TECHNICAL REVIEW

Introduction to CAE R&D Center

In October, 2018, CAE R&D Center was established to enhance the R&D and Manufacturing operations and increase the efficiency of various departments (Design, Development, Prototyping, Testing, Manufacturing, etc.), reorganizing the existing CAE Department.

CAE (Computer Aided Engineering) is a technology to validate if the planned product/peripheral structure satisfies the required performance by computer simulation. This helps us to improve design accuracy where design validation was conventionally difficult. This even allows us to study the design safety factors of products including the peripheral components. By simulating fabrication of prototypes and experiment/evaluation of the prototypes in advance, we can reduce the number of prototype builds and testing to improve the efficiency of design/experiment and provide cost reductions.

The recent improvements of CAE have been remarkable and CAE technology has been introduced and enhanced in all the industrial fields. **NTN** Next Generation Research Alliance Laboratory at Osaka University also adopts CAE in its research projects for establishing next generation technologies and quickly applying them to products.

By reducing the R&D man-hours with CAE technology, researchers and engineers are allowed to dedicate themselves to higher-value activities. The development period can be reduced and competitive products can be introduced to the market faster. As **NTN** transforms its operations from the development of single products to modules and system products, we are appling technology to more complex mechanisms and simulations of composite and different materials.

As an example of CAE simulation technology, the following are some of the calculations of the force applied from rolling elements to the cage in bearings used to support transmissions which are the power transmitting devices in automobiles. CAE simulation technology enables the following:
· Calculation of the load acting on each rolling element in the bearings of a moving automobile.
· Calculation of the force from the above rolling elements to the cage and the generated stress.
⇒ These calculations help optimize the number and diameters of the rolling elements and improve the bearing load capacity by precisely determining the required strength of the cage.
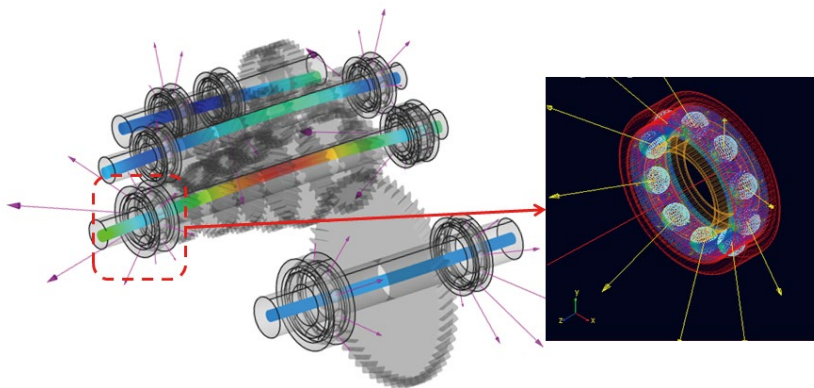
Simulation of force applied to cage of transmission bearings and initiation of stress

NTN

TECHNICAL REVIEW

No.87

NTN corporation

NTN TECHNICAL REVIEW No.87

CONTENTS

A message for the special issue on "Automotive Products for Electric, Autonomous and Low Fuel Consumption"

Representative Executive Officer,
Senior Managing Executive Officer and CTO (Chief Technology Officer)
Yoshinori TERASAKA

The automotive industry is facing a huge transformation period. All the companies in the world associated with automobiles are in the midst of fierce competition in technology, performance and cost, in an industry which is swept away by the market trend characterized by "CASE," such as the agreement of controlling global average temperature at the COP 21 Paris Agreement, electrification to improved fuel economy as a response to global warming, autonomous driving providing improved safety and the idea of a shared economy.

We are a bearing manufacturer with 100 years of history since its foundation; however, we have been proactive in advanced development ahead of the market trend so that we can achieve "sustainable growth" and be a "surviving company" into the next generation. The origin of **NTN**'s development is our core competence including tribology technology but we have also expanded our development philosophy from original development to partnership with third parties.

Our foundation is our core competence in tribology. We think that this core competence continuously enhances the companys value when it is applied to new products. In our company, the Advanced Technology R&D Center is in charge of core technology, New Product Development R&D Center is in charge of new product development and the Process Engineering R&D Center is in charge of manufacturing technology. The **NTN** Next Generation Research Alliance Laboratory at Osaka University was founded in 2017 for research of next generation technologies which are expected to grow in the future such as AI and IoT. The **NTN** Next Generation Research Alliance Laboratory is responsible for incorporating those technologies as our new core competence, and for the training of our researchers. In addition, the CAE R&D Center was newly founded in October, 2018. Its purpose is to advance simulation technologies we have been developing to work on tasks such as engineering challenges of all **NTN** groups, faster development/refinement and accuracy improvement. Since simulation technologies are a research area to be further actively pursued, we are continuing our research at the **NTN** Next Generation Research Alliance Laboratory, as well as elevating the applicability of these technologies to our development and using them in our products.

We have also realized vehicle autonomous driving and electrification, with advanced development of module and system products, which increased our value in the industry. Those products include IWM (In-wheel motor systems), among others, such as electrical module products that can be used for electrical accessory devices such as oil pumps, water pumps and vacuum pumps. There are also multifunctional products such as eHUB and sHUB, which consist of axle bearings (our main product), motor and controller. We are also contemplating development of "sensorized bearings" . With the integration of special sensors, we can transform wheel bearing operations offering service solutions such as status monitoring and fault prevention using the output of those sensors and analyzing them with advanced programs equipped with an AI algorithm.

We have been preparing for the drastic transformation of the automotive industry by reorganizing our R&D and production systems. We believe that the success of our challenge of "sustainable growth" and being a "surviving company" depends on how we can achieve competitive products fast, taking advantage of the technologies and know-how accumulated so far. The foundation for this challenge is our mid-term business plan "**NTN**100" of 2015. In "DRIVE **NTN**100" of 2018, we set a plan to promote new products.

We would be grateful if these plans can contribute to further development of the entire industry.

Perspective for Advanced Vehicle Technology into CASE Era

Hideo INOUE

Professor, Faculty of Creative Engineering, Chair of Department of Vehicle System Engineering, Kanagawa Institute of Technology

What is the CASE (Connected, Autonomous, Shared & Services, Electric)[1] era? The integration of information and mobility has begun a paradigm change that will drastically change the ecosystem of people, cars, and transportation society, and it can be said that it is a borderless competition and collaborative era of Silicon Valley players, European car manufactures, new comers, and developing countries. Looking back on the history of automotive technology, I would like to discuss this perspective with you based on the examples of the evolution of safety, deepening driving, and mobility city systems that are the foundation of the eco-system.

1. Introduction

Automobiles have contributed to the development of industry and culture by expanding free and safe transportation of people and goods since the end of the 19th century. In 1885, Karl Benz of Germany succeeded in running a 3-wheel vehicle with a newly invented gasoline engine on a public road. The glorious first-ever automobile's name was Benz Patent Motorwagen. It created the basic form of the current automobile. In 1908, the king of automobiles, Henry Ford, introduced the mass-production "Model T," as he "wanted a vehicle as fast as a train that can run anywhere like a horse," which created an "automotive revolution."

And today, the environment surrounding the automotive industry is in a foregoing period of a large paradigm shift, such as diversification of power train led by electrification, global competition of autonomous driving, acceleration of "intelligent vehicles with IoT" and transformation of "ownership and use of vehicles" as can be seen in "emergence of sharing services."

From the perspective of the global industry competition, energy, IT and automotive industries are actively partnering with each other across the borders for innovation and acquisition of new business segments while competing with each other. Even in this environment, however, we cannot overlook the fact that Tesla's fast growth quickly achieved entry to the automotive industry from Silicon Valley, by not just building an EV but by building a vehicle platform through electrification that cannot be achieved by the conventional internal combustion engine power train. Tesla created a vehicle with very high fundamental performance that is fun, comfortable and attractive to consumers.

Also, the European automotive industry, led by Germany, is diligently working on the evolution of environment-friendly, comfortable, easy-to-drive and intelligent vehicles incorporating advanced technologies such as drive assistance and connectivity backed up by the respective state through the collaboration among the industry, academia and government. In addition, these new trends have potential to quickly expand to the automotive markets of emerging countries such as China, India and South-East Asian countries. The Japanese automotive industry also needs to be competitive to win in this paradigm shift both in global competition and competition with other industries such as IT.

These global trends can be interpreted as a solution to the compelling social problems such as global warming, traffic jams/accidents, declining birthrate and an aging population while achieving a rich and comfortable mobility society. In other words, the automotive innovations with better and smarter vehicles are the "primary units" and "driving force" for enriching the communities and the citizens **(Fig. 1)**.
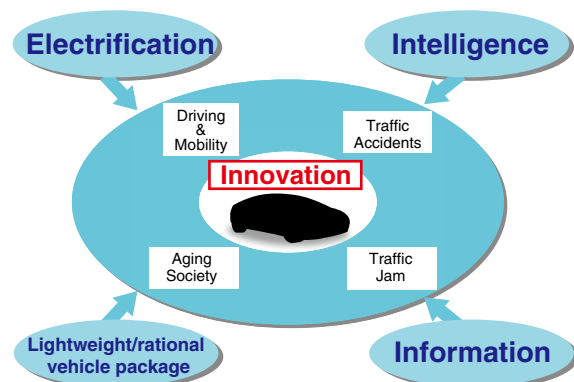

Fig.1 Direction of vehicle innovation

"The real automobile innovation is starting now!" "Vehicle development" and "human development" with "integration of advancement and foundation" will make or break is not an overstatement.

Now, let me discuss the perspective raised in the title of this paper by looking back at the ITS (Intelligent Transport System) activities so far. Although CASE (Connected, Autonomous, Shared & Services, Electric) is a term that expresses the current paradigm shift of the automotive and IT industries well, it is not so different from the change nurtured by the long ITS activities aiming for the "sustainable mobility society." The biggest difference is the automotive industry is forced to make a big transformation in the era of new entrants from the IT industry of Silicon Valley such as GAFA[2], energy industry and new industries through electrification and autonomous driving. However, this was also included in the discussion of ITS activities, as it expressed the importance for the automotive industry to have a perspective of an ecosystem consisting of people, transportation community and the use ICT (Information and Communication Technology) for building a rich and comfortable mobility community (maximizing) by solving social problems (minimizing) such as traffic accidents/jams, energy/environment and aging society[3, 4]. Then, what are the real differences?

· The evolution of electrification, autonomous driving and ICT raised the expectation that the dream of a mobility community may come true
· It revealed the change cannot be coped with using the conventional framework of the automotive industry alone and a new ecosystem from both the industrial and social system perspectives needs to be built
· A ubiquitous and global borderless era facilitated by the Internet made it easier for the new entrants to play with new ideas
· Due to all of the above, the design structure of the automobile itself, needs to be innovated

Are the above not the real differences from the perspective of the history of the automotive industry? This also shows the conventional structure and mechanism of production is close to the limit and a new S curve needs to be built for breaking the limit representing the needs of the times. Although the threat from IT, energy and new industries exist, the automotive industry should not take them as the entire picture. The real challenge is:
· if the automotive industry can transform itself, and
· if the automotive industry can take the leadership while repeating collaboration and competition with other industries,
aiming for a comfortable and rich mobility community.
In order for the automotive industry to take the

leadership, its own core technology is needed.

Thus, the ecosystem raised by CASE can also be expressed as the cyber physical system **(Fig. 2)**[5].
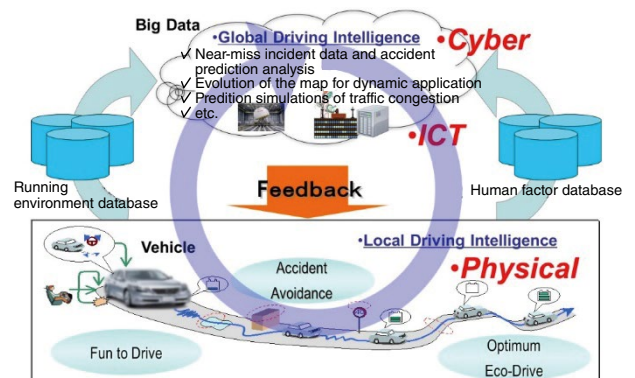
Fig. 2 Example of cyber physical system

The cyber physical system is a system of cyber space (virtual space) and physical space (real space) highly integrated by ICT.

I highly expect the automotive industry to achieve self-transformation and take the leadership of other industries by putting the people (citizens) in the center of mobility **(Fig. 3)**.
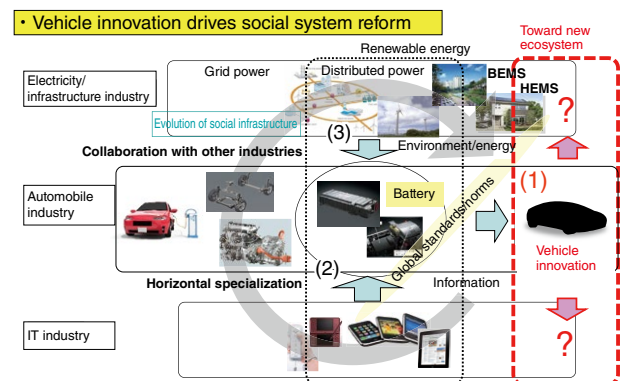
Fig. 3 Relationship among industries

In this paper, I would like to think about the mobility community of the 21st century together with the readers, introducing cases from the viewpoints of "driving" and "mobility" on how the ecosystem and cyber physical system in this mobility change in the era of CASE.

2. Autonomous Driving; "Unity of Rider and Horse" and "Driving Intelligence Aiming for Further Safety"

2.1 What Are "Autonomous Driving" and "Driving Intelligence"?

Information on autonomous driving technology is constantly publicized at the media, industry and state level in the world. Although with rather excessive expectation, the autonomous driving technology is promoting a big dream in the mobility community where the people have foresight of innovation in vehicles, transportation system and even information services.

Let us track down the history of autonomous driving. Leonardo da Vinci dreamed of an autonomous driving vehicle when he thought of a mechanical vehicle. In the 1960s to 1970s, the first smart car "Stanford Craft" was conceived for investigation of the lunar surface. Long cables were equipped for a video camera and remote control which contributed to obstacle avoidance technology and higher image processing performance later in the development. However, the biggest impact on the automotive industry and society came as autonomous driving vehicles from colleges and companies participating at two DARPA (Defense Advanced Research Projects Agency) Challenges subsequent autonomous driving vehicle from Google. Google has continued the driving experiment on public roads since 2010, totaling 700 thousand miles (approx. 1,130 thousand km) by April, 2014. In Europe, state level projects such as HAVEit are making progress through a collaborative framework among industry, academia and government[6]. In 2013, Daimler announced that it would introduce autonomous driving vehicles into the market by 2020, disclosing that its vehicle traveled autonomously on a German public road for over 100 km. Furthermore, European project PEGASUS recently created and proposed a framework for the development and evaluation process based on systematic driving scenarios. Also recently reported is the announcement of establishing a research center for autonomous driving taxis by the U.S. car sharing company Uber, and a plan of an on-demand autonomous car service from Google. As such, the competition of research and development has heated up with participants worldwide from the automotive, IT, car sharing service and logistics industry which combine engineering and business operations with the actual introduction reportedly around 2020. When we consider the advantage/value of autonomous driving from the viewpoint of the social challenges,

(1) Improvement of traffic flow (reduction of congestion/ CO_2)

(2) Reduction of accidents due to human errors (carelessness/distraction/fatigue)

(3) Reduction of accidents due to health problems/ unconsciousness

(4) Safe driving under low visibility (nighttime/rain/snow)

(5) Reduction of accidents by aged drivers/securing means of transportation (decline of driving ability due to physical impairment)

(6) Improvement of comfort by reduction of driving load can be expected. However, "autonomous driving" is not necessarily "safe" all of sudden. I think there is "good driving" and "bad driving" for "autonomous driving," as well. With the technology today, it should not be difficult to run the vehicles automatically, however, "good driving" is a different matter. Driving by an expert driver requires observation of the surrounding environment predicting possible changes based on the knowledge, experience, and understanding of his/ her own vehicle's behavior and motion characteristics with prediction of possible outcomes. The driver enjoys the value of transportation, freely, safely and comfortably by doing all of the above but it is not as easy for a machine to do that on behalf of human beings. Recognition of the surroundings is not sufficient. It requires "driving intelligence." Also, neither people nor machines are 100% safe or trustworthy. They grew (learn from each other) by enhancing their advantages and complementing disadvantages to improve the driving quality by continuously creating "better" and "safer" driving operation under various driving conditions. Regardless of who drives the vehicle, people or machines, safe driving technique is common. Therefore, I think incorporating more "driving intelligence" into the vehicles and driving its evolution specifically is the most important challenge. In the history of mankind, the relationship between machines and people is commonplace. There has been a lot of evolution when transportation changed from the horse to vehicle; however, there are things horses can do but vehicles cannot. I do not think the vehicles have achieved the value of so-called "unity of rider and horse" such as the "safety instinct where the horse would not jump off from the cliff even if the rider instructs so and running with comfort together," "ability of the rider, who may or may not want to drive, to communicate and act on the context of the wills of each other between the rider and the horse," and "not to be isolated in the communication between the riders."

In the context of CASE, this aspect of "driving" is not largely raised. In addition, we cannot ignore the development of the people (drivers) and traffic environment (infrastructure) along with the development of vehicles in the context of the relationship among the people, vehicles and traffic environment. As mentioned before, the driving technique of an expert driver

comes from the information learned under various driving conditions and knowledge accumulated over a long driving experience. An expert driver internalizes the dynamic vehicle motion reaction against the driving maneuver and holds it as "driving intelligence" in the physical model. Therefore, the driving technique of an expert driver can be understood as a cyber physical system integrating the "experience/knowledge information model" and "physical model of vehicle motion." Is this "driving intelligence" not the important aspect where the autonomous driving technology makes the real difference?

Recognizing these challenges, I would like to step into the discussion of the evolution of "safe driving technique" and "autonomous driving with unity of rider and horse (shared control)" based on "driving intelligence," which can be interpreted as the instinct of a vehicle, not only remaining in the generalized concept of "autonomous driving."

The following is based on the research and development conducted since 2011 on a collaborative framework between universities and industry "Driving Intelligence System to Enhance Safe and Secured Traffic Society for Elderly Drivers"[7] which is the theme adopted by the "Japan Science and Technology Agency (JST) Strategic Innovation Promotion Program (SIP)" and my own view.

2.2 Driving Intelligence Aiming for Further Safety
2.2.1 Driving Support System and Autonomous Driving Technology

The safe driving technology has evolved from collision safety to preventative safety. The recent idea of "integrated safety,"[8] which covers the entire safety phases from the normal driving phase to collision and rescue/emergency response phase for reviewing and responding is an important philosophy showing "there is no compromise for safety." With this philosophy, adoption of a driving support system that recognizes the driving surrounding environment and obstacles using sensors such as cameras and radar expanded very quickly. Devices such as collision damage reduction/preventative automated brake systems are deployed in many products as their benefit is easily recognized and its adoption is recently expanded even in light vehicles under the name of AEB (Automated Emergency Brake). This way, the capability of accident avoidance is a little over a second before collision, such as rear-end collision, has greatly improved. On the other hand, systems for reducing the driving load during normal operation have been deployed, such as the ACC (Adaptive Cruise Control), LKA (Lane Keeping Assist) and LDW (Lane Departure Warning (& Prevention)). From the safety standpoint, driving phases consist of the "normal driving" phase for smooth driving without any risk and the "emergency

avoidance" phase, which is a few seconds before potential collision and with increased potential/apparent risk. In the former phase, it is necessary to drive with caution while predicting potential risks as the driving schools often teach with "risk predictive driving" **(Fig. 4)**. So far, the driving support system has been effective in "normal driving" and "emergency avoidance" phases. As the autonomous driving technology evolves, we must not overlook the technology of "look-ahead driving" that corresponds to the risk increasing phase. Also, as mentioned earlier, since 90% of the traffic accidents are caused by human errors, the evolution of driving support systems to deal with the various causes, such as elderly drivers, distraction, health problems, distracted, congestion, etc. is expected. However, adding individual systems will not be effective. It should be necessary to complement driver errors by the autonomous /intelligent driving systematically.
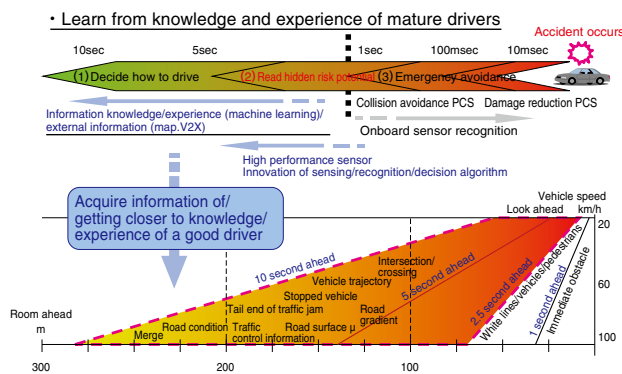
Fig. 4 Concept of risk phases for preventative safety (SIP)[9]

2.2.2 Driving Intelligence with Risk Prediction Capability

Now, how can we specifically capture the driving intelligence? First, it is essential to "observe well" the surrounding environment, namely, improve the ability of "recognition" with sensing technologies. In addition, it is necessary to create the basic drive planning ability such as generating the path to the destination from the recognized information[10] and pass around the stopped vehicles. In addition essential drive planning and risk prediction intelligence will be required by looking ahead and anticipating risks **(Fig. 5)**.
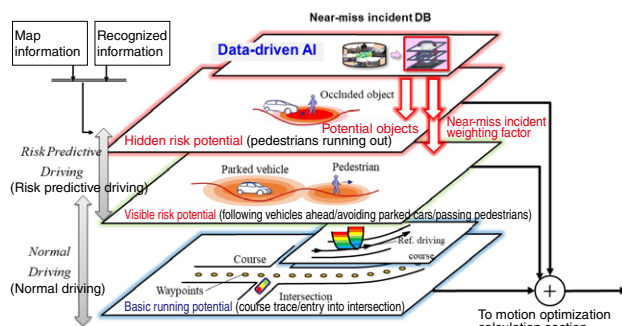
Fig. 5 Layered structure of risk predictive control (SIP)[11]

Risks include apparent risk such as a bicycle or pedestrian who is visible but "may" change the behavior in the next instance, and potential risk such as a pedestrian who is hidden and may jump out from behind a stopped vehicle. There are two important points for making the risk prediction technology. The first is the model to define the possibility of collision a few seconds away while running and to physically express the present margin toward the risk. There are some methods such as the potential field, but this is an important model expression for generating the optimum driving path with smaller risk and control of the vehicle speed. The second is the learning process based on the experienced running information. The ontological approach based on rich information is also necessary in order to determine the risk from the apparent conditions. Building prediction model's integrating the physical model and information model is a new challenge for the automotive industry. The "near-miss incident data"[12), 13)] currently accumulated at Tokyo University of Agriculture and Technology is very useful as a source of information. Since this is the information source determining risk events such as "emergency brake was applied even if it did not lead to accidents," learning the data may lead to risk prediction. As described above, it is indispensable to implement the intelligent behavior of people, such as feeling "somewhat risky" from general observation and slowing down, to the machine (vehicle) for evolution of safety and technical challenge called autonomous driving.

Fig. 6 shows the physical model expressing the risk as the potential field (hereafter, "risk potential") in the SIP project. By making the space information recognized by various peripheral monitoring sensors risk potential, the risk image of driving environment such as the parked vehicles can be continuously presented as the physical expression. Furthermore, this potential field facilitates driving control since it can optimize the target course and speed (I am omitting the detailed explanation. Refer to the reference for more information)[14)].

$$\text{Ref. yaw rate } \gamma^*(t) = \min_{r_p} \sum_{j_y=1}^{N_y} \left(U_t \left(X_{P\_y}(i_y, j_y), Y_{P\_y}(i_y, j_y) \right) + r_y \gamma_P^2 \right) \quad (5)$$
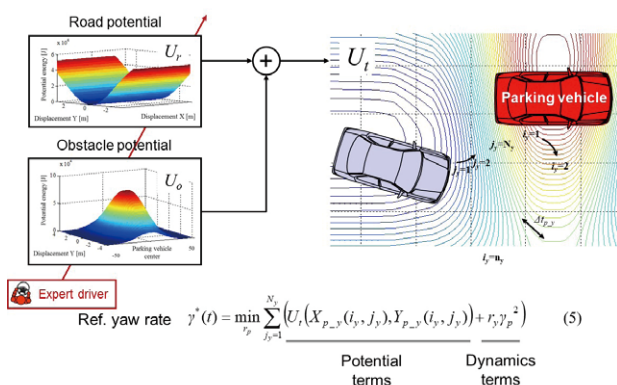
Fig. 6 Optimization of target trajectory by risk potential

2.3 Near-Miss Incident Database and Information Risk Model

We learned a lot from the near-miss incident data in the SIP project[15).] We made progress in building the "Data Driven Risk Prediction Model" which predicts the risk potential in the future from the near-miss incident empirical data, not only from the risk potential of the physical model. **Fig. 7** shows the framework leading to the risk prediction control built in this project[16)].
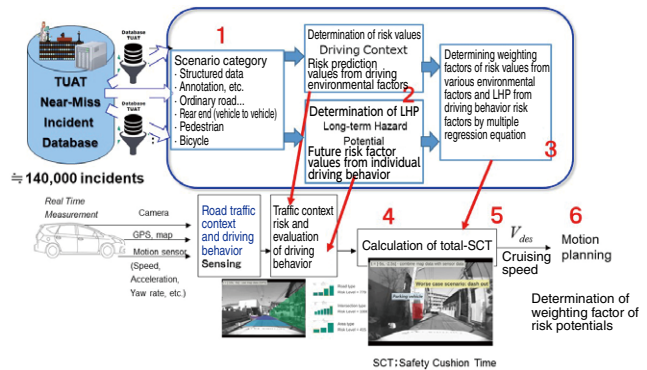
Fig. 7 Framework of data-driven risk predictive control

The causes and effects of "driving behavior factors" and "driving environmental factors" to the near-miss incident events are expressed by the quantitative indices, LHP (Long-term Hazard Potential) and Rv (Risk value). These 2 risk quantitative values are determined by the data between approx. 10 seconds and 3 seconds before the risk events. The value of these not-so-complex quantitative indices, LHP and Rv, which show 2 key non-stationary factors of the "human drivers" and "driving environment" in vehicle driving is significant. Furthermore, by incorporating them in the virtual driving/traffic simulation to make it a framework of prediction from near-miss incidents to accidents, we could make probabilistic predictions from the "risk prediction control," such as "risk predictive driving." **Fig. 8** shows an example of its results[16)].
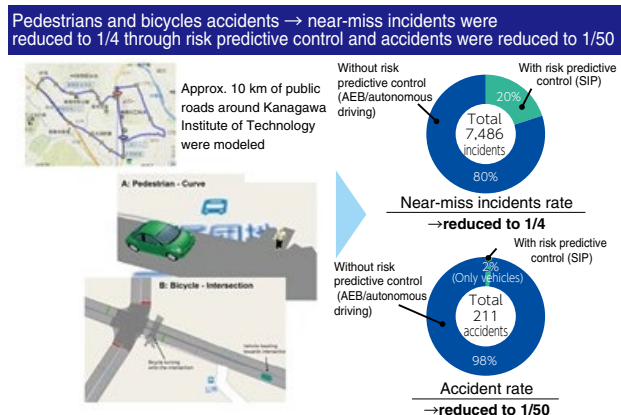
Fig. 8 Prediction of risk predictive control through driving/traffic simulation

We have simulated intersections and jumping-out of pedestrians and bicycles on public roads of approx. 10 km around the Kanagawa Institute of Technology and built a virtual model considering the LHP and Rv indices. This dynamic simulation result shows a reduction of near-miss incidents to approx 1/4 (total of 7,486 near-miss incidents) and a reduction of accidents to approx 1/50 by the introduction of risk prediction control (slowing down by risk predictive driving). This result indicates the difference between "autonomous driving to apply brake after observation (recognition)" and "driving intelligence of slowing down by looking ahead for something jumping out from the visible environment." This kind of simulated effect prediction does not have enough credibility, yet, as the history of weather forecast shows. However, it shows a direction of risk prediction technology both as the system control technology and as the digital twin virtual validation technology integrating the "information model" and the "physical model." This framework that we could build this time is important but we have to note that this database might not be effective in the area/country where the traffic environment is different, similar to the fact that the people familiar with the area can drive effectively. Our challenge is how to build near-miss incident database for each community and how to structure them.

2.4 Autonomous Driving with Unity of Rider and Horse (Shared Control)[17)-19)]

The machines are only used by the people when trusted. As mentioned earlier, the people may want to drive or may not when tired or under monotonous situation. Elderly people feel uncomfortable driving, recognizing poor physical conditions. Enabling them to drive worry-free to the destination should be the role of the intelligent machine, not taking away the driving privilege from the elderly people. The benefit of cars is not only providing means of flexible transportation but also driving pleasure. Use of machines by people has an aspect of stimulus to the instinct where the people become active and motivated. Recently, "use of information" significantly expanded through the use of smartphones. If the information provides value for "knowing," "things" have value "to be seen, touched and felt." The question is not to determine which is better, but the important point they both offer in common is if the context the machines provide can be understood by the people who use them (or easily understood). This does not immediately jump into the discussion of HMI (Human/Machine Interface) or driver monitor, but rather, we have to check if the machines provide the outcomes (performance) that meet or exceed expectation of the people who use them (this is the baseline for the trust). The machines should predict the result (performance), provide the context of their action to the people and be understood. In this context, the

smartphones are ahead. The vehicles are still behind the curve. By providing the road conditions and recognition that the machines determine optimal as rational as possible to the people and expressing them through the steering wheel, acceleration and braking which the people can touch and feel while the frontal view that the people can see and understand, the machines can become closer to the horses. It is imperative not to add new interfaces and increase the load of driving. Can the context of driving be firmly grasped and communicated to the people? This is also what is expected from the intelligence of autonomous driving (i.e. driving intelligence).

An example of the research achievements of SIP project is shown in the following. **Fig. 9** shows a conceptual diagram of Haptic Steering Shared Control[11)]. It aims for guiding the vehicle to a better course trace by applying the difference between the steering operation modeled after an expert driver and steering operation of a real person to the steering torque reaction force. It revealed that this control improves both traceability of the model course and smooth operation **(Fig. 10)**[14), 20), 21)].
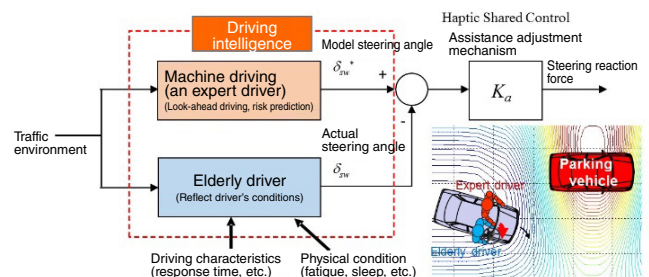

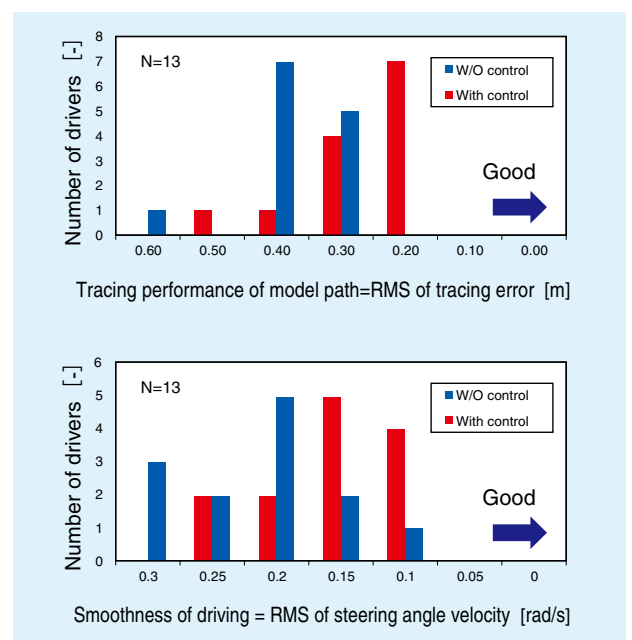**Fig. 9** Haptic Steering Shared Control

Fig. 10 Effectiveness of Haptic Steering Shared Control

I have discussed "driving intelligence aiming for further safety" and "autonomous driving with unity of rider and horse" in the evolution of autonomous driving technology as my expectation. I welcome participation of those who share my view in this discussion.

3. Connected; Mobility Ecosystem Connected by Information

3.1 Overview

Now, let us think about the transformation of transportation system as the ecosystem of people, vehicle and traffic environment. That is, MaaS (Mobility as a Service). The possibility of service businesses is unlimited in the cyber physical network where information and mobility are integrated. Services to use multiple means of transportation in an integrated fashion are beginning and expected to grow worldwide. In Finland and Singapore, collection of traffic information and creation of database for dynamic communication are led at the government level. The initiatives at ITS include solution of mobility divide, that is, safe mobility and active life support of elderly and disabled people who are vulnerable road users, and revitalization of local communities and improvement of QOL (Quality of Life) of citizens. Therefore, the concept of "provision of equal mobility to everybody" is also important.

The above is an example focused on the information/software aspects but formation of ecosystem as an infrastructure that includes IoT and physical space is also important as the information and mobility are integrated. Let me introduce a research and development project in Singapore, "TUMCREATE," as an evolution of mobility from transformation of transportation system.

3.2 TUMCREATE

A project of Technical University of Munich, TUMCREATE (TUM: Technical University of Munich), adopted by the CREATE (Campus for Research Excellence and Technological Enterprise) program of Singapore's National Research Foundation is a good research example that shows a new mobility community.

This project is joined by Singapore's NTU (Nanyang Technological University) and thus contributing to the development of young Asian engineers. The first phase was conducted from 2010 to 2016 with the theme of "The Center for Electromobility in Megacity" and the second phase is being conducted from 2016 to 2021 under the theme of "Towards the Ultimate Public Transport System." Over 100 engineers and researchers will participate in this project from both universities and the professors from the Technical

University of Munich are also stationed in Singapore dedicated to 5 years of research.

In the first phase, NTU's engineers learned the architecture of vehicles including package design as the foundation of automotive engineering, in addition to building an EV. They also digested the foundation of the electric motor system such as the design of battery pack and test bed and fabricated a research vehicle taxi EV suitable for megacities in South East Asia, called EVA **(Fig. 11)**.

(Source: TUMCREATE website)

Fig. 11 TUMCREATE EVA – Tropical taxi EV [22]

In addition, they conducted simulation of the traffic conditions in Singapore, as well as to the simulation of the battery management in the vehicle. They even built a data management system for optimization of driving and battery charging.

The research theme of the second phase is traffic congestion, energy and security in Singapore, which is precisely the solution aimed at problems of megacities in the new ecosystem proposed by the ITS activities.

First, the mobility called SRT (Semi Rapid Transit) System is planned, which uses units of 30 person capacity to form a flexible caravan of autonomous driving. This is a mobility capability aimed for increased efficiency in urban transportation, between MRT (Mass Rapid Transit) System which is high speed/high capacity with sparse passengers and a bus service which is slow and low capacity **(Fig. 12)**.
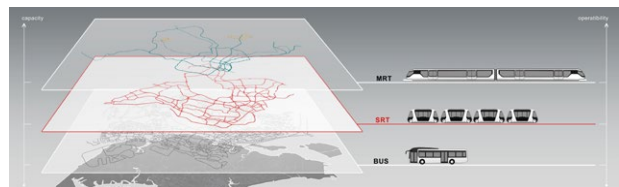
(Source: TUMCREATE website)

Fig. 12 Semi Rapid Transit System [22]

Naturally, the electric vehicle with the technology developed in phase 1 is used. The SRT System is characterized by the following, in addition to the service offering of seamless use of multiple means of transportation (mobility X).

· Multifunctional capability by autonomous driving as the module
· Clean urban environment by electric vehicles
· Dynamic and flexible passenger transporting capability up to 10 units (300 passengers) in a caravan during peak hours
· Quick response to demand reducing wasted time
· Quick loading/unloading at the SRT stops

Next, the SRT-MODULE is not a stand-alone project but a component of an integrated ecosystem with SRT-CENTRAL, SRT-INFRASTRUCTURE, SRT-CONNECT and SRT-POWER **(Fig. 13, 14)**.
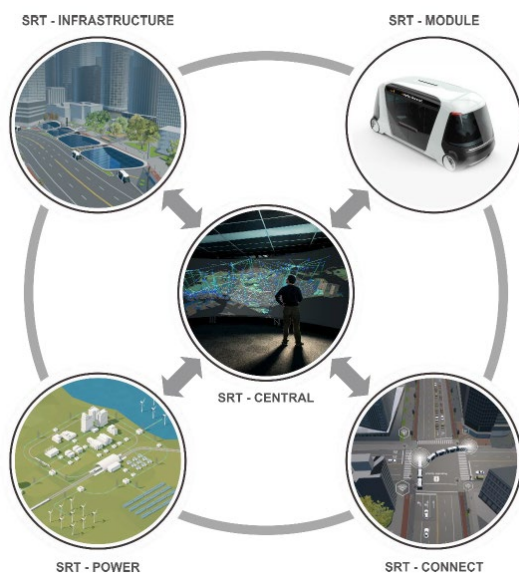
The SRT vehicle unit is designed with user-friendly features, such as an air curtain to contain the conditioned air in the vehicle while loading/unloading, all wheel independent steering mechanism for a small turning radius and easy parallel parking **(Fig. 15)**, low-floor and guidance technology with road projection for easy access, adopting many novel ideas.

(Source: TUMCREATE website)
Fig. 13 Semi-Rapid Transit(SRT) System [22]
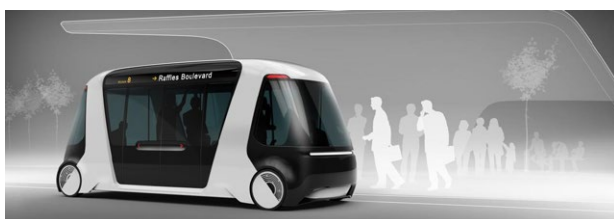
(Source: TUMCREATE website)
Fig. 14 SRT-MODULE [22]
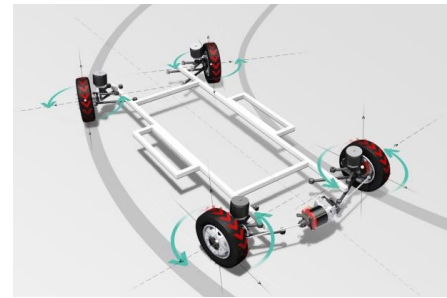
(Source: TUMCREATE website)
Fig. 15 All wheel steering system [22]

They can be evaluated/designed on the virtual space using VR (Virtual Reality). The most spectacular point is that they have built a dynamic simulation of the entire city of Singapore, called CityMoS **(Fig. 16)**.

This is the system with layers of power system, sensor network and a traffic system for the entire city not only providing simulation (virtual world) but also actual data sensing (real world), so it is built as a cyber physical system. In other words, the city-state of Singapore itself, as the "Cyber City," has become an intelligent system.
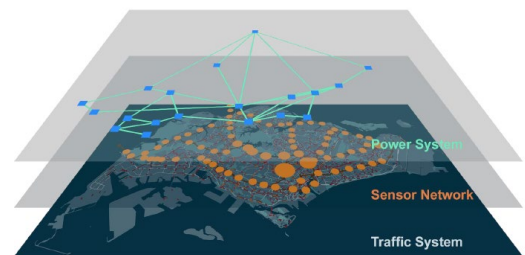
(Source: TUMCREATE website)
Fig. 16 SRT – CENTRAL (CityMoS) [22]

As an advisor of this project, I am impressed with the young engineers of TUM and NTU who are excited and confidently working on their respective R&D subjects. Post doctoral researchers, doctors, professors and engineers of NTU from the international alliance are increasing their capabilities through automotive design and manufacturing while acquiring a high skill set of the cyber physical system. The level of these R&D activities is equivalent to forefront R&D activities at large corporations. Some companies seem to participate in the actual manufacturing process but most of the basic design is decided by this project. Also, the project offers a powerful human development opportunity for young engineers.

3.3 Disaster-Resilient Ecosystem for Japan

In this Chapter, I have only mentioned good projects from the overseas but now I would like to mention universal concepts originated from Japan which (in my opinion) should also work worldwide.

In the era of Heisei, Japan was struck by many disasters and many people had a bad experience.

However, the Japanese culture had strength to overcome these disasters. Based on these lessons, we have to build an ecosystem suitable for Japan in the era of Reiwa, which is highly active in normal period and resilient to disasters.

In the Great East Japan Earthquake of March 11, 2011, the entire nation of Japan grieved over the death of many people. I would like to express my deepest sympathy to the deceased and encourage the people who are working hard in the aftermath.

Personally, I also experienced the earthquake on March 11, when I was holding a conference in Sendai. I experienced the infrastructure risk firsthand. An experience of loss of social infrastructure with information completely blocked, energy risk of electric power and gasoline, disruption of means of transportation, lack of food and water, etc. The following is an unofficial proposal we made to the government and business community, which is based on my own note of lessons I learned as one of the citizens working on the mobility industry and contribution from colleagues.

3.3.1 Lessons from the Experience of Infrastructure Risk

· Mobile phones did not work as the base stations were dysfunctional.
  → Internet and WiFi spots are effective. Distribution-optimized ad-hoc base stations are needed.
· It was unfortunate that a Prius generator could not be used for 12V output. (Toyota provided this feature soon after the disaster.)
  → Electrification means having optimum battery capacity; yet, having generators is also important. Especially a multi-fuel generator.
· Real-time mobility connection information is required on how to coordinate public transportation, automobiles and other mobility modal.
· Autonomous distributed power management system is also required, not only overall optimization such as the power grid.
· It is important to "have the ability to communicate with strangers," "take action when scared" and "believe in one's own sense of risk."

3.3.2 Proposal for Disaster-Resilient System

· Locally generated/locally consumed distributed energy community
  → Autonomous management of local power system for energy saving and efficient use based on management of local energy information such as a stationary battery. Control of demand and supply balance with the power grid by dynamic pricing during normal operation.

· Building autonomous and distributed mobile wireless communication network
  → Use vehicles as the temporary wireless tandem stations for ad-hoc communication network using WiFi functionality during disasters or in remote areas, as a limited emergency communication system.
· Multi-fuel range extender
  → Effective during normal and disaster periods.
· Automatic driving system for remote control and autonomous driving
  → The questions of security need to be addressed, but remote control driving is effective during disasters. Vehicles with ability to run on bad terrain such as SUVs are also effective.

Some of the above have made good progress but having built the cyber physical ecosystem with autonomous and distributed system in addition to overall optimization system must be particularly important for the ecosystem of Japan where many disasters strike.

4. Summary

In this paper, we have discussed the evolution of advanced automobile technologies toward the era of CASE and evolution of ecosystem of people, automobile and traffic environment, although the discussion may have been generalized towards the end. For example, the discussion included much of my personal views, which may not reflect the trends of the time objectively. We are certainly in the midst of a once in a century paradigm shift and we should have a sense of urgency as global competition intensifies; however, this change is an inevitable result of evolution and is also important to have originality in our vision and ideas based on the Japanese culture and history, for the requirements of the mobility society and automotive technologies. I believe that these views and ideas will have a positive global impact.

References

1) https://mb-live.jp/mercedes-benz/case/

2) https://ja.wikipedia.org/wiki/GAFA

3) Okazaki Teruo, Watanabe Hiroyuki, Oohata Akira, Inoue Hideo, Amano Kaoru, Chapter 9. Technology Diffusion and Development, Climate Change Mitigation - A Balanced Approach to Climate Change - , Yamaguchi Mitsutsune(Ed.), Springer,(2012), 179-221.

4) Teruo Okazaki, Hiroyuki Watanabe, Akira Oohata,Hideo Inoue, Kaoru Amano, Climate Change Mitigation - a Balanced Approach to Climate Change - Edited by Mitsutsune Yamaguchi, Chapter 9 Technology Dissemination/Development, Maruzen Publishing, (2013), 213-238.

5) Hideo Inoue, et al. Intelligent Vehicles for Super Mature Society, Symposium of the Society of Automotive Engineers of Japan (No. 06-14) Presentation on "Latest Technology Innovation of Autonomous Driving" (May, 2014).

6) Bauer, E. et al., "PRORETA3 : An Integrated Approach to Collision Avoidance and Vehicle Automation", Automatisierungstechnik, Vol. 60, No.12, (2012), 755-765.

7) Hideo Inoue, Masao Nagai, et.al, Driving Intelligence System to Enhance Safe and Secured Traffic Society for Elderly Drivers, 2014 JSAE Annual Congress(Spring), Yokohama Japan, (May 22 2014).

8) Toyota Motor Corp. News Release, "Toyota Strengthens Efforts to Develop Safe Vehicles - Integrated Safety Management Concept Forms Base of New Safety Technologies -" (August, 2006). https://global.toyota/jp/detail/1532213

9) Hideo Inoue, et al. Vehicle Intelligence toward Aging Society, Japan Science and Technology Agency (JST) Strategic Innovation Promotion Program (SIP), Interim Report Symposium, presentation material, (January, 2015).

10) Kim, W., Kim, D., Yi, K and Kim, H. J., "Development of a Path-Tracking Control System Based on Model Predictive Control Using Infrastructure Sensors", Vehicle System Dynamics, Vol.50, No.6, (2012), 100-1023.

11) Hideo Inoue, et al. Autonomous Driving Intelligence System to Enhance Safe and Secured Traffic Society for Elderly Drivers, Japan Science and Technology Agency (JST) Strategic Innovation Promotion Program (SIP) Symposium, presentation material, (September, 2016).

12) Hideo Inoue, Research into ADAS with Driving Intelligence for Future Innovation, 26th IEEE International Electron Device Meeting 2014, Keynote Speech, (15 December 2014), 1.3.1-1.3.7.

13) Pongsathorn Raksincharoensak, Drive Recorder Database for Accident/Incident Study and Its Potential for Active Safety Development, FOT-NET Workshop Tokyo Japan, (October 13 2013).

14) Hideo Inoue, et al, "Intelligent Driving System for Safer Automobiles", Journal of Information Processing, Vol.25, (November 2016).

15) Wongwaiwit, P., Raksincharoensak, P., Michitsuji, Y., "Analysis on Pedestrian and Bicycle Behavior in Unsignalized Intersection Based on Near-Miss Incident Database", Proceedings of 20th JSME Transportation and Logistics Conference, (2011), 19-22.

16) Hideo Inoue, Mohanad El-Haji, Thomas Freudenmann, Haipeng Zhang, Pongsathorn Raksincharoensak, Yuichi Saito, "Validation Methodology to Establish Safe Autonomous Driving Algorithms with a High Driver Acceptance Using a Virtual Environment", FAST-zero, (September 2019).

17) Abbink, D. A., Mulder, M. and Boer, E. "Haptic Shared Control: smoothly shifting control authority", Cognitive Technology Work, Vol.14, (2012), 19/28.

18) Diomidis Katzourakis, Claes Olsson, Nenad Lazic and Mathias Lidberg, "Driver Steering Override Strategies for Steering Based Active Safety Systems", Proceedings of 2nd International Symposium on Future Active Safety Technology Towards Zero-Traffic Accidents (FAST-zero '13) , Paper no. 20134591, (2013), 1-7.

19) Ryota Nishimura, Takahiro Wada, and Seiji Sugiyama, "Haptic Shared Control in Steering Operation Based on Cooperative Status Between a Driver and a Driver Assistance System", Journal of Human-Robot Interaction, Vol.4, No.3, (2015), 19-37.

20) Shintaro Inoue, Hideo Inoue, Hiroyuki Aikawa, Raksincharoensak Pongsathorn, Study on Human-Machine Shared Driving System Using DYC and Steering Assistance (Second Report), Transactions of Society of Automotive Engineers of Japan, Vol. 48, No. 1, 20174062, (January, 2017), 111-118.

21) Shintaro Inoue, Yutaka Hirano, Hideo Inoue, Takumi Ozawa, Raksincharoensak Pongsathorn, Study on Human-Machine Shared Driving System Using DYC and Steering Assistance - Effectiveness of Assistance on Elderly Drivers in Course Tracking Maneuver -, Transactions of Society of Automotive Engineers of Japan, Vol. 47, No. 3, 20164339, (May, 2016), 734-737.

22) https://www.tum-create.edu.sg/

〈 Author Biography 〉

Hideo Inoue
Professor, Faculty of Creative Engineering, Chair of Department of Vehicle System Engineering,
Kanagawa Institute of Technology

1978	Graduated from Mechanical Engineering, Faculty of Science and Engineering, Waseda University
1978	Joined Toyota Motor Corporation
1997	Head of BR-Vehicle Control Room
1998	Head of No. 2 Vehicle Engineering Dept. Vehicle Control Development Room
2004	Manager, Integrated System Development Dept.
2008	Head of Advanced Technology Strategy Room (Equivalent to Dept. Head)
2013	Manager, FP Advanced Vehicle Research (Equivalent to Dept. Head)
2016	Professor, Faculty of Creative Engineering, Chair of Department of Vehicle System Engineering, Kanagawa Institute of Technology
2017	Director, Advanced Vehicle Research Institute, Head of Automotive Technology Center, Kanagawa Institute of Technology
2018	Dean of Faculty of Creative Engineering
2011-present	Project Manager, "Autonomous Driving Intelligence System to Enhance Safe and Secured Traffic Society for Elderly Drivers" which is the theme adopted by the "Japan Science and Technology Agency (JST) Strategic Innovation Promotion Program (SIP)"
2013-present	Visiting Professor, Division of Advanced Mechanical Systems Engineering, Institute of Engineering (Graduate School), Tokyo University of Agriculture and Technology
2013-present	Advisory Committee Member, TUMCREATE, a Germany-Singapore International Partnership Project
2018-present	Project Leader, "Development of Autonomous Driving Evaluation Environment Maintenance Method in Virtual Space" which is adopted in the "Strategic Innovation Promotion Program (SIP), Phase 2 Autonomous Driving (System and Service Enhancement)"

[Specialty]

Vehicle motion control, driving assistance/autonomous driving, advanced safety/preventative safety, vehicle integrated control, etc.

[Society Activity]

2017-present	Reviewer of technical papers, Member of Activity Safety Committee, Society of Automotive Engineers of Japan, Inc.
2018-present	Delegate, Society of Automotive Engineers of Japan, Inc. Member, Technical Paper Editorial Committee

[Awards]

1992	FISITA Paper Award, Development of Vehicle Integrated Control System
1998	Japan Society for the Promotion of Machine Industry, 31st Minister of International Trade and Industry Award "Development of a sideslip prevention rolling stock stability control system"
2009	The US Government Award from NHTSA for Special Appreciation for contributions to the development and popularization of safety technology
2016	The Japan Society of Mechanical Engineers, Transportation and Logistics Award for Achievement

NTN's Approach and Effort for CASE

Koji KAMETAKA*

Currently, it is said that automotive industry enters a phase of major change which comes "once in a century".
One of the representative development trends is CASE.
"CASE" consists from initials of Connected (External connection), Autonomous (Autonomous driving), Shared & Services (Car sharing and service or Car sharing only) and Electric (Electrical vehicles).
CASE is advocated by Dr. Dieter Zetsche (ex-CEO of Daimler AG) at Paris Motor Show 2016.
This paper introduces our developing activities with this major trend which we are greatly concerned with.

1. Introduction

Automobiles are a useful means of transportation, but a significant change to electrification is now underway due to recent environmental issues. Autonomous driving is another area of research for a safer and more efficient transportation system. Research of autonomous driving involves both control of a single vehicle and a safe and highly efficient autonomous driving system that incorporates various types of information. Particularly in Japan, with a large aging society, autonomous driving should be effective means in avoiding accidents.

In addition, the car sharing system is also expanding, particularly in urban environments where automobiles are being shared instead of owned.

As such, the automobile industry is in an era of transformation so-called "once in a century", which is driving an alliance among automobile manufacturers in order to reduce the burden of development expenses. As new entrants are making strides into autonomous driving from outside the automobile industry, such as communication companies, it is not clear from the consumers who the decision makers of the automotive industry will be in the future.

The impact of these large trends on product development is significant for **NTN**, and as a result we have been developing electric module products. We have also conducted development of energy saving features on the existing products.

This paper describes our approach for development of new electric module products to support CASE, which is depicted in **Fig. 1**, as well as an overview of new development to our existing products for faster,

more reliable, quieter and more durable operation in addition to our continuous efforts to reduce size/weight and lower friction.
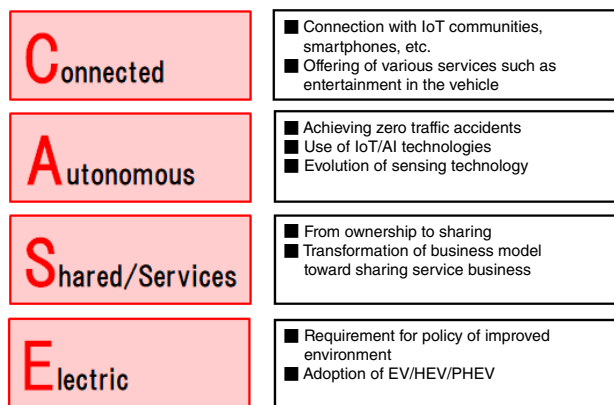
Fig. 1 Overview of CASE for automobile

2. Approach to Support CASE

2.1 Development of the Electric Actuator and Its Applications

NTN has developed the "Electric Motor and Actuator" series, which is essential for by-wire control that is expected to be widely used for vehicle drive and control.

Significant electrification is now underway in the

* Executive Officer, Deputy Corporate General Manager, Automotive Business Headquarters, General Manager, Electric Module Products Division

automotive industry, particularly with by-wire control as the core technology along with the various systems that support drive and control, in response to the requirements needed for autonomous driving and improved fuel efficiency.

To address such market trends, **NTN** developed the "Electric Motor and Actuator" series shown in **Table 1** and **Fig. 2**, combining its core technology of bearings and ball screws with motor design and electronic control technology for controlling vehicles. The product line-up features common components and specifications with a variety of shapes and sizes, which eliminates the need for individual designs and reduces development time.

The developed products can be applied to various on-board applications, but should be applicable for a wider range of fields in the future that is beyond automotive. **NTN** is aiming to establish early volume production and promote global distribution for on-board applications first, and then expand applications to other devices that use actuators.

Table 1 Types of electric actuators

|	Type	Feature
1	Parallel shaft Type B II	• Lightweight with resin housing • Can be equipped with a reverse input rotation prevention unit that can be used for parking brakes, etc. • Add-on reducer unit that can be used for high-thrust applications • Integrated non-contact linear position sensor
2	Coaxial Hollow Shaft Type B III **(Fig. 2)**	• Compact design with coaxial configuration • Optimum size, torque and output by layering the magnet and core • Common magnets and coils that are the core components of motors • Integrated non-contact linear position sensor

Hollow ball screw Motor
Direct output shaft
Motor coil Planetary gear
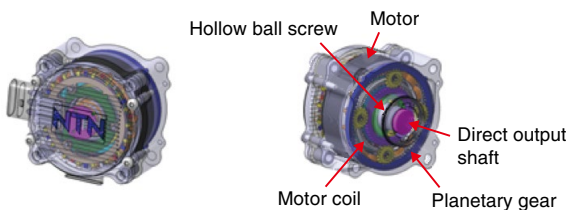
Fig. 2 External view and configuration of Coaxial Hollow Shaft Type B III

2.1.1 Electric Oil Pump for Transmission

An example of this development is the electric oil pump for idling stop function. Idling stop is provided as one of the methods to reduce fuel consumption and requires a lightweight/compact, more efficient

and higher energy savings electric oil pump, which requirement is met by the pump that uses **NTN**'s "Electric Motor and Actuator."

In addition, the ZEV (Zero Emission Vehicle) regulations in the U.S. and China, for example, require EV mode driving of approx. 50 km or more for HEVs and PHEVs, which is only met by electric oil pumps with higher output than those for idling stop.

2.2 Module Product with Added Functionality for Axle Bearings
2.2.1 Hub Bearing with Motor Generator Function "eHUB"

"eHUB **(Fig. 3)**" is a product already developed which combines a motor generator with a hub bearing to support wheel rotation. As improvement of fuel efficiency of vehicles progresses and regulation of CO_2 emission is strengthened, the adoption of the "48V Mild Hybrid System" (hereafter, 48V MHEV), which improves fuel efficiency by adding power at start or acceleration of vehicles, has increased.

The "48V MHEV" is a system that uses the engine as the main power source and provides additional power using a small motor while driving the engine when starting and accelerating. Also, the energy can be recovered as electric power in deceleration (regeneration) resulting in even better fuel efficiency.

When "eHUB"s are used for front-wheel drive vehicles they are also mounted on the rear wheels (non-driven wheels) to provide driving assist power with the motor in order to reduce engine load and also act as power generators to regenerate energy into electric power when decelerating. When "eHUB" is combined with the "48V MHEV" already in use (such as starter generators), an improvement of up to 25% in fuel efficiency is expected compared to conventional vehicles with only engines. It can also be used for EV creep and vehicle stability control on slippery roads (low friction roads).
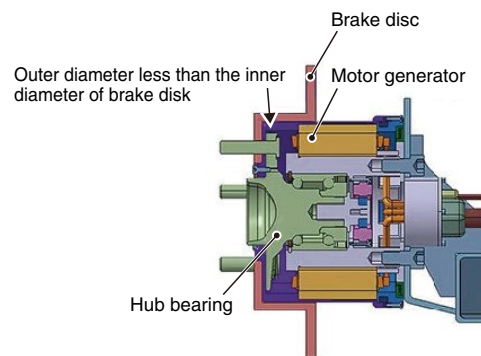

Outer diameter less than the inner diameter of brake disk
Brake disc
Motor generator
Hub bearing

Fig. 3 Cross-section of Hub Bearing with Motor Generator Function

2.2.2 Hub Bearing with Steering Assist Function "sHUB"

NTN has developed a hub bearing with a steering assist function, "sHUB", which integrates the hub bearing and steering angle adjustment mechanism. "sHUB" combines motor and motion control technology with the design and manufacturing technology that has been acquired over many years with the development of the hub bearing, which **NTN** has the No. 1 global share.

With conventional vehicles, the tires and the steering device placed on the front wheels are mechanically connected and therefore the turning angles of both front tires are fixed to the angle of the steering wheel being operated. While driving it was not possible to change to an optimal setting for each driving condition, such as driving straight or cornering.

"sHUB" (shown in **Fig. 4**) is a module product that can correct the steering angle at the left and right wheels separately and be installed onto a vehicle's front wheel steering and the suspension system without replacing the existing steering device. Optimum correction of the turning angles of each tire based on the data on the speed and steering wheel operating angle while driving improves the cornering performance and high-speed stability, as well as vehicle stability in emergency against skidding, for example, and fuel efficiency.

It is expected that "sHUB" will be used as part of a system to provide a safer risk avoidance performance in full-autonomous driving vehicles and it is anticipated that this product will expand in the market in the future.
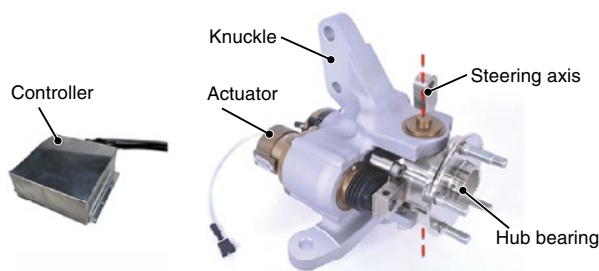

Fig. 4 General structure of Hub Bearing with Steering Assist Function

3. Improvement of the Existing Products for Reduced Size/Weight and Lower Friction

3.1 "Ultra-low Friction Sealed Ball Bearing" for Transmission

NTN developed the "Ultra-low Friction Sealed Ball Bearing" for automotive transmissions that reduces rotating torque by 80% compared to the conventional contact sealed type bearing by adopting a proprietary shape of the ultra-low friction seal.

Lower torque is required for better fuel efficiency in addition to a longer life for transmission bearings used for automobiles. Use of the contact sealed type was standard for longer operating life by preventing hard foreign objects, such as wear debris from the gears in the transmission, to penetrate the bearings. However, this resulted in drag torque due to the seal contacting the inner ring when rotating. Furthermore, in applications where high-speed rotation is required, such as recent EVs and HEVs, use of the contact sealed type was difficult due to the restriction of the peripheral speed limit of the seal.

"Ultra-low Friction Sealed Ball Bearing" has achieved an 80% rotating torque reduction compared to conventional products and provides a low torque effect equivalent to that of the non-contact sealed type. This is achieved by adopting a newly developed contact type seal which arranges arc-shaped (half-cylindrical) micro convexes at evenly spaced intervals on the sliding contact section of the seal lip, as shown in **Fig. 5**. During rotation an oil film is formed between the sliding surfaces of the seal and inner ring due to the wedge film effect of the micro convexes. This significantly reduces the drag torque of the seal, even if it is a contact sealed type. Also, because the seal lip convexes are microscopic, they allow lubricant to pass through but prevent harmful hard foreign matter from entering the bearing, which contributes to longer bearing life.
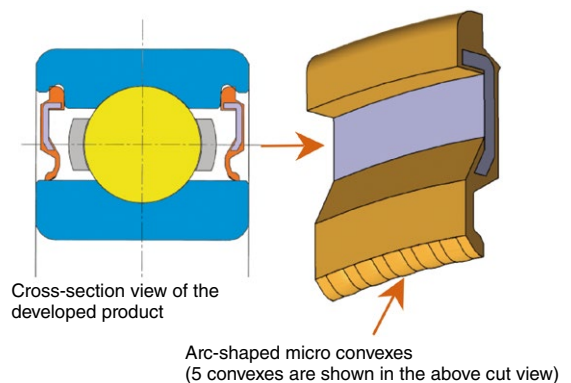

Cross-section view of the developed product

Arc-shaped micro convexes
(5 convexes are shown in the above cut view)

Fig. 5 General structure of "Ultra-low Friction Sealed Ball Bearing" for Transmission

3.2 ULTAGE Tapered Roller Bearings for Automotive Application

"ULTAGE Tapered Roller Bearing for Automotive Application **(Fig. 6)**" is introduced in the following paragraphs, which delivers the world's highest standard load capacity and rotational speed performance by optimizing the internal design of the bearing.

Tapered roller bearings for automobiles are used in components such as transmissions and differentials, and need to have a high-load capacity in order to operate in conditions that are becoming increasingly more harsh, including greater loads due to a higher power output, as well as greater unbalanced loads caused by the lower rigidity due to lightweight housings. The bearings also need to provide the low torque required for lower fuel consumption and high-efficiency and high-speed rotational performance with a low temperature rise.

"ULTAGE Tapered Roller Bearing for Automotive Application" improved on the optimal design technology that maximizes the rolling operating life developed for the Large Size Tapered Roller Bearing and applied it to the compact series lineup. This was done to realize the maximum potential of the bearing operating life even under increased and high unbalanced loads by making the contact stress even between the rolling elements (rollers) and the raceways (inner/outer rings).

This developed product has realized a load capacity 1.3 times higher and a rated life over 2.5 times longer than the conventional product. In addition, the permitted rotational speed increased by approximately 10% to offer the world's highest level in load capacity and rotational speed performance by optimizing the sliding contact zone between the rollers, inner ring and cage.

Fig. 6 ULTAGE Tapered Roller Bearing for Automotive Application

3.3 "Low Friction Hub Bearing III" Reducing Rotational Friction by 62%

"Low Friction Hub Bearing III" reduces rotational friction by 62% compared to the conventional product and is introduced in the following paragraphs.

Hub bearings that support wheel rotation are now being required to further reduce rotational friction in addition to satisfying the basic performance, such as operating life and strength.

NTN has been researching and developing hub bearings for many years in pursuit of lighter weight, longer operating life, and higher efficiency. We have also promoted to unitize bearings and components (GEN1 to GEN3) to improve fuel efficiency and ease of assembling by making them smaller and lighter. We also developed hub bearings with longer operating life and lower friction by improving materials, greases, seals, and other items, for use in the global market. Today, **NTN** has the world's largest market share in hub bearings.

"Low Friction Hub Bearing III" reduces rotational friction by 62% compared to the conventional product and improves the fuel efficiency by approximately 0.53%, by developing a low friction grease as shown in **Fig. 7**. The newly developed product has improved operating life and resistance to fretting wear in low temperature. In addition, by optimizing the preload inside the hub bearing, the developed product reduces the rotational friction of the bearing itself while still maintaining the required performance.
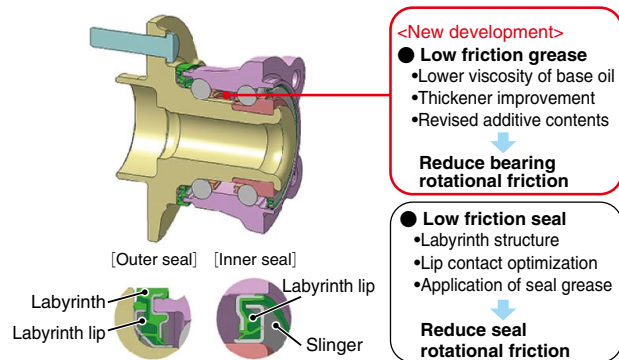

Fig. 7 Low Friction Hub Bearing III

3.4 Compact Plunging Type Constant Velocity Joint for Propeller Shafts "HEDJ-P"

"HEDJ-P" **(Fig. 8)** is a plunging type constant velocity joint for propeller shafts that achieves the world's highest level of compactness and lightweight with 17% weight reduction and 6% decrease in outer ring outer diameter when compared to conventional products.

Propeller shafts are used on vehicles, such as ones with 4WD, and take the role of transferring transmission rotation to the front and rear of the vehicle, as shown in **Fig. 9**. Also, constant velocity joints for propeller shafts have increased in application as there is now an increase emphasis on NVH (Noise, Vibration and Harshness) for luxury passenger vehicles as well as SUVs (Sports Utility Vehicle).

The conventional HEDJ, which this development was based on, provides excellent balanced NVH

characteristics, as well as easy mounting ability on a vehicle since a greater slide amount and operating angle can be used, which improves the flexibility of vehicle layout and is suitable for use on SUVs which use large angles.

NTN has been widely distributing HEDJ's, which have been adopted by a great number of users around the world since the first product roll out. The newly developed "HEDJ-P" is redesigned based on the conventional HEDJ in order to make the outer ring even more compact and the inner ring thinner for dedicated use with propeller shafts. As a result, it achieved 17% weight reduction and 6% reduction in the size of the outer diameter while maintaining the same performance as the HEDJ.

Fig. 8 Compact Plunging Type Constant Velocity Joint for Propeller Shafts HEDJ-P
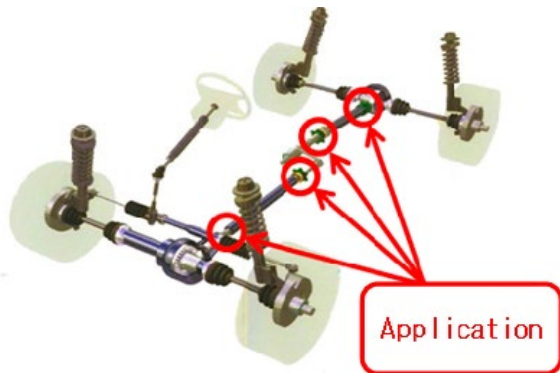

Fig. 9 Application of Compact Plunging Type Constant Velocity Joint for Propeller Shafts HEDJ-P

4. Conclusion

This paper introduced **NTN**'s current development and products regarding one of the main development trends, CASE (Connected, Autonomous, Shared & Services, Electric), which represents a "once in a century" transformation of the automotive industry.

We described our approach for development of new electric module products, as well as an overview of new development items to our existing products for faster, more reliable, quieter and more longer life operation in addition to our continuous efforts to reduce size/weight and lower friction.

Numerous items in development are based on **NTN**'s core competency of tribology technology, high-precision processing technology, high-precision measurement technology and analytical technology such as simulation, as well as our alliance with external agencies in view of increased speed and expansion of fields of application.

We hope to provide a major contribution to the development of the automotive industry and to the community at large through our technologies and products.

Photo of author

Koji KAMETAKA

Executive Officer
Deputy Corporate General
Manager, Automotive Business
Headquarters,
General Manager, Electric
Module Products Division

Hub Bearing Module with Steering Adjust Function

Satoshi UTSUNOMIYA*   Norio ISHIHARA*
Yuusuke OOHATA*   Atsushi ITO*

We have developed a hub bearing module, 'sHUB' with steering adjust function incorporating the steering angle adjustment mechanism in the hub bearing. We demonstrated that the prototype successfully modified the steering angles of the left and right wheel independently according to the driving situation of the vehicle and the operation of the driver. The developed hub bearing module will hence make a significant contribution to the dynamic performance improvement of the vehicle.

1. Introduction

In conventional vehicles the tires and the steering device placed on the front wheels are mechanically connected and therefore the turning angles of both front tires are fixed to the angle of the steering wheel being operated. When making a big turn at slow speed, the turning radii of the right and left wheels are significantly different. Therefore, in order for a smooth turn they should follow the Ackermann geometry (larger angle for the inner wheel with smaller angle for the outer wheel). On the other hand, parallel or reverse Ackermann geometry is suggested to improve the turning performance in mid to high-speed maneuvers.

The Ackermann characteristics are determined by the geometric configuration of the steering device; therefore, volume production vehicles choose to emphasize either maneuverability at low speed or turning ability at high-speed depending on the vehicle concept.

Also, the toe angle of the outer wheel, which supports a heavy load while turning at mid to high-speed, is passively controlled by the damping characteristics of the suspension bushings; however, it is more desirable to actively control the optimum steering geometry based on the turning radius and turning acceleration.

As the top manufacturer of hub bearings, **NTN** has developed a brand new "Hub Bearing with Steering Assist Function" (hereafter, sHUB®)[1] which combines a mechanism that adjusts the steering angle of the tires on the hub bearing, for actively controlling the steering geometry depending on the driving conditions while solving the above mentioned trade-off.

sHUB provides safe and comfortable driving by controlling the left and right wheels independently to the optimum angles depending on the running conditions of the vehicle. This module system improves straight-running and cornering stability and contributes to risk avoidance in emergencies, for example when a wheel skids on a low-μ road surface. In normal driving conditions it contributes to energy saving by minimizing the cornering drag while turning in a curve. It could also be applied to avoidance maneuvering in upcoming autonomous driving vehicles.

Fig. 1 shows an overview of how sHUBs are installed on a vehicle. They can be installed on vehicles together with the existing steering devices without making large modifications to the suspension system. The controller of sHUBs independently calculates and controls the target angles of the sHUBs on the left and right wheels based on the vehicle information, such as the vehicle speed and steering angle.
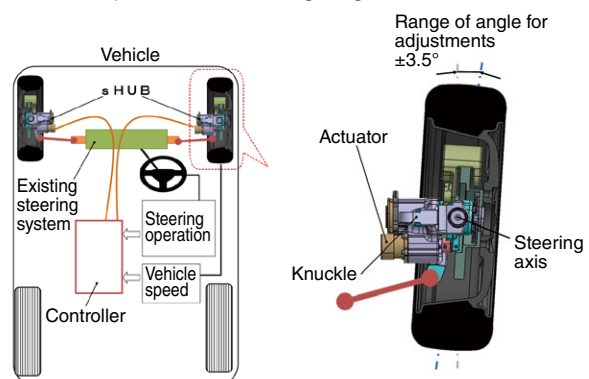

Fig. 1 Vehicle with sHUB installed (on front wheels)

2. Concept

The following parameters were set as the design concept for achieving improved vehicle dynamic performance, as well as safe and comfortable driving.

*New Product Development R&D Center

(1) Installed on the left and right wheels in order to independently control steering angles of both wheels
(2) Optimum control to the best angles depending on the driving conditions
　　・Energy saving driving minimizing cornering drag
　　・Maintain vehicle stability even in an emergency situation, such as risk avoidance
(3) Able to be installed on the driven wheels (front or rear wheels) of existing vehicles regardless of the type of steering/suspension systems without requiring a large modification
(4) Compact and lightweight based on the optimum internal design

Fig. 2 shows the appearance of the prototype (for right wheel) to be used with the strut type suspension for front wheels. As shown in **Fig. 3**, the small size allows installation on both front wheels of a vehicle without modifying the surrounding structure, such as the suspension.
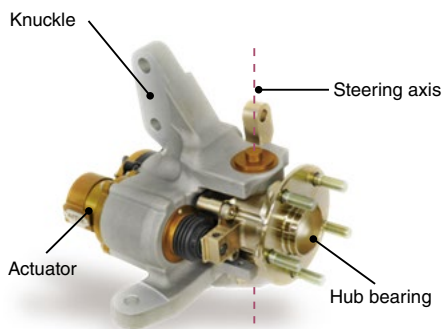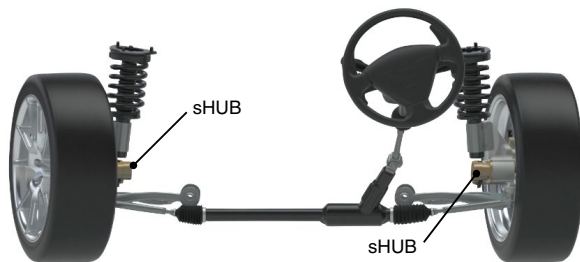

Fig. 2 Prototype of sHUB

Fig. 3 sHUBs installed on front wheels

Fig. 4 shows the basic design of sHUB when it is installed on the front wheel. The kingpin axis which is the central axis of the tire during normal steering and the steering axis of sHUB are two different axes. It was designed so that those two axes cross at the ground surface. With this structure the amount of sliding is reduced by the steering-assist of sHUB, which improves safety.
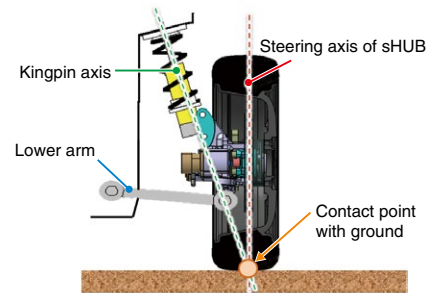

Fig. 4 Basic design of sHUB installed on front wheel

Fig. 5 shows an example of sHUB installed on the rear wheel. Similar to the case of the front wheels, it can be installed with modification only to the knuckle. In this case, the suspension system is a regular rigid axle (torsion beam). The rear wheel steering was easily achieved by merely installing sHUB on the torsion beam where the hub bearing is normally installed.
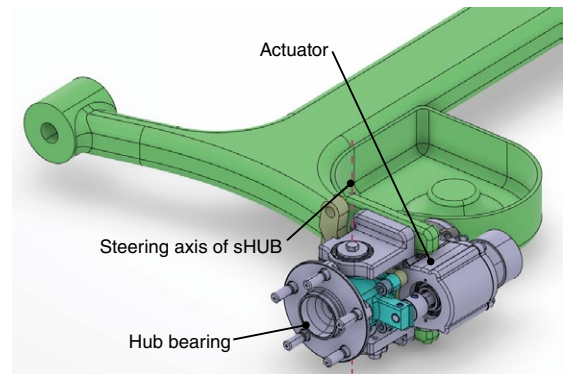
Fig. 5 sHUB installed on rear wheel

3. Configuration and Specification

3.1 Components
Fig. 6 shows the components of sHUB. sHUB is comprised of an actuator, hub bearing and knuckle. The function of the respective components is described as follows:

・Actuator
　Fixed to knuckle and steers hub bearing
・Hub bearing
　Rotary support of tire; rotary support of the steering axis of sHUB against the knuckle
・Knuckle
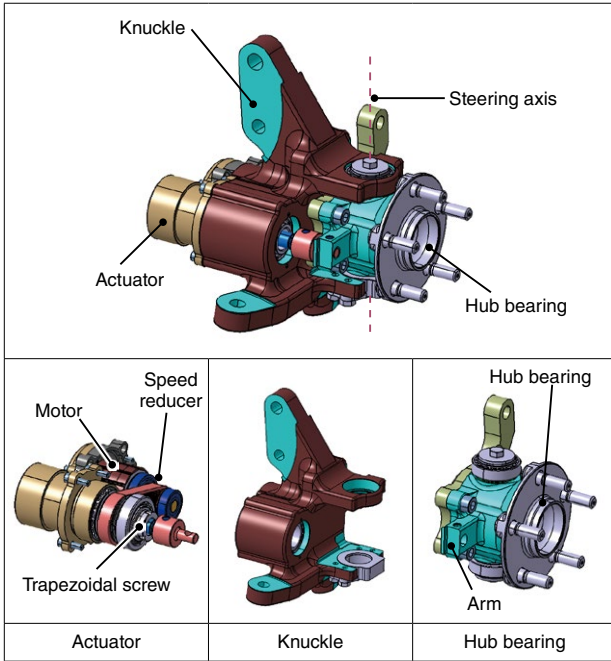　Connection with vehicle suspension

Fig. 6 Components of sHUB

The motor of the actuator is controlled by the controller based on an input, such as the vehicle speed and steering wheel angle in order to achieve the best tire angle. The rotation from the motor, through the reducer, is converted to linear motion by the trapezoidal screw, which drives the end of the arm installed on the hub bearing and steers the tire around the steering axis.

The reverse input from the tire due to the reaction force from the ground is blocked by the self-lock mechanism of the trapezoidal screw. Therefore, power consumption of the motor can be saved.

3.2 Specification

Table 1 shows the specification of the prototype, which was designed for front wheels of a C-segment vehicles with rear wheel drive. The weight of the prototype was 13.8 kg, which only adds 5 kg or less to the standard components (knuckle and hub bearing) of the original vehicle.

Table 1 Specification of prototype

Item	Values
Maximum steering torque	350 Nm
Supply voltage	24 V
Maximum steering angle	±3.5 deg
Maximum steering angular speed	16 deg/s
Weight	13.8 kg

4. Basic Performance Test

A C-segment rear-wheel drive vehicle was chosen as the test vehicle with the sHUBs described in Section 3.2 being installed on the front wheels.

4.1 Frequency Response Characteristics Test

A frequency response characteristics test was conducted in a stationary state by mounting the front wheels of the sHUB installed on the vehicle to a turntable. The actual angles were verified by giving an angle command in the form of a sinusoidal wave (0.5 deg. of amplitude and 1, 2, 4, 6 and 8 Hz of frequencies).

Fig. 7 shows the test results. The dashed curve indicates the command angle and the solid curve indicates the actual angle of sHUB. As the frequency increased, the delay of the actual angle against the command angle increased; however, the maximum frequency in practical use is 5 Hz or less and in this range the delay of the actual angle from the command angle was 0.025 sec or less, which is sufficiently small.
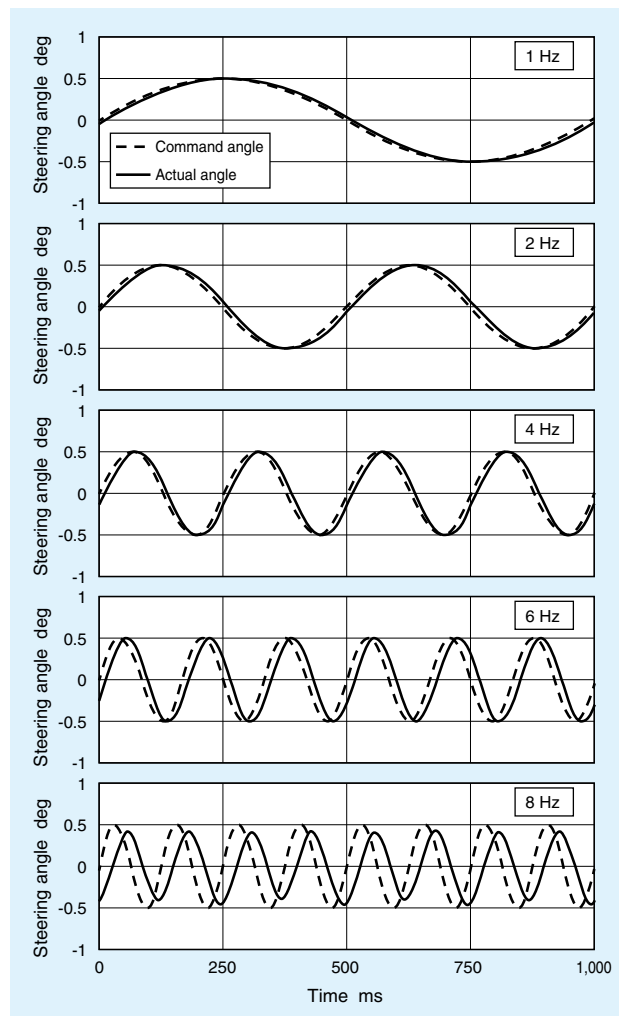

Fig. 7 Frequency response characteristics

4.2 Steering Response Speed Test

The steering response speed was obtained by steering the sHUB while a steering torque is applied to the hub bearing. The command value shown in **Fig. 8** (dashed line) was given to the controller to determine the steering response speed of sHUB. The steering response speed was determined from the slope of the actual measurement (solid line).
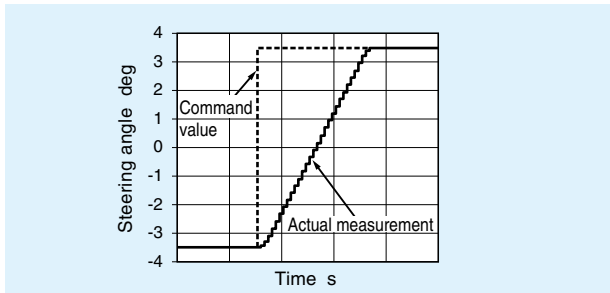

Fig. 8 Command value and measured value of steering angle

Fig. 9 shows the steering response speed of sHUB against the steering torque. As the steering torque increased, the steering response speed decreased. However, it satisfied the target response time of 10 deg/s or more in the entire range of the steering torque.
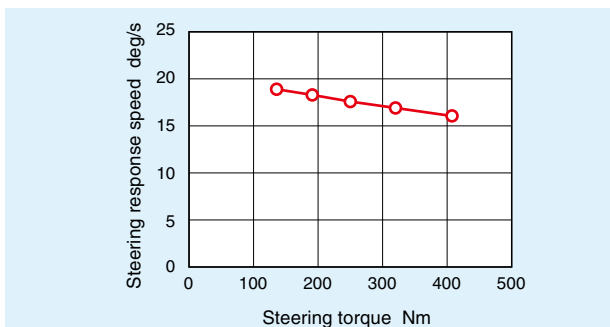

Fig. 9 Relationship between steering torque and steering response speed

4.3 Rigidity Test

The rigidity of the axle of a turning vehicle was verified against a moment load being applied to the tires. **Fig. 10** shows the flange angles of a standard hub bearing and sHUB for the same type of vehicle for comparison of moment rigidity.

As a result of the optimization of internal specification of the hub bearing, which is a component of sHUB, steering axis support bearing and bearing preload, the flange angle of sHUB increased 5% compared with standard hub bearings in the high-load range.
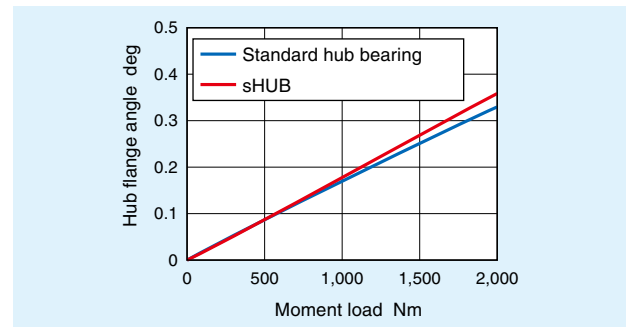

Fig. 10 Flange angle

5. Vehicle Motion Control by the Front Wheel Steering

A joint development with Yamakado/Kano Laboratory of Kanagawa Institute of Technology was conducted for verification of effective control method of sHUB.

"Control to Improve Transient Response" which improves the vehicle response in transient mode and "Control to Improve Turning Characteristics" which optimizes the lateral skidding angle of the tires in a steady turn of a vehicle were developed.

5.1 Control to Improve Transient Response[2), 3)]

This control adjusts time constants of 3 responses, namely, lateral skidding angle, yaw rate and lateral acceleration against the vehicle speed and steering by the correction of steering operation of sHUB for improvement of vehicle dynamic performance.

In order to verify the improvement of the vehicle responsiveness by this control law, a "pulse steering input" test was conducted using a test vehicle with sHUB according to the "Transient Response Test Procedures for Passenger Cars (JASO Z110:2003)."[4)] A test condition of 80 km/h vehicle speed and a triangular wave with pulse width of 0.5 s for drivers steering operation was used.

The results of frequency response of yaw rate and lateral acceleration against the steering wheel angle are shown in **Fig. 11**.

By using this control, it revealed that the vehicle responsiveness against steering operation improved, as the peak value increased and the phase lag improved, both for yaw rate and lateral acceleration in the frequency range (0.5 to 2.0 Hz) of the steering wheel angle, which is equivalent to normal driving.
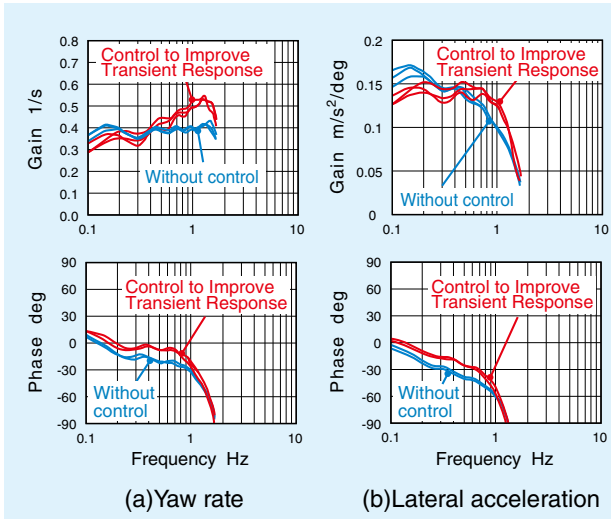
(a)Yaw rate (b)Lateral acceleration

Fig. 11 Test result of frequency response characteristics

Next, the change of vehicle behavior was evaluated with the actual vehicle, with and without this control, by conducting a single lane change at the speed of 80 km/h on an asphalt course shown in **Fig. 12. Fig. 13** shows the change of yaw rate and lateral acceleration in the test. It revealed that this control decreases the required steering wheel operation and improves the response of yaw rate and lateral acceleration.
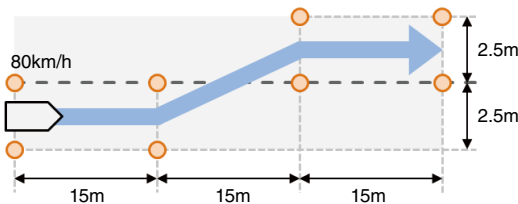

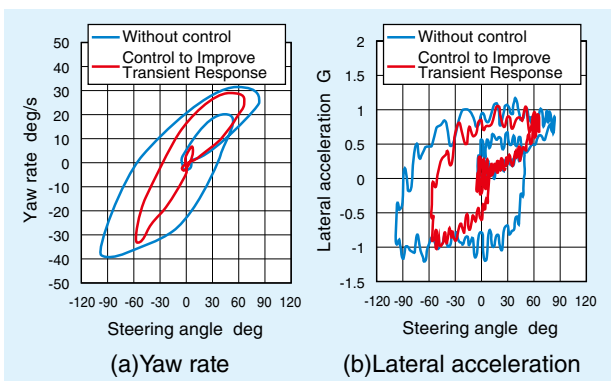**Fig. 12** Actual driving test course (single lane change)

(a)Yaw rate (b)Lateral acceleration

Fig. 13 Test result (yaw rate and lateral acceleration)

5.2 Control to Improve Turning Characteristics (SAHS)[5]

The following shows the control law to efficiently utilize the maximum tire performance in response to the load shift during turns, in the entire speed range from ultra-low speed to mid/high speed when the load shift on the left and right wheels increases. This control law is called SAHS (Super Ackermann Hub Steer).

When a running vehicle makes a turn, load shift between the left and right wheels and lateral skidding occur. When the load on the inner wheel and outer wheel during a turn are represented by W_i and W_o respectively, and the lateral skid angle by β_n, (inner wheel: β_i, outer wheel: β_o), then the relationship between the cornering force and lateral skid angle is similar against the change of the load, which can be depicted as **Fig. 14**.
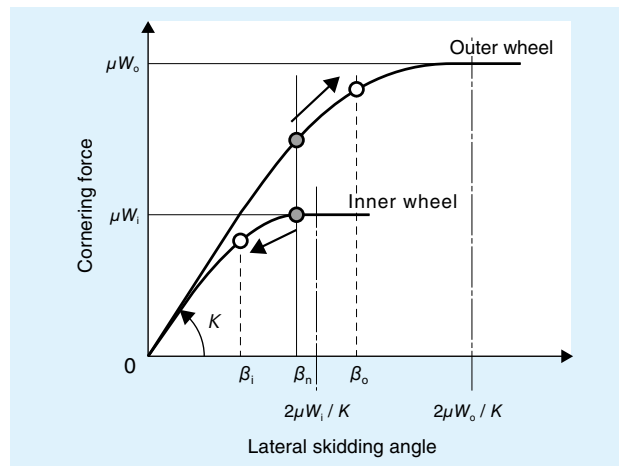
Fig. 14 Relationship between lateral skidding angle and cornering force

In SAHS control, the lateral skidding angle of the inner wheel is decreased and that of the outer wheel is increased by sHUB so that the loads on the right wheel and left wheel become equal($\beta_i/W_i = \beta_o/W_o$)(to the direction of the arrows in **Fig. 14**). With this control, the sum of the cornering forces can be increased without changing the average steering angles of the left and right wheels, utilizing both tires effectively during turns. In other words, at ultra-low speed where lateral acceleration (load shift) can be ignored, the control realizes an ideal Ackermann geometry and at mid/high-speed where lateral acceleration increases, reverse Ackermann geometry is followed.

An evaluation test was conducted for verifying the effect of SAHS using a test vehicle with sHUB. **Fig. 15** shows the layout of the test course. The change of vehicle behavior was evaluated with and without this control by inputting a steering maneuver ramping up to 130 degrees at 0.5 sec intervals starting from point A after straight running at a speed of 50 km/h. The control parameters were determined based on the sensitivity evaluation during driving.

Fig. 15 J-turn test course layout

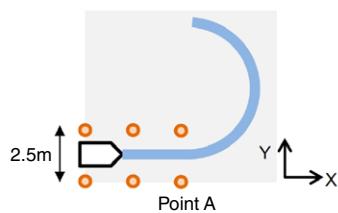**Fig. 16** shows the result of test. Without the control, the ratio of skidding angle against tire load (burden on the tire) is significantly different between the inner and outer wheels. On the other hand, with the control the load is equivalent between the inner and outer wheels. Therefore, the force from both tires is efficiently transmitted on the road surface. As a result, the turning radius decreased as shown in **Fig. 17**.
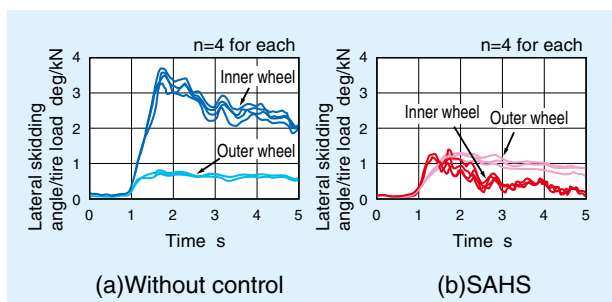

(a)Without control (b)SAHS
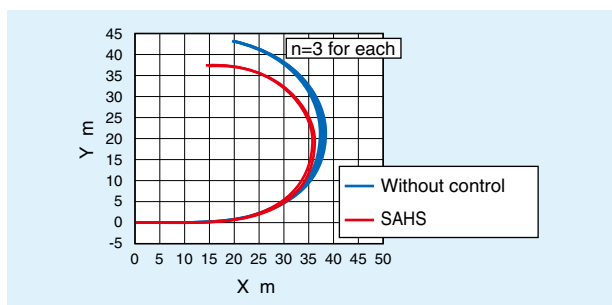
Fig. 16 Test result (load on tires)

Fig. 17 Test result (driving trajectory)

6. Conclusion

Structure, specification and basic performance of the "Hub Bearing with Steering Assist Function (sHUB®)" were introduced.

Also, it was confirmed that two control methods (Control to Improve Transient Response and Control to Improve Turning Characteristics (SAHS)) can significantly improve the vehicle characteristics by applying correction to the steering angles of the left and right wheels against the driver's steering operation for improved vehicle dynamic performance, as shown in the driving test with sHUB installed on an actual C-segment vehicle. In addition, we are currently working on building an integrated control combining these two control methods.

Moving forward, we will study control methods to take advantage of sHUB more effectively for its application on many vehicles including being applied for the driving wheels. We believe in the high potential of sHUB for increasing the driving degrees of freedom in the "steering by wire" system which is expected to be a technology of the future in order to increase responsiveness even more, as it can apply corrective control at the closest position from the contact point between the tire and the ground.

References
1) **NTN**'s home page
   https://www.ntn.co.jp/japan/news/new_products/news201800050.html.
2) Norio Ishihara, Mitsunori Ishibashi, Hirokazu Ooba, Atsushi Ito, Makoto Yamakado, Yoshio Kano, Masato Abe, Hub Bearing with Integrated Active Front Steering Function that Improves Vehicle Dynamic Performance, Proceedings of Society of Automotive Engineers of Japan, (2018) 20185263.
3) Norio Ishihara, Hirokazu Ooba, Atsushi Ito, Mitsunori Ishibashi, Makoto Yamakado, Yoshio Kano, Masato Abe, Hub Bearing with Steering Function that Improves Vehicle Dynamic Performance, NTN TECHNICAL REVIEW, No. 86, (2018) 84-90.
4) JASO Z110:2003 "Automotive Standard: Transient Response Test Procedures for Passenger Cars".
5) Norio Ishihara, Mitsunori Ishibashi, Hirokazu Ooba, Atsushi Ito, Makoto Yamakado, Yoshio Kano, Masato Abe, Hub Bearing with Integrated Active Front Steering Function that Improves Vehicle Dynamic Performance [2nd Report], Proceedings of Society of Automotive Engineers of Japan, (2019) 20191269.

Photo of authors

Satoshi UTSUNOMIYA
New Product Development
R&D Center

Norio ISHIHARA
New Product Development
R&D Center

Yuusuke OOHATA
New Product Development
R&D Center

Atsushi ITO
New Product Development
R&D Center

Hub Bearing Module with Motor and Generator Function

Kentaro NISHIKAWA* **Mitsuo KAWAMURA***
Hiroki YABUTA* **Atsushi ITO***

NTN has developed the hub bearing module combined with a motor generator, 'eHUB'. This module is mounted on an existing vehicle with less modification of the chassis. It will make a contribution to the improvement of the fuel efficiency and vehicle dynamics practically when it is applied to a 48V mild hybrid vehicle. This article focuses on the improvement of the vehicle dynamics.

1. Introduction

As environmental regulations are strengthened globally, each country has established stringent regulations for automobiles toward reduction of CO_2 emissions. Along with this trend, the electrification of automobiles has been accelerating with the active development of hybrid vehicles including plug-in, battery powered electric vehicles and fuel cell vehicles. **Fig. 1** shows the production forecast of passenger vehicles globally. 48V mild hybrid vehicles (hereafter, 48V MHEV) are expected to grow to 25% of all the production vehicles by 2025 since electrical handling is easy and the implementation costs are low. It is known however, that the rate of improvement of fuel efficiency is about 15% maximum even if the effect to fuel cost against implementation costs are large. The implementation rate of these vehicles in terms of low fuel consumption such as electric vehicles and plug-in hybrid vehicles is expected to be slow due to the promulgation of infrastructure, battery supply and cost issues. ; Improvement of fuel efficiency of 48V MHEVs, which are expected to grow faster, is required to address the strengthening regulatory requirements on fuel efficiency in the near term.
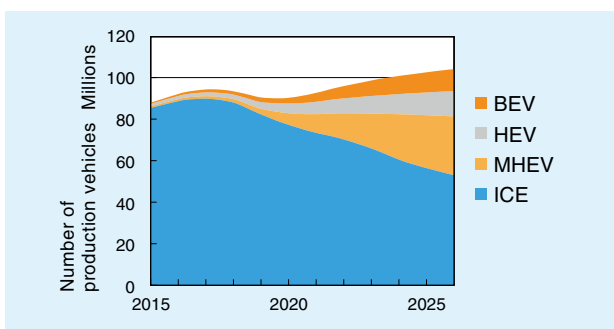
Therefore, **NTN** has developed a Hub Bearing with Motor Generator Function (hereafter, eHUB), to be installed on the rear wheels (driven wheels) of front wheel-driven 48V MHEVs[1]. The following shows the development concept of eHUB.

(1) Improved fuel efficiency of 48V MHEV vehicles
(2) Improved vehicle dynamic performance
(3) Installable on existing suspension systems

In the previous article, we reported that the eHUB improved fuel efficiency by 3.2% in WLTC mode when installed on the rear wheels of a front wheel-driven internal combustion engine vehicle (ICE vehicle)[1]. Additionally, eHUB can drive the left and right wheels independently with good responsiveness as it transmits torque directly to the wheel, and controls regenerative torque. These characteristics contribute to driving stability and ride comfort. In this article, improvement of vehicle dynamic performance based on the independent control of eHUBs on the left and right wheels is discussed, focusing on concept (2) above.

2. Basic Configuration

2.1 Structure and Specification

We set the following goal for the size of the outer diameter so that it can be installed on an existing suspension system.

・Outer diameter less than the inner diameter of brake disk
・Same axial length as a conventional hub bearing

A three-phase brushless DC motor was adopted to obtain as much output as possible in a limited amount of space. **Table 1** shows the specification of the eHUB used for evaluations. The prototype eHUB was larger than the target size (width) requiring modification to the test vehicle. **NTN** is currently working on size modifications to the design achieving the same output and results.

Fig. 1 Production forecast of global passenger vehicles
(Our own analysis and forecast based on IHS Markit)

*New Product Development R&D Center

Table 1 Specification of eHUB

Item	Target value	Prototype
Appearance		
Outer diameter mm	ϕ 160	ϕ 159
Width mm (Hub bolts not included)	80	126
Weight kg	10	14
Driving voltage V	48	48
Maximum output kW	5.0	4.5
Maximum torque Nm	60.0	59.2
Maximum rotational speed min^{-1} (Equivalent vehicle speed km/h)	1,700 (200)	1,200 (130)

Fig. 2 Power train configuration of the test vehicle

Table 2 Test vehicle specification

Item	Specification	Remark
Driving method	Front wheel-driven	
Main drive power	ICE	
Transmission type	MT	
Number of passengers	2	Rear seats were removed
Tire size	195/45/R17	
Vehicle weight kg	1,207	No load
ABS system	OFF	
Electronic stability control system	OFF	
eHUB	Prototype	Refer to Table 1
eHUB installation	Rear wheels (left and right)	Torsion beam is modified

2.2 Test Vehicle

Improvement of vehicle dynamic performance was reviewed by installing the eHUB on the front wheel-driven application of a B segment vehicle. The vehicle used for measuring fuel efficiency in the previous report was used for this test. The power train configuration is shown in **Fig. 2** and the vehicle specification is shown in **Table 2**. A commercially available internal combustion engine vehicle (ICE vehicle) was modified to install the eHUB on the rear wheels. As shown in **Fig. 3**, the torsion beam was modified to install the eHUB and existing hydraulic brakes. The controller unit and battery were installed in the rear seating area and cargo space **(Fig. 4)**. The eHUB was built as a control system independent from the existing vehicle system, that obtains information such as steering angle, acceleration and speed from the vehicle. Commercially available products were used for the 48V battery and controller unit, building an environment where the control model created for simulation can be directly evaluated with the actual vehicle.
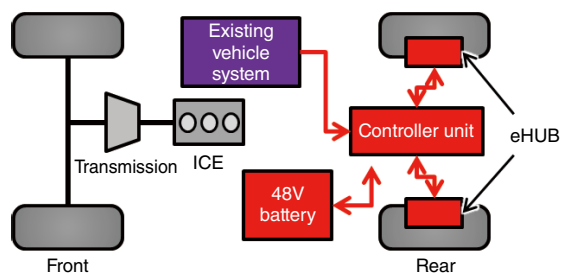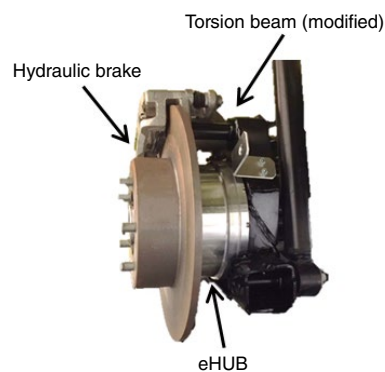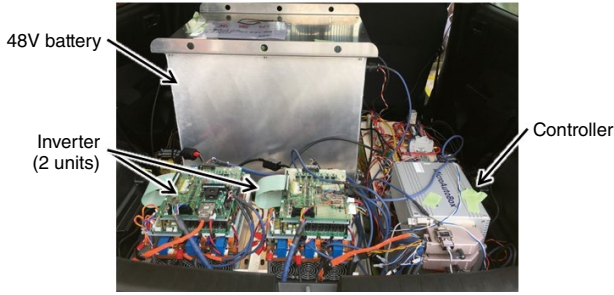

Fig. 3 eHUB installed

Fig. 4 Controller unit and battery

3. Direct Yaw Moment Control (DYC)

We worked on vehicle dynamic control taking advantage of the benefits of eHUB, which can drive the left and right wheels independently and regenerate energy. Vehicle dynamic performance can be improved by appropriately operating eHUB depending on the vehicle information such as the speed, steering angles and changing the vehicle behavior.

The approach to actively producing different driving inputs to the left and right wheels to directly control the vehicle yaw moment is called Direct Yaw Moment Control (hereafter, DYC)[2), 3)]. DYC is expected to improve the responsiveness of yaw rate against steering and vehicle maneuverability on slippery road surfaces such as roads with compacted snow or ice.

An approach to produce yaw moment from the difference of driving inputs to the left and right wheels to compensate for the difference between the target yaw rate and vehicle yaw rate is known as the DYC yaw rate response. The target yaw rate r_t is expressed by Equation (1) in conventional DYC.

$$r_t(s) = G_\delta^r(0) \frac{1 + T_r s}{1 + \frac{2\beta\zeta}{\alpha\omega}s + \frac{1}{(\alpha\omega)^2}s^2} \delta(s) \tag{1}$$

Where,

r_t : target yaw rate [rad/s]
δ : steering angle [rad]
ω : natural frequency of yaw rate response
ζ : damping ratio of yaw rate response
T_r : time constant of yaw rate response [s]
$G_\delta^r(0)$: steady gain of yaw rate response
α : control parameter of natural frequency
β : control parameter of damping ratio

Equation (1) shows that the natural frequency and damping ratio of the yaw rate response to steering can be changed by arbitrarily setting the control parameters α and β. The yaw moment M_Z necessary to achieve this yaw rate is expressed by Equation (2).

$$M_Z(s) = \frac{G_\delta^r(0)}{G_m^r(0)} \frac{1 + T_r s}{1 + T_m s} \left(\frac{1 + 2\frac{\zeta}{\omega}s + \frac{1}{\omega^2}s^2}{1 + 2\frac{\beta\zeta}{\alpha\omega}s + \frac{1}{(\alpha\omega)^2}s^2} - 1 \right) \delta(s) \tag{2}$$

Where,

T_m : time constant of yaw moment response [s]
$G_m^r(0)$: steady gain of yaw moment response
M_Z : required yaw moment [Nm]

Equation (2) shows that the yaw moment is determined depending on the steering angular velocity and angular acceleration in the conventional DYC. By adjusting α and β to maximize the effect of DYC, the yaw moment becomes large due to the term that depends on the steering angular velocity, resulting in the required maximum torque of several hundreds of Nm per wheel, on both wheels. Therefore, the conventional DYC cannot be applied to eHUB, which has the maximum torque of a magnitude of tens Nm.

Therefore, we focused on the stability of maneuverability on slippery roads and adjusted the control parameters for improving the yaw rate response at the beginning of steering operation. If we set $\beta = \alpha$ in Equation (1), the target yaw rate can be expressed by Equation (3) and the required yaw moment by Equation (4), respectively, improving the torque response against the steering angular acceleration. This enables improved response to the initial steering operation even with relatively low torque.

$$r_t(s) = G_\delta^r(0) \frac{1 + T_r s}{1 + \frac{2\zeta}{\omega}s + \frac{1}{(\alpha\omega)^2}s^2} \delta(s) \tag{3}$$

$$M_Z(s) = \frac{G_\delta^r(0)}{G_m^r(0)} \frac{1 + T_r s}{1 + T_m s} \left(\frac{1 + 2\frac{\zeta}{\omega}s + \frac{1}{\omega^2}s^2}{1 + 2\frac{\zeta}{\omega}s + \frac{1}{(\alpha\omega)^2}s^2} - 1 \right) \delta(s) \tag{4}$$

The yaw motion of the initial steering operation is enhanced when $\alpha > 1$, and suppressed when $\alpha < 1$. Torque of the eHUB to achieve the yaw moment of Equation (4) is Equation (5).

$$T_L = -\frac{R}{D}M_Z, \quad T_R = +\frac{R}{D}M_Z \tag{5}$$

Where,

D : rear wheel tread [m]
R : dynamic effective radius of tire [m]
T_L, T_R : torque of eHUB (left and right) [Nm]

Fig. 5 shows the result of the simulation for the required torque against the steering angles. In the ordinary DYC, the torque is determined according to the change of steering angular velocity and steering

angular acceleration. In contrast, in the DYC for the eHUB, since the torque responds to the change of steering angular acceleration, the increase in torque is faster compared with ordinary DYC. A driving test of a single lane change on a low μ road was conducted using this method for setting parameters. As shown in **Fig. 6**, the vehicle's speed is adjusted to 30 km/h in the speed adjustment zone and the acceleration pedal is released at a predetermined point to coast for a lane change. **Fig. 7** shows the driving trajectory of the vehicle. The figure shows an average of 3 runs under the same conditions. Without control and with DYC (α = 0.8), the vehicle turned wide when steering back (at around 20 - 30 m in the figure), but the vehicle with DYC (α = 1.2) turned smoothly and remained stable. **Fig. 8** shows the change of yaw rate against the steering angle. Applying DYC (α = 1.2) improved traceability of yaw rate to steering angle and the amount of steering significantly reduced compared to the vehicle without control. That means that the vehicle behavior responds well to the steering operation and the vehicle turns more easily. On the other hand, in the case of DYC (α =0.8), the amount of steering is almost the same as the case without control but the area inside the curve is larger. That means that the yaw rate response is delayed against the steering operation, the vehicle behavior does not respond well and the vehicle turns less easily. As such, we could verify that even a small amount of torque, such as the eHUB, can change the vehicle behavior by driving/regenerating the left and right wheels separately.
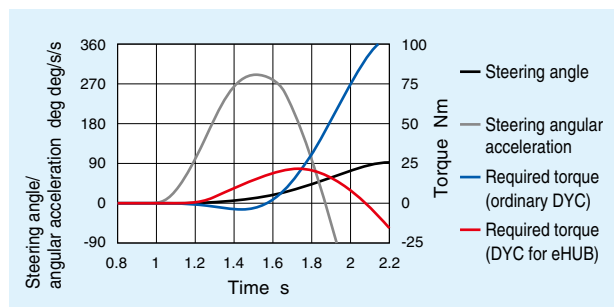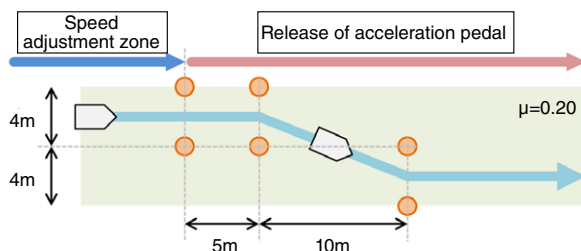

Fig. 5 Torque of eHUB against steering

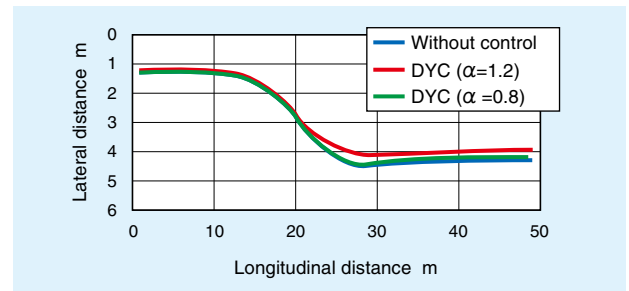**Fig. 6** Driving condition
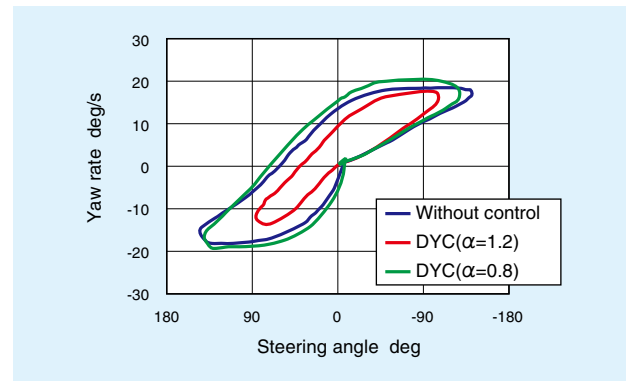

Fig. 7 Vehicle driving trajectory

Fig. 8 Change of yaw rate against steering angle

4. Longitudinal Acceleration Control According To Lateral Acceleration

DYC in the previous Chapter is effective when the friction coefficient between the tire and the road surface is low. However, these driving conditions are limited so another method for controlling vehicles more cohesively with longitudinal and lateral acceleration is being proposed by adding longitudinal acceleration according to lateral acceleration[4].

Fig. 9 shows a graphical representation of longitudinal and lateral acceleration during turns of everyday drivers and expert drivers in regular driving conditions. Ordinary drivers tend to decelerate before a turn and only maneuver the steering wheel while turning. Therefore, the lateral acceleration abruptly changes after deceleration as shown in (a) in the figure. The passengers feel significant change of inertial force that may cause carsickness or discomfort. On the other hand, expert drivers adjust acceleration/deceleration along with steering operation, which makes the combined acceleration of longitudinal and lateral acceleration transition along with a smooth curve. Therefore, the passengers feel a smoother change of inertial force and a improved comfort level[5].

The driving technique of expert drivers can be achieved by adding longitudinal acceleration to lateral acceleration, which can be expressed in Equation (6). The left and right torque from the eHUBs are the same to realize this and can be expressed in Equation (7).
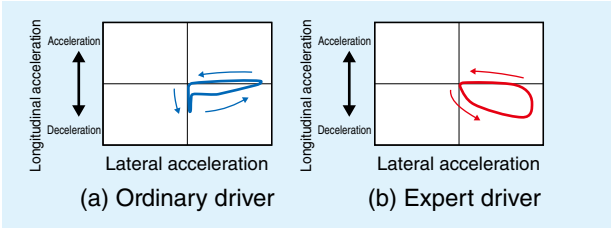
Fig. 9 Lateral/longitudinal acceleration during a turn (graphical representation)

$$G_x = -\mathrm{sgn}(G_y \cdot \dot{G}_y)\frac{\alpha_x}{1 + T_x s}|\dot{G}_y| \qquad (6)$$

$$T_L = T_R = \frac{1}{2}RmG_x \qquad (7)$$

Where,

G_y : vehicle lateral acceleration [m/s^2]

$\dot{G}_y$: vehicle lateral jerk (time derivative of G_y) [m/s^3]

G_x : vehicle target longitudinal acceleration [m/s^2]

T_x : first-order lag time constant [s]

m : vehicle weight [kg]

α_x : control parameter of longitudinal acceleration

Fig. 10 shows the graphic representing longitudinal acceleration control. The longitudinal acceleration is controlled with the torque produced by eHUB according to lateral acceleration. Deceleration is added when the vehicle enters into a curve so that the load moves from the rear wheels to the front wheels and the yaw moment to assist turning is created. On the other hand, acceleration is added when the vehicle exits from the curve so that the load moves from the front wheels to the rear wheels and the yaw moment to restore the vehicle stability is created.

Fig. 11 shows the result of the driving test with an actual vehicle similar to that in Chapter 3 to verify the effect of the longitudinal acceleration control through drive/regenerating brake control of the eHUB. Two control conditions were used: without control and longitudinal acceleration control. The results show an average of 3 runs, similar to the test with DYC. The longitudinal/lateral acceleration transitioned in a smooth curve when longitudinal acceleration control was applied.

These results suggest high potential for improvement of vehicle dynamic performance if appropriate vehicle operation is implemented, even with a motor/generator of small output such as eHUB. In the next stage, we will build an integrated control combining DYC, longitudinal acceleration control and optimum logic for fuel efficiency, etc.
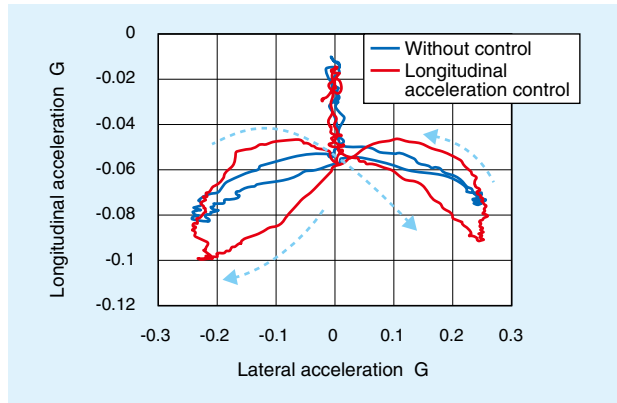
Fig. 11 Result of longitudinal acceleration control driving

Fig. 10 Concept of longitudinal acceleration control

5. Conclusion

In this paper, the effect of vehicle dynamic control was verified with the eHUB, which improves fuel efficiency and driving performance of 48V MHEVs without significant modification to the vehicles, and the following result was obtained.

(1) Direct Yaw Moment Control
It was verified that DYC with higher sensitivity to the steering angular acceleration was effective for the stability of driving trajectory and the reduction of the amount of steering in a single lane change on a low μ road.

(2) Longitudinal Acceleration Control Coupled with Lateral Acceleration
It was verified that application of longitudinal acceleration, which is said to contribute to the improvement of ride comfort, was effective for the smoother change of lateral/longitudinal combined acceleration and the improvement of ride comfort in steering.

In the next phase, we will work on improvement of the eHUB for higher output and higher efficiency to enhance the effect of reduced fuel consumption, as well as the improvement of vehicle dynamic performance for practical applications.

References

1) Kentaro Nishikawa, Yuuji Yada, Yasuyuki Fujita, Mitsuo Kawamura, Hiroki Yabuta, Hub Module with Motor and Generator Function, NTN TECHNICAL REVIEW, No. 85, (2017) 26-32.

2) Masato Abe, Automotive Vehicle Dynamics (2nd Edition), Tokyo Denki University Press (2012) 236-247.

3) Ryou Yukishima, Yusuke Makino, Hidenori Karasawa, Takeshi Kanda, Aiko Myouki, Tomohiro Sugai, Katsunori Satou, Two Motor On-board Drive System, NTN TECHNICAL REVIEW, No. 83, (2015) 20-25.

4) Yuta Suzuki, Weipeng Cheng, Shuichi Kosaka, Influence of Vehicle Body Motion on the Effects of G-Vectoring Control, NTN TECHNICAL REVIEW, No. 85, (2017) 33-39.

5) Makoto Yamakado, Junya Takahashi, Shinjiro Saito, Masato Abe, New Vehicle Dynamics Control Concept "G-Vectoring" for Enhancement of Safe Driving, Hitachi Review, (2009) 46-49.

Photo of authors

Kentaro NISHIKAWA
New Product Development
R&D Center

Mitsuo KAWAMURA
New Product Development
R&D Center

Hiroki YABUTA
New Product Development
R&D Center

Atsushi ITO
New Product Development
R&D Center

Development of Control Platform for Electric Module

Tatsuji INOUE*　　Kazuhiro AOSHIMA*
Yuichi SUGIMOTO*　Keigo MOTOKUBO*

　　In the automotive industry, the development of CASE (Connected, Autonomous, Shared & services, Electric) has proceeded. Many devices (such as cameras, sensors, actuators, motors, etc.) are used for autonomous driving and electrification. And the software for controlling those devices increase year by year. The functional safety standard ISO 26262 has been established and development to ensure safety is proceeding. However the development which is based on ISO 26262 requires larger number of people, costs, and much more skills than conventional development which is based on IATF 16949. **NTN** is developing electric motors, actuators, and controllers that contribute to electrification and By-wire-system. In this article, we introduce the development of control platform for **NTN** electric motors and actuators.

1. Introduction

　Various companies are developing initiatives for Connected, Autonomous, Shared & Services, and Electric (CASE) with the aim of reducing traffic accidents, providing safe and secure freedom of transportation, usefulness to users and environmental measures. **NTN**, in view of these trends, has developed a universal series of electric modules containing various motors and actuators so that we can contribute to the "Autonomous" and "Electric" aspect of CASE. **NTN** achieves this through the use of our core expertise and technologies which includes bearings and ball screws, as well as our research into the design technology of motors and control technology of vehicles. The following are descriptions related to some of the electric modules we have developed as well as their proposed uses.

1) Overview of Electric Module Series
(1) B II Series **(Fig. 1)**
　・Electric actuator using paired gears to reduce the speed and convert rotation motion to linear motion through the use of a ball screw
　・Through the use of optional components such as a planetary reducer or a reverse lock out, the driving power can be increased as well as the ability to maintain actuator position

(2) B III Series **(Fig. 2)**
　・A compact electric actuator that combines a high output brushless DC motor, a ball screw and a linear motion mechanism within a hollow structure.

・For use in applications where it will be directly installed on components

Fig. 1　Outlook of B II Series (B II 00)

Fig. 2　Outlook of B III Series (B III N)

---

(3) SP Series **(Fig. 3)**
・ Brushless DC motor series
・ For use in applications that require a thin and high torque rotational actuator. This is based on the hollow motor structure of the BIII series but with a reducer in the hollow part.

Fig. 3 Outlook of SP Series

2) Examples of proposed uses of Electric Module Series
(1) Transmissions as an electronic shift selector (B II Series)
    The shift lever of both AT and CVT are usually connected to the transmission with a mechanical wire, etc. for selecting the shift position. Using the B II Series module it would be possible to electrify the shifting of the transmission.
(2) Electric hydraulic brake (B III Series)
    Applying the coaxial type B III Series with built-in ball screw to the master cylinder shaft contributes to reducing the overall size of an electric hydraulic brake system
(3) Electric variable valve timing control (SP Series)
    Space efficient electric variable valve timing mechanism can be created by incorporating the SP Series into cam shafts
(4) Electric oil pump (SP Series)
    Integrating a thin and highly efficient SP motor and controller contributes to reducing the size of an electric oil pump

　　With the development of the different Electric Module Series, the software needed to support each Electric Module and application also needed to be developed, which increased man-hours for development and maintenance.
　　Failure rate was also increased due to the complexity of the electronic system, in addition to increased risk of new failure modes due to the application of new technologies. Out of these backgrounds, the Automotive Standard for Functional Safety, ISO 26262 was issued. It became imperative to build a new process for efficient software development not only to cope with the requirements of ISO 26262 but also to address the need of software support for each application of electric module series.

2. Background of Control Platform Development

　　The electric module series was developed as a product line-up for applications such as chassis, engine and transmission, and are selected to meet the application specification. Various software versions have been developed for different applications by using the existing asset, which created the following issues:

・ Complexity due to many changes, enhancements, and reproduction of code
・ Side effect of software changes causing degradation and failure of existing functions

　　To address the issues of the conventional development approach of using the existing asset and to cope with ISO 26262, we decided to analyze the current situation and introduce two development methods.

1) Development of software product line
　　The characteristics of the Electric Module series of products were defined by the external variability (characteristics/values of the system viewed from outside) and the internal variability (elements to compose a system). Using a variety of systems and software it was possible analyze the dependencies and differences between the Electric Module product series. As a result, the software product line was introduced, which is effective at reducing the number of man-hours by creating a core asset of software, and for improving quality by repetitive use of the core asset. This is further described in Section 3.2 in details.

2) Model Based Development
　　In general, it is said that validation by simulation during the requirement definition and basic design phases reduces the man-hours of test phase and rework **(Fig. 4)**.
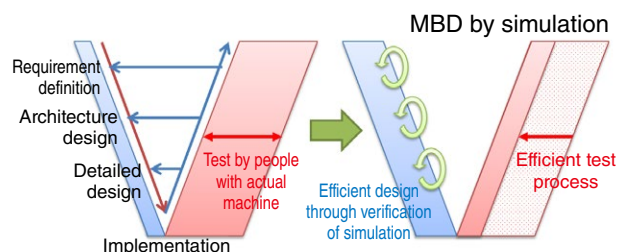

Fig. 4 Shift of development to design process

Conventionally, simulation of responsiveness, etc. was conducted by spreadsheet software, which had its own limitations. In order to increase the simulation accuracy and to understand the basic characteristics of a motor at the design phase, JMAG[*1] is used for motor design.

It is also required to conduct simulation of the system including controller (motor control part) and plant (JMAG-RT[*2] model created from JMAG).

As ISO 26262 also suggests validation using simulation, fault injection test[*3], which intentionally creates faults in the model, can be easily conducted in shorter time and at less cost than using actual machines. Validation by simulation can also be conducted at the requirement definition phase. We decided to use the Model Based Development to address the above.

We are currently conducting the development of the Control Platform using these two development methods, which is described in the following Chapter.

*1: JMAG: Simulation software made by JSOL for development of electric equipment design
*2: JMAG-RT: A high-speed and high-accuracy plant model for system-level simulation derived from the FEA model
*3: Fault injection test: Validation to review if the system turns into a safe condition as designed, by intentionally injecting faults

3. Control Platform Development

3.1 Overview of Process

The entire process was built with compliance to the functional safety standard ISO 26262, which is subject to quality management, and is based on the internal process that conforms with IATF 16949, adding Automotive SPICE (system development process model for on-board systems) which is highly compatible with ISO 26262 **(Fig. 5)**. The following shows the features.

· Since Automotive SPICE only defines the framework, requirements on methods and safety specified by ISO 26262 are incorporated into the process to make it compliant to the standard.
· Process definition (where work flow is specified) is made available to software developers at any time, using EPF Composer (a tool that defines the development process and converts it to HTML) via the Intranet **(Fig. 6)**.
· The software process is separately defined for core asset development and new product development aligned with the Product Line newly introduced for efficient development of software (Section 3.2).
· The following was introduced mainly for validation of motor control in the Model Based Development (Section 3.3):
  In the system requirement phase: MILS[*4]
  In the software design phase: MILS, RCP[*5]

*4: MILS: Model In the Loop Simulation; Simulation that operates the control specification written in the model, combining with the plant model
*5: RCP: Raid Control Prototype; Validation of the actual machine subject to control, which incorporates the control specification written in the model into the general purpose controller
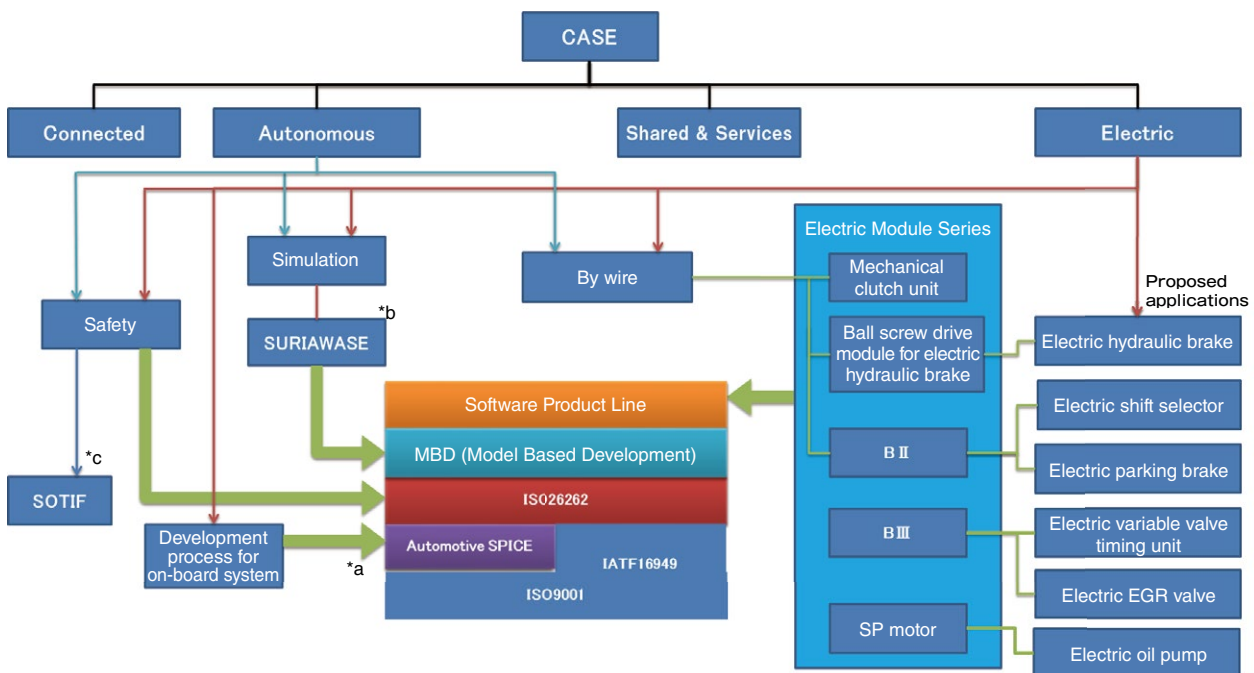
*a Automotive SPICE: process improvement model for on-board system development
*b SURIAWASE: Strategy that Ministry of Economy, Trade and Industry (METI) compiled to enhance harmonization by taking advantage of a model-based development (MBD) process that uses virtual simulations instead of physical machines.
*c SOTIF: safety of the intended functionality

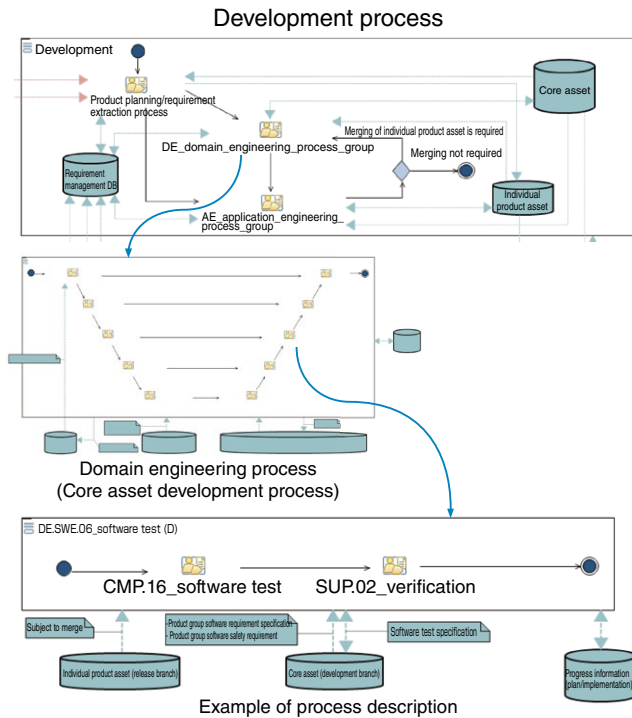**Fig. 5** Foundation of the development process

Development process

Domain engineering process
(Core asset development process)

Example of process description

Fig. 6 Process definition created by EPF

3.2 Software Product Line

The Software Product Line is a method to analyze the products to be developed and to categorize certain portions into the common part and product specific part. Using this method, the common part is defined as assets to be reused and the product specific part is developed efficiently. It is effective in reducing the development period and man-hours while improving quality. In applying the Software Product Line, the scope (range of specifications that covers a product group) was defined as the existing motor series. The deliverables were defined as the software requirements, architecture, detailed design specification, Simulink®*6 model, hand implementation code and test specification. The flow of the Software Product Line is explained in the following, along with **Fig. 7**.

*6: Simulink®: Block diagram environment for Model-Based Design developed by MathWorks

1) Development of core asset

(1) The common part and variable part of the product group **(Fig. 8)** are created by the feature model that defines the variability of functions and features which are used to generate the base of the configuration model (model to select the product properties)

(2) Reusable assets are incorporating into the deliverables (requirement specification, architecture, Simulink® model, codes) which helps develop the feature model of the common and variable parts of the product group

2) New product development

(3) The requirement specifications of the new product are classified into "common part/variable part" and "product specific part"

(4) The common/variable parts of the requirement specification of new products are selected from the configuration model

(5) The configuration model created in (4) and based on the reusable assets created in the core asset development (2) is loaded into the Binding Tool. This is then used for binding and deliverables based on the required specification of the new product

(6) The deliverables for the product specific part are newly created

(7) The deliverables to conform to the new product requirements are created by combining the deliverables extracted from the core asset (5) and the deliverables newly created for the product specific parts (6)
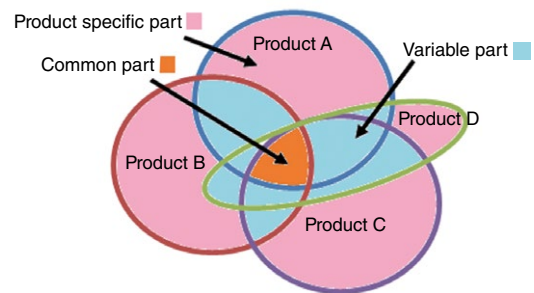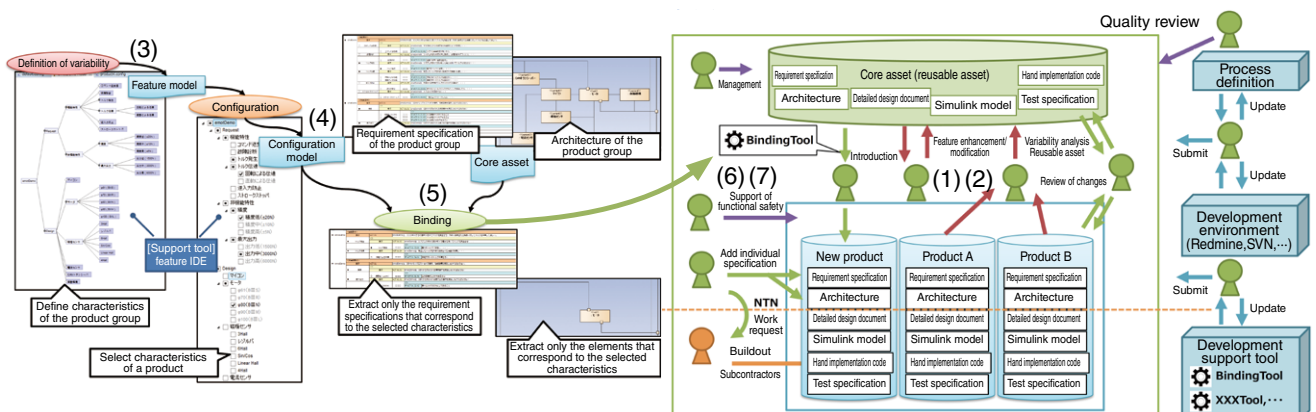

Fig. 8 Common part and variable part

Fig. 7 Total view of Software Product Line

Tools could be created in-house in a short time, by using FeatureIDE an open source product for creating the feature model and configuration model and developing the Binding Tool.

We used a sample core asset for binding (5) and verified that the required deliverables were extracted. With this, we completed creating the mechanism of the process.

Currently, we are converting the requirement specifications and architectures of the existing products into parts to be reused. In this process, since the difference (variability) needs to be considered for design and implementation, some of them need to be modified before turning them into parts.

In the Product Line, since specifying and managing the variability that exist in the product group are important, we plan to thoroughly analyze the differences (variability) of the software platform for functional safety under development to make the design easily reusable.

3.3 Model Based Development

In order to verify the system to conduct simulation of the controller model, where the motor control algorithm and the controlled objects are incorporated into the plant model, the Model Based Development was applied.

In the process definition, the process was identified with system requirement review phase, software architecture design phase and simulation (MILS, RCP) in the detailed design phase **(Fig. 9)**.

3.3.1 Result of Simulation and Future Plan

As the target of simulation, in MILS, JMAG and RCP, the relative error of N-T and I-T characteristics, which are regarded as the basic characteristics of the motor, were set to ±10%.

Firstly, the motor control (vector control) algorithm was modeled reverse engineered from the existing C source code, to create the controller model by Simulink®. The vector control algorithm that was modeled was bound to the motor model (JMAG-RT) in order to conduct MILS with the general purpose controller. This control was connected to the inverter and motor to be evaluated and RCP was conducted. The comparison of N-T and I-T characteristics from MILS and RCP **(Fig. 10)** revealed that the I-T characteristics almost matched and the N-T characteristics were within ±10% when no load was applied but as the current increased, the N-T characteristics exceeded ±10%. Since the motor phase voltage dropped by 1.73V against the power source voltage of 12V, the voltage drop may have occurred due to the internal resistance or wiring resistance in the inverter used in RCP **(Fig. 11)**. We plan to investigate the cause of this error by comparing the theoretical calculation and the actual measurement of the voltage drop due to internal resistance, etc. and improve the model.
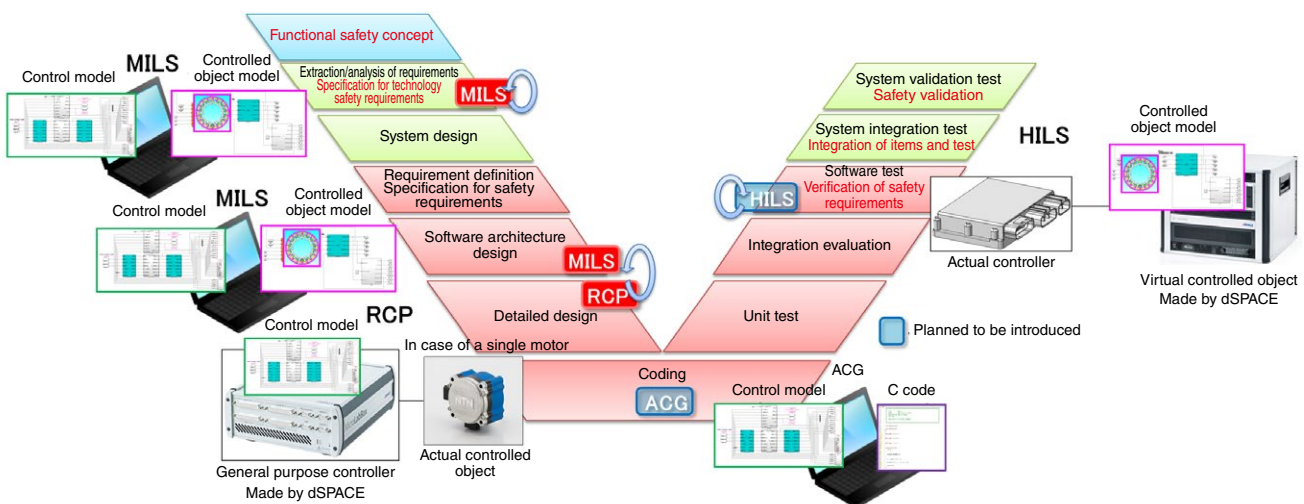

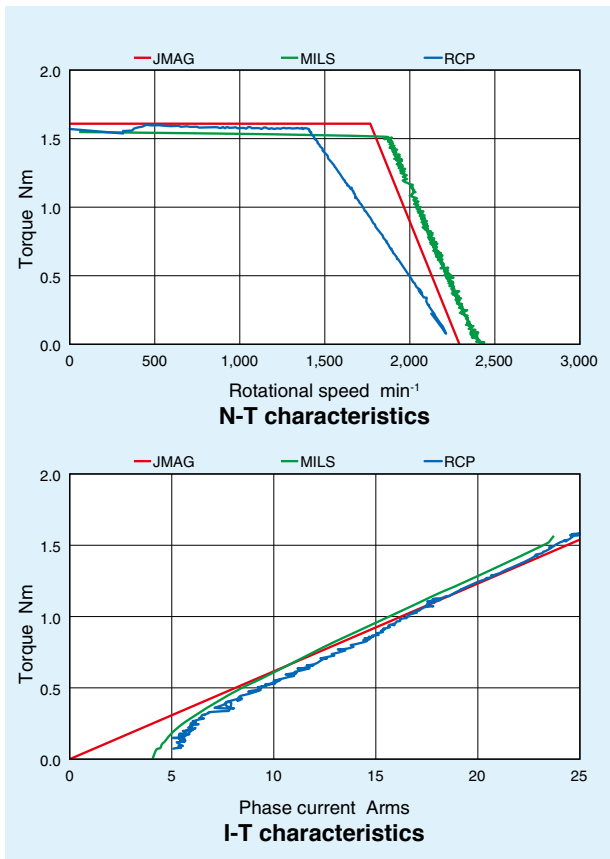
Fig. 9 V-shape development model

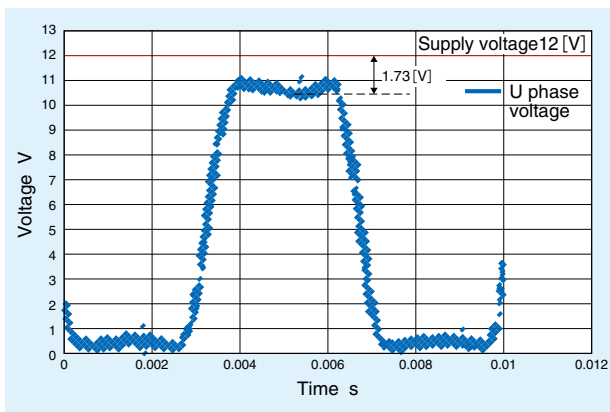**Fig. 10** Simulation result (N-T, I-T characteristics)

Fig. 11 U phase voltage when phase current effective value is 25Arms

3.3.2 Result of Controller Model and Future Plan

In the controller model, we are promoting the use of the core asset (reusable asset) anticipating the forthcoming auto code generation. As one subsystem meets multiple requirements, the subsystems were recreated to correspond to each requirement in the requirement specification.

Then, the switch of subsystems where made in three patterns based on "with/without" requirement. The three patterns determine the binding time depending on "when" the variability is realized for each subsystem **(Fig. 12)**.

1) Required model elements are edited (added/deleted) by the Matlab script
2) Required model is selected by the Variant SubSystem and Configurable SubSystem
3) Processing is dynamically selected by If/Switch Case SubSystem and Switch block

Switch is applied at the design phase for 1), code generation or compiling phase for 2) and software execution phase for 3). The model unit test was defined in the process to verify the output result per SubSystem.

By conducting the simulation test per subsystem, faults can be removed before implementation with auto code generation. The model based development comes with a rich set of test tools; however, in order to eliminate variance of quality of manual tests and for efficiency purposes, a tool for automatic testing that works with different tools was developed. This enabled automatic generation of test specifications, simulation models and test results, easy retesting and recording of evidence **(Fig. 13)**.

For applying auto code generation to the products in the coming years, we will prepare the environment and process for conducting verification of consistency between the model and codes (Back to Back testing) required by ISO 26262 (SILS, PILS).
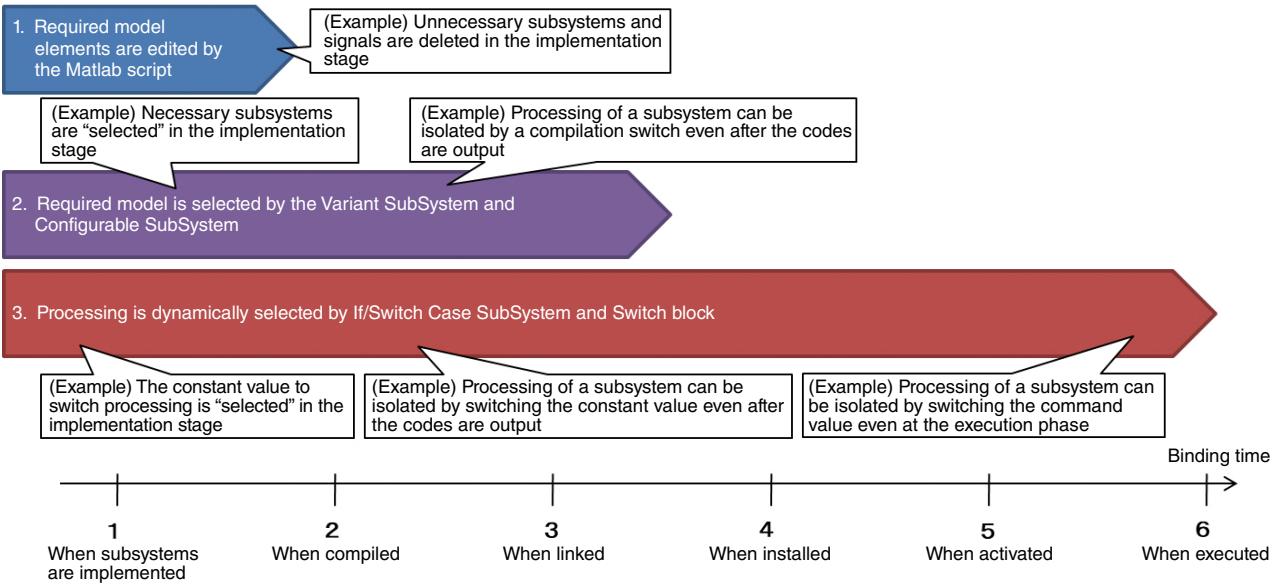
1. Required model elements are edited by the Matlab script

(Example) Unnecessary subsystems and signals are deleted in the implementation stage

(Example) Necessary subsystems are "selected" in the implementation stage

(Example) Processing of a subsystem can be isolated by a compilation switch even after the codes are output

2. Required model is selected by the Variant SubSystem and Configurable SubSystem

3. Processing is dynamically selected by If/Switch Case SubSystem and Switch block

(Example) The constant value to switch processing is "selected" in the implementation stage

(Example) Processing of a subsystem can be isolated by switching the constant value even after the codes are output

(Example) Processing of a subsystem can be isolated by switching the command value even at the execution phase

Binding time

1	2	3	4	5	6
When subsystems are implemented	When compiled	When linked	When installed	When activated	When executed

Fig. 12 Relationship of replacement measures between the binding time and Simulink® subsystem

Test specification

Model is automatically generated from the test specification

Automatic execution of the simulation

Waveforms of input values and expected values

Waveforms of expected values and results

The red circles indicate deviation from the expected values
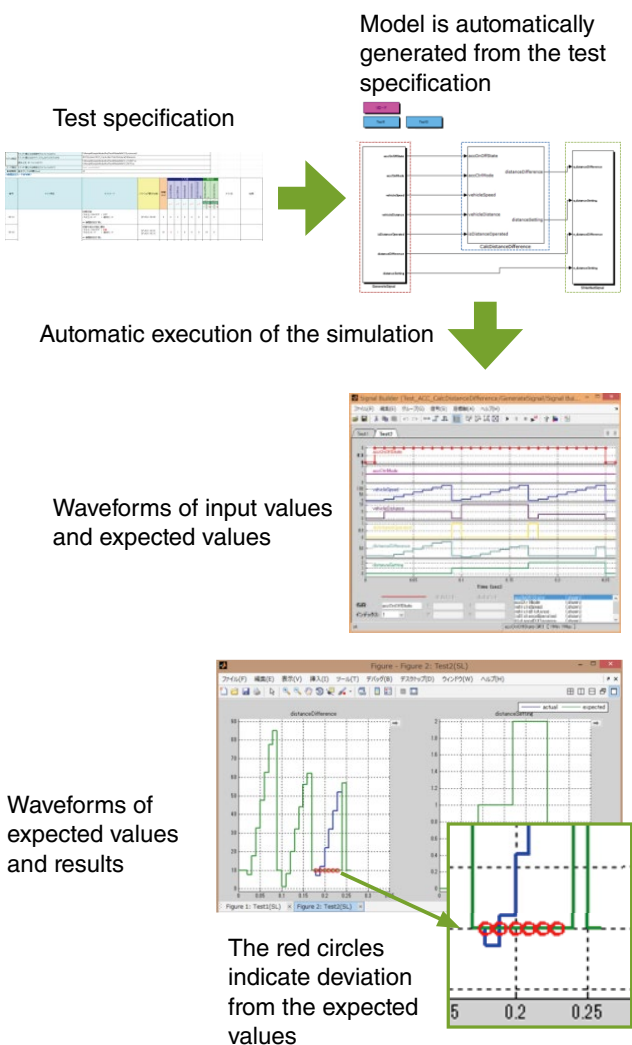
Fig. 13 Flow of unit test tool of automatic model

4. Conclusion

NTN will continue developing electric module products, which can be applied to various applications efficiently, taking advantage of our base technologies, and contribute to the promotion of autonomous driving and electrification, which is evolving in the automotive industry.

Photo of authors

Tatsuji INOUE

Business Promotion Department
Electric Module Products Division
Automotive Business Headquarters

Kazuhiro AOSHIMA

Business Promotion Department
Electric Module Products Division
Automotive Business Headquarters

Yuichi SUGIMOTO

Business Promotion Department
Electric Module Products Division
Automotive Business Headquarters

Keigo MOTOKUBO

Business Promotion Department
Electric Module Products Division
Automotive Business Headquarters

Introduction of Sensor Modular Products and Technologies for Autonomous Driving and Electrification of Automobiles

Yasuyuki FUKUSHIMA*   Hiroyuki HAKAMATA*
Christophe DURET**

This article describes what **NTN** is challenging to meet the emerging requirements on automobiles, 'CASE' , focusing on newly developed sensor modular products and technologies applied to the existing automotive bearings.

1. Automotive Market Trend and NTN's Approach

The automotive industry is facing a significant transformation period that only happens once in a century. Responses to the new requirements of "CASE" are needed, in addition to the improvement of conventional vehicle performance: "driving", "turning" and "braking". CASE stands for "Connected", "Autonomous", "Shared & Services" and "Electric"[1]-[3].

・Connected
  Exchange of information between an automobile and everything else connected to the network, such as roads, homes, dealers and other automobiles via wireless transmission pathways such as 5G networks.
・Autonomous
  Autonomous vehicle driving represented by vehicle driving assistance and driverless taxis.
・Shared & Services
  Sharing and service offerings including MaaS (Mobility as a Service).
・Electric
  Not only the electric power train of electric vehicles (EVs), but also electrification of every moving element of vehicles.

NTN provides the automotive sector with hub bearings and CVJs (driveshaft), and module products that incorporate them. Hub bearings are important components in many vehicles that support rotation of the wheels and are equipped with ABS sensors (wheel rotational speed sensors) to detect the rotational speed of each wheel. **NTN-SNR** has been leading the field of wheel speed active sensing technology since the 1990s, by developing a technology to integrate the rubber magnet with the seal of hub bearings (ASB®: Active Sensor Bearing; shown in **Fig. 1**) as the global standard[4]. In this article, **NTN**'s sensor products/ technologies that can satisfy the new requirements of CASE are introduced, which have been developed after the above mentioned technology.
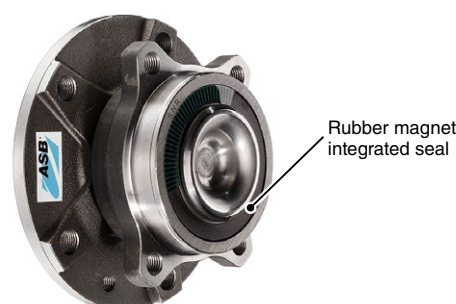

Rubber magnet integrated seal

Fig. 1 ASB® (Active Sensor Bearing) hub bearing

2. Hub Bearing with Integrated High Resolution Rotation Sensor

NTN developed the "Hub Bearing with Integrated High Resolution Rotation Sensor"[6] which is equipped with wheel speed sensor technology that achieves a max. 40 times higher resolution by using a high-resolution rotation sensor (MPS40S)[5], without changing the specification of the conventional hub bearing. The improved resolution promotes accurate estimation of the tire and road conditions. The Hub Bearing with Integrated High Resolution Rotation Sensor is shown in **Fig. 2**. In this section, an overview and the evolution of the Hub Bearing with Integrated High Resolution Rotation Sensor are discussed, with focus on its application to autonomous driving.

*New Product Development R&D Center
** NTN-SNR ROULEMENTS Research & Innovation Mechatronics

Fig. 2 Hub Bearing with Integrated High Resolution Rotation Sensor

2.1 Overview of Hub Bearing with Integrated High Resolution Rotation Sensor

An overview of the Hub Bearing with Integrated High Resolution Rotation Sensor equipped with the high-resolution rotation sensor (MPS40S) is shown in **Fig. 3**. The high-resolution rotation sensor, which is the detection component, is molded together with the fixing core grid with resin, and press fit onto the stationary ring (outer ring). The component to be detected is a magnetic ring with alternating North and South-poles (48 poles total), which is press fit onto the rotating ring (inner ring). The high-resolution rotation sensor (MPS40S) creates high resolution output signals by electrically interpolating (multiplying) the length of the pole-pair of the magnetic ring. The multiplier can be set up to 40 times, with output of 1,920 pulses/rotation.
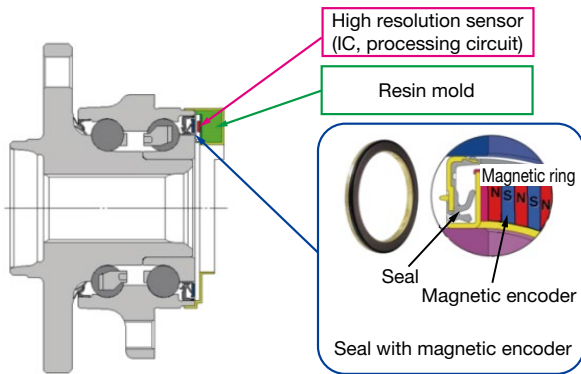

Fig. 3 Overview of Hub Bearing with Integrated High Resolution Rotation Sensor

2.2 Application to Estimation of Tire/Road Conditions

NTN has been working on the approach to estimate the tire and road conditions by extracting and analyzing the information of the changes of the rotational speed from the wheel rotation signals of a running vehicle using the Hub Bearing with an Integrated High Resolution Rotation Sensor. The rotational speed variation includes information about the variation of the road surface/tire and vehicle propulsion condition, as shown in **Fig. 4**. **Fig. 5** shows an example of signal processing for obtaining the rotational speed variation. The tire and road conditions are estimated by analyzing patterns obtained by

extracting the rotational speed variation of one tire rotation. The data is extracted under the condition that the driving speed is constant in order to obtain highly accurate information. The rotational speed variation patterns are generated from the signals of multiple rotations to reduce the random noise that comes from the road surface while the vehicle is running. The rotational speed variation patterns obtained this way provide characteristic waveforms dependent on the tread patterns. It is estimated that they show the rotational speed variation caused by the deformation of the tread when the tread comes in contact with or separates from the road surface. In high speed driving, the deformation of the tread cannot be captured easily because the tire-specific vibration mode becomes dominant. Therefore, the detection accuracy can be increased by obtaining data in low speed driving. The conventional ABS sensor cannot extract the rotational speed variation with sufficient resolution since it provides much fewer pulses per rotation. Therefore, the signals from the high-resolution rotational sensor can be used to increase accuracy of the estimation of the tire and road surface conditions. Sections 2.2.1 to 2.2.5 discuss the result of test verification with different conditions of the tire, such as a foreign object inserted in the tread, tire type, wear, air pressure, as well as different conditions of the road surface. The multiplier of the high-resolution rotational sensor was set to 10 (output of 480 pulses from AB phase per rotation).
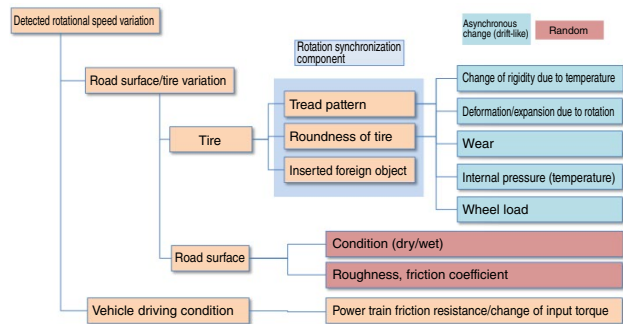

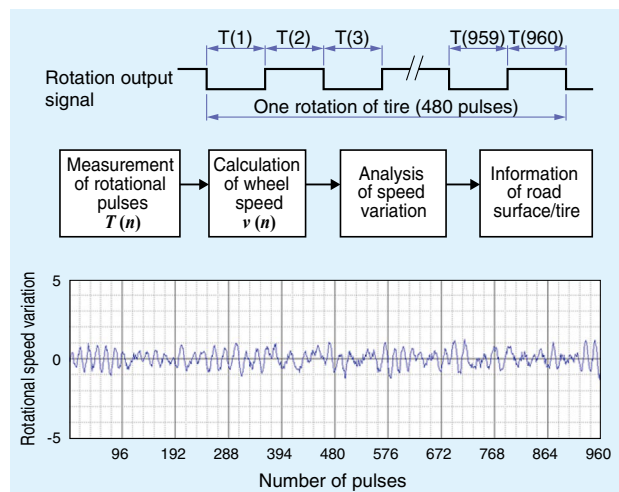**Fig. 4** Information contained in the rotational speed variation components

Fig. 5 Example of rotation pulse signal processing

2.2.1 Detection of Foreign Objects in the Tire Tread

To simulate the condition of foreign objects in the tire, a screw was set between the treads of the tire without puncturing it **(Fig. 6)**. **Fig. 7** shows the rotational speed variation patterns with and without a screw. A part of the rotational speed variation pattern significantly changed due to the presence of the foreign object in the tread, verifying the difference of rotational speed variation patterns with/without the foreign object.
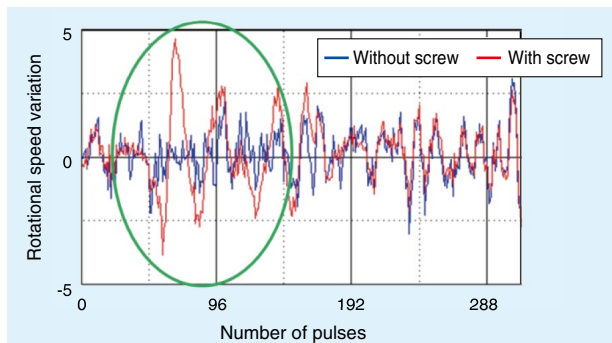

Fig. 6 A screw is inserted in the tread

Fig. 7 Comparison of rotational speed variation patterns with and without the screw

2.2.2 Detection of Tire Types

Improvement in vehicle safety and fuel consumption can be expected by optimally controlling propulsion/braking based on the characteristics of the detected tire type. Two types of tires, A and B, which have different tread patterns, were prepared. The rotational speed variation patterns of tires A and B were obtained, and in order to clearly observe the characteristics of the tread patterns, an autocorrelation value (cyclic nature of signals) was calculated by shifting the phase of each rotational speed variation pattern, and the resulting patterns were compared **(Fig. 8)**. The autocorrelation pattern of each tire is clearly different, which verified that the tire types could be differentiated.
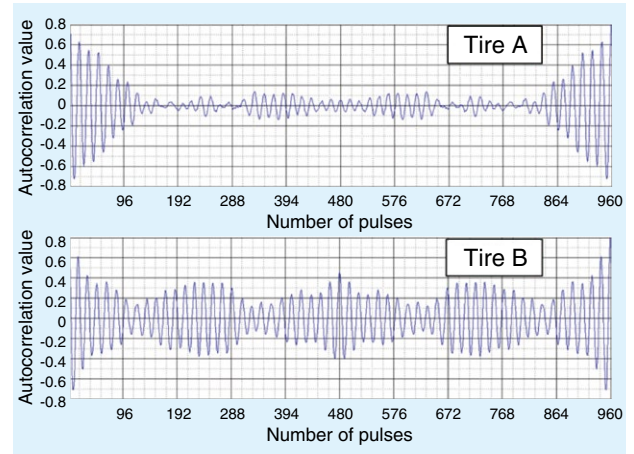

Fig. 8 Comparison of autocorrelation patterns of 2 types of tread patterns

2.2.3 Detection of Tire Wear

Fig. 9 shows the results of the rotational speed variation patterns of two sets of tires with the same tread pattern and different tread depths of 8 mm and 2 mm. It was verified that the amplitude level of the rotational speed variation patterns are different depending on the tread depth.
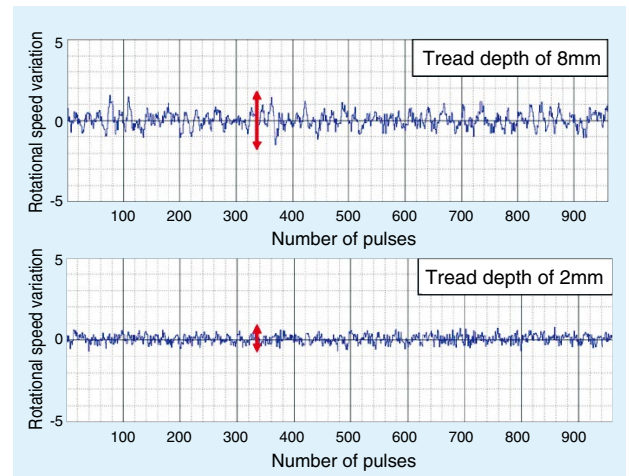

Fig. 9 Comparison of rotational speed variation patterns with different tread depths

2.2.4 Detection of Air Pressure

Tires with eight levels of air pressure (0.14, 0.15, 0.16, 0.17, 0.18, 0.2, 0.23, 0.26 MPa; the standard level is 0.23 MPa) were prepared to obtain rotational speed variation patterns of four wheels (FL: front left, FR: front right, RL: rear left and RR: rear right). To verify the difference due to the air pressure levels, the cross-correlation values (similarity of signals) of the rotational speed variation patterns of different air pressures versus the variation patterns at the air pressure of 0.23 MPa were calculated and plotted in **Fig. 10**. As the air pressure changes, the contact position between the tread and the road changes and the rotational

speed variation pattern changes; therefore, the cross-correlation values decrease. From this test result, it was verified that the change of air pressure could be detected from the relative change of rotational speed variation patterns.
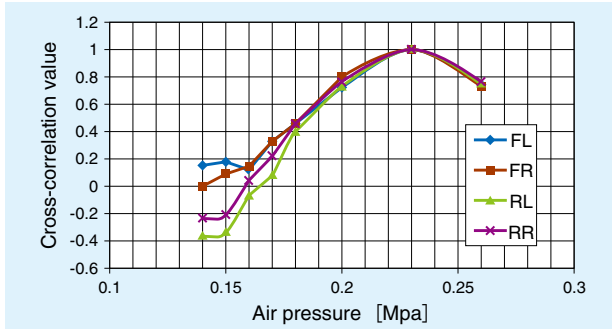

Fig. 10 Comparison of cross-correlation values with different air pressures

2.2.5 Estimation of Road Conditions

Fig. 11 shows the cross-correlation values of the rotational speed variation patterns of an asphalt paved road and a road with compacted snow; the baseline rotational speed variation pattern was obtained from a different asphalt paved road. When the friction coefficient of the tire and road surface decreases, the cross-correlation value also decreases, which verifies the possibility of detecting the change of road conditions.
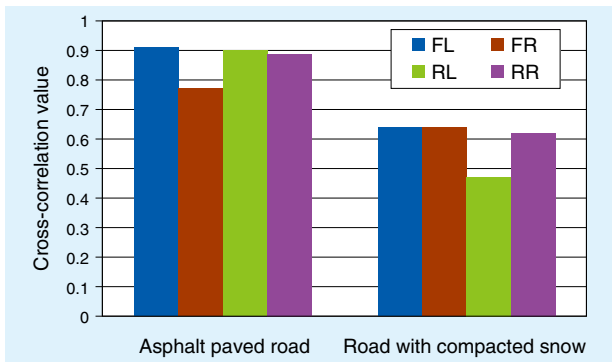

Fig. 11 Comparison of cross-correlation values with different road conditions

2.3 Application to Autonomous and Shared & Services

For autonomous driving, especially automated vehicle parking, accurate information is needed about the traveling distance of a vehicle so that the vehicle can move exactly to the desired position. This information can be gathered by detecting the rotation of the wheels. The wheel speed sensors widely used today do not output a rotation pulse until the wheel rotates approximately four centimeters or more. That means that vehicle movement of a few centimeters cannot be detected; the vehicle may contact an obstacle due to detection error of the vehicle position based on the wheel rotation. When

high-resolution rotation sensor technology is applied, the rotation signal frequency increases by a factor of forty (maximum of approx. 1.4 kHz) compared with the conventional wheel rotation speed sensor, with the output of a rotation pulse when the wheel travels approximately 1mm. This has the potential to contribute to riding comfort and improve operating stability. This technology is expected to address the requirements of autonomous driving.

Autonomous driving vehicles where users do not drive, and shared vehicles which a large unspecified number of drivers drive only for a short time present problems that the users may not become aware of, namely risky vehicle conditions such as tire wear and low tire pressure. As mentioned above, this technology can detect the variation in the contact condition between the tires and the road surface based on the resulting rotational speed variation and provide the information of the conditions to the users and administrators. This helps prevent accidents and enables scheduled maintenance, as well as secures the safety of autonomous driving and shared vehicles and improves their availability.

3. Application of high-resolution rotation sensor technology

NTN has bearings with rotation sensors[7] in its product line. Therefore, **NTN** developed bearings with high-resolution rotation sensors by combining the high-resolution rotation sensor technology with bearings similar to the case of hub bearings. In addition, **NTN** promotes CASE by proposing use of the magnetized ring, which is the key component of the high-resolution rotation sensors.

3.1 Bearing with High-Resolution Rotation Sensor

In autonomous driving, it is necessary to recognize the environment surrounding the vehicle as accurately as possible. The components currently used to accomplish this, such as cameras, LiDAR and millimeter-wave radars, are listed in **Table 1** with their respective characteristics[7].

Table 1 Sensors for recognizing the surrounding environment

Sensor type	Range	Advantage	Disadvantage
Camera	300m	Resolution Color identification	Poor Environmental resistance
LiDAR	200-300m	Distance finding performance	Poor Environmental resistance
Millimeter-wave radar	200-300m	Speed measurement Environmental resistance	Resolution

Created based on Reference 7)

LiDAR acquires distance data by measuring the time of the reflected light from two-dimensional scanning of a near-infrared laser beam. Currently, rotating mirrors are used to scan the laser light. Although the development of non-mechanical light scanning technology is expected that uses no mechanical movement or rotating components for achieving light and compact LiDAR with high reliability, challenges remain for both wide scanning angles and stability.

The rotating mirror scanning method requires accurate detection of the rotational angle of the rotating mirror in high resolution for further segmentation of the distance data for the scanned surface. Currently, application of magnetic rotational angle sensors has begun for mass production automobiles considering both the environment and cost.

NTN is proposing the "Bearing with High-Resolution Rotation Sensor" using the MPS40S sensor for this application[8]. **Fig. 12** shows the appearance of the Bearing with High-Resolution Rotation Sensor. The MPS40S sensor is certified by the reliability test for automotive electronic components, AECQ100, which proves its high environmental performance. It also has a compact structure that allows installation in the same way as conventional bearings. Therefore, information on rotation and angle can be acquired with high accuracy by simply replacing the existing bearings. For example, it can be used in the application where highly accurate angle detection is required with small and light form factor such as LiDAR of the rotational mirror scanning type. **NTN** is prepared to apply this technology in a broad range of applications in vehicle electrification.
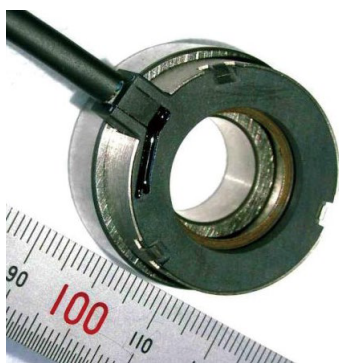

Fig. 12 Bearing with High-Resolution Rotation Sensor

3.2 Tube Type High Resolution Rotation Sensor

When the Bearing with High-Resolution Rotation Sensor discussed in Section 3.1 is used in a muddy water or oily environment, the magnetic detection elements need to be protected by a waterproof/oil proof structure, because the sensor detects magnetic fields by Hall elements. **NTN** started proposing the use of the Tube Type High Resolution Rotation Sensor **(Fig. 13)** where the elements and peripheral circuits are sealed by a tube-shaped thin laminate structure. **NTN**'s proposal began in Europe, where it is beginning to be used on agricultural tractors and small autonomous buses. With this sensor, high-resolution pulse signals can be acquired by a factor of 4 to 200 more times over the N-S magnetic pole pair width (standard width is 5 mm). **Table 2** shows the key specifications. The multiplication factor, magnetic pole width, sensor size and mounting method can be customized, which allows its use in broad applications.

.

Fig. 13 Tube Type High Resolution Rotation Sensor

Table 2 Key specifications of Tube Type High Resolution Rotation Sensor

Size (excluding wiring)	Φ 15.2 × L73mm
Output	Two-phase square wave (phase A, phase B)
Input voltage range	8-32V
Magnetic pole width	5mm(1, 2.5 mm selectable)
Air gap	3 mm or less
Waterproof structure	IP67

3.3 Multi-track Magnetic Ring[9]

The next topic to be discussed is the application of the multi-track magnetic ring **(Fig. 14)** in car sharing. The driver of a shared vehicle needs to adjust the seat position and the mirror angle every time he/she drives depending on his/her physical size or preference. If electric adjustment mechanisms such as power seat and the position data are available, the vehicle can automatically adjust to the driver-specific seat position. A driver who uses a vehicle sharing service can register

his/her seat position setting data into the cloud and the vehicle can set the adjustment position the next time he/she drives the car using that data and the electric adjustment mechanism. An angle sensor is required to reproduce the rotational angle of the electric actuator for adjustment. Drivers often feel discomfort when the seat position is off even a little bit. The Bearing with High-Resolution Rotation Sensor, which provides high resolution and accuracy, along with an angle detection system equipped with a multi-track magnetic ring for acquiring absolute angle without initialization, can be used in these situations.

The multi-track magnetic ring has two magnetic tracks with a different number of pole pairs and can detect absolute angle with high accuracy (±0.1°) and resolution without the need of initialization, by the dedicated magnetic sensor using the difference of the number of pole pairs. A series of radial type (magnetized on the circumferential direction) and axial type rings (magnetized in the axial direction) as well as different numbers of pole pairs are available to be used depending on the application and layout.
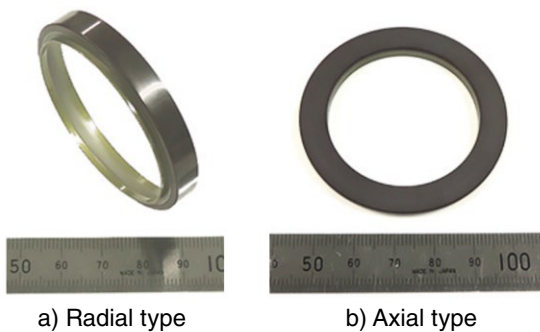

a) Radial type   b) Axial type

Fig. 14 Multi-track magnetic ring

3.4 Rotation angle sensor as an alternative to resolvers

Electrification of vehicle power trains, such as in hybrid electric vehicles (HEVs) and electric vehicles (EVs), is expected to grow due to the trends of global environment protection (including legal regulations), and innovative battery technology reducing cost and improving performance. Along with the drivetrain, accessories are being electrified like those that use the power generated by the internal combustion engine, such as the air conditioner, and devices that use negative engine pressure and hydraulic pressure, such as the brake.

Together with the trends of electrification, compliance to international standard ISO 26262 is required regarding vehicle functional safety. This standard requires measures on the vehicle system, hardware, and software depending on the ASIL (Automotive Safety Integrity Level) considering the severity of any risk factors. They are ranked from A to D depending on the probability of

exposure, controllability and severity. For items that directly involve lives, such as the EPS (Electric Power Steering), where the highest safety is required, measures of ASIL-D are mandatory. For example, misdetection of angles of a motor, which is controlled by detecting the rotation angle, may result in a major functional loss. In this case, the functional loss is prevented by redundancy, placing multiple detectors. For redundancy, if multiple detectors of the same type are implemented, they may fail altogether with the same cause; therefore, implementing detectors with different detection methods will be a safer choice.

Redundancy of rotation angle detection is expected to be achieved by inexpensive and highly accurate rotation angle sensor technology, to respond to the demand of functional safety. Currently, resolvers are widely used as the rotation angle detection sensors for motors; however, magnetic type rotation angle sensors are attracting attention as a redundancy sensor due to their cost and detection method.

Resolvers are widely adopted for controlling motors for propulsion, and have become an inexpensive and secure detection means due to the volume production effect and broad adoption of processing circuits with signal processing hardware. Magnetic-type rotation angle sensors for automotive applications have also been widely adopted as wheel speed sensors and crank angle sensors, but they are not cost competitive against resolvers for achieving highly accurate absolute angle detection functionality.

NTN developed a new rotation angle sensor combining a magnetic ring that uses special magnetization technology and an inexpensive magnetic sensor. Absolute angles can be calculated from the output signals of sine/cosine waves according to the rotation angles, and highly accurate angle information can be acquired by the proprietary magnetization technology and signal processing. **Fig. 15** shows the external view of the developed Bearing with High-Resolution Rotation Sensor.

Fig. 15 Bearing with rotational angle sensor

4. Summary

In this article, **NTN**'s activities around bearings, and bearing module products/technologies to respond to the new demands of CASE are discussed. These demands can significantly change the business structure of the automotive industry, as part of a transformation that happens once in a century. **Table 3** shows the summary of the discussion. These products/technologies are required in global markets including Japan. **NTN**, as a group, will continue to devote ourselves to this development.

Table 3 Summary of **NTN** sensor related products for CASE

	Hub Bearing with an Integrated High Resolution Rotation Sensor	Hub Bearing with an Integrated Rotation Sensor	Tube Type High Resolution Rotation Sensor	Multi-Track Magnetic Ring	Rotation Angle Sensor as an alternative to Resolvers
Connected	○	○	○	○	
Autonomous	○	○	○	○	○
Shared & Services	○		○	○	
Electric				○	○

References

1) Journal of Society of Automotive Engineers of Japan, Vol. 73, No. 7 (2019).
2) CASE Revolution; Automotive Industry of 2030, Nikkei Publishing Inc., (2018).
3) Age of CASE; Exploring New Mobility, Jihyo Co., Ltd. (2018).
4) ASB Technology https://www.ntn-snr.com/sites/default/files/2017-03/technologie_asb_en.pdf.
5) NTN TECHNICAL REVIEW No.75 (2007) 36-41.
6) NTN TECHNICAL REVIEW No.81 (2013) 52-57.
7) Three Kingdom Saga of Onboard Sensors, Nikkei Electronics, March Issue, 2018 (2018).
8) NTN TECHNICAL REVIEW No.78 (2010) 70-76.
9) NTN TECHNICAL REVIEW No.86 (2018) 45-49.

Photo of authors

Yasuyuki FUKUSHIMA
New Product Development R&D Center

Hiroyuki HAKAMATA
New Product Development R&D Center

Christophe DURET
NTN-SNR ROULEMENTS Research & Innovation Mechatronics

Vehicle Motion Control with In-Wheel-Motors

Junichi HIRATA*
Yuta SUZUKI*

A vehicle equipped with In-Wheel-Motors can control the braking / driving force independently in the left and right wheels. **NTN** has developed a vehicle motion control that balances turning performance and attitude stability by adjusting the braking / driving force of the In-Wheel-Motors according to the driving attitude of the vehicle. This paper mainly introduces, among the developed vehicle motion control, the effect of yaw moment control that we verified by the actual vehicle test.

1. Introduction

Recently, various policies for promoting electric vehicles (EVs) as a measure to solve environmental issues such as global warming and air pollution have been put in place globally[1]. With EVs, the driving power source changes from the conventional internal combustion engine to electric motors, which also enables active use of regenerative braking[2),3)].

The methods for using the motor for driving vehicles include on-board method[4] which places the motor on the body and transmits the power to the tires via driveshafts and in-wheel motor method[5] which places the motor inside the wheels and transmits the power to the tires directly without the use of driveshafts. Adopting the in-wheel motor method means that the braking/driving power to the left and right wheels can be independent, responsive and precisely controlled because the driveshaft is not used.

NTN developed vehicle motion control technology to improve both the turning performance and attitude stability by controlling the braking/driving power of in-wheel motor (hereafter IWM) according to the vehicle driving conditions. In this article, the effect of the yaw moment control is introduced from the developed vehicle motion control technology, among others.

2. Vehicle Motion Control

Fig. 1 shows the block diagram of integrated control, which is the developed vehicle motion control. The integrated control consists of 4 functional blocks. The μ estimation is the block to estimate the friction coefficient of the road surface and the anti-skid control is the block to control the skidding of tires by reducing

the torque commanded to IWM when skidding begins. The turning performance improvement control and attitude stability control are the blocks to control the vehicle yaw moment.

The concept of the yaw moment control operation is shown in **Fig. 2**. The vehicle in **Fig. 2** is equipped with IWM on the front wheels, similar to the test vehicle introduced in Chapter 3. The yaw moment is generated to the vehicle by creating different braking/driving powers to the left and right front wheels (orange arrows in **Fig. 2**). When the yaw moment is created to the same direction as the turning direction of the vehicle, turns can be assisted (**Fig. 2** (a)). When the yaw moment is created to the opposite direction of the turning direction of the vehicle, excessive turns such as the spinning can be reduced (**Fig. 2** (b)).

The control shown in **Fig. 1** is integrated so that these 4 blocks can seamlessly work together.
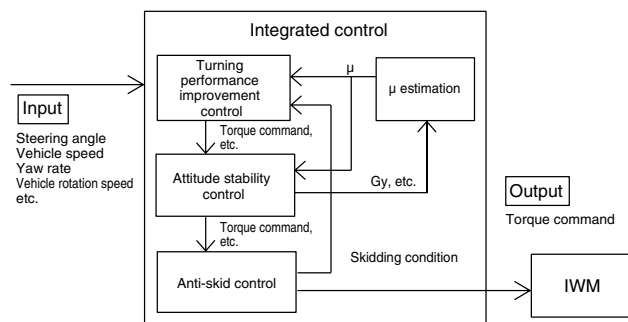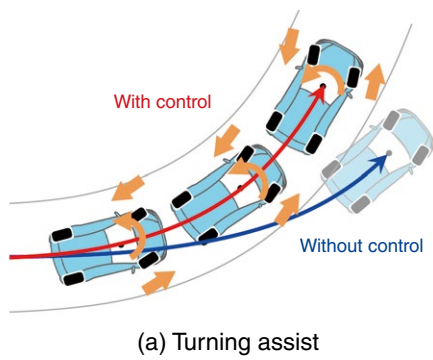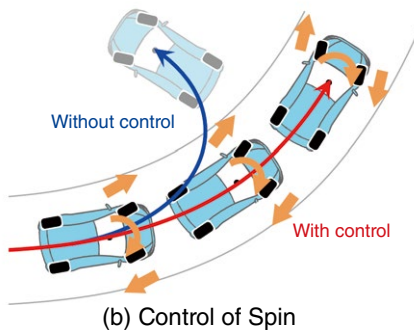

Fig. 1 Block diagram of integrated control

* Engineering Dept., EV Module Division

(a) Turning assist

(b) Control of Spin

Fig. 2 Concept of yaw moment control

3. Actual Vehicle Test

In this Chapter, the verification result of the effect of the developed control is introduced from an actual vehicle test.

3.1 Test Vehicle

Fig. 3 shows the vehicle used in the test. IWMs **(Fig. 4)** were installed on the front wheels of a Suzuki Splash (front wheel driven) to convert it into an EV. **Table 1** shows the vehicle specification.
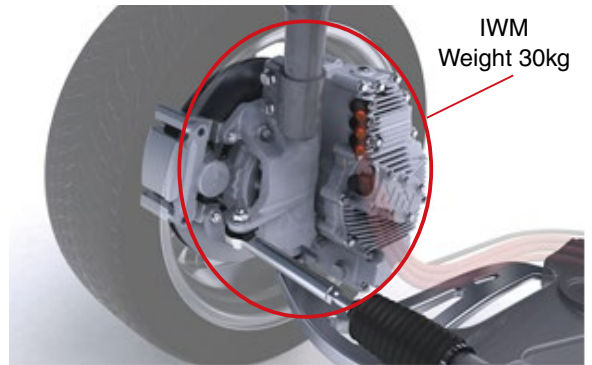

Fig. 3 Test vehicle

Fig. 4 In-wheel motor (IWM)

Table 1 Vehicle specification

Overall length	3.775m
Overall width	1.69m
Wheel base	2.36m
Tread front/rear	1.46m/1.47m
Vehicle weight	Approx. 1,200 kg
Driving method	Front wheel IWM
Maximum output	60 kW(30 kW × 2 wheels)
Battery type	Lithium ion battery

3.2 Verification of Turning Performance Improvement Effect

The effect of turning assist by turning performance improvement control was verified by driving the slalom course shown in **Fig. 5** at a speed of 50 km/h. As shown in **Fig. 6**, the delay from the steering operation to the generation of vehicle yaw rate was reduced from 75 ms to 60 ms and the amplitude of the steering angle was also reduced from 300 deg. to 270 deg. by applying the control. This result revealed that the turning performance improved from the control.
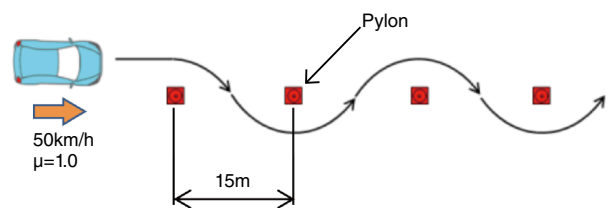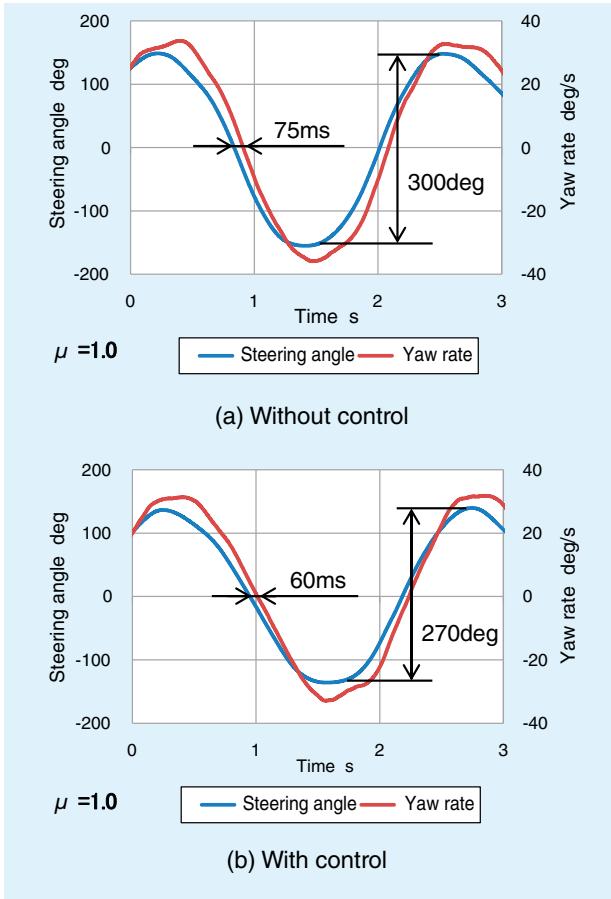

Fig. 5 Slalom course

μ =1.0

(a) Without control

μ =1.0

(b) With control

Fig. 6 Slalom test result

Fig. 7 J-turn course

Fig. 8 J-turn

3.3 Verification of Attitude Stability Improvement Effect

The vehicle condition representing turning instability can be categorized into plow (drift out) where the vehicle is pushed outside of the course as it turns around the curve and spin where the vehicle is pulled inside the curve. The attitude stability control to control these conditions is developed and its effect was verified using a test vehicle.

3.3.1 Control of Plow

The effect of the plow control by the attitude stability control was verified by driving the J-turn course in **Fig. 7**. The pylons were placed in the position with a 20 m radius, to make the J-turn target radius of 18 m. The vehicle speed entering the course is approx. 60 km/h. **Fig. 8** shows the vehicle in the driving test and **Fig. 9** shows the driving trajectory. **Fig. 9** shows that the vehicle without control significantly deviated from the course whereas the vehicle with control was on the track proving that the plow was reduced by the control.
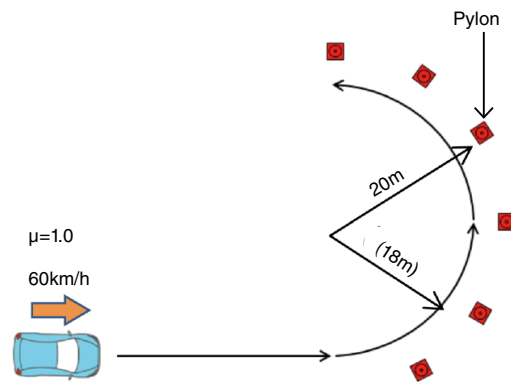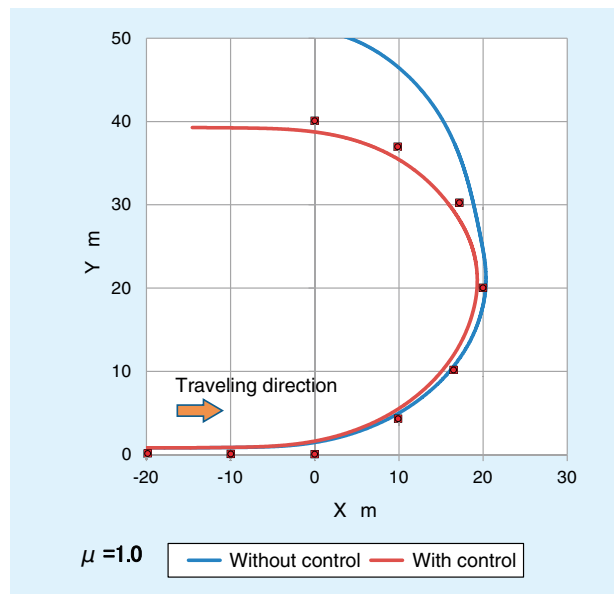

μ =1.0

Fig. 9 J-turn test result

3.3.2 Control of Spin

The vehicle test with a steering maneuver to induce spinning was conducted at a vehicle speed of 60 km/h to verify the effect of attitude stability control against spinning and the yaw rates and driving trajectories with and without control were compared. **Fig. 10** shows the test result. In the case where no control was applied, the yaw rate continued to increase inducing a spinning condition even if the steering angle was reduced at 2 1/2 seconds. The trajectory also indicates spinning

condition as the turning radius suddenly became small. On the other hand, when control was applied, the yaw rate turned to zero as the steering angle returned to zero after 3 seconds without causing spinning and the vehicle was under control as the driver intended to steer it. The trajectory also shows stable driving without unsteady behavior.
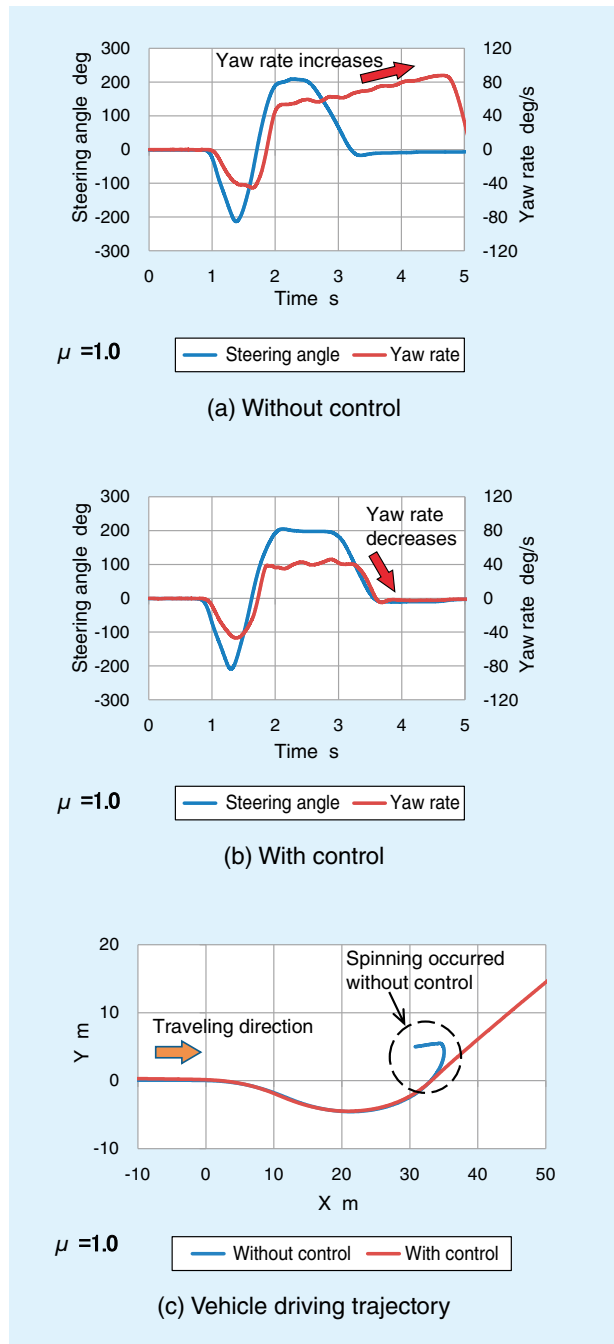

(a) Without control

(b) With control

(c) Vehicle driving trajectory

Fig. 10 Stability evaluation test result

3.4 Anti-Skid Control

In order to make the yaw moment control effective, it is important to ensure the braking/driving power of the front wheels (braking/driving torque of IWM) is securely transmitted to the road surface. For that reason, anti-skid control is applied to prevent tire spin while driving and tire lock while braking **(Fig. 1)**. A start/acceleration test was conducted on a road surface equivalent to frozen roads (friction coefficient μ = 0.2: course design value) to verify the anti-skid control effect. When anti-skid control is not applied, giving a large driving torque command to IWM creates spinning of the driving wheels preventing good acceleration.

Fig. 11 shows the wheel speed of both front wheels, vehicle speed is measured by GNSS (Global Navigation Satellite System) and the vehicle longitudinal acceleration as the vehicle starts moving. The driving wheels steadily rotate at a rate slightly faster than the GNSS vehicle speed (maintains the constant skid rate) without remarkable skidding, producing acceleration equivalent to the course design value of 0.2 ($\approx 2m/s^2$) to the vehicle. This confirmed that the driving power was securely transmitted to the road surface with the anti-skid control.
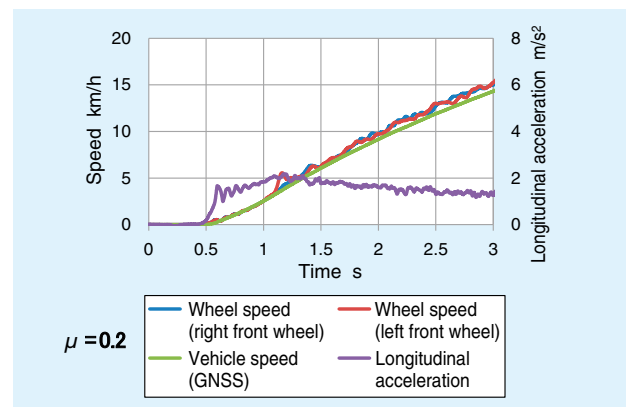

Fig. 11 Low μ road starting test result

3.5 Integrated Control

The integrated control integrates all of the controls introduced in the previous Sections so that they work seamlessly together. The following are the effect of the integrated control on a high μ road and low μ road.

3.5.1 High μ Road (dry asphalt surface)

The effect of the integrated control was verified on the high μ road in the double lane change course shown in **Fig. 12**. The vehicle speed entering the course was 60 km/h. **Fig. 13** shows the test results.

Fig. 13 reveals that the steering angle and the delay of the yaw rate are both reduced by the effect of the turning performance improvement control at the first steering maneuver immediately after entering the course (at around 1 second). In the latter half of the course (after 2 seconds), the yaw rate follows the steering operation preventing spinning from occurring due to the effect of the attitude stability control. The driving trajectories also show that the vehicle without control significantly deviated from the course whereas

the vehicle with control could follow the targeted course. **Fig. 14** shows the vehicle attitude when it exited the course. The vehicle without control shows the spinning behavior heading in the lateral direction from the course but the vehicle with control maintained a stable vehicle attitude, proving the effect of the control.
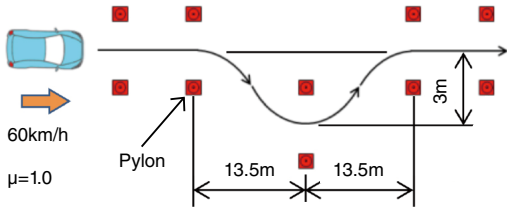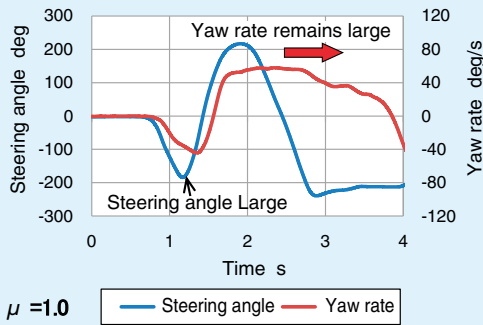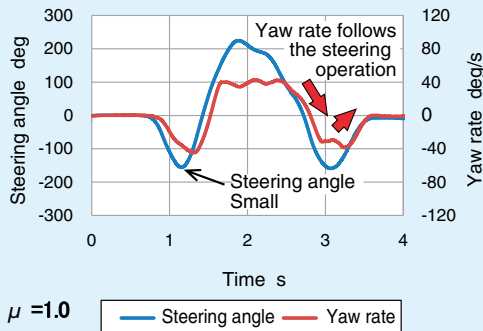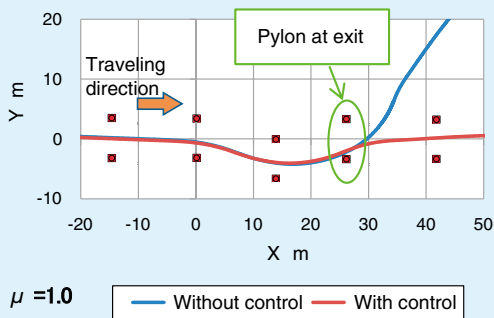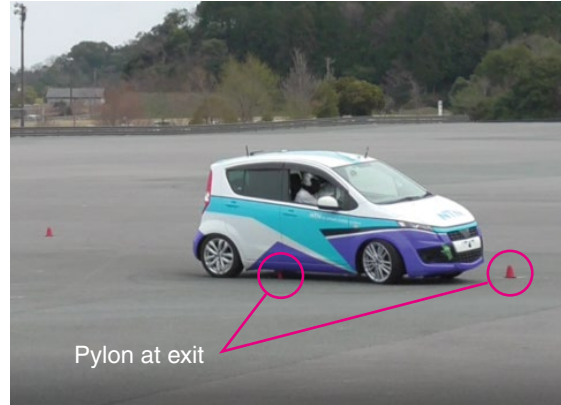

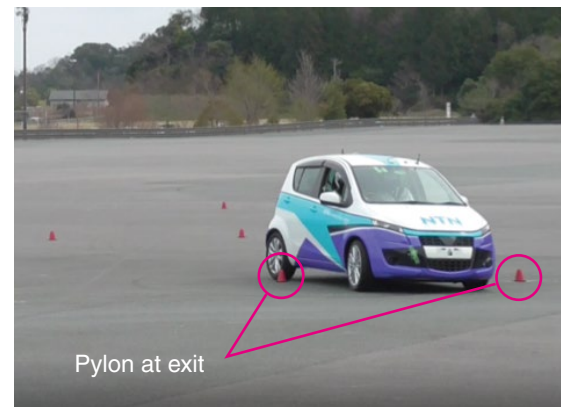**Fig. 12** Double lane change course

(a) Without control

(b) With control

Fig. 13 Double lane change test result

(a) Without control

(b) With control

Fig. 14 Vehicle attitude during double lane change test

3.5.2 Low μ Road (equivalent to frozen road μ = 0.2)

The integrated control has a function to estimate the road surface μ **(Fig. 1)** to detect the change of the road surface μ from different kinds of information, such as the vehicle behavior, and automatically adjust various parameters to control the vehicle not only for high μ roads but also low μ roads. The effect of the low μ road was verified on the road surface equivalent to a frozen road (μ = 0.2) by setting a single lane change course as shown in **Fig. 15**. The vehicle speed entering the course was 40 km/h.

Fig. 16 shows the driving trajectories. No differences were noted in the vehicle trajectory by steering operation immediately after entering the course between the vehicles with and without control; however, in the latter half of the course, the vehicle without control showed a spinning behavior, similar to the high μ road, significantly deviating from the course. On the other hand, the vehicle with control could drive the course without spinning behavior. This result shows that the developed integrated control is effective with a change to the road surface friction coefficient and can handle the low μ road instantaneously, as well as the high μ road.
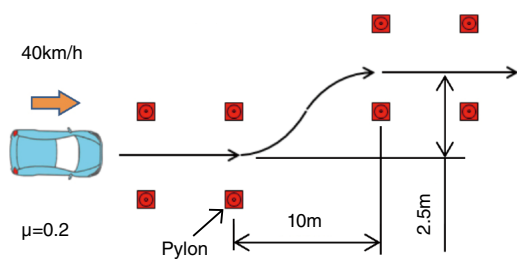
Fig. 15 Single lane change course
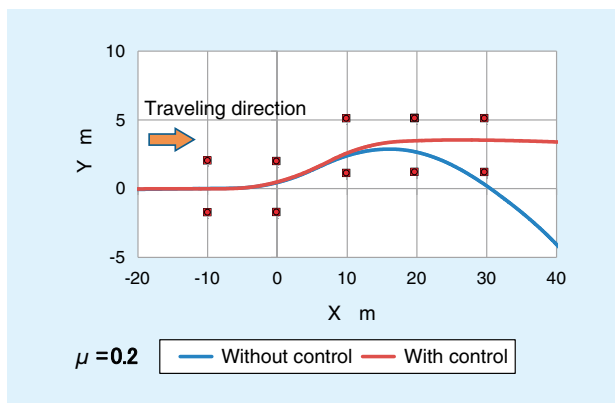
Fig. 16 Single lane change test result

4. Conclusion

In this article, the effect of the yaw moment control is introduced from the vehicle motion control technologies developed by **NTN**. We will further explore the possibilities of control with IWM through development of vehicle motion control using IWM.

References

1) Ministry of the Environment, Ministry of Economy, Trade and Industry, Ministry of Land, Infrastructure, Transport and Tourism, Next-Generation Automobile Guidebook 2017-2018 (2018).

2) Kimura et al., Development of New-generation e-POWER Hybrid Powertrain, Nissan Technical Review, No 80, (2017) 6-14.

3) Tomokazu Honda, Development of Handling Performance Control for SPORT HYBRID SH-AWD, Proceedings of the Society of Automotive Engineers of Japan Annual Congress. No. 102-14, (2014) 25-28.

4) Yukishima et al., Two Motor On-board Drive System, NTN TECHNICAL REVIEW, No. 83, (2015) 20-25.

5) Itoh et al., In-Wheel Motor System, NTN TECHNICAL REVIEW, No. 79, (2011) 9-16.

Photo of authors

Junichi HIRATA

Engineering Dept.
EV Module Division

Yuta SUZUKI

Engineering Dept.
EV Module Division

History of Development of Bearings for Automobiles Aiming at Low Fuel Consumption

Takashi YASUNISHI*

Hybrid vehicle/Electric vehicles (HEV/EV) that represent the next-generation vehicles, future expansion are expected.

On the other hand, in emerging countries such as Asia and Africa, there is still high demand for conventional vehicles (engine type) on a global basis due to population growth. In addition, from the point of environmental regulation, each automotive manufacturer is focusing on the development of vehicles with low environmental impact. We will introduce the history of the development as a bearing for automobiles, about "Low Fuel Consumption" required for automobiles.

1. Introduction

Since the structure of bearings for automotive use are simple, specification differences are not often noticeable by appearance. However, a look at the history of bearing specifications from the 1980's till present reveal that basic performance continued to evolve ahead of market needs. In this article the transition of automotive bearing technology (deep groove ball bearing and tapered roller bearing) is introduced up to the latest specification in regards to low fuel consumption (low torque).

2. History of Development of Bearings for Automotive Use

2.1 Deep Groove Ball Bearing

In response to the market demands of high efficiency multi-stage AT and CVT, the functionality of the deep groove ball bearing, mainly used for transmission, has been improved. This includes high-speed use and lower torque. In addition to requirements of being compact, lightweight and a long operating life, bearings for driving motors of electric vehicles also face similar specification demands.

The demand for lower torque is met with a compact and lightweight design. This is achieved with the material and thermal treatment, change of internal design specification and improvement of components such as the seal, cage and grease **(Fig. 1)**.

Table 1 shows the characteristics of the structure and performance of each specification of deep groove ball bearings. **Fig. 2** shows the history of technology since the 1980s comparing the running torque.

The deep groove ball bearings used for transmission were generally the open type without a shield or seal. However, contact seals (LU seal/LH seal) are now adopted to prevent reduction of operating life due to penetrating hard foreign objects contained in the oil.

Bearings with contact seals have higher torque than the open type due to the sliding nature of the seal so the open type is used when the requirement for lower torque is critical. Improvements of material and thermal treatment have been made to achieve longer operating life even in an environment where foreign objects may penetrate.

The latest specification (LE Seal) developed has improved seal material and seal lip geometry achieving low torque while maintaining the seal performance. These improvements result in lower torque equivalent to non-contact type seal under oil lubrication.
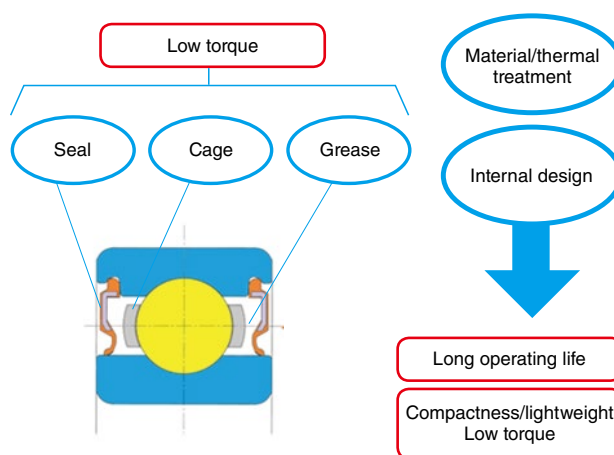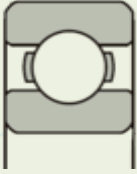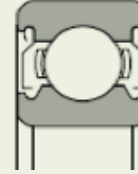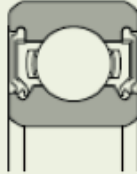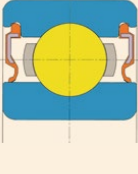

Fig. 1 Deep groove ball bearing and characteristics

* Automotive Bearing Engineering Dept., Automotive Business Headquarters

Table 1 Characteristics of deep groove ball bearing[1]

Type and code		Open type	Shield type	Seal type		Seal type
			Non-contact type ZZ	Contact type LU	Low torque type LH	Low torque type LE
		Specification of standard type				*Specification of developed product*
Structure						
		No shield or seal to seal the bearing.	Metallic shield is fixed on the outer ring to form labyrinth seal with the seal groove of the inner ring.	Seal of steel plate with synthetic rubber adhered by vulcanization is fixed to the outer ring and the tip of the seal is in contact with the seal groove of the inner ring for sealing the bearing.	The same basic structure as LU with improved seal tip to reduce the contact force and achieve low torque by providing slits for avoiding absorption.	Low torque is achieved with non-contact seal by creating a wedge film effect of fluid under the oil lubrication environment by providing multiple arc-shaped micro convexes on the sliding surface of the seal tip.
Comparison of performance	Low torque	☆☆☆	☆☆☆	☆	☆☆	☆☆☆
	Dust proof	—	☆	☆☆☆	☆☆☆	☆☆☆
	High speed	☆☆☆	☆☆☆	☆	☆☆	☆☆☆

Order of superiority: excellent ☆☆☆＞☆☆＞☆ poor

Deep Groove Ball Bearing

Fig. 2 Transition of development of deep groove ball bearings[2]

2.2 Tapered Roller Bearing

Tapered roller bearings used for transmission and differential gears have more design elements than deep groove ball bearings. As a result, various characteristics brought by the design parameters have been explored. In addition to lower torque, improvements on materials and thermal treatment as well as long operating life has been achieved **(Fig. 3)**.

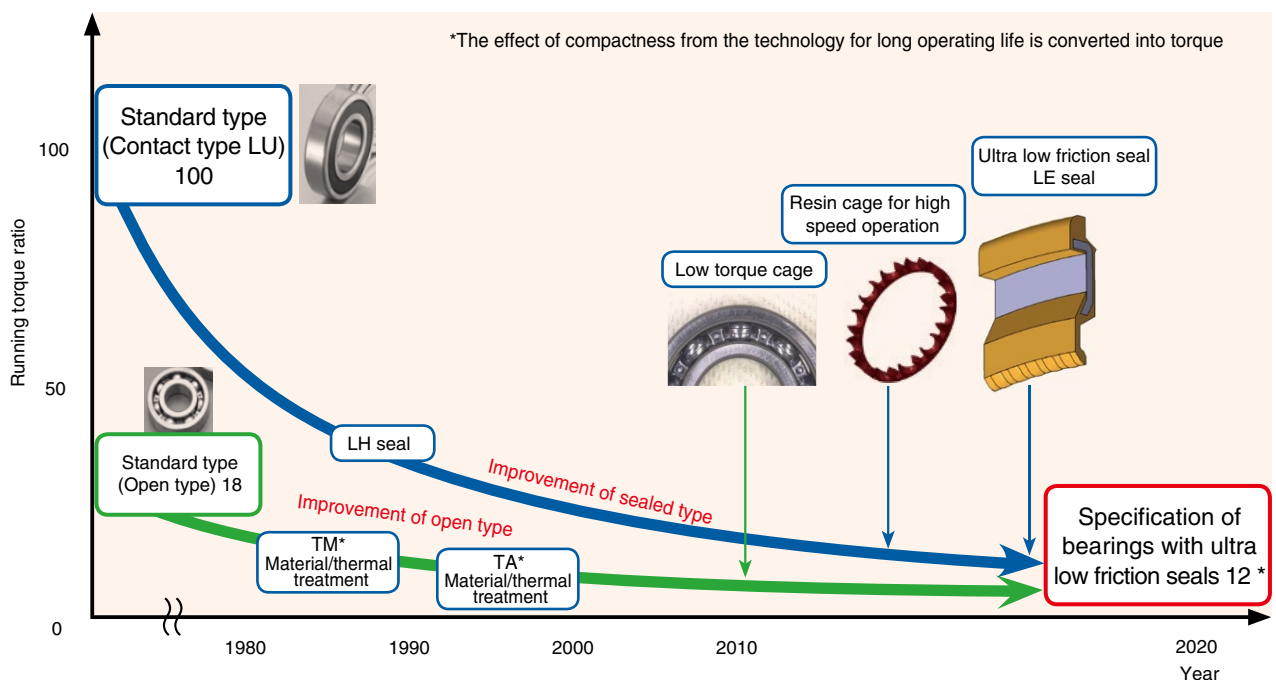In this Section, improvements on the internal design and material/thermal treatment are discussed in the transition to lower torque. The ST specification, which reduced the torque by improving the sliding characteristics of the rollers, was established for the improvement of internal design. This is primarily accomplished with special shape and processing of the inner ring collar. As for the improvement of the material/thermal treatment, special thermal treatment was applied to the carburized steel as the base. This contributes to long operating life due to an increase in retained austenite on the surface of the raceway. (The torque calculation result due to compactness is shown in **Fig. 4.**)

The ECO-Top specification was later established with improvements to micro curvature (crowning) of inner/outer ring raceway and development of products which integrated this technology and other material/thermal treatment technology. Furthermore, the stirring resistance of oil was significantly reduced by changing the design of steel plate cage. In the latest specification, ULTAGE*1 Tapered Roller Bearing for Automotive Application was developed with improved design of crowning and establishing of volume production

processing technology. This also addresses the needs for being lightweight and compact for the recent application of HEVs/EVs.

In addition, the long-life thermal treatment "FA process" was developed based on the bearing steel globally available for procurement. The ULTAGE Tapered Roller Bearing has achieved an increased operating life and a significant torque reduction compared to the standard specification **(Fig. 4)**. Improvements such as optimization of contact stress distribution, which is mentioned later, contribute to the longer life.
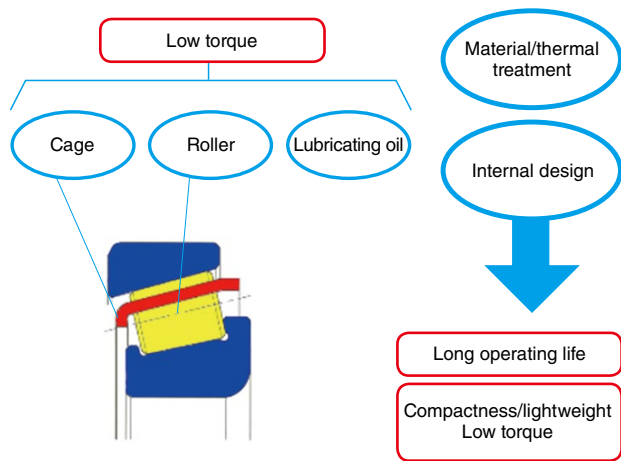
Fig. 3 Tapered roller bearing and characteristics

*1 ULTAGE® is a name created from the combination of "ultimate," signifying refinement, and "stage," signifying **NTN**'s intention that this series of products be employed in diverse applications. Additionally, ULTAGE® is also the general name for **NTN**'s new generation of bearings that are noted for their industry-leading performance.

Tapered roller bearings
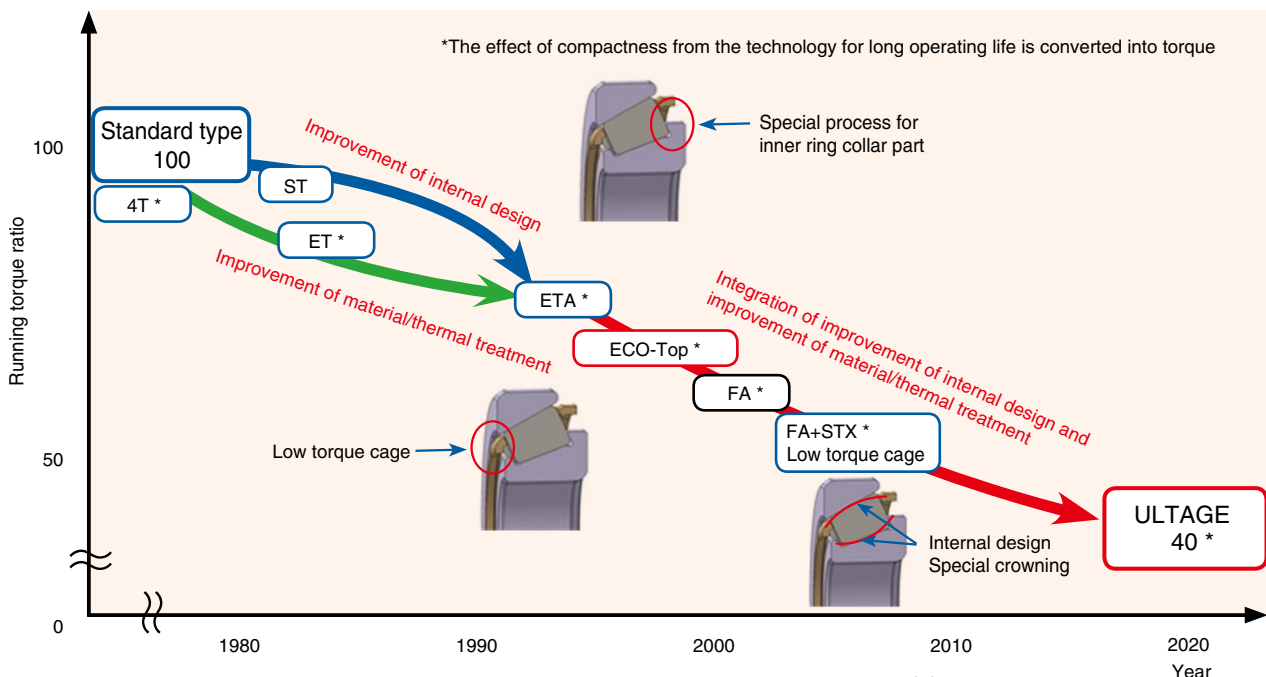
Fig. 4 Transition of development of tapered roller bearing[2),3)]

3. Introduction of Next-Generation Bearings for Automotive Use

The following is the introduction of the next-generation deep groove ball bearings for automotive use for "low fuel consumption" and the latest development of tapered roller bearings.

3.1 Ultra Low Friction Sealed Ball Bearing[4]

In order to prevent reduction of operating life due to severe environments where hard foreign objects are present in the transmission lubrication oil, contact type seals are generally used. Contact type seals increase resistance to foreign objects such as the wear particles from gears. However, bearings with contact seals have larger torque due to the sliding resistance of the seal. The LE Seal optimizes the shape and material of the seal to achieve low torque while maintaining the sealing effect of the contact seal. This seal successfully reduces running torque and raises the circumferential speed limit. It accomplishes this by promoting formation of oil film between the seal lip and the sliding surface of the bearing inner ring for fluid lubrication condition, from the pressure wedge effect of the arc-shaped (half-cylindrical shaped) micro convexes **(Fig. 5)** placed on the sliding contact section of the seal lip **(Table 2, Fig. 6)**.

**Fig. 6** Relation between bearing temperature and running torque

3.2 ULTAGE Tapered Roller Bearing for Automotive Application[5]

Tapered roller bearings used in the power train such as the transmission and differential gears are required to be small and light, in addition to having long operating life and low torque.

ULTAGE Tapered Roller Bearing for Automotive Application is introduced in the following, which delivers the world's highest standard of high-load capacity and high-speed rotational performance with robust crowning optimization technology to maximize the rolling fatigue life of bearing **(Fig. 7)**.

Fig. 5 Characteristics of ultra low friction sealed bearing

Features of developed product

(1) Reduction of 80% or more of running torque (compared to contact type seal)
(2) Support of high circumferential speed of 50 m/s or more
(3) Prevention of harmful foreign objects from penetrating

Table 2 Test condition

Item	Condition
Radial load	0.05 C (C: dynamic load rating)
Rotational speed (min⁻¹)	1,500
Lubricating oil	CVT fluid
Bearing temperature (°C)	35-120

Fig. 7 Structure of ULTAGE tapered roller bearing for automotive application

Features of developed product

(1) World's highest standard of high-load capacity
  · Basic dynamic load rating - 1.3 times*
(2) Long operating life (compared with the basic rating life)
  · Standard type (bearing steel; standard quenching)
    2.5 times or more*
  · High-functionality type (FA process)
    3.8 times or more*
(3) High speed rotational performance at the world's highest level
  · Permitted rotational speed - approx. 10% improvement*
(4) Permitted inclination (magnitude of misalignment)
  · Permitted inclination - max. 4 times*
                    * Comparison of standard catalog values

The contact stress at the rolling contact area of the tapered roller bearing was minimized and a special crowning shape to reduce the excessive pressure on the edge of the contact area (edge load) was applied to the rollers. **Fig. 8** shows an example of calculation of contact stress distribution at the axial cross section of raceway. With ULTAGE Tapered Roller Bearing for Automotive Application, the bearing operating life is improved by suppressing the edge load at the edge of the contact area and equalizing the overall contact stress distribution by the adoption of special crowning.

In addition, because of the long operating life effect due to equalized contact stress distribution, the bearing can be designed for smaller and lighter form factor under the same operating life. Using a compact and lightweight design while maintaining operating life and the restriction of contact pressure, the bearing running torque was reduced by 60% compared to the standard bearing **(Fig. 9)**.

Furthermore, superior seizure resistance property was confirmed with the temperature rise of 1/3 of the standard bearing in the temperature rising test, as shown in **Fig. 10**. Optimization of the shape of the collar and the roller end surface shown in **Fig. 7** resulted in the superior seizure resistance property.
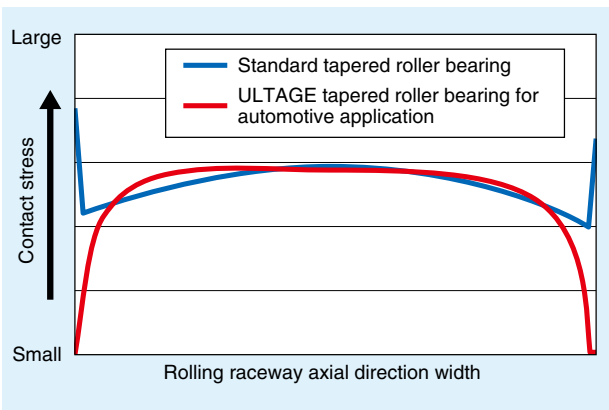
Fig. 8 Contact stress distribution on the raceway
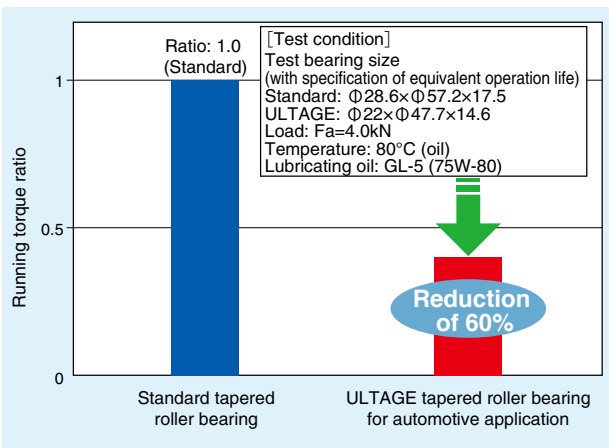
Fig. 9 Running torque ratio of bearings
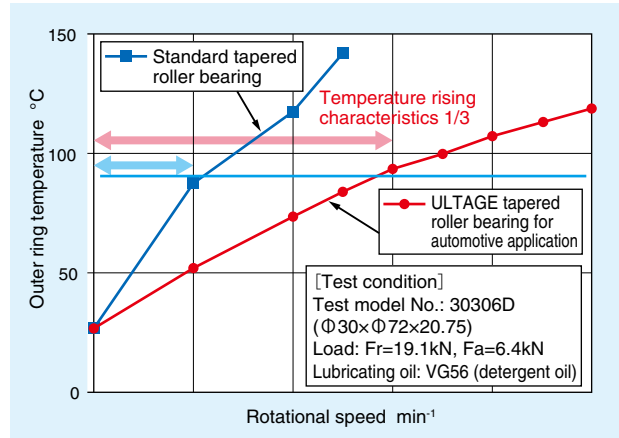
Fig. 10 Seizure resistance test (temperature rising test)

4. Conclusion

The development history of bearings for automotive application was reviewed from the viewpoint of reducing torque. As we have been proposing products ahead of market needs through the development of various technologies, we intend to support the coming stricter and rapidly changing demands. We hope we can continue to contribute to society, so that we will continue to be indispensable in the quest for development of more environmentally friendly, more comfortable and more useful next-generation vehicles.

References

1) NTN Catalog CAT. No. 3015- Ⅳ , P2
2) Hirokazu Nakashima, Trends in Materials and Heat Treatments for Rolling Bearings, NTN TECHNICAL REVIEW, No. 76 (2008), 10-16.
3) Chikara Ohki, Development of High Performance Bearing with Strengthened Grain Refinement, NTN TECHNICAL REVIEW, No. 78 (2010), 128.
4) Katsuaki Sasaki, Takahiro Wakuda, Tomohiro Sugai, Ultra-low Friction Sealed Ball Bearing for Transmission, NTN TECHNICAL REVIEW, No. 85 (2017), 62-66.
5) Yasuhito Fujikake, Takanori Ishikawa, Susumu Miyairi: ULTAGE Tapered Roller Bearing for Automotive Application, NTN TECHNICAL REVIEW, No. 85 (2017) 51-55.

Photo of author

Takashi YASUNISHI

Automotive Bearing
Engineering Dept.
Automotive Business
Headquarters

History of Development of Axle Bearings Aiming at Low Fuel Consumption

Makoto SEKI*

Axle bearing has been innovated by integrating the surrounding components. This article introduces the transition of axle bearing type and the latest **NTN**'s technology.

1. Introduction

While roller bearings for general use are regulated by standards such as ISO and JIS, roller bearings for supporting vehicle wheels (axle unit bearings) have gone through significant transitions over the years.

Also, in recent years restrictions on size, weight, fuel consumption, and environmental consciousness of automotive components have been imposed[1]. The axle unit bearings have evolved to meet those requirements. In this article, the history of these developments is discussed, focusing on reduction of weight and fuel consumption (low torque) of axle unit bearings.

2. Overview of Market Demand for Axle Unit Bearings

The design specifications of axle unit bearings are diversely based on automotive manufacturer needs (mounting methods, allowable space and bearing size, bearing load carrying capacity, low torque performance, muddy water resistance, rigidity and strength, etc.). Their past and current requirements can be categorized as follows:

a) Ease of assembly
b) Simplification or elimination of bearing clearance adjustment
c) Compact, lightweight and large load carrying capacity
d) Maintenance-free
   Particularly, elimination of greasing operation and external seal for sealed bearings
e) Reduction of quantity of components
f) Overall cost reduction including bearing units, secondary components and labor cost

Responding to the above requirements, **NTN** has been developing and marketing the production of the 1st generation, 2nd generation and 3rd generation products (GEN1, GEN2 and GEN3) for approximately 40 years[2].

In addition, environmental regulations have been introduced in many countries with continuous enhancements. This demands the improvement of fuel efficiency to reduce CO_2 emissions. Therefore, lightweight and low torque products are required for axle unit bearings, in addition to the above mentioned requirements.

3. History of Axle Unit Bearings

3.1 History of Bearing Type

Until the 1970s, placing two single row roller bearings was the norm. However, the single row roller bearing had limitations for reducing the weight and size. Therefore, the evolution of unitized products was done to ease assembly, which had the potential to accommodate the weight and packaging requirements.

The first of such products were the Sealed Double Row Angular Contact Ball Bearing (Angular Unit) and Sealed Double Row Taper Roller Bearing (Tapered Unit), then named GEN1 bearings. These were widely used in the themed to late 1970s. In the 1980s, the bearings were unitized with their secondary components, such as hubs and housings (knuckles) to reduce the number of components. This also aided in the efforts to reduce weight, which eventually resulted in the GEN2 bearing.

The aim to further reduce the amount of individual components led to the creation of the GEN3 bearing. Because the GEN3 bearing encompassed more components than the previous GEN2, the installation of the axle unit bearing on the vehicle assembly line was simplified.

Table 1 shows the transition and characteristics of **NTN**'s axle unit bearings by generation, including the time when two single row bearings were used (before unitization efforts began).

* Automotive Unit Engineering Dept., Automotive Business Headquarters

Through the multiple generations of bearings, more secondary components have been incorporated into the single product. This helped reduce the total number of individual components contributing to a more compact design and overall lighter axle weight. Similarly, as the axle unit bearings evolved with further unitization, press fitting the inner/outer rings onto the secondary components is no longer necessary. On driven bearings, fixing the inner ring by swaging it makes preload management easier resulting in significant reduction of variability. This improved preload optimization to achieve reduction of running torque.

3.2 Development of Next Generation Hub Joint

After the creation of the GEN3 for production, **NTN** completed the development of the next generation axle unit bearing: the GEN4. This bearing combines the axle unit bearing with the constant velocity joint (CVJ). This technology has not been adopted because it requires significant modification to the vehicle assembly lines at the auto manufacturers.

Therefore, **NTN** developed a new assembly method for CVJ and axle unit bearings, which can be done without changing the assembly lines at the auto manufacturers. The Press Connect Hub Joint (PCS H/J) method achieves a significant reduction in weight **(Fig. 1)**.

Conventionally, the CVJ and axle unit bearing are connected with a spline and tightened with a nut. The spline teeth are generally designed for interference fit with the helix angle to eliminate backlash, which requires a long spline fit length. The new press connect fit method finishes securing the spline by tightening a bolt, which results in a tighter interference fit than the CVJ stem spline on the

hub bearing bore diameter. This enables the torque to be applied to the entire spline area, resulting in significant reduction of spline fit length.

The adoption of the PCS H/J method achieves about a 65% reduction in CVJ stem length and a 12% reduction in weight (max.). This is due to the hollow structure of the hub ring inner diameter, conversion of nut to bolt, etc., and no spline fit backlash[3].

Fig. 1 Structure of PCS H/J

3.3 Development of Lightweight Bearings

As mentioned above, **NTN** has been reducing the size and weight of the entire axle structure through multiple generations of increasingly unitized axle unit bearings. However, after the adoption of the GEN3 as the mainstream product, further weight reduction of the bearing was required, but unitization has become more difficult.

Table 1 Transition and Characteristics of **NTN**'s Axle Unit Bearings by Generation

Generation		Conventional	GEN1	GEN2	GEN3
Start of production		- 1970s	Mid - 1970s	1983 -	Mid - 1980s -
Structure	Driven Wheel				
	Non-Driven Wheel				
Feature		· Two single row roller bearings.	· Combined two single row roller bearings.	· Integrated mounting flange and outer ring.	· Integrated mounting flange and outer ring, inner ring. · No need to press bearing to mating component.
Ease of Assembly to Vehicles		☆	☆☆	☆☆☆	☆☆☆☆
Compactness		☆	☆☆	☆☆☆	☆☆☆☆
Rigidity		☆	☆☆	☆☆☆	☆☆☆☆
Preload Control		☆	☆☆	☆☆☆	☆☆☆☆
Running Torque		☆	☆☆	☆☆☆	☆☆☆☆

Order of Superiority: Excellent ☆☆☆☆＞☆☆☆＞☆☆＞☆ Poor

Requirements for the GEN3 axle unit bearing, as the strength member, are different from those for the individual bearing, in terms of strength of hub ring, strength of outer ring, overall bearing rigidity, etc. Weight reduction was required while maintaining these strengths, particularly with GEN3. The weight of the hub ring and outer ring account for more than a half of the entire unit, so optimizal design of these components is very important for reducing weight.

NTN uses FEM analysis to determine weight abatement while maintaining the strength and rigidity to satisfy the required functionality. In the past, the optimal shape was developed using topology optimization[4]. An ultra-light hub bearing shape shown in **Fig. 2** was also developed. Therefore, NTN employs the accumulated technologies to provide the optimal shape for the minimum weight, while meeting the required specifications.
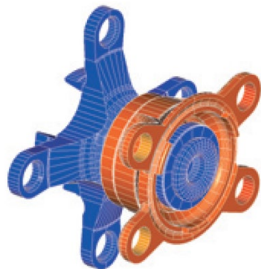
Fig. 2 Shape of developed product by topology optimization

3.4 Development of Torque Reduction

Reduction of torque has always been required for axle unit bearings to improve the vehicle fuel efficiency. However, the requirements are becoming stricter since many countries introduced environmental regulations. NTN has developed various low torque products to respond to market demands for hub bearing applications. **Fig. 3** shows the progression of hub bearings reducing torque.

The torque of axle unit bearings consists of rolling resistance from the rolling balls that follows the rotation of the bearing and the sliding resistance of the seal, which is equipped to seal the bearing. Each represents approximately 50% of the entire torque. Therefore, reducing them is the general approach to reducing the overall torque.

3.4.1 History of Grease Development

The rolling resistance of the bearing is determined by the bearing design and the grease contained in the bearing. The bearing design is optimized to satisfy the customer's demands. The grease contained in the bearing has been developed over many years based on the needs of the customers and the market.
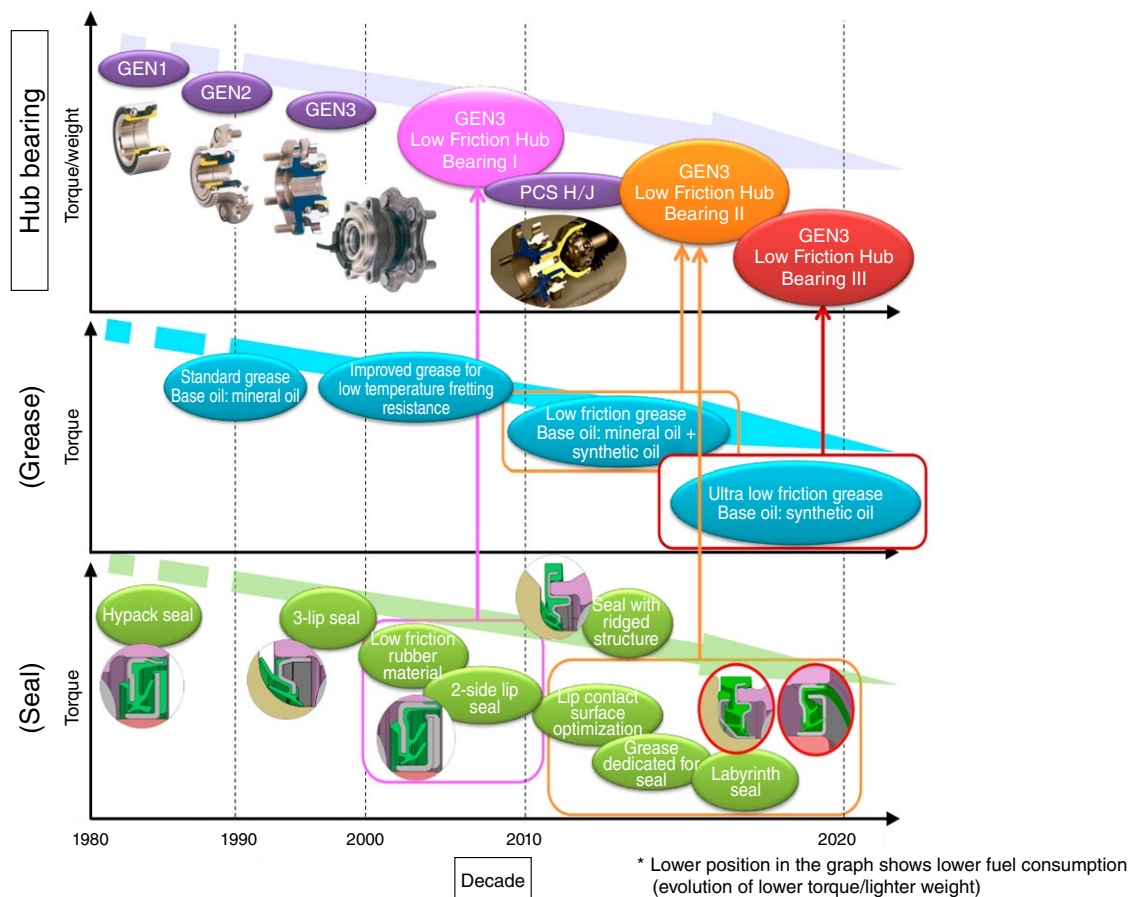

Fig. 3 History of development of hub bearings

The standard grease used in production currently is based on that used for GEN1 production, with improvements made to better its rust resistance properties. In the mid-2010s low friction grease was developed[5] and used on vehicles requiring lower torque. In 2019 the ultra-low friction grease was created further reducing torque. The difference between the three greases are the base oils. The standard grease uses mineral oil, the low friction grease uses a mixture of mineral oil and synthetic oil and the ultra-low friction grease uses synthetic oil. Adopting superior base oil can reduce the viscosity resistance in the low to mid temperature range and, in turn, reduce torque. **NTN** has been optimizing, not only the base oil, but also the thickener and additives which compose the grease, improving the torque property and other grease properties.

3.4.2 History of Seal Development

Various elements of seal sliding resistance have been developed and introduced to the market, such as the optimization of the seal design structure, rubber material, lip contact surface, lip rigidity, etc. without degrading the seal property. By incorporating these elements, the seal torque has been significantly reduced compared to previous seals.

Further torque reduction can be achieved by reducing the number of lips in contact with the rotating components. However, this would degrade the seal function. A new seal was developed adopting a labyrinth structure to combat these issues[5].

For the driven wheels, CVJ does not have to be inserted in the inner diameter. Therefore, a design that seals the inboard side (vehicle side) with a cap is implemented, as shown in **Fig. 4**, which significantly reduces torque by eliminating one of the two seals of the conventional unit.
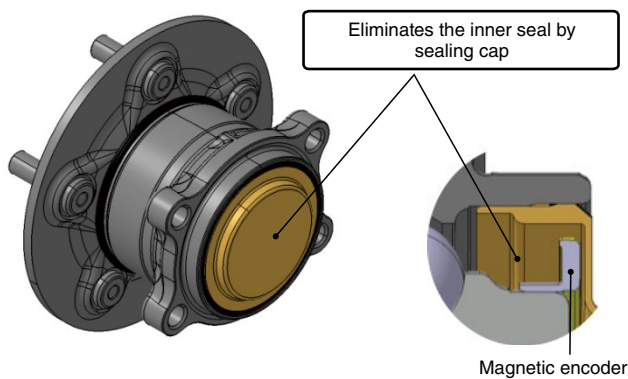
4. Summary

NTN has been working to develop axle unit bearings for over 40 years and has expanded its market with the merger of **NTN-SNR** in 2008, which has enabled its market share has grown to the top. By continuously working to meet the market's needs, we are able to offer products with lower weights and torque than in the past while maintaining reliability. We are excited to continue our development of the next generation of products with new ideas for further reduction of weight and torque.

In this article, we have reviewed the history of axle unit bearings development focusing on reduction of weight and torque. We owe this to the efforts of our pioneers, which we are very proud of, and hope to continue these efforts to construct vehicles with greater functionality and comfort.

References
1) Eiji Funahashi, NTN TECHNICAL REVIEW, No. 70, (2002) 52-57.
2) Masao Kato, Hiroshi Morishita, Kenji Hibi, Kunishige Ototake, NTN TECHNICAL REVIEW, No. 52, (1986) 40-53.
3) Takayuki Norimatsu, Tsutomu Nagata, NTN TECHNICAL REVIEW, No. 81, (2013) 58-63.
4) Haruo Nagatani, Tsuyoshi Niwa, NTN TECHNICAL REVIEW, No.73, (2005) 14-19.
5) Makoto Seki, NTN TECHNICAL REVIEW, No. 85, (2017) 67-71.

Eliminates the inner seal by sealing cap

Magnetic encoder

Fig. 4 Example of sealing cap structure

Photo of author

Makoto SEKI

Automotive Unit Engineering Dept.
Automotive Business Headquarters

History of Development of Constant Velocity Joints Aiming at Low Fuel Consumption

Tatsuro SUGIYAMA*

NTN commercialized the constant velocity joint for the first time in Japan in 1963, and after that, worked on lightweight, compact and high efficiency to meet the evolving needs of automobiles. This article looks back on the history of **NTN**'s constant velocity joints contributing to lower fuel consumption in automobiles.

1. Introduction

Recently, environmental concerns such as global warming have been highlighted globally. For reducing CO_2 emissions, which is the main factor of global warming, auto manufacturers are working on various aspects to reduce fuel consumption.

Under these circumstances, reducing weight and improving torque transmission efficiency are required, for lower fuel consumption, to the Constant Velocity Joint (hereafter, CVJ), which is a component to transmit the vehicle power.

The power from the vehicle engine is transmitted to the tires through the transmission, differential and driveshaft. The CVJ is used to smoothly transmit torque at the same rotational speed when the input and output of the driveshaft rotate at an arbitrary work angle. As shown in **Fig. 1**, "the sliding type CVJ" which can slide in the axial direction is used on the differential side of the driveshaft and "the fixed type CVJ" which has a larger work angle is used on the tire side.
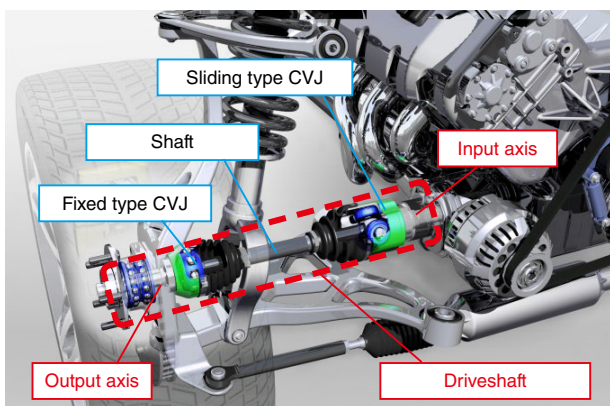

Fig. 1 Placement of driveshaft

* CVJ Development Dept., Automotive Business Headquarters

2. Market Trend/Need

The CVJ has contributed to solving challenges that automobiles face such as safety, environmental protection, low fuel consumption, and ride comfort.

Historically, the fixed CVJ was required for its reduced weight and compactness and then later addressed the increased efficiency requirement. The sliding CVJ was required for its low vibration characteristics and then later addressed the requirement of lightweight and compactness.

Improvements to the grease for CVJ lubrication, higher shaft strength and development of the lightweight E-series have greatly contributed to the above development requirements of CVJs and high efficiency, contributing to lower fuel consumption of vehicles.

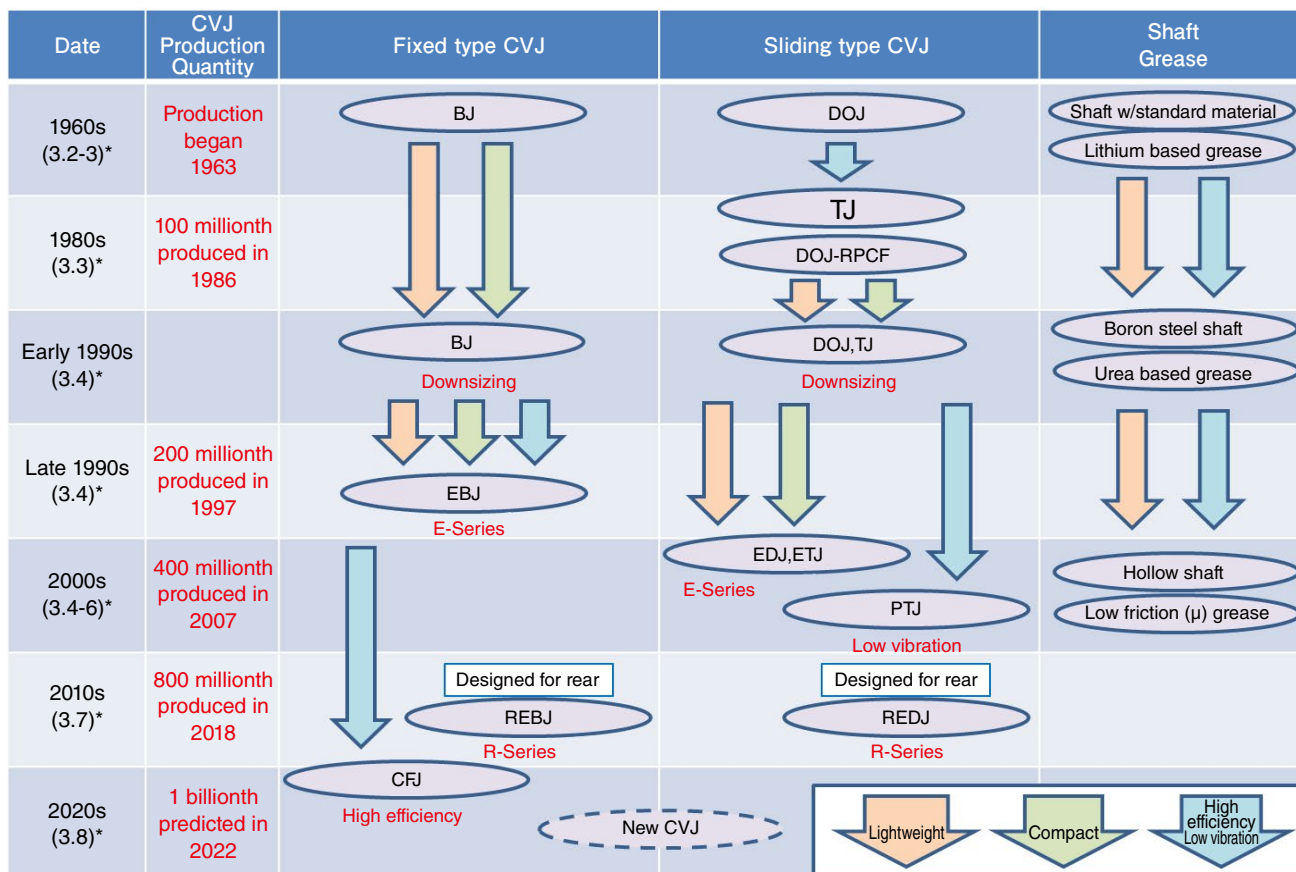## 3. History of Development of CVJ[1)-3)]

3.1 Before Development of CVJ

Vehicles before the 1960s were mostly front engine/rear drive type where power was transmitted to the rear wheels through a rigid axle and a CVJ was not necessary. A CVJ was not necessary for the front wheels either, as they were used only for steering, not for driving.

3.2 Adoption of CVJ to Automobiles (in the 1960s)

In front wheel drive (FF) vehicles and 4-wheel drive (4WD) vehicles, the power is transmitted to the front wheels; therefore, a driveshaft to steer and transmit driving power became necessary. Initially, a cross joint (Cardan joint) was used for the driveshaft. However, since it was not a constant velocity joint, the cross joint produced vibration and noise while driving with a large work angle and steering stability during cornering was poor.

Date	CVJ Production Quantity	Fixed type CVJ	Sliding type CVJ	Shaft Grease
1960s (3.2-3)*	Production began 1963	BJ	DOJ	Shaft w/standard material / Lithium based grease
1980s (3.3)*	100 millionth produced in 1986		TJ / DOJ-RPCF	
Early 1990s (3.4)*		BJ — Downsizing	DOJ,TJ — Downsizing	Boron steel shaft / Urea based grease
Late 1990s (3.4)*	200 millionth produced in 1997	EBJ — E-Series		
2000s (3.4-6)*	400 millionth produced in 2007		EDJ,ETJ — E-Series / PTJ — Low vibration	Hollow shaft / Low friction (μ) grease
2010s (3.7)*	800 millionth produced in 2018	Designed for rear / REBJ — R-Series	Designed for rear / REDJ — R-Series	
2020s (3.8)*	1 billionth predicted in 2022	CFJ — High efficiency / New CVJ		Lightweight / Compact / High efficiency Low vibration

* ( ) following the date indicates the corresponding paragraph in the document text

Fig. 2 History of development of **NTN**'s light weight, compact and high efficiency CVJ

To solve these problems, the Weiss joint, and Double Cardan joint, etc. were developed as the pseudo constant velocity joint; however, their performance was not sufficient enough for the driveshaft of automobiles.

Then, Hardy-Spicer in the UK developed the Birfield joint (BJ) which is a predecessor of the current CVJ for automobiles and **NTN** introduced that technology in their products. At that time, the sliding motion in the axial direction was absorbed by the slide spline installed on the shaft, but the sliding double offset joint (DOJ) developed by **NTN** provided smooth sliding. These CVJs were superior in performance and reliability, improving driving stability significantly, and contributed to the development of FF vehicles.

Fig. 2 shows the history of development of **NTN**'s lightweight, compact and highly efficient CVJ.

3.3 Application to FF vehicles (1963 -)

When automobile manufacturers started developing FF vehicles at full scale, **NTN** worked with Suzulight (Suzuki) to develop the BJ in 1963 and succeeded with volume production of CVJs for the first time in Japan. Then in 1965, the BJ+DOJ, which is the current driveshaft style, was first adopted by the Subaru 1000 model vehicle.

In the 1970s, various auto manufacturers introduced FF vehicles into the market. The second oil crisis of 1978

accelerated the adoption of FF vehicles and the demand for **NTN**'s CVJs expanded. In addition, **NTN**'s CVJs greatly contributed to the expansion of the front engine/rear drive (FR) vehicles, which introduced independent suspension, from the rigid axle style, for improved ride comfort and the development and expansion of 4WD vehicles.

3.4 Lightweight and Compactness (1990 -), E-Series

The manufacturing process of the outer ring of CVJs was changed to induction hardening using medium carbon steel rather than carburized steel to increase strength and reduce weight. Also, urea-based grease was developed to facilitate a long operating life. With these developments, in around 1992, **NTN** started providing driveshafts of one size smaller and lighter than the conventional products.

Furthermore, from around 1995, **NTN** started the next phase of development of fixed/sliding type CVJ for lightweight/compactness and from 1998, started market introduction of the E-Series CVJ. The E-Series CVJ (EBJ) which is the fixed type CVJ, was developed by reducing the ball size and increasing the number of balls from 6 to 8 in order to achieve lighter and smaller units, while maintaining the load carrying capacity equivalent to BJ. Along with this, the sliding type CVJ, "EDJ" was also developed by increasing the number of balls from 6 to 8.
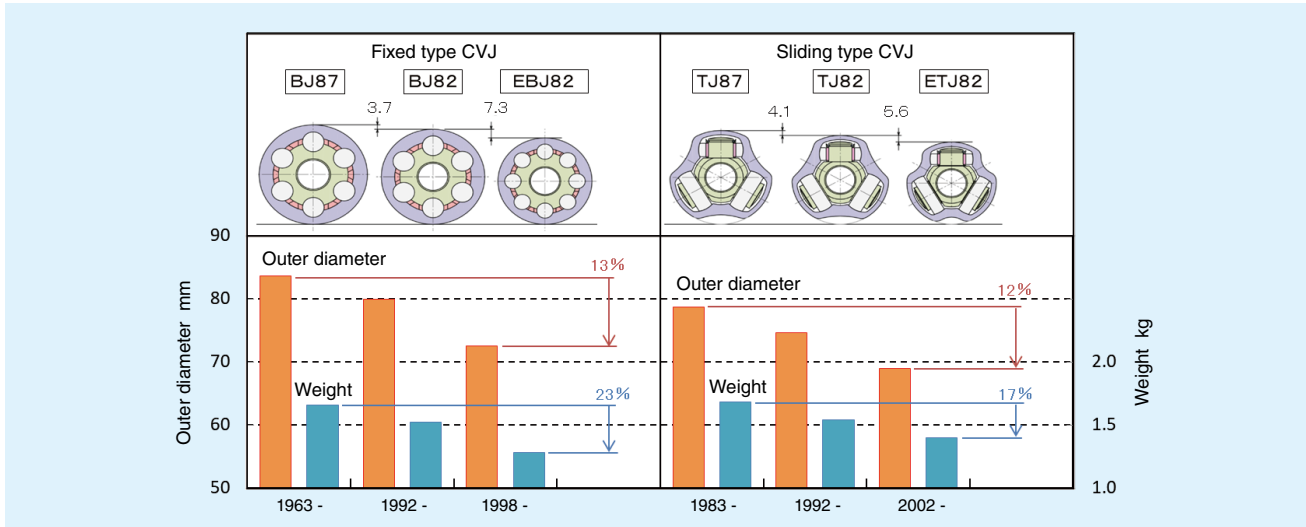
The internal design of the roller type sliding TJ was

Fig. 3 Transition of outer diameter and weight of CVJ (example of the initial #87 size)

also improved at the same time to achieve a smaller unit without degrading strength from the inherent longer operating life than ball type, resulting in the development of "ETJ."

The transition of reduction of weight and size mentioned above is shown as a comparison with the size #87 fixed type BJ and sliding type TJ as the baseline **(Fig. 3)**. The size #87 was downsized to size #82 by application of long-life grease and high-strength shaft and then further reduction equivalent to 2 sizes by introduction of E-Series. Compared to the initial volume production, the current product achieved 13% reduction in size and 23% reduction in weight for fixed type BJ and 12% reduction in size and 17% reduction in weight for sliding type TJ.

3.5 Low Vibration Driveshaft

Along with the development of automobiles, the need for comfort and quietness increased for improved ride comfort, which increased the demand for low vibration sliding type CVJ.

The first developed sliding type CVJ was the ball type DOJ which had large sliding resistance. In 1984, the sliding resistance was successfully reduced by the adoption of *RPCF cage which has a structure to allow a small amount of ball rolling in the axial direction to absorb small amplitude vibrations.

In 1983 the roller type tripod joint (TJ), which was a newly structured sliding CVJ, was developed. Because of its structure of rolling rollers, sliding resistance was significantly reduced compared to DOJ and its adoption by FF AT vehicles expanded due to issues with idling vibration.

Later, TJ was also improved and in 2002, low vibration sliding type CVJ "PTJ" was developed, which allowed rollers to roll smoothly, even in the high work angle range, by combining elliptical trunnion journal shape and roller cassette, for addressing further low vibration and low

sliding resistance **(Fig. 4)**. The history of the development of the sliding type CVJ reduced sliding resistance, which contributed to the reduction of vibration and fuel consumption of vehicles over time.

*RPCF cage: Cage with a structure to allow movement between the cage and inner ring by opening a gap in the axial direction between them, which allows a ball to roll by opening gap between the cage window and the ball.
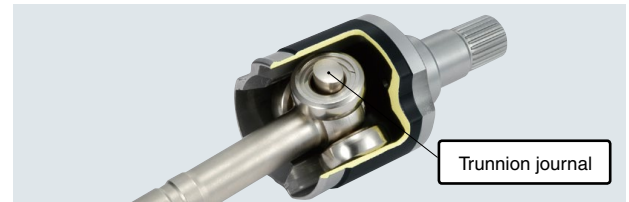
Fig. 4 Structure of PTJ

3.6 Lightweight Shaft (Hollow Shaft)

The shaft is a component to transmit power, connecting the fixed type CVJ and the sliding type CVJ. After achieving reduction of weight by enhancing the strength of the material of the solid shaft, a hollow shaft was developed, which increased rigidity and reduced weight. Volume production of hollow shaft started from the 2000s.

The hollow pipe raw material shown in **Fig. 5** was processed to have the both ends squeezed so they can be inserted to the inner rings of a CVJ. Applying a hollow shaft achieved 20-30% reduction of weight compared with the conventional solid shaft with the same torsional stiffness.
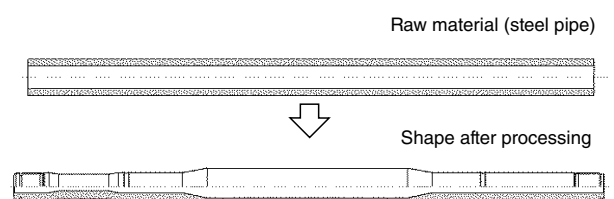

Fig. 5 Structure of hollow shaft

3.7 Light and Compact Rear CVJ (R-Series)[4]

Conventionally, commonly designed CVJs were used for the rear driveshaft of FR vehicles and front driveshaft of FF vehicles. However, since the rear driveshaft of FR vehicles does not require a high work angle, a light and compact R-Series CVJ was developed specifically for rear driveshafts, as shown in **Fig. 6**. Together with the adoption of the hollow shaft and compact boot with less grease, the R-Series accomplished approx. 30% weight reduction compared with the conventional product.
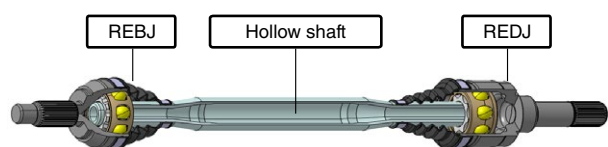
Fig. 6 Structure of R-Series

3.8 Development of High Efficiency Fixed Type CVJ (CFJ)[5]

In 2013, a structure to reduce sliding resistance among the internal components of the fixed type CVJ was developed, as the current structure was causing increased friction loss and thus reduced transmission efficiency as the angle increased. "CFJ" shown in **Fig. 7** places the adjacent arc-shaped tracks mirror-symmetrically, so that the forces that the balls push on the cage with are alternately directed to the open side of the outer ring and the opposite side. These forces have the same magnitude and opposite directions; therefore, they are canceled out resulting in reduced axial displacement of the cage. This design significantly reduces the contact force of the spherical parts between the cage and the outer ring, as well as between the cage and the inner ring. As a result, the torque loss rate against the EBJ improved by approx. 50% (work angle of 9 deg) achieving the world's highest level of efficiency, contributing to low fuel consumption.
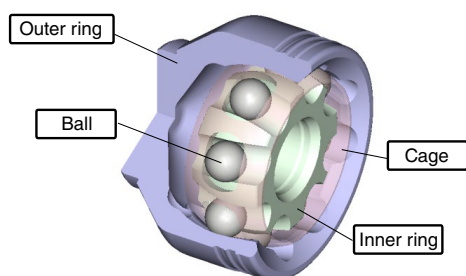
4. Future Development

Although electric vehicles (EVs) are gaining traction, which changes the driving method, the requirement for the driveshaft will stay the same. Therefore, we will continue developing light, compact, highly efficient and quiet CVJs while optimizing strength and durability suitable for the application, use and vehicle characteristics by anticipating the future trends and needs of vehicles.

5. Summary

In this article, the history of the development of the constant velocity joint (CVJ) for driveshaft, which was aimed for low fuel consumption, was reviewed. The performance of vehicles is constantly improving. The functional improvement of constant velocity joints directly and indirectly contribute to this vehicle performance, and therefore, **NTN** will continue developing and supplying CVJs that contribute to vehicle development and are friendly to the global environment.

References

1) Takeshi Ikeda, History of CVJ Design for Automobiles and Recent Technology, NTN TECHNICAL REVIEW, No. 70, (2002) 8-17.
2) Shin Tomogami, Technical Trends in Constant Velocity Universal Joints and the Development of Related Products, NTN TECHNICAL REVIEW, No. 75, (2007) 10-15.
3) Shinichi Takabe, History of Constant Velocity Joints, NTN TECHNICAL REVIEW, No. 85, (2017) 40-45.
4) Tomoshige Kobayashi, Light Weight Drive Shaft for FR vehicle "R series," NTN TECHNICAL REVIEW, No. 85, (2017) 78-83.
5) Teruaki Fujio, Next-generation High Efficiency Fixed Type Constant Velocity Joint "CFJ," NTN TECHNICAL REVIEW, No. 81, (2013) 64-67.

Fig. 7 Structure of CFJ

Photo of author

Tatsuro SUGIYAMA

CVJ Development Dept.
Automotive Business
Headquarters

Low Friction Hub Bearing III

Makoto SEKI*

The Fuel efficiency regulations have been strengthening, therefore the good fuel efficiency is one of the important requirements from the field. Based on this background, **NTN** has been developing the low friction Hub Bearing continuously.

The Low Friction Hub bearing III applicable to such around 60% low torque requirement is introduced in this report.

1. Introduction

Recently, regulations on fuel efficiency and CO_2 emissions have been enhanced globally which has increased the importance of vehicle energy consumption reduction. As a result hub bearings that support wheel rotation are required to further reduce running torque in addition to satisfying basic performance such as operating life and strength.

NTN, which has a high share of hub bearings for vehicles, has long been dedicated to R&D of low consumption technologies for hub bearings. **NTN** has proposed various technologies to achieve the objective[1)-3)].

In this article Low Friction Hub Bearing III is discussed which reduced running torque by 62% when compared to conventional products. It accomplishes this by combining existing items with newly developed grease for reducing torque.

2. Development of Low Torque Hub Bearings

2.1 Structure of Hub Bearings and Contributing Factors for Increasing Torque

An example of the 3rd generation hub bearings is shown in **Fig. 1**.

The torque of hub bearings consists of rolling resistance of the bearing and the sliding resistance of the seals (outer seal and inner seal). Each of them represents approx. 50% of the entire torque. Various reduction technologies have been developed for each of the contributing factors shown in **Fig. 2**. For rolling resistance, optimization of bearing specifications and improvement of bearing internal grease are included. For sliding resistance, improvement of seal rubber material and improvement of seal structure and seal interference are included.

* Automotive Unit Engineering Dept., Automotive Business Headquarters
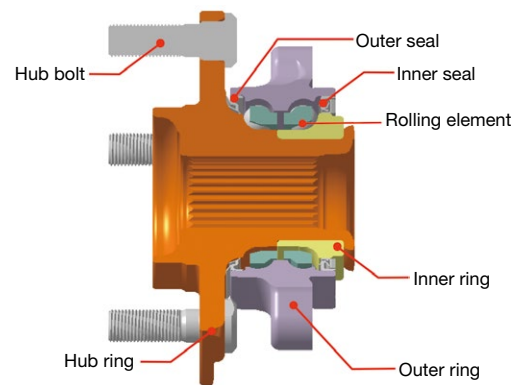
Fig. 1 Example of the 3rd generation hub bearing structure
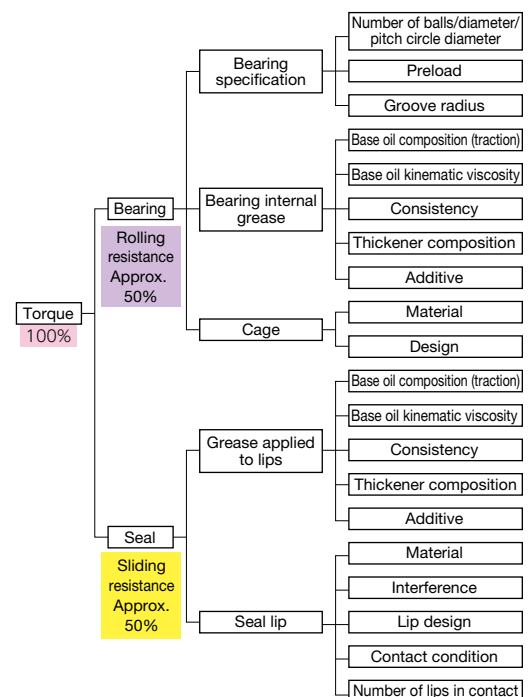
Fig. 2 Contributing factors of bearing torque

2.2 Transition of Low Friction Hub Bearings

NTN has been developing and proposing design specifications for reducing torque. The hub bearings have evolved into Low Friction Hub Bearing I, II and III by applying these design specifications.

An overview of the evolution is shown in **Table 1** and torque reduction ratios to the conventional products are shown in **Fig. 3**. For Low Friction Hub Bearing I, design optimization was mainly applied and for Low Friction Hub Bearing II, improvement of injected grease and

adoption of low friction seals were applied to achieve a significant reduction.

The newly developed Low Friction Hub Bearing III further reduced the torque to achieve a 62% reduction compared to conventional products. This reduction was accomplished by applying the specifications developed in the past and newly developed grease which improved the bearing internal grease used in the Low Friction Hub Bearing II.

Table 1 Transition of Low Friction Hub Bearings

Applied low torque technologies		Low Friction Hub Bearing		
		I	II	III
Bearing	Bearing specification	○	←	◎ * Further improvement
	Bearing internal grease		○	◎ * Further improvement
Seal	Grease applied to lips		○	←
	Lip design	○	←	←
	Lip contact condition		○	←
	Number of lips in contact		○	←
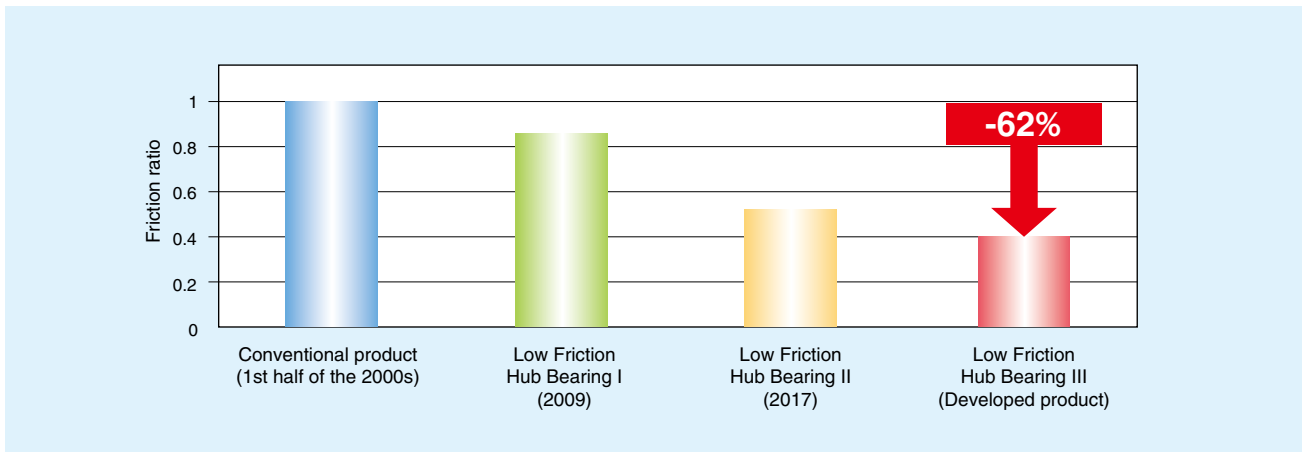
Fig. 3 Transition of development for torque reduction

3. Newly Developed Grease (Reduction of Rolling Resistance)

3.1 Functional Requirements and Specifications of the Developed Grease

The internal grease of hub bearings is required to have the following functions in addition to low friction.

(1) Maintain long operating life by providing sufficient oil film and preventing seizure under the load, temperature and speed conditions of hub bearings
(2) Provide superior fretting resistance under low temperature
(3) Sufficient rust resistance and leakage resistance

Based on the above requirements, the specification of the developed grease was determined as follows: The final concept of the developed grease is shown in **Table 2**.

3.1.1 Reduction of Friction While Maintaining Bearing Operating Life

A microscopic view of the rolling contact point between the ball and groove includes the element of sliding as well. As a result, grease with base oil for reduced kinematic viscosity and low traction coefficient was applied to reduce friction caused by sliding.

When kinematic viscosity of the base oil of the grease is reduced, the risk of insufficient oil film increases. This results in damage to the raceway, as a trade-off condition. Attention is especially required in high load condition as the bearing temperature rises and the grease base oil viscosity further decreases. Low traction base oil was used to control the locally rising temperature for maintaining sufficient oil film thickness and high viscosity index. Vaporization resistance and oxidation resistance were improved

to secure long-term lubricity in the high load region, resulting in an operating life equivalent to or better than conventional products.

3.1.2 Fretting Resistance under Low Temperature

In the long-haul transportation of newly manufactured vehicles on railroad freight cars, small vibrations are generated between the raceway and the rolling elements of a hub bearing. As shown by the red arrows in **Fig. 4**, these vibrations squeeze out grease between the raceway and rolling elements creating metal-to-metal contact causing fretting wear. Fretting wear becomes more significant in low temperature conditions where grease tends to be harder and fluidity decreases. If a vehicle in this condition is driven, abnormal noise may be generated.

In order to ensure grease fluidity in low temperature, base oil of low pour point is applied and thickener and additive were optimized resulting in improved low temperature fretting performance.

Table 2 Concept of developed grease

Grease property	Comparison with the conventional product
Base oil	· High viscosity index · Superior vaporization resistance and oxidation resistance · Low pour point · Low traction
Base oil kinematic viscosity	· Low to room temperature: reduce · High temperature: aim for equivalent to conventional product
Thickener	· Improved composition for low friction
Additive	· Selection of additives to compensate the disadvantages brought in by change of base oil

The condition caused by shaking of the vehicle on the railroad freight car **during the long-haul transportation. The resultant motion while the freight car passes over the rail joints.** (Vehicle is fixed on the bed of the freight car)

Vehicles in transportation

Tire

Small vibrations between the raceway and the rolling elements

Top part of the groove

Bottom part of the groove

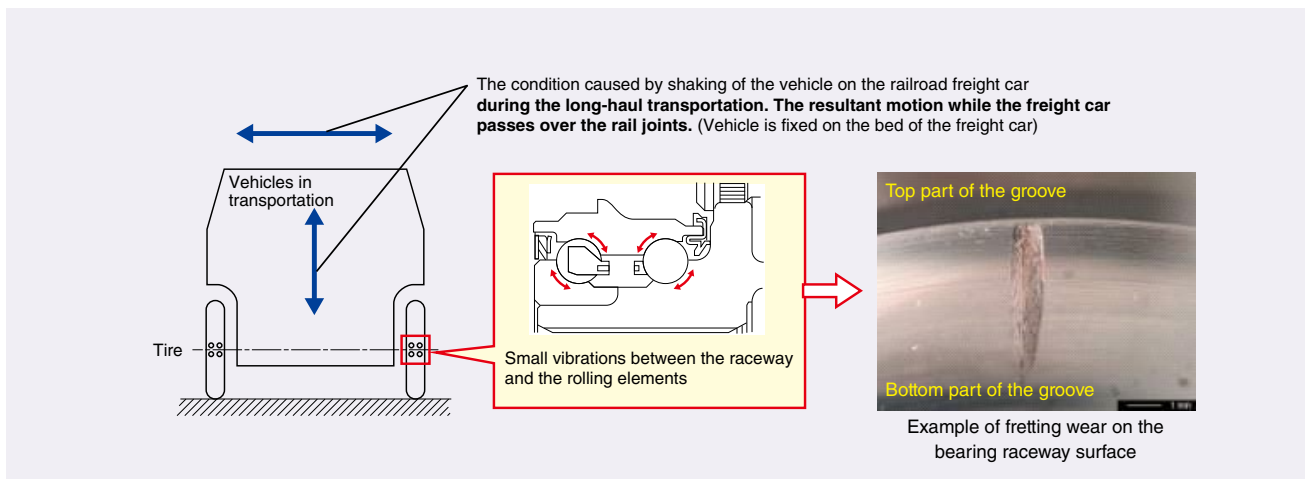Example of fretting wear on the bearing raceway surface

Fig. 4 Mechanism to produce fretting wear

3.2 Evaluation Test

A running torque test was conducted with a hub bearing filled with the developed grease and seals with the rubber lip removed.

The result is shown in **Fig. 5**. The ratio of torque reduction reached to 56% compared to the conventional product (initial 3rd generation hub bearing), validating the reduction effect of rolling resistance of the improved bearing internal grease.

A reliability evaluation test was also conducted to verify the required functionality, as shown in **Table 3**. The bearing with the developed grease satisfied all the development objectives in the test items, fulfilling all the functions required of the bearing internal grease.
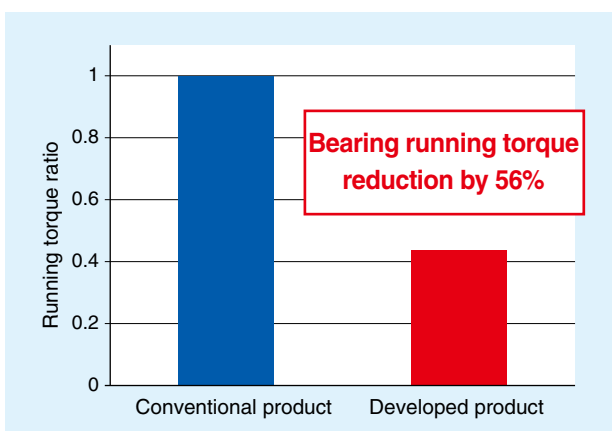
Fig. 5 Running torque test (room temperature)

Table 3 Bearing internal grease reliability evaluation test

Test item	Result
Bearing life from vehicle turns[*1]	More than 3 times over the rated operating life
Seizure during high-speed rotation[*2]	No trace of seizure on the bearing raceway surface
Low temperature fretting[*3]	Wear rate Reduction of 80% compared to the conventional grease

*1 Turning load: 0.6 G load condition
*2 Rotating speed condition when the vehicle speed is 200 km/h
*3 Wear test with small vibrations under the environment of -20°C

4. Ultra Low Friction Seal (Reduction of Sliding Resistance)

The structures of the outer seal and the inner seal adopted by the initial 3rd generation hub bearings (conventional seal) and low friction seals are compared in **Fig. 6**.

Generally, three contacting lips are used to ensure necessary protection against muddy water. However, low friction seals use less contacting lips to further reduce friction. Protection against muddy water, which is degraded by reduction of contacting lips, is preserved by introducing a labyrinth structure and elaborating the lip shape.

Reduction of friction is not only due to the structure but also the rubber material with low friction coefficient, optimized design of the lip contact surface and application of grease dedicated to the lips. Altogether, these items contributed to a reduction of 70% of seal torque compared to conventional products as shown in **Fig. 7**.
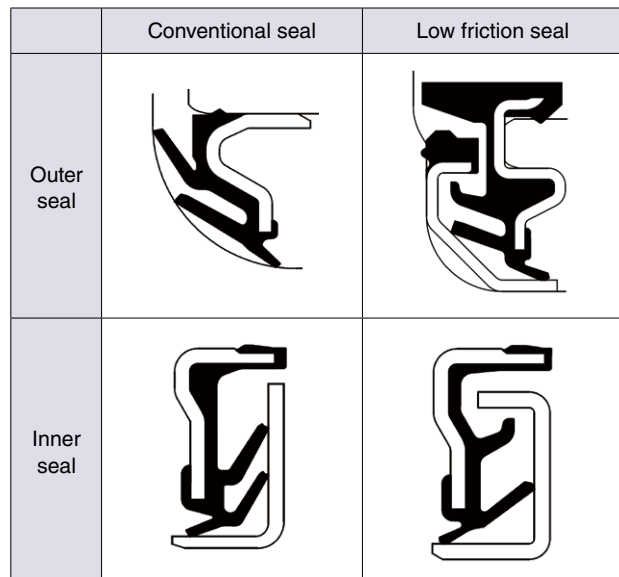
Fig. 6 Structure of conventional seal and low friction seal
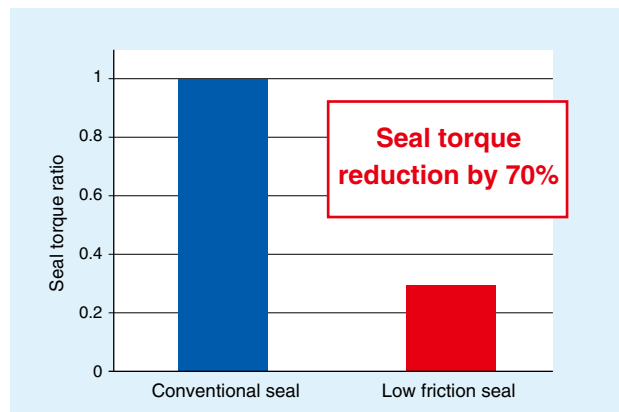
Fig. 7 Seal torque test (room temperature)

5. Low Friction Hub Bearing III

The newly developed bearing internal grease was combined with the existing low friction seal. **Fig. 8** shows the running torque ratio of this bearing. By reducing rolling resistance and sliding resistance of both inner seal and outer seal, 62% of torque reduction effect was obtained for the entire hub bearing.

Fig. 9 shows the performance evaluation chart of the main functional requirements of hub bearings.

It shows that the developed product performed equivalent to or superior to the conventional product in all the functional requirements. The developed product should also be adequate in applications with more severe environments as the fretting resistance in low temperature has significantly improved. In addition, the Low Friction Hub Bearing III decreases the preload upper limit by narrowing the preload range to reduce and stabilize the running torque.

6. Conclusion

In response to the demand for low fuel consumption, new bearing internal grease was developed and combined with the existing technology to introduce Low Friction Hub Bearing III to the market. It has reliability equivalent or greater than the existing products while reducing torque. Some of the technology used in the developed product is already adopted by auto manufacturers.

We will continue to strive to contribute to society and develop products to address the global need for further torque reduction and improved reliability.

References

1) Haruo Nagatani, Tsuyoshi Niwa, Application of Topology Optimization and Shape Optimization for Development of Hub-Bearing Lightening, NTN TECHNICAL REVIEW, No. 73, (2005) 14-19.
2) Kiyotake Shibata, Takayuki Norimatsu, Technical Trends in Axle Bearings and the Development of Related Products, NTN TECHNICAL REVIEW, No. 75, (2007) 29-35.
3) Makoto Seki, Low Friction Hub Bearing, NTN TECHNICAL REVIEW, No. 85, (2017) 67-71.

Fig. 8 Example of running torque ratio of hub bearings

Fig. 9 Performance evaluation chart

Photo of author

Makoto SEKI

Automotive Unit
Engineering Dept.
Automotive Business
Headquarters

Fuel-efficient Compact Chain Tensioner

Kouichi ONIMARU*
Ikumi AGATA**

The fuel efficiency regulations have been forwarded, therefore the automotive industry is developing electrical technology. On the other hand, efforts are being made to reduce engine fuel consumption.

Based on this background, The "Fuel-efficient compact chain tensioner" that achieves downsizing and a significant reduction of oil supply for a hydraulic chain tensioner that adjusts the tension of the timing chain is introduced in this report.

1. Introduction

Recently, regulations on vehicle fuel efficiency and gas emissions have been intensified considering the impact on the global environment, with further regulatory developments planned globally in the coming years.

Therefore, development of electrified technologies, including hybrid technology, is actively pursued in the automotive industry. More efficient internal combustion engines are also being pursued.

NTN develops and manufactures auto tensioners used for timing belt systems and timing chain systems, which transmit the rotation of the crankshaft of internal combustion engines (hereafter, "engines") synchronously to the cam shafts and accessory belt systems for driving accessory devices[1].

The role of an auto tensioner is to appropriately maintain the tension of the belts and chains to reduce the system noise and extend operating life. It also contributes to low fuel consumption by reducing system friction through selecting the optimum specifications to fit particular engines.

NTN has developed a "Fuel-efficient Compact Chain Tensioner" (hereafter, "Chain Tensioner") **(Fig. 1)** as a product to contribute to lower fuel consumption from timing chain systems.

In general, the chain tensioner used in vehicle engines employs a damping mechanism using engine oil supplied from the engine. The aim of **NTN**'s development was to reduce the energy loss and fuel consumption by significantly reducing the amount of engine oil used by the chain tensioner so that the load of the oil pump, which supplies engine oil to the entire engine, is reduced.

In addition, this development included simplification of the internal structure of the tensioner itself for reducing its size and weight to address the market demand for cost reduction. In this article, the structure and features of **NTN**'s developed chain tensioner are introduced.
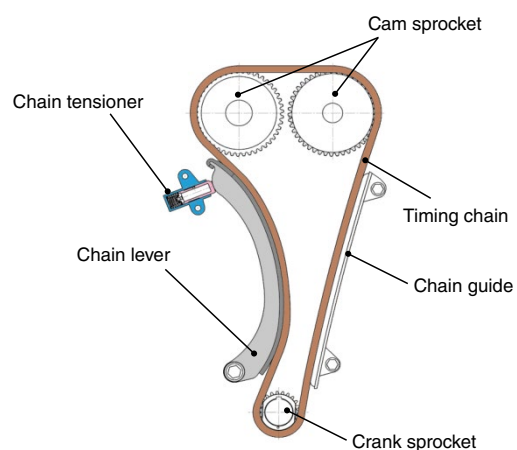
Fig. 1 Example of chain system layout

* Automotive Unit Engineering Dept., Automotive Business Headquarters
** Automotive Testing Dept., Automotive Business Headquarters

2. Structure

Simplified diagrams of the structure of the developed product and the conventional product are shown in **Fig. 2** and **3**. The developed product uses a newly adopted oil circulating structure and oil storage structure, described later in section three. Adoption of an oil storage structure helped eliminate the anti-backlash mechanism shown in **Fig. 3** to simplify the structure. Also, modification of the return spring to a conical spring helped reduce the total length and achieve a more compact size. In case the plunger thrust power is insufficient in certain applications, an assist spring, also shown in **Fig. 3**, can be added for additional power.

Cylinder
Plunger
(Mounting side)
Oil supply port (Cylinder and plunger)
Check valve
Assist spring (purple)
Return spring (green)
(Pressure chamber)

Valve seat
Steel ball
Valve spring
Valve retainer

Check valve
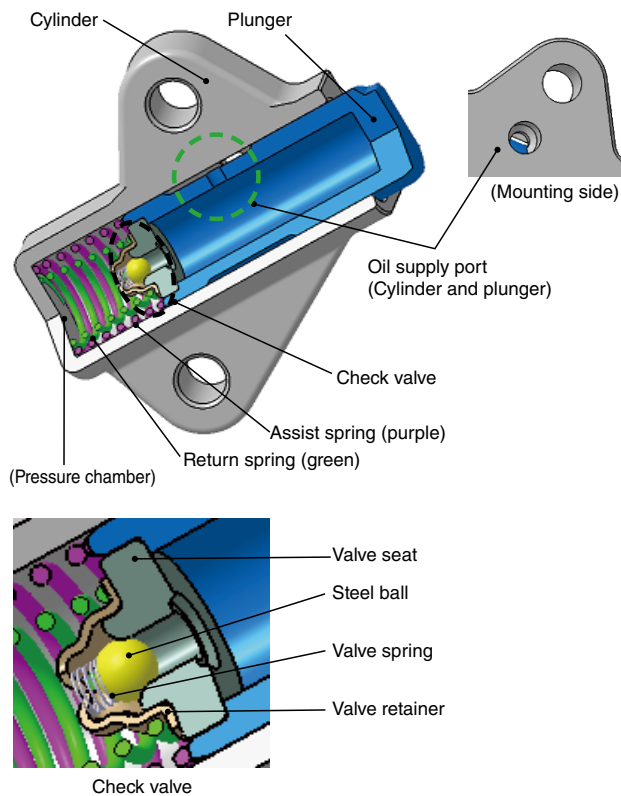
Fig. 2 Structure of Fuel-efficient Compact Chain Tensioner

Groove on cylinder bore
Groove on plunger outer diameter
Register ring
Anti-backlash mechanism
Check valve
Oil supply port
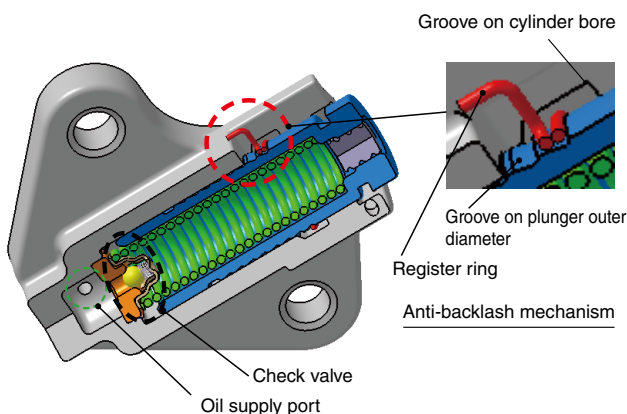
Fig. 3 Structure of conventional chain tensioner

3. Features

The features of **NTN**'s chain tensioner are listed below, compared to our conventional chain tensioner:
(1) Reduction of the oil amount used by adoption of oil circulating structure: 1/10 or less
(2) Activation of damping force from the initial stage by adoption of oil storage structure: elimination of anti-backlash mechanism
(3) Compactness by modification of internal structure **(Fig. 4)**: reduction of total length by 18%, reduction of weight by 10% or more

Reduction by 18%
Weight reduction of 10% or more by the internal parts
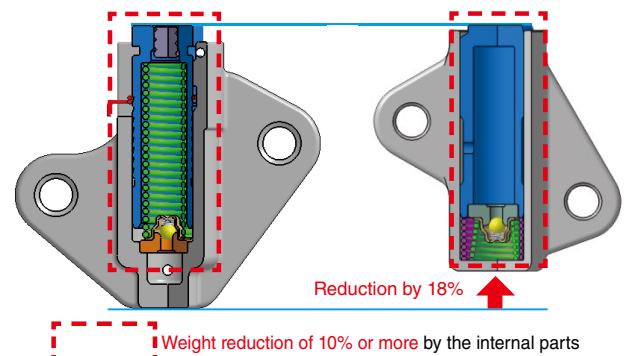
Fig. 4 Compact and light structure

3.1 Contribution to Low Fuel Consumption by Adoption of Oil Circulating Structure

Conventionally, the oil supplied to the chain tensioner is released from the tensioner through the gap between the outer diameter of the plunger and the cylinder bore (leak gap) when damping force is generated. The released oil is stored in the oil pan below the engine to be re-supplied to various parts of the engine by the oil pump. The oil pump is required to have the supply capacity to also return the oil released from the tensioner.

In contrast, the developed product can significantly reduce the amount of oil released out of the tensioner by returning the oil that leaks out through the leak gap (when damping force is generated) back inside the plunger through a side hole on the outer circumference of the plunger **(Fig. 5)**. This enables a significant reduction of the necessary amount of supplied oil while maintaining high reliability and durability as the conventional product. The reduction of the amount of oil used reduces the load the pump is required to drive, which can reduce the size of the oil pump, leading to lower fuel consumption from the engine.
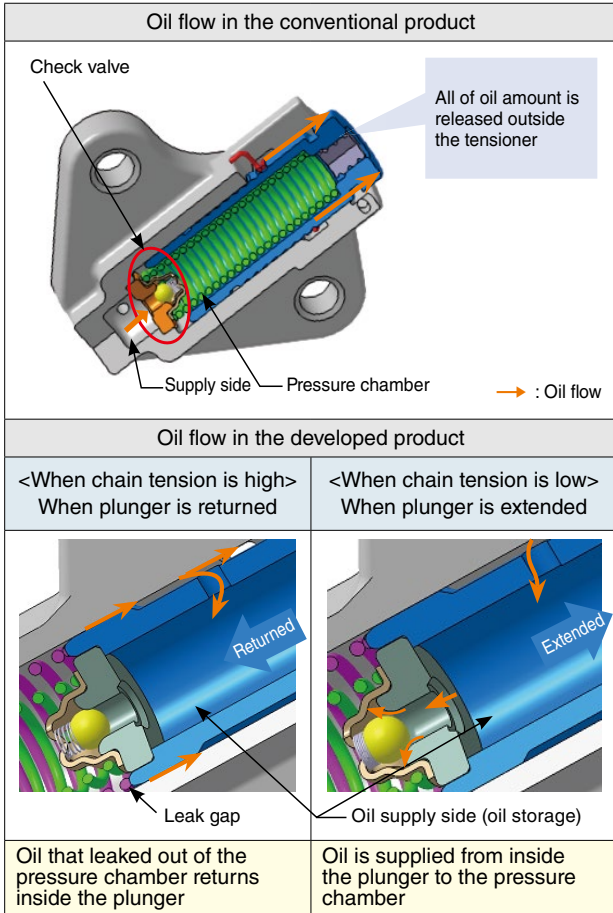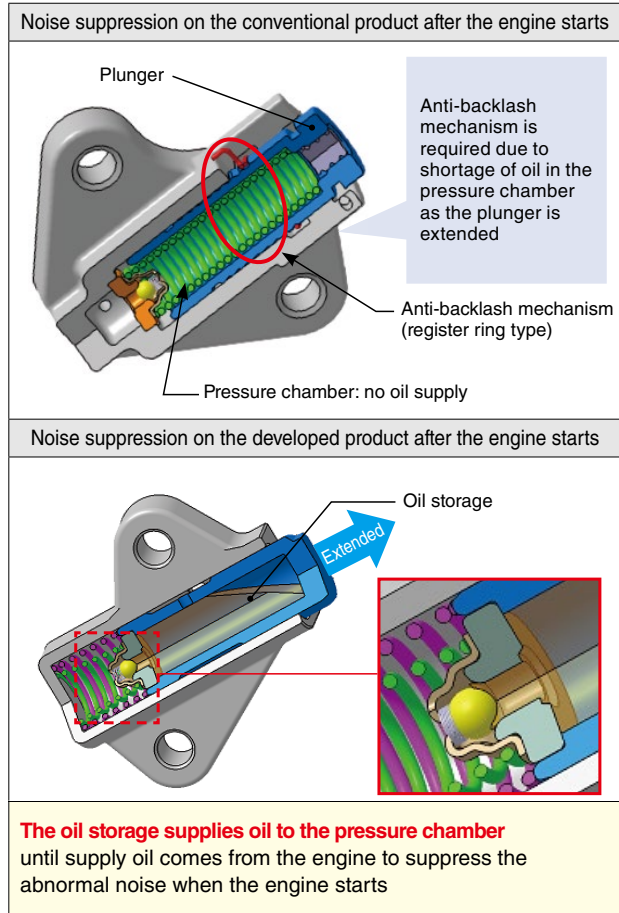
Oil flow in the conventional product

Check valve

All of oil amount is released outside the tensioner

Supply side — Pressure chamber   → : Oil flow

Oil flow in the developed product

<When chain tension is high> When plunger is returned	<When chain tension is low> When plunger is extended

Returned

Extended

Leak gap — Oil supply side (oil storage)

Oil that leaked out of the pressure chamber returns inside the plunger

Oil is supplied from inside the plunger to the pressure chamber

Fig. 5 Oil circulation structure

Noise suppression on the conventional product after the engine starts

Plunger

Anti-backlash mechanism is required due to shortage of oil in the pressure chamber as the plunger is extended

Anti-backlash mechanism (register ring type)

Pressure chamber: no oil supply

Noise suppression on the developed product after the engine starts

Oil storage

Extended

The oil storage supplies oil to the pressure chamber until supply oil comes from the engine to suppress the abnormal noise when the engine starts

Fig. 6 Oil storage structure

3.2 Structure benefit from oil storage

A hydraulic chain tensioner generates the required damping force for adjusting the chain tension using oil supplied from the oil pump. However, as mentioned later, when the engine stops, the oil pump also stops supplying oil, which causes a delay of oil supply to the chain tensioner when the engine restarts. Conventionally, a mechanical anti-backlash mechanism was required to suppress abnormal noise generated due to insufficient tension from the above-mentioned delay for a few seconds after the engine starts.

The developed product adopts a structure to store oil inside the plunger to eliminate the anti-backlash mechanism. By adopting this structure, this stored oil is used until oil is supplied from the oil pump to the chain tensioner after the engine starts to compensate the delay of oil supply, producing appropriate damping force immediately after the engine starts **(Fig. 6)**. Therefore, undesirable noise can be mitigated even when the anti-backlash mechanism is eliminated.

3.3 Compactness/lightweight Design

The developed product achieved reduction of axial length by 18% and reduction of weight by over 10% compared to the conventional product by modifying the

internal specifications and simplifying the structure/ The following are some examples of adopted designs.

1) Size reduction of internal spring **(Fig. 7)**

The total length of the internal spring was reduced by adopting a conical return spring as the main spring. In addition, providing an assist spring on the outer perimeter made it possible to cope with a wide range of thrust requirements.

Reduction

Adoption of conical spring   Assist spring
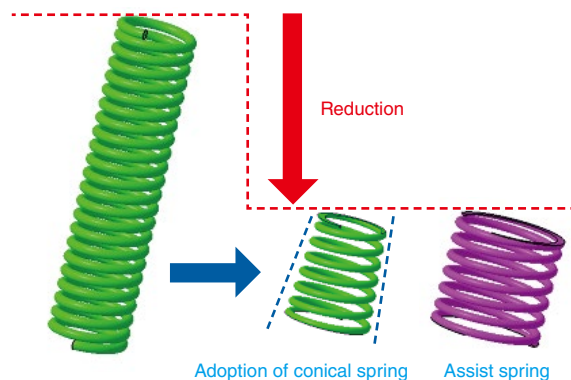
Fig. 7 Spring shape

2) Streamlined cylinder

Eliminating the anti-backlash mechanism also eliminated the need for the register ring and multiple grooves on the outer diameter of the plunger. The groove to accommodate the register ring on the cylinder bore is not required any more, making it possible to streamline the cylinder outer diameter.

(Additional notes)

(1) Anti-backlash mechanism (conventional product)

A mechanism to suppress vibration of the timing chain due to no oil supply immediately after the engine starts even when no damping force is produced on the chain tensioner. **NTN** has two mechanisms: a buttress thread type, which uses the frictional force of the screw and has small backlash and quiet operation, and a register ring type, which has a simplified structure with a ring and stepped grooves[1), 2)].

(2) Role of the check valve **(Fig. 8)**
- When the chain has tension, the plunger is pushed back and the pressure of the pressure chamber (a) becomes higher than the oil supply pressure (b), the check valve is closed and damping force is produced.
- When the chain loses tension, the plunger is extended and the pressure of the pressure chamber (a) becomes lower than the oil supply pressure (b), and the steel ball moves and oil flows into the pressure chamber.

<When chain tension is high>	<When chain tension is low>
Check valve closed	Oil inflow
Pressure a>b	Pressure a<b
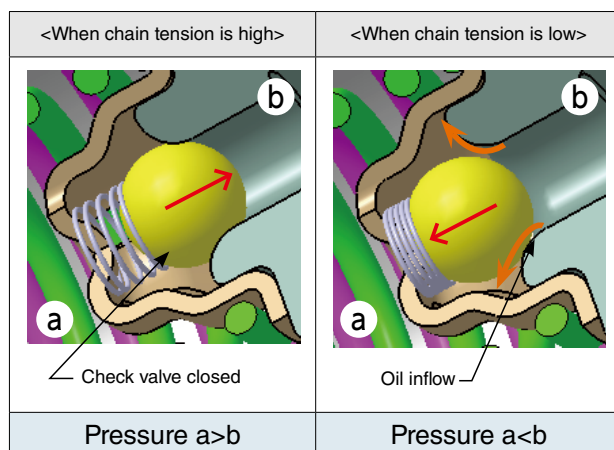
Fig. 8 Role of check valve

(3) Delay of oil supply when the engine starts **(Fig. 9)**

In general, oil is supplied to the chain tensioner by the oil pump, which pumps out oil in the oil pan located at the bottom of the engine. Since rotation of the oil pump usually works together with rotation of the engine, oil is not supplied while the engine stops. Therefore, oil in the piping of the engine drops back into the oil pan a while after the engine stops.

When the engine starts, oil is re-supplied to the chain tensioner through the piping, which causes a delay before the chain tensioner is supplied with oil again.
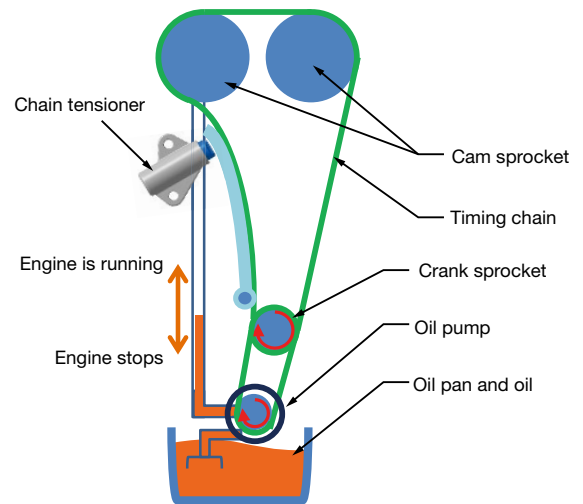
Fig. 9 Concept of oil supply

4. Functional Evaluation

4.1 Comparison of oil consumption

To evaluate the oil circulating structure, which is a feature of the developed product, operation with the actual product was simulated to measure the amount of oil released from the chain tensioner (oil consumed) under vibration and the result was compared with the conventional product. During the test, oil was supplied to the chain tensioner and the orientation of the sample was horizontal **(Fig. 10)**. Below is an example of the evaluation conditions and the evaluation result. The comparison was made with the samples having an equivalent damping capacity (load generated when vibration was applied).

<Example of the evaluation conditions>
- Amplitude of applied vibration : ± 0.2mm
- Frequency of applied vibration : 100Hz
- Supply oil pressure : 0.2MPa
- Oil type : SAE 10W-30
- Oil temperature : 35°C, 100°C
- Measurement of oil amount : 30s
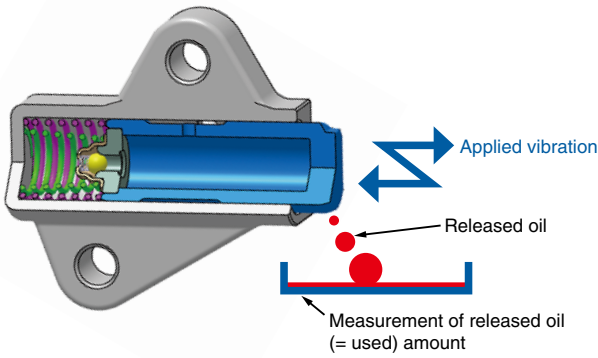
Fig. 10 Measurement of used oil amount

The developed product could reduce oil consumption to 1/10 or less compared with a conventional product with the equivalent damping capacity **(Fig. 11)**.
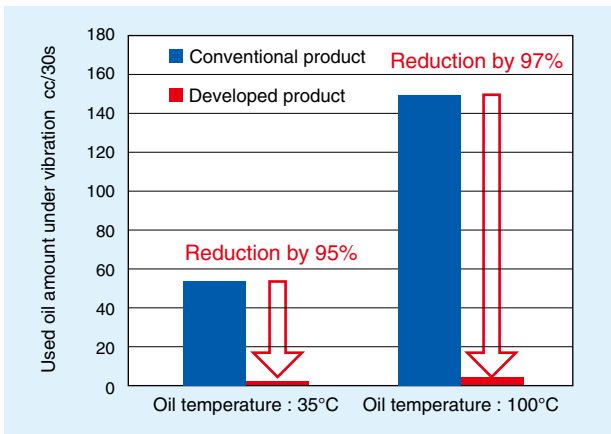

Fig. 11 Measurement result of used oil amount

4.2 Evaluation at Start-up of the Engine

In order to verify the impact of eliminating the anti-backlash mechanism and verify the function of the oil storage structure, a test was conducted simulating the engine start-up using the actual engine. By verifying the displacement of the plunger and the input load, the effect of the aforementioned delay of oil supply at the engine start-up was determined. The following are some examples of the evaluation results.

When the plunger is quickly extended due to the start-up of the engine (the condition from (1) to (2) in **Fig. 12**) and no oil is supplied from the engine, damping force is produced by internal oil stored in the oil storage giving an appropriate tension to the chain, in an early stage, which suppressed the vibration of the chain (amplitude of the plunger displacement). The result verified that the anti-backlash mechanism can be eliminated.
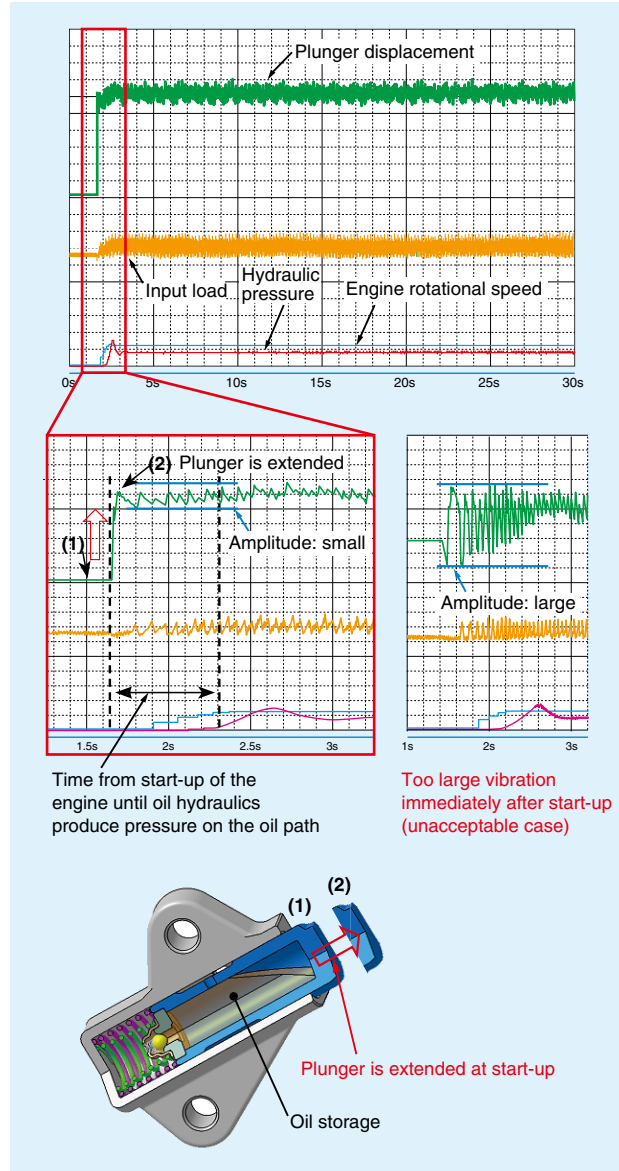
Fig. 12 Result of evaluation of behavior at start-up of the engine

4.3 Oil Hydraulics Damping Property

A dynamic characteristics evaluation test was conducted to evaluate the dynamic reaction force of the chain tensioner when vibration is applied to index the basic damping force of the hydraulic chain tensioner. In the dynamic characteristics evaluation, the load generated by the applied vibration is verified while supplying oil to the chain tensioner; therefore, the impact of various parameters such as the leak gap, check valve load and spring load can be verified. The evaluation can be conducted on the platform simulating the operation with the engine. The following is an example of the evaluation conditions:

<Evaluation conditions>
- Amplitude of applied vibration : ± 0.2mm
- Frequency of applied vibration : -200Hz
- Supply oil pressure : 0.3MPa
- Oil type : SAE 10W-30
- Oil temperature : 35°C

Fig. 13 shows the comparison of the evaluation results of the developed and conventional product. The developed product shows load generation up to higher frequencies, similar to the conventional product, which verifies good followability? and basic damping capacity. The maximum and minimum values in **Fig. 13** are the results obtained from the Lissajous figure (**Fig. 14** Amplitude-Generated Load) at various frequencies.
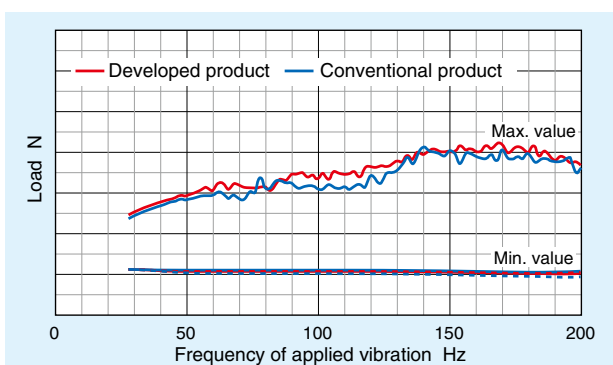
Fig. 13 Dynamic characteristics evaluation test result
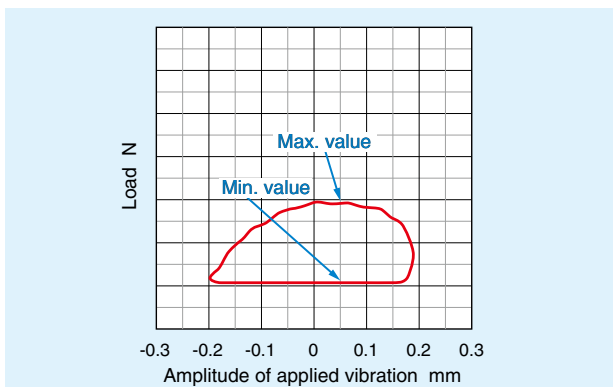
Fig. 14 Lissajous figure (developed product)

Photo of authors

Kouichi ONIMARU

Automotive Unit
Engineering Dept.
Automotive Business
Headquarters

Ikumi AGATA

Automotive Testing Dept.
Automotive Business
Headquarters

5. Conclusion

In this article, the Fuel-efficient Compact Chain Tensioner was introduced. The developed product achieved reduced oil consumption in the tensioner to 1/10 or less, compared to the conventional product. The functionality of the conventional product was maintained by adopting the structure to circulate oil in the tensioner, which contributes to lower fuel consumption of the engine by reducing the load to the oil pump. In addition, the developed product achieved a reduction in length by 18% and a reduction of weight by 10% by simplifying the structure and reducing the size of the tensioner.

We will devote ourselves to further development and promote product development for higher functionality.

References
1) Seiji Sato, Technology Trends in Auto Tensioners, NTN TECHNICAL REVIEW, No. 79, (2011) 83-89.
2) Kouichi Onimaru, Chain Tensioner for Motorcycle Engine, NTN TECHNICAL REVIEW, No. 85, (2017) 72-77.

Fixed Constant Velocity Joint with Ultra High Angle and High Efficiency "CFJ-W"

Masashi FUNAHASHI*
Mika KOHARA*

In the future, it is increasingly required to improve the energy efficiency of automotive parts and the added value of automobiles. So, by applying **NTN**'s proprietary technology, we have developed the fixed constant velocity joint "CFJ-W" with the highest maximum working angle and high efficiency in the world.

1. Introduction

In 2015, parties agreed via the Paris Agreement, to maintain the average global temperature rise attributed to greenhouse gas emissions from human activities, to below 2 degrees Celsius. Automobiles account for approx. 18% of the CO_2 emissions of energy origin, and therefore, energy efficiency improvement of automotive components is an urgent issue[1].

At the same time, longer wheelbases for larger passenger compartments, and larger size tires for driving stability, have become the vehicle trend. These trends affect the vehicle's minimum turning radius and require a larger wheel angle in order to maintain the same turning radius of conventional vehicles.

The wheel angle is determined by vehicle design restrictions and the maximum bending angle (hereafter, "maximum working angle") of the fixed type constant velocity joint (hereafter, "fixed type CVJ") installed on the tire side.

So in this article, the fixed type CVJ, "CFJ-W", is introduced. The CFJ-W has the world's highest level of both efficiency and working angle and can contribute to the reduction of CO_2 emissions, deliver larger passenger compartments and increase vehicle driving stability.

2. About the Driveshaft

The driveshaft is a component that smoothly transmits engine power (both rotation and torque), to the tires at constant speed, even when the input shaft (differential gear shaft) and the output shaft (wheel shaft) are rotated at an angle. In general, the driveshaft consists of a fixed type CVJ, a sliding type CVJ, and a shaft to connect them together **(Fig. 1)**. The fixed type CVJ can have a large working angle, but cannot slide in the axial direction; the sliding type CVJ has a small working angle, but allows for movement in the axial direction.

In 1997, ahead of the competition, **NTN** developed the "EBJ (with a maximum working angle of 47°)[2]", a light, compact and highly efficient joint. Then in 2012, for a light, compact, wide-angle, fixed type CVJ, **NTN** started production of the "VUJ (with a maximum working angle of 50°)". Also in 2012, **NTN** introduced the "CFJ (with a maximum working angle of 47°)[3]", which through **NTN** proprietary design, reduced torque loss by half in comparison to **NTN**'s EBJ. As such, **NTN** has shown a track record of improving on joint efficiencies and widening angles.
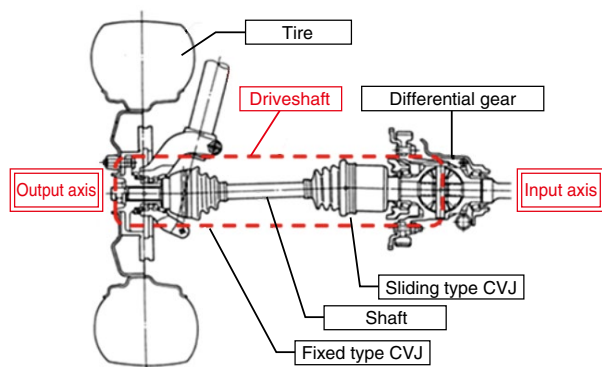
Fig. 1 Placement of driveshaft

3. CFJ-W Structure and Features

3.1 Structure

The CFJ-W basically follows the structure of the existing already developed CFJ; it consists of an inner race and an outer race, both of which have raceway grooves (hereafter, "tracks") for the 8 balls that transmit running torque, a cage that holds the balls and a boot that can operate to the maximum working angle of 55° **(Fig. 2)**.

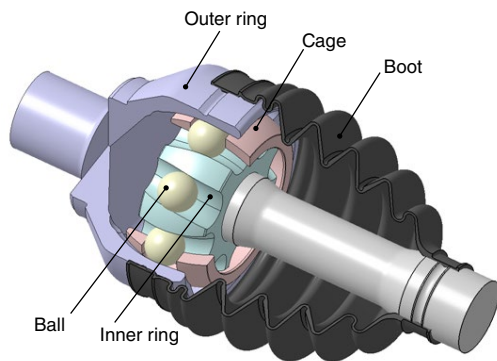* CVJ Development Dept., Automotive Business Headquarters

Fig. 2 Structure of CFJ-W

3.2 Features

Adopting **NTN**'s proprietary spherical cross groove structure technology **(Fig. 3)** made it possible to reduce the force generated within CVJ (internal force) upon torque load, as well as to increase the load carrying capacity. This enabled smooth operation of the CVJ internal components, even under tough operating conditions. Additionally, applying **NTN**'s technology helped the CFJ-W achieve the world's largest maximum working angle and transmission efficiency, while maintaining an outer race diameter and weight similar to a conventional high-angle fixed type CVJ (i.e. VUJ). (**Table 1** and **Fig. 4**)

To ensure quality, the associated boot shape was redesigned to withstand the wider CFJ-W angle, while maintaining outer race diameter dimensions that are equivalent to those of conventional boots.
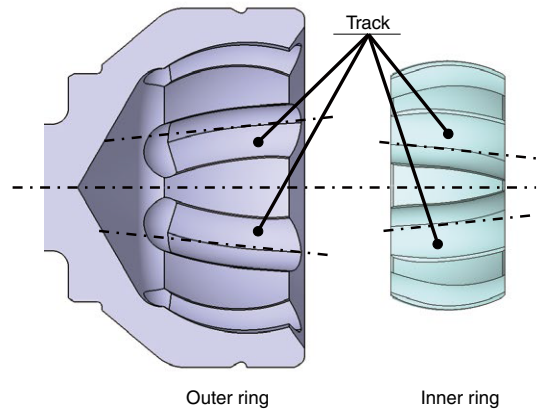
Feature 1: The arc-shaped tracks of the inner and outer rings are tilted in the axial direction, and adjacent tracks are mirrored.
Feature 2: The inner track and the outer track cross the slope of each other, and the ball is placed at the intersection.

Fig. 3 Spherical cross groove structure

Table 1 Comparison of VUJ and CFJ-W

Item	Conventional Product VUJ92	Developed Product CFJ92W
Max. Working Angle (°)	50	55
Outer Race Outer Diameter mm	Φ87.8	Φ88
Number of Balls	6	8
Ball Diameter mm	Φ17.462	Φ15.081
Weight kg	1.64	1.60
Torque Loss	−	Over 50% reduction compared to the conventional product

VUJ92 (Maximum working angle 50 degrees)　　　CFJ92W (Maximum working angle 55 degrees)
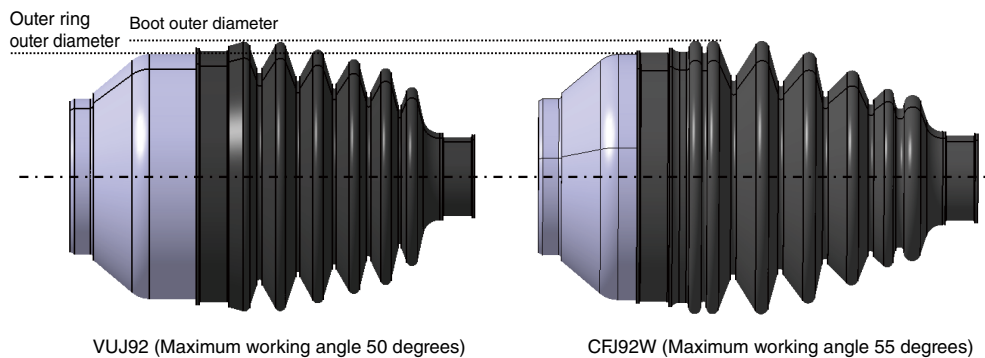
Fig. 4 Appearance of VUJ and CFJ-W

3.3 Achieving High Efficiency & a Large Maximum Working Angle (50 Degrees-Plus)

Within conventional joint (i.e. EBJs, VUJs) structures, the ball tracks on the inner and outer race are formed in an arc shape (shown in **Fig. 5**), with the arc centers offset in opposite directions from each other from the center of the joint. On the other hand, the CFJ-W inner and outer races' arc-shaped track centers are not offset, but slanted in the axial direction, with adjacent tracks symmetrically placed with the angles of the inner and outer race tracks crossing each other (shown in **Fig. 6**). This ensures the functionality of the CVJ and greatly contributes to the achievement of both a large maximum working angle (working angle of over 50 degrees) and high efficiency.
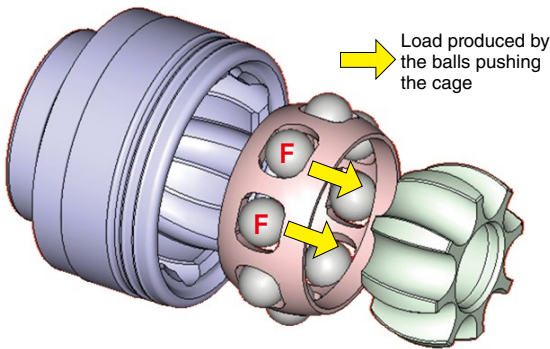
Fig. 5 Structure of EBJ (conventional product), internal force
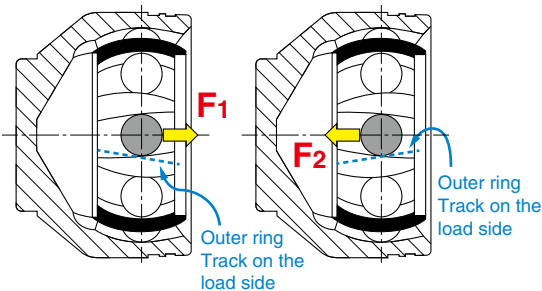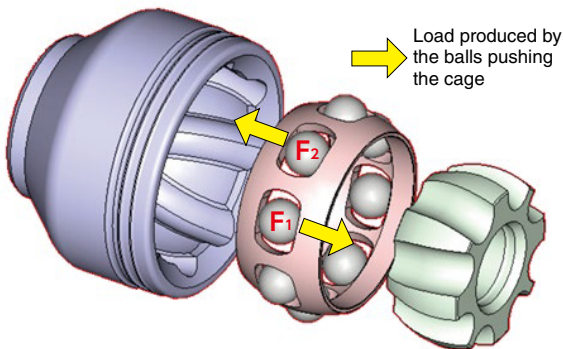
Fig. 6 Structure of CFJ and CFJ-W, internal force

1) CVJ Internal Force

As mentioned above, the CFJ-W has adjacent arc-shaped tracks axially inclined and placed symmetrically relative to each other. The intended affect for this design is to have the adjacent balls push the cage in opposite directions, canceling out the resultant forces that suppress the axial displacement of the cage (shown in **Fig. 6**). This significantly reduces the spherical contact force between the cage and outer race, and between the cage and inner race, which greatly improves torque loss ratio.

Also, it is known that as the CVJ working angle increases, the load produced inside the CVJ increases independent of torque input[4]. Along with this increased load, the load on the CVJ internal components also increases resulting in increased heat and degraded strength. At the high working angle range, the CFJ-W's spherical cross groove structure reduces the contact force produced inside the CVJ. As evidenced by the spherical contact force analysis in **Fig. 7**, the aforementioned structure nearly eliminates the contact force in the normal operating range. Even at the high working angle range, close to the maximum working angle, the contact force is reduced in comparison to that of the conventional product, contributing to the achievement of functionality in the range beyond 50 degrees.
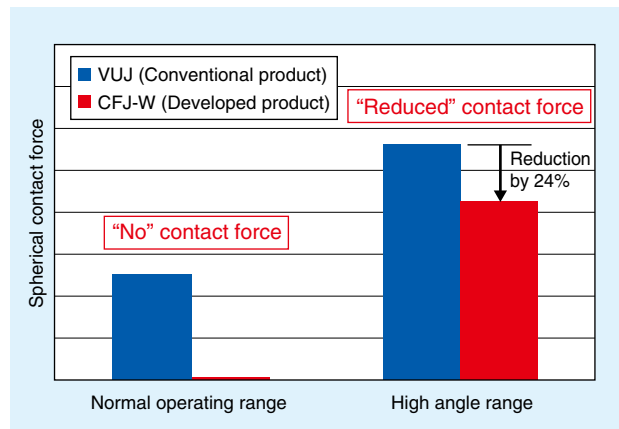

**Fig. 7** Analysis result of spherical contact force

2) Load Carrying Capacity

For achieving a maximum working angle beyond 50 degrees, it is important to control deformation of the internal components. Internal component deformation is mainly a product of ball and track contact at high working angles and high torque inputs. Therefore, it is necessary to keep sufficient track depth at the high working angle range. The CFJ-W's spherical cross groove structure positions the CFJ-W inner and outer races' arc-shaped track center in the same plane as the center of the joint which ensures the same track depth at any range (**Fig. 8** hatched area), improving the load carrying capacity of the CFJ-W at the high

working angle range. This differs from that of the conventional joint which has the inherent problem of reduced track depth at the high working angle range.

Enlarged

Inner ring track depth

Outer ring track depth
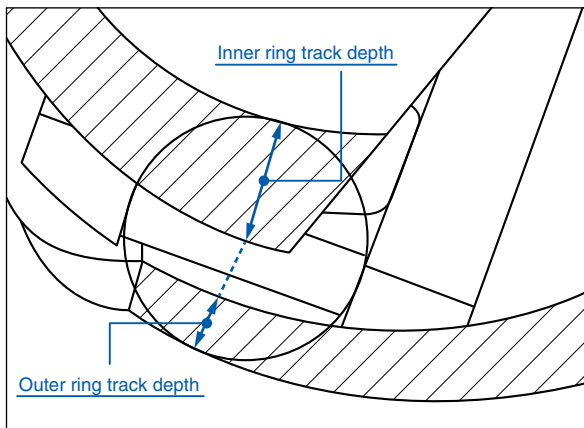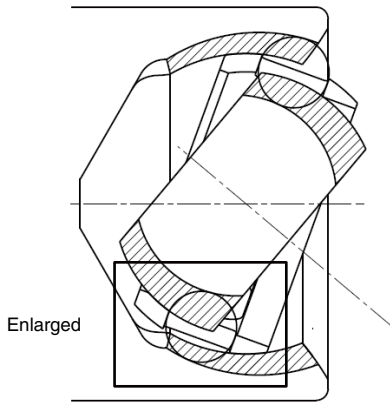
Enlarged view of EBJ (conventional product)

Inner ring track depth

Outer ring track depth
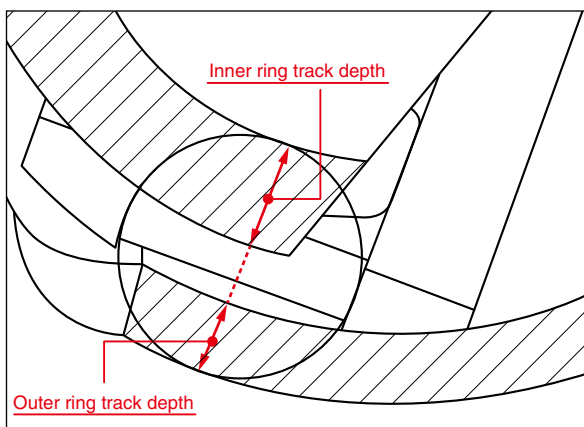
Enlarged view of developed product

Fig. 8 Comparison of track depths

3) Grease

NTN has developed various high-functional greases used selectively in various CVJ types and applications. In order to achieve a 50-plus degree maximum working angle and high efficiency, internal force reduction as well as lubrication improvement is required.

By optimizing the thickener and additive, which resulted in outstanding grease fluidity and lower friction respectively, the CFJ-W grease reduced the friction coefficient in the SRV (vibration/friction/wear) test, as shown in **Fig. 9**. In the Torque Loss Test (**Fig. 9**) for an EBJ (conventional joint), this grease showed a 22% improvement in performance in comparison to the general-purpose grease's performance in the same test. This supports that this grease's use in a CFJ-W, can further reduce torque loss and heat generation.

Joint under evaluation: EBJ (conventional product)

Friction coefficient

Improved by 22%

General purpose grease   Applied grease
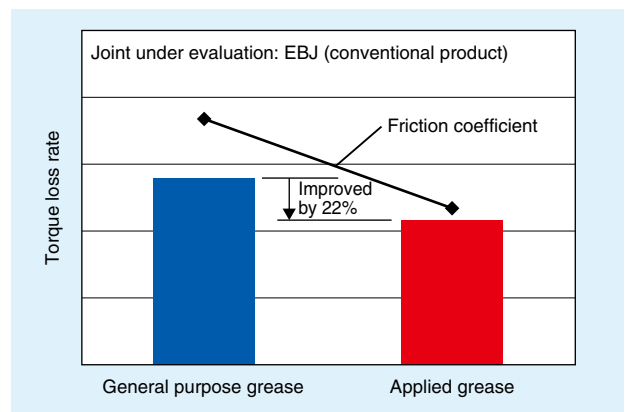
Fig. 9 Comparison of torque loss rate by grease

4) Functional Evaluation

The results of the CFJ-W (developed joint) and VUJ (conventional joint) dynamic high-angle torsional strength evaluation, transmission efficiency (torque loss rate) evaluation and temperature rise characteristics (joint surface temperature) are shown in **Fig. 10**, **Fig. 11** and **Fig. 12**, respectively of the developed product, CFJ-W, and the conventional product, VUJ, are shown in **Fig. 10**, **Fig. 11** and **Fig. 12**, respectively.

At high angles, close to the maximum working angle, the CFJ-W and VUJ show equivalent strength. Transmission efficiency evaluation confirmed similar performances between the CFJ-W and the current high-efficiency fixed type CVJ, the CFJ; the torque loss was reduced by over 50% at any angle range in comparison to the VUJ (the current high-angle fixed type CVJ). Additionally, the temperature rise characteristics comparison show a 55% joint surface temperature reduction between the CFJ-W and CFJ.

These results show that the CFJ-W has the world's highest level of efficiency in its normal operating range, as well as low temperature rise and sufficient strength at the severe operating conditions of working angles over 50 degrees.
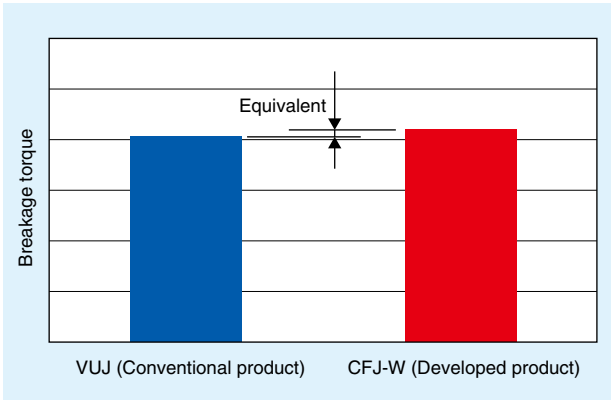
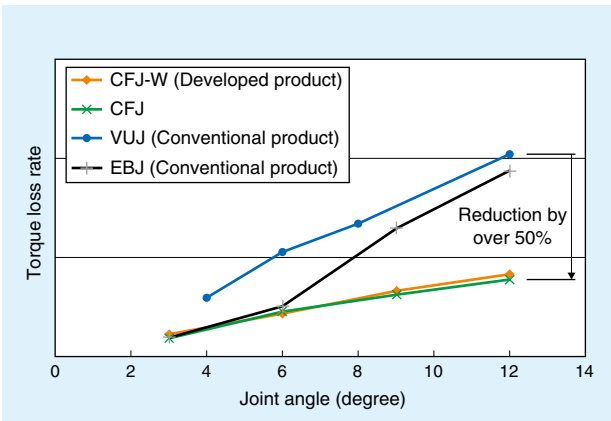**Fig. 10** Comparison of high-angle torsional strengths

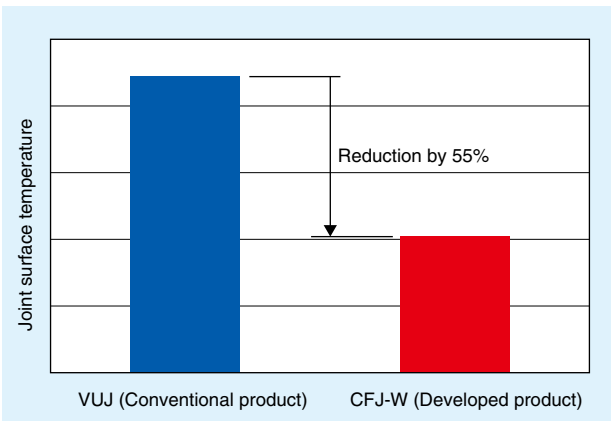**Fig. 11** Comparison of torque loss rates

Fig. 12 Comparison of joint surface temperatures

4. Development of CFJ-W Dedicated Resin Boot

Since this joint achieved the maximum working angle of 55 degrees, which is the world's greatest for vehicles' front driveshafts, the boot applied also had to match this capability. This boot would be required to withstand angles higher than that of a conventional high-angle boot (for 50 degrees) and demanded boot shape improvements.

The CFJ-W boot needed to achieve the ultra-high working angle, while meeting the same functional and performance requirements of other fixed type CVJs, specifically the following items:

   (1) Durability and Sealability:
      equivalent to the conventional joint
   (2) Compactness:
      equivalent to the conventional joint
   (3) No clamp interference:
      no clamp interference at the maximum angle

4.1 Durability

An appropriate boot bellow length is required to ensure boot durability. There are different approaches to accomplish this, such as increasing the number of convolutes, increasing the boot large diameter and decreasing the boot small diameter. However, each of these techniques brings unfavorable consequences such as:

   (1) increasing vehicle space needed for boot packaging and installation
   (2) decreasing boot flexibility
   (3) increasing the friction between adjacent boot convolutes
   (4) increasing the chance of interference of the small diameter inner convolute with the IC shaft
   (5) increasing the axial load on the clamp when the boot bellows are retracted

The boot developed for the CFJ-W addressed all the aforementioned issues through the addition of multiple, smaller multiple convolutes on both ends of the boot with these convolutes the same size as those used by conventional boots (as indicated by the circles in **Fig. 13**). In addition, to protect against friction at larger working angles, when considering the increased contact surface pressure between convolutes, a suitable material was selected. As a result, this boot achieved comparable durability to conventional boots.
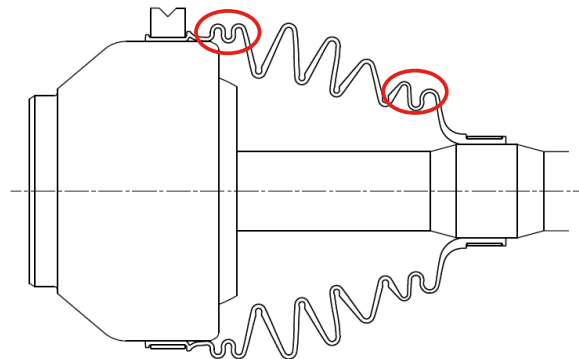

Fig. 13 Sectional view of the boot (working angle: 0 degrees)

4.2 Clamp Compactness and Interference Control

CVJ boots are designed considering interference with the joint and peripheral components, in addition to needing to be flexible at higher working angles. The bellow of the CFJ-W boot was designed with the optimum ratio of large and small diameter convolutes to achieve a small packaging requirement, even at high angle operations. Also, this design, while allowing the bellow to be convoluted on the outer diameter of the outer race, including the addition of the small convolutes with no clamp interference, protects the boot from being damaged by the clamp (as shown in **Fig. 14**).

Clamp
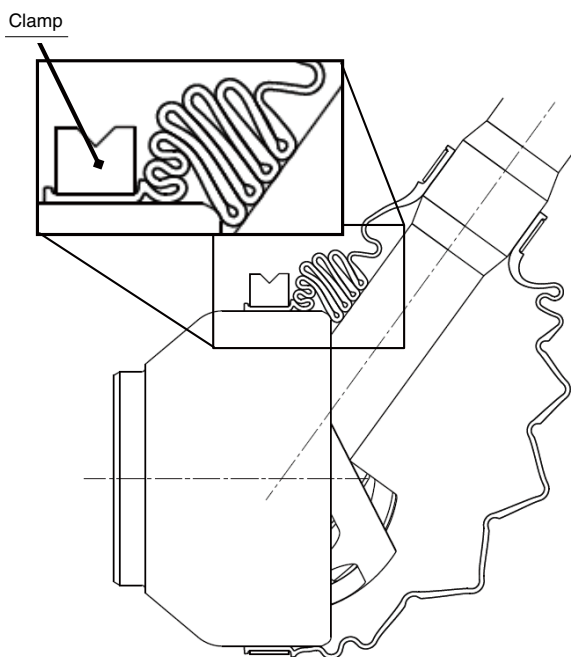
Fig. 14 Sectional view of the boot (working angle: 55 degrees)

5. Conclusion

In this article, the features and performance of "CFJ-W" were introduced; the CFJ-W achieves both the "world's highest maximum working angle of 55 degrees" and "reduction of approx. 50% of torque loss rate in comparison to the conventional CVJ (VUJ)" by improving the load carrying capacity of each component and enhancing lubrication of **NTN**'s proprietary "CFJ" product, which was announced in 2012.

This developed product can be applied to the front wheels of 4-wheel drive vehicles, while achieving the same minimum turning radius as the rear wheel drive vehicles, as well as to reduce the adverse impact on fuel consumption due to increase of vehicle weight.

NTN hopes to introduce this product globally as the world's benchmark for fixed type CVJs, achieving both high functionality and low CO_2 emission which are becoming increasingly required for vehicles globally.

References

1) IEA, CO_2 emissions from fuel combustion,(2018).
2) Keisuke Sone, Kazuhiko Hozumi, High Efficiency Compact Fixed Constant Velocity Universal Joints (EBJ), NTN TECHNICAL REVIEW, No. 66, (1997) 28-31.
3) Teruaki Fujio, Next-generation High Efficiency Fixed Type Constant Velocity Joint "CFJ," NTN TECHNICAL REVIEW, No. 81, (2013) 64-67.
4) Yoshihiko Hayama, Dynamic Analysis of Forces Generated on Internal Parts for Ball Type Constant Velocity Joint, NTN TECHNICAL REVIEW, No. 70, (2002) 36-43.

Photo of authors

Masashi FUNAHASHI
CVJ Development Dept.
Automotive Business
Headquarters

Mika KOHARA
CVJ Development Dept.
Automotive Business
Headquarters

Compact Plunging CVJ for Propeller Shaft "HEDJ-P"

Masazumi KOBAYASHI*

Constant velocity joints for propeller shaft have been applied to 4WD and FR vehicles since the 1970s. And further small size and light weight are desired to CVJ for propeller shaft.
This article introduces the new product "HEDJ-P" for propeller shaft.

1. Introduction

Propeller shafts are used on a variety of vehicles and take the role of transferring transmission rotation to the front and rear driving shafts, as shown in **Fig. 1**. Application of the constant velocity joint (CVJ) for propeller shafts has recently increased in Luxury Car and SUV's applications due to emphasis on reducing NVH (Noise, Vibration and Harshness) and ongoing demands to further reduce size and weight for lower fuel consumption.

Although **NTN** has existing production of compact and lightweight sliding type propeller shaft CVJ joints, known as "HEDJ" here we introduce the new "HEDJ-P". This new joint is dedicated for propeller shafts to address the need for further size and weight reductions and has achieved the world's highest level in these categories.
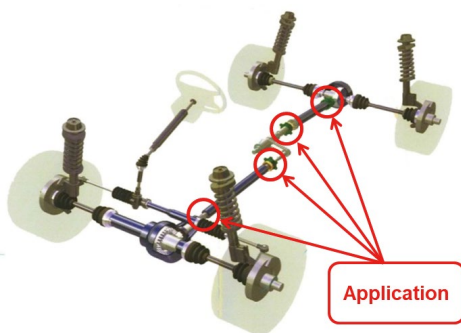
Fig. 1 Application of CVJ for propeller shaft

2. Features of CVJ for Propeller Shafts[1)-3)]

NTN's CVJ was first adopted for propeller shafts of automotive vehicles in the first half of the 1970s. The demand significantly increased from the latter half of the 1980s with a increased need of high functionality and diversification of vehicles. Due to noise and ride comfort requirements of 4WD vehicles and complex powertrain configurations CVJs have been adopted replacing the conventional Cardan joint (not constant velocity joint, using cross shaft). **Fig. 2** shows the manufacturing timeline of **NTN**'s CVJs for propeller shafts.

The main operating conditions of CVJ are rotation, load torque and work angle. The propeller shaft transmits power between the transmission and differential and the driveshaft transmits power between the differential and the wheels. With the position of the propeller shaft the rotational speed is higher and the load torque is smaller than the driveshaft. In general, the propeller shaft does not require a large work angle as the driveshaft due to its layout and functional requirements.

NTN has a lineup of various types and sizes of the CVJs for propeller shafts to meet the increase in propeller shaft structures and functional requirements in vehicles. Initially the design was common with CVJ's for driveshafts (BJ/DOJ/TJ/LJ); however, addressing the market demand for high speed rotation, CVJs modifications of internal clearance and surface treatment were offered as the CVJs for propeller shafts (conventional series). CVJs for driveshafts were modified to be more compact/light type, E-Series (EBJ/EDJ/ETJ), to address the demand for smaller and lighter components. In addition, H-Series for supporting high speed operation are enhanced to address the needs of every type of vehicles **(Fig. 3)**.

An appropriate sliding type CVJ must be selected based on the required sliding amount, outer diameter size, characteristics and operating condition. **Table 1** shows the main basic performance of H-Series sliding type CVJs and a comparison of their characteristics.

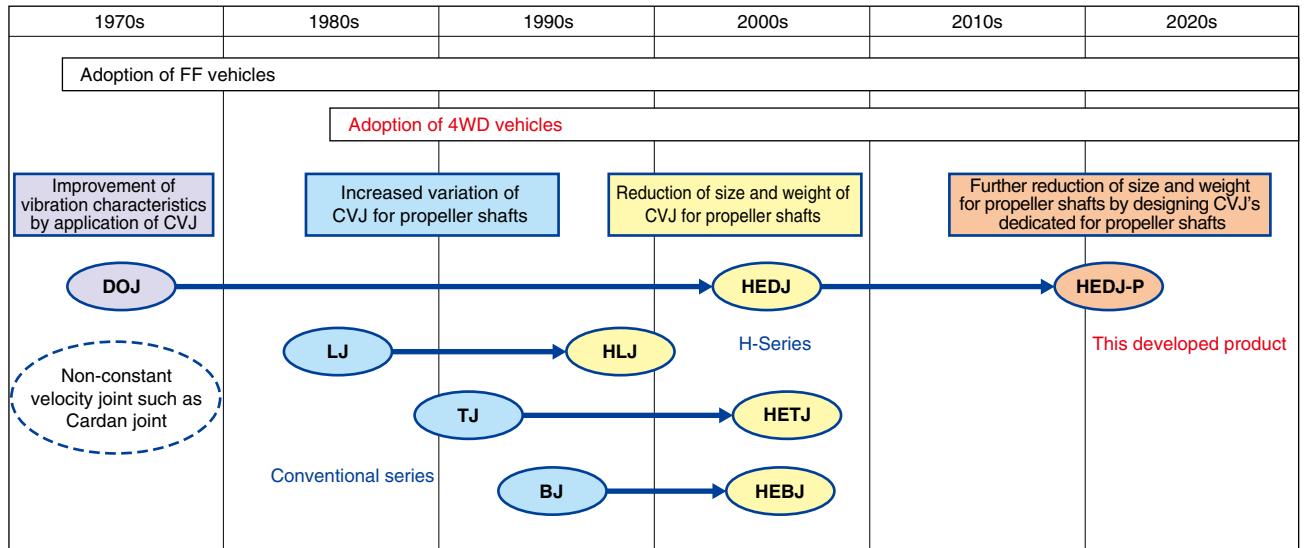* CVJ Development Dept., Automotive Business Headquarters

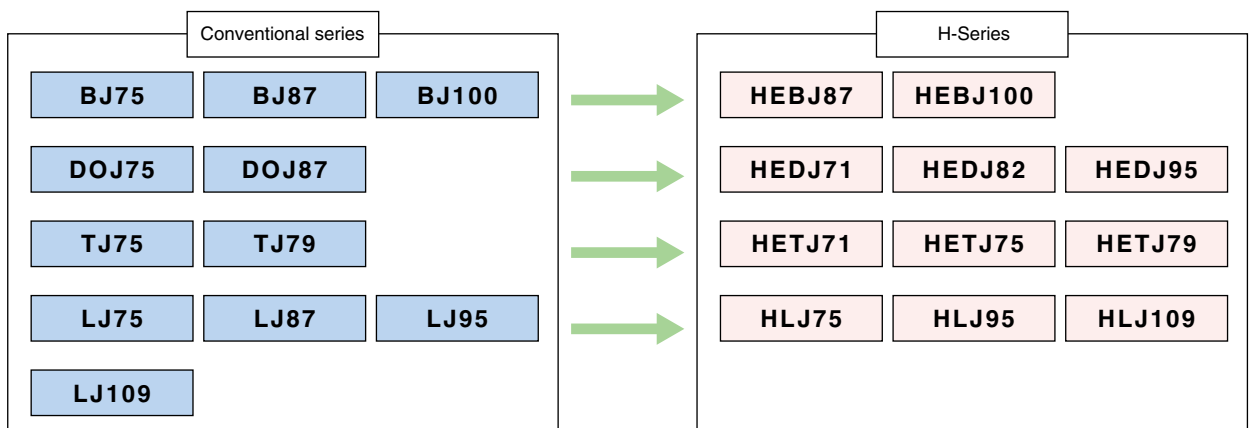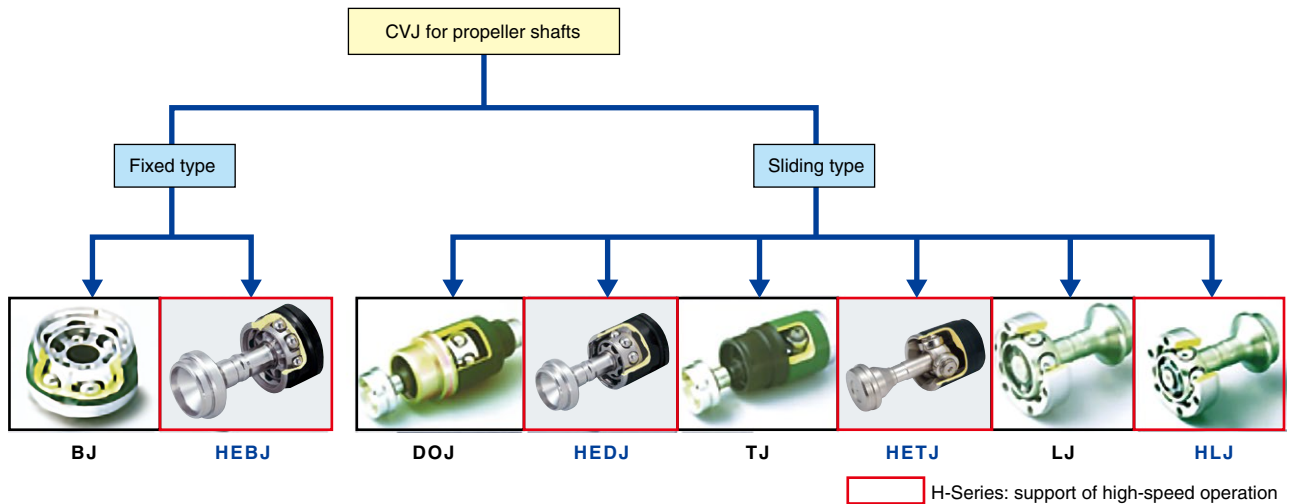**Fig. 2** Manufacturing timeline of CVJ for propeller shafts

BJ   HEBJ   DOJ   HEDJ   TJ   HETJ   LJ   HLJ

H-Series: support of high-speed operation

Fig. 3 Type and size of CVJ for propeller shafts

Table 1 Comparison of characteristics of various sliding type CVJs

		Sliding type		
		HEDJ	HETJ	HLJ
Sliding amount		+++	+++	++
Allowed angle		+++	+	++
High speed operation		++	+	+++
Heat generation		++	+++	+
NVH characteristics	Sliding resistance	++	+++	+
	Induced force	8th order	3rd order	6th/3rd order
Backlash	Axial	++	+	+++
	Radial	++	+	+++

+++: Excellent ++: Good +: Fair

3. Structure and Features of Developed Product

The newly developed HEDJ-P is redesign of the conventional HEDJ to make the outer ring even more compact and the inner ring thinner for dedicated use with propeller shafts.

As shown in **Table 1**, HEDJ has relatively superior balance of NVH characteristics and large sliding amount/angle. These attributes contribute to the increased degree of freedom for vehicle design and ease of mounting on vehicles. It is suitable especially for SUVs which have larger operating angles, and adopted by many vehicle models. That is the reason why it was selected as the base of the new development.
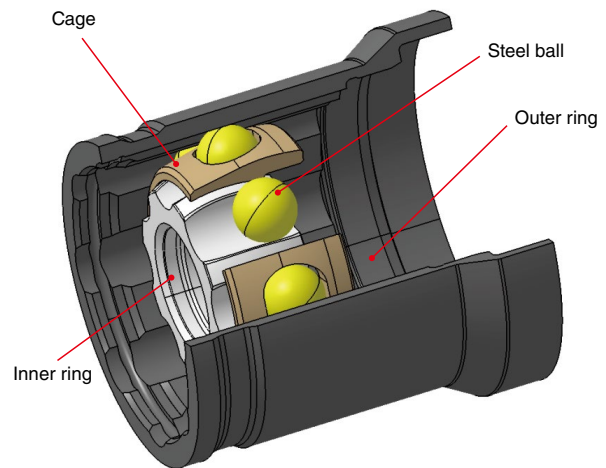
3.1 Structure

The joint itself consists of an inner ring, outer ring, cage and 8 steel balls, as shown in **Fig. 4**, similar to the conventional HEDJ.

For the cage, the RPCF cage was adopted so that it can absorb small vibrations of vehicles, similar to the conventional product. **Fig. 5** shows the structure of the RPCF cage. The RPCF cage has a clearance between the steel ball and the cage pocket and a cylindrical part on the inner diameter of the cage so that the inner ring and the cage can mutually move in the axial direction.

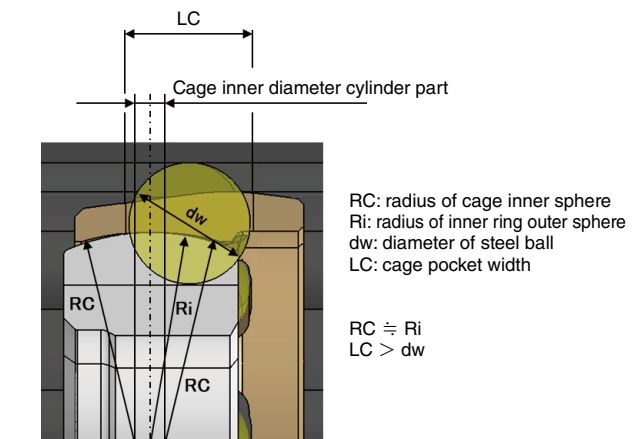This allows the small vehicle vibrations to be absorbed in the joint, blocking the vibrations.

Fig. 4 Structure of the developed product

RC: radius of cage inner sphere
Ri: radius of inner ring outer sphere
dw: diameter of steel ball
LC: cage pocket width

$RC \fallingdotseq Ri$
$LC > dw$

Fig. 5 Structure of RPCF cage

3.2 Compactness/lightweight

Since the inner ring and cage of the conventional HEDJ are common with EDJ for driveshafts, the maximum work angle of the joint alone (without the boot installed) is 25 degrees.

On the other hand, CVJs for propeller shafts only require the maximum work angle of around 10 degrees for vehicle assembly (with the boot installed) and around 15 degrees for the joint alone.

HEDJ-P focused on the functions required by the propeller shafts limiting the maximum work angle to 15 degrees and to achieve reduction of outer diameter by 6%, weight by 17% while maintaining the equivalent performance as HEDJ in the same operating range. This was achieved by reducing the outer diameter of the outer ring and PCD (ball pitch circle diameter), thinning the inner ring and reducing the widths of inner ring and the cage.

Fig. 6 shows a comparison of the developed product with the conventional HEDJ, **Fig. 7** shows a comparison of the outer diameters, and **Fig. 8** shows a comparison of weights.
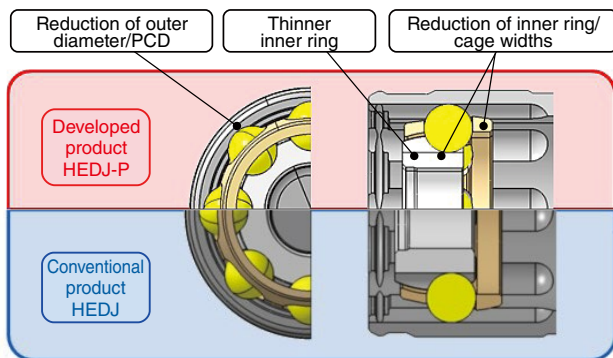
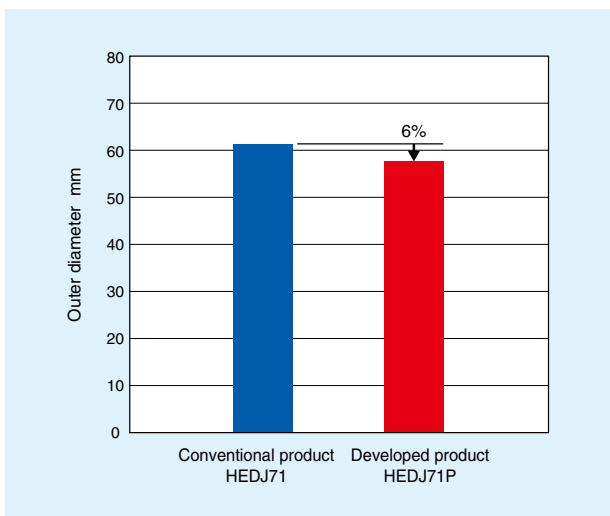**Fig. 6** Comparison of developed product and conventional product

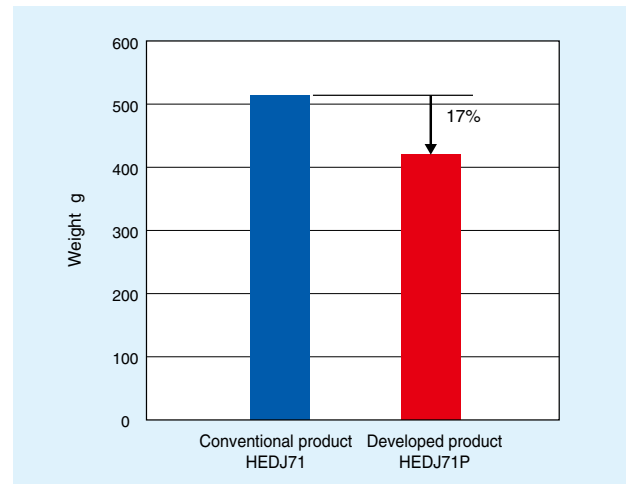**Fig. 7** Comparison of outer diameters

Fig. 8 Comparison of weights

3.3 Functional Evaluation

Fig. 9 shows the result of the static torsional strength test of the developed product HEDJ71P.

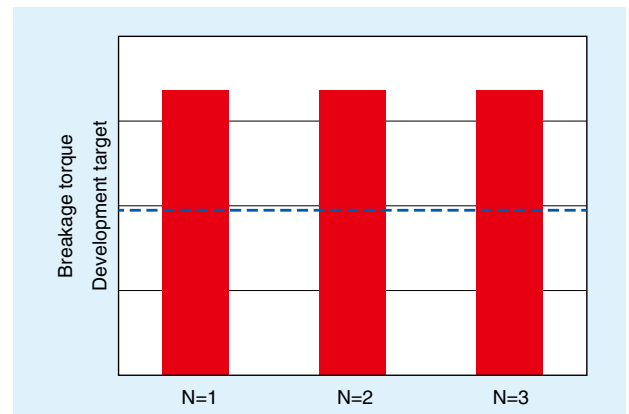HEDJ71P has sufficient static torsional strength compared to the conventional product.

Fig. 9 Static torsional strength test result (mounting angle: 15°)

Fig. 10 shows an example of the results from the durability test.

HEDJ71P has sufficient durability compared to the conventional product.

CVJ type	Operating time		
Developed product HEDJ71P	○⋯⋯○⋯⋯○ ○⋯⋯○⋯⋯○		
Conventional product HEDJ71	○⋯⋯○⋯⋯△ ○⋯⋯○⋯⋯△		

○ : No problem   △ : Minor problem

Fig. 10 High-speed rotation durability test result

The temperature rise characteristics which are used as an index of high-speed performance is shown in **Fig. 11**.

HEDJ71P shows about 30% lower temperature rise

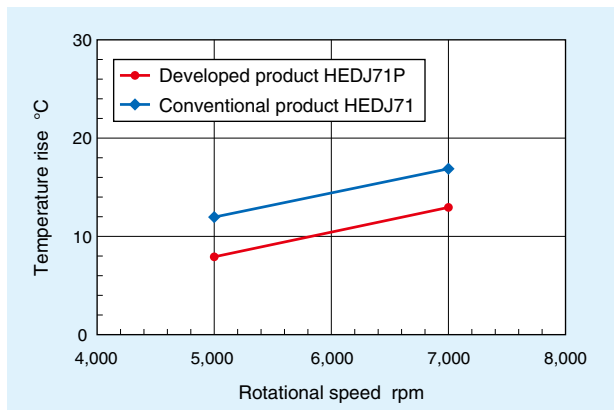than the conventional product, revealing superior high-speed performance.

Fig. 11 Temperature rise characteristics (inner ring driven)

Table 2 shows other performance evaluation results. It shows that the developed product performed equivalent to the conventional product in all items.

Table 2 Other performance

Evaluation item	Developed product
Sliding resistance	Equivalent to HEDJ
Induced force	Equivalent to HEDJ
Radial backlash	Equivalent to HEDJ
Axial backlash	Equivalent to HEDJ
Bending torque	Equivalent to HEDJ

3.4 Transmission Efficiency Analysis Result

The following is an introduction of the optimization of the internal design to achieve the highest level of size and weight while keeping performance.

Since CVJ for propeller shafts is used in high-speed rotation, the most critical issue is how to contain heat generation of the joint. Some of the methods for containing heat generation of the joint include surface treatment of the internal components and application of temperature controlling grease. However, it would achieve higher propeller shaft performance if heat can be contained by the optimum design of the joint.

Since the temperature rise inside the joint is caused by friction among internal components, an analysis of the torque loss within the joint was conducted using the mechanism analysis. The results are shown in **Fig. 12**.

It revealed that the developed product reduced torque loss rate by approx. 45% compared to the conventional product. It also matches with the result of the actual temperature rise test shown in **Fig. 11**, in that the temperature rise of the developed product is small.
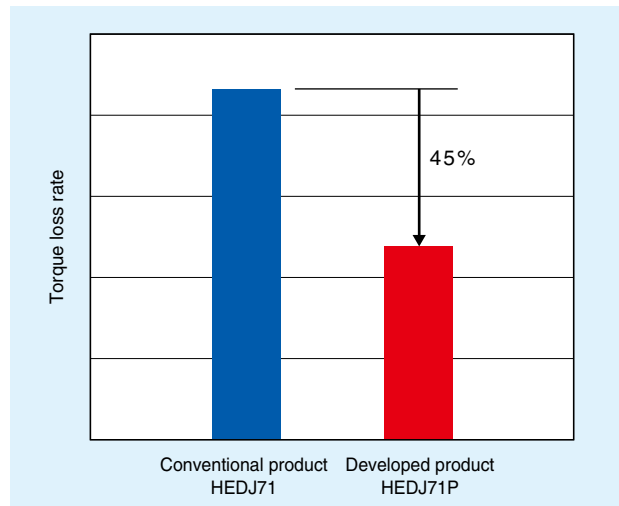

Fig. 12 Calculation result of torque loss rate (inner ring driven)

4. Conclusion

The structure, features and performance of the compact sliding type CVJ for propeller shafts "HEDJ-P" were introduced in this article.

The demand for CVJs for propeller shafts continues to grow along with the recent popularity of SUVs and 4WD vehicles. The developed product has achieved the world's highest level of size and weight reduction and is expected to be globally adopted as it contributes to increased degree of freedom for vehicle design and low fuel consumption at high-speed operation.

References

1) Akio Sakaguchi, Yoshimasa Ushioda, Masahide Miyata et al., Constant Velocity Universal Joints for Propeller Shafts, NTN TECHNICAL REVIEW No. 66, (1997) 37-44.
2) Tomoshige Kobayashi, Teruaki Fujio, Summary of E Series, Constant Velocity Joint for Propeller Shaft, NTN TECHNICAL REVIEW No. 73, (2005) 88-91.
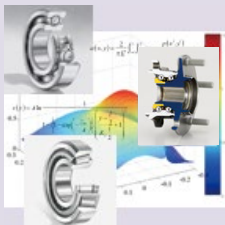3) Shinichi Takabe, History of Constant Velocity Joints, NTN TECHNICAL REVIEW, No. 85 (2017) 40-45.

Photo of author

Masazumi KOBAYASHI

CVJ Development Dept.
Automotive Business
Headquarters

New Technology of Rolling Bearings Contributing to Low Fuel Consumption of Automobiles

Takayuki KAWAMURA*   **Hiroki FUJIWARA***
Kouya OOHIRA*

To reduce the fuel consumption of automobiles, rolling bearings are required to be lighter, smaller and have lower torque. Additionally, for electric automobiles, the rolling bearings that are used at high speed rotation and prevent electrolytic corrosion are also required.

In this paper, the technologies for these requirements are explained from the viewpoints of lubrication, numerical analysis, and materials.

1. Introduction

Recently, development of automobiles is drastically shifting from the conventional vehicles with an engine as the power source to hybrid vehicles (HEV and PHEV), which combine the engine and motor, fuel cell vehicles (FCV) and electric vehicles (BEV) which are driven only by motor. One of the reasons for this trend is the stricter global regulations on fuel consumption originated from environmental issues such as air pollution and global warming. Emphasis on reduction of CO_2 emissions while driving vehicles continues and enhanced regulations on fuel consumption take effect in Japan, the U.S., Europe and China toward 2021. Therefore, auto manufacturers and automotive component manufacturers are racing to introduce new technologies successively into the global market. On the other hand, engines are also used in HEVs and PHEVs; therefore, improvement of fuel/electricity efficiency is a critical challenge, too.

Based on the above situation, this article introduces "new technologies contributing to low fuel consumption of vehicles" with rolling bearings.

2. Challenges of Rolling Bearings Regarding Low Fuel Consumption

Approximately 100 to 150 bearings are used in a vehicle and rolling bearings are some of the components required for safe and comfortable driving. Rolling bearings are used in many parts of a vehicle, such as engine peripheral, transmission, various motors as accessories and driving axle units. There are broadly two characteristics for reducing fuel consumption of conventional vehicles powered by engines. One is lower torque and the other is compactness and lightweight for reducing the vehicle weight.

The requirements for rolling bearings toward electrification of vehicles include high-speed technology to support high-speed rotation of motors and avoidance of electrical corrosion in the vehicles with complex electrical current paths.

There may be other technological challenges specific to HEVs and PHEVs, as well as to FCVs and BEVs, but the main challenges overall are (1) lower torque, (2) compactness and lightweight, (3) high-speed rotation and (4) avoidance of electrical corrosion, which are inherent from electrification.

The following are the topics of the discussion in this article on those challenges:

(1) Lower torque: While grease lubricated rolling bearings are frequently used in vehicles, improvement of grease technology made a significant contribution to reducing torque. This article will discuss those cases.

(2) Compactness/lightweight: Technologies discussed in the past article[1] for improvement of materials/thermal treatments are making a good track record of results for contributing to compactness/lightweight. This article discusses improvement of bearing load carrying capacity by numerical analysis.

(3) High-speed rotation: High-speed rotation is usually supported by ball bearings and an accurate understanding of cage transformation in high-speed rotation is required. In this article, some cases of numerical analysis are discussed.

(4) Avoidance of electrical corrosion: While insulating film may be applied on the outer diameter of the raceway, this article discusses about ceramic ball bearings which are expected to provide highly reliable insulation capability and significant weight reduction.

3. Lower Torque

Reduction of torque is required to grease lubricated rolling bearings from the viewpoint of energy efficiency and resource conservation. Reducing viscosity of grease base oil can reduce torque. However, a simple reduction of viscosity is not effective as it degrades the oil film formation and increases the risk of reduced bearing life. The following is an introduction of bearing torque reduction technology based on rheology characteristics of grease[2].

3.1 Relation of State of Existence of Grease Within Ball Bearings and Bearing Torque

The state of existence of grease within ball bearings can be broadly divided into a churning state where grease churning continues and torque is high and a channeling state where most grease is squeezed out from the rolling elements and torque is low. To observe the difference between those states, the condition of grease adhesion inside the bearing was investigated using X-ray CT, which is becoming a standard method for observing grease behavior.

Inner/outer rings, balls, cage and seals made of resin were used for the bearing to be observed, so that X-ray can be transmitted. For a better contrast between the grease and the other materials, 5% tungsten (by weight) was added in the grease as a tracer. As shown in **Fig. 1**, state of existence of grease between the balls and cage pocket was observed running the grease lubricated bearing while torque is measured. In the initial stage (after 5 hours of operation) where the bearing was stopped in the churning state (torque: 13 Nmm) and when the bearing was assumed to reach the channeling state after a long hours (23 hours) of operation (torque: 5 Nmm). It revealed that there was a large difference in the amount of grease between the balls and the cage pockets between the two states, as shown in **Fig. 2**.

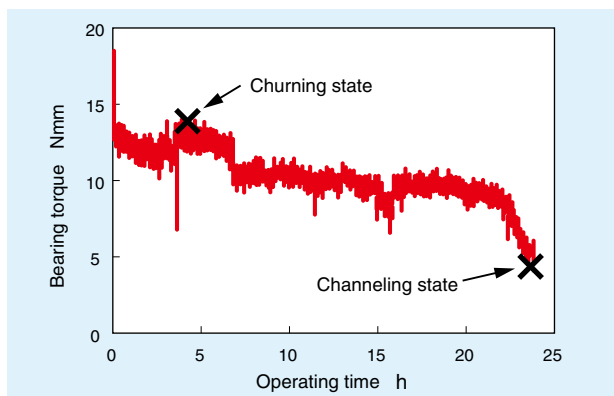<Resin-made bearing torque measurement condition>
6204, 25 °C, Fa=19.6 N, 3,600 min^{-1}

Fig. 1 Chronological change of bearing torque of resin made bearing

Churning state
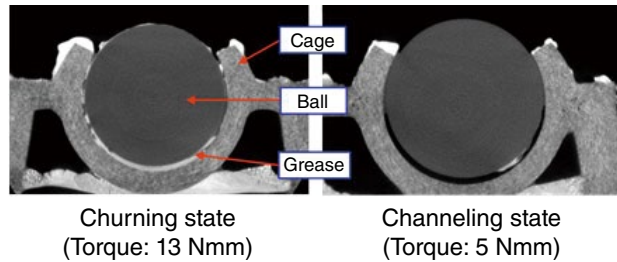(Torque: 13 Nmm)

Channeling state
(Torque: 5 Nmm)

Fig. 2 State of grease adhesion in resin made bearing (between ball and cage pocket surface)

3.2 Basic Concept of Lowering Torque by Grease

The observation of X-ray CT revealed that shear stress of grease between the balls and the cage pocket surface needs to be reduced in order to reduce torque in grease lubrication. That is, two points, namely, 1) reduction of grease viscosity and 2) faster transition to channeling state, are effective. The following is an example of verification of these effects by using 4 types (grease A to D) of grease for rolling bearings **(Table 1)**.

Table 1 Sample grease

		Grease A	Grease B	Grease C	Grease D
Thickener		Lithium soap	Urea	Urea	Urea
Base oil	Type	Synthetic oil	Synthetic oil	Synthetic oil	Mineral oil
	Kinematic viscosity mm^2/s (40°C)	25	40	23	95
Consistency		250	250	280	290

1) Reduction of Grease Viscosity

Grease viscosity is a function of grease shear velocity, therefore viscosity needs to be reduced in the shear velocity zone between the balls and the cage pocket surface under the operating condition of rolling bearings. If the balls are assumed to be at the center of the cage pockets and the inner ring of a ball bearing (6204) rotates at 1,800-10,000 min^{-1}, then the grease shear velocity of the cage pocket is 24,000-130,000 s^{-1}.

Fig. 3 shows the relation between the shear stress at the cage pocket obtained by calculating the actual grease viscosity measured with a rheometer multiplied by the shear velocity, and the bearing torque actually measured at the initial stage of operation. Except for grease D at 1,800 min^{-1}, the more the shear stress, the greater the bearing torque in all the conditions (any grease types and rotational speeds). Reduction of grease viscosity at the shear velocity equivalent to the cage pockets and reduction of shear stress between the balls and the cage pocket surface are effective for reducing torque.

2) Faster Transition to Channeling State

In grease lubrication, the difference between the churning state and channeling state has a major impact on bearing torque. For low torque, the channeling state, where the grease between the balls and the cage pocket surface is quickly squeezed out, is more desirable. Grease D at 1,800 min^{-1} in **Fig. 3** is considered to be in the channeling state and the other conditions are considered to be in the churning state.

By changing angle of oscillation with the rheometer, the storage modulus G', which indicates grease property as solid, and the loss modulus G', which indicates the grease property as liquid, are measured and the shear stress, where the ratio of those two ($tan \delta$ = G"/G') is 1, is obtained as the yield stress **(Fig. 4).** As shown in **Fig. 5**, it was verified that the grease with high yield stress (grease C and D) can transition from the churning state (high torque) to the channeling state (low torque) within the operating time of 120 min., the grease with low yield stress (grease A and B) cannot transition to the channeling state (low torque).

The grease in the bearing with a rotating inner ring moves from the raceway surface to the inner diameter of the outer ring by the centrifugal force and stays there as agglomeration. It is assumed that the agglomerated grease or oil separated from it flows back to the raceway lubricating the bearing[3]. As shown in **Fig. 6**, it is considered that the grease agglomerated on the inner diameter of the outer ring with higher yield stress is harder to move to the raceway surface by vibration and temperature rise, allowing more stable channeling state.

<Bearing torque measurement condition>
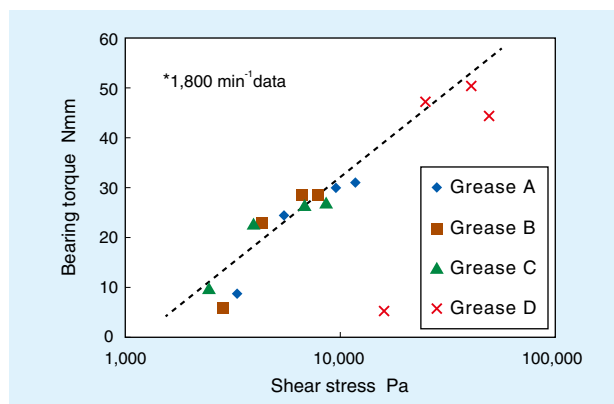6204, 25 °C, Fa=19.6 N, 1,800-10,000 min^{-1}

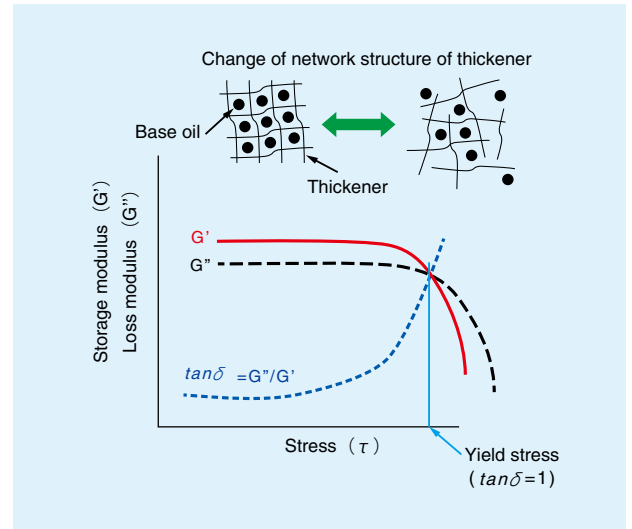**Fig. 3** Relationship between bearing torque and cage pocket shear stress

Fig. 4 Example of measurement of yield stress by rheometer

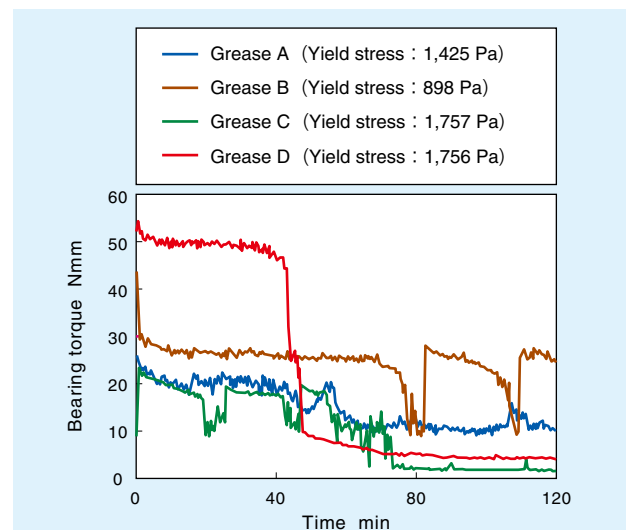<Bearing torque measurement condition>
6204, 25 °C, Fa=19.6 N, 1,800 min^{-1}

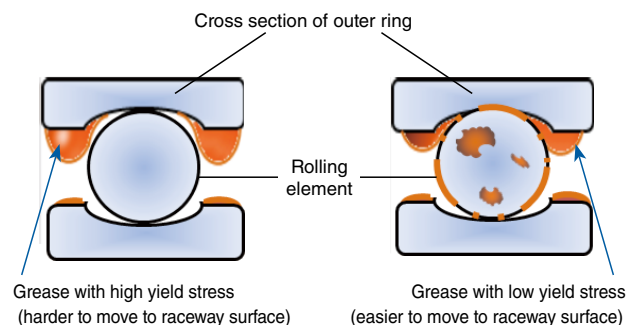**Fig. 5** Relationship between grease yield stress and bearing torque

Fig. 6 Schematic diagram of grease flow agglomerated on the inner diameter of outer ring

3.3 Application to Grease for Hub Bearings

NTN is developing different types of grease for various applications based on the low torque technologies by grease described in 3.2. As an example, the case of application of the grease for hub bearings, which has particularly strong demand for low torque among automotive components[4] is introduced.

In this development, reduction of grease shear stress between the raceway and rolling elements is also elaborated in addition to the reduction of the grease shear stress between the balls and cage pocket surface.

(1) Reduction of Grease Shear Stress Between the Balls and Cage Pocket Surface

Fig. 7 and **8** show the comparison of the grease viscosity and yield stress between the conventional product and the developed product. The developed product provides lower viscosity and higher yield stress in the shear velocity zone above 2,000 s^{-1}, which is important in hub bearings, than the conventional product, as a result of elaboration on grease composition. Control of these physical properties made it possible to reduce grease shear stress between the balls and cage pocket surface and achieve low torque.

<Grease viscosity measurement condition>
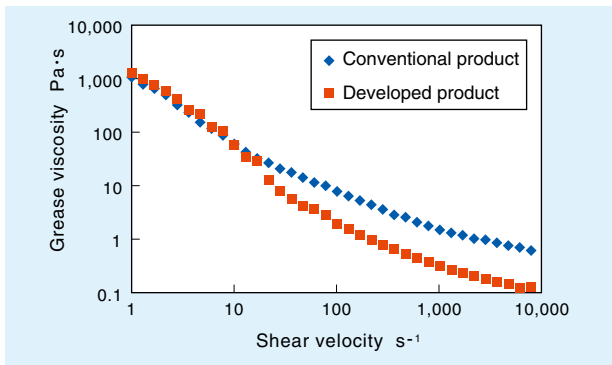Cone-plate rheometer, 25°C, 1 ⇒ 8,000 s^{-1}, steady flow

Fig. 7 Relationship between shear velocity and grease viscosity

<Yield stress measurement condition>
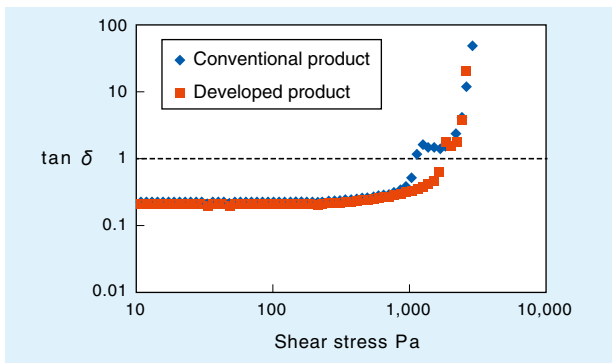Parallel plate rheometer, 25°C, 1 Hz, 10 ⇒ 3,000 Pa

Fig. 8 Measurement result of yield stress

(2) Reduction of Grease Shear Stress Between Raceway and Rolling Elements

With ball bearings, it is known that the small sliding between the raceway and the rolling elements, which is called differential slips and spins, cause friction (traction)[5]. **Fig. 9** shows the investigation result of the impact of the molecular structure of grease composition on the traction. It was revealed that the traction can be reduced by reducing circular/branching structure in the molecular structure of the base oil and making the straight-chain structure as the dominant structure. The developed product improved the molecular structure in addition to the rheology property of the grease for achieving torque reduction.

<Traction measurement condition>
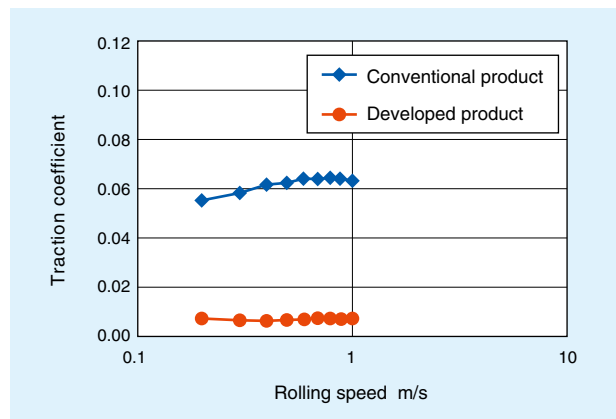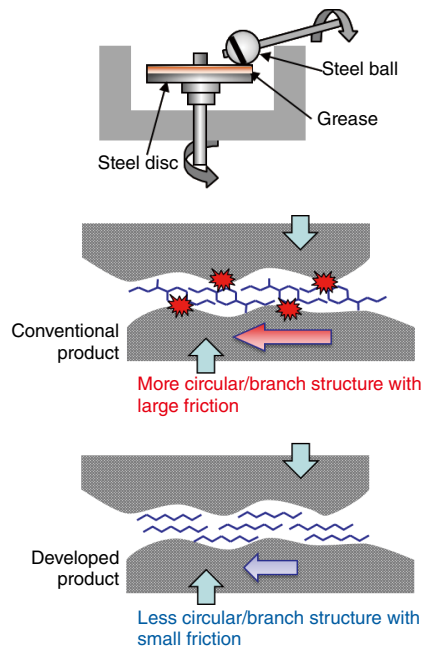25°C, 0.65 GPa, 0.2 ⇒ 1.0 m/s (3% slip)

Fig. 9 Relationship between molecular structure of grease component and traction

4. Compactness/lightweight

For low fuel consumption, it is necessary to reduce the size and weight of each individual component of a vehicle. In case of rolling bearings, a simple downsizing causes reduction of system life. Therefore, past efforts were focused on the improvement of material to reduce the size while maintaining the required system life[1]. In this article, a technology for long system life is introduced, with a new viewpoint of changing the design of the bearing internal shape, which contributes to downsizing.

The rolling element and raceway are in line contact as they are basically cylinders; however, if they are made of simple cylinders, excessive stress is concentrated on both ends of the contact called "edge load." Therefore, the radii of both ends of the rolling elements and raceway are reduced by a few μ m, called "crowning." Edge loading can be prevented by applying large crowning even in the misaligned condition; however, that causes large maximum stress at the center of the roller, causing reduction of operating life. Although the theoretical shape to minimize the maximum stress while preventing the edge load was known to be a logarithmic curve, the ideal curve could not be actually processed and the impact of misalignment, which is realistically unavoidable could not be eliminated. **NTN** developed a proprietary logarithmic function formula for crowning with improved degree of design freedom, as well as an automated design method using mathematical optimization method[6].

Fig. 10 shows a diagram of the distribution of stress. The logarithmic crowning reduces the edge stress even if the amount of processing at the edges is almost the same as the conventional crowning, resulting in longer operating life. By using this technology, compact and light bearings can be developed maintaining equivalent life as the conventional products, which contribute to lower torque and lower fuel consumption.
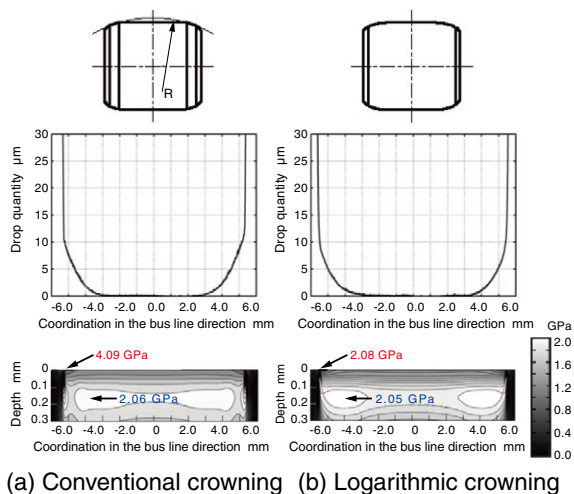

(a) Conventional crowning (b) Logarithmic crowning

Fig. 10 Crowning geometry and distribution of Mises equivalent stresses[7]

5. High-speed Rotation

The motor, as the power source of an EV, becomes larger if designed with the low speed/high torque specification; therefore, it is designed with the high speed/ low torque specification for compactness and the required torque is created by reducing the speed. This requires the rolling bearings for EV motors to support high-speed rotation.

The type of bearings suitable for high-speed operation is ball bearings. Resin made cages, which exhibit superior self-lubricating property, are frequently used to reduce friction loss. An ordinary resin-made cage has a shape asymmetric with respect to the axial direction called a "snap cage," as shown in **Fig. 11**. The pocket has an open end in the axial direction where a ball is snapped in. The claws on the open end of the pocket can open to the outer diameter side when operated in high speed, by the centrifugal force, as shown in **Fig. 12**, with deformation like flower petals. This type of deformation of claws can interfere with the balls and outer ring, causing an increased friction loss and wear.
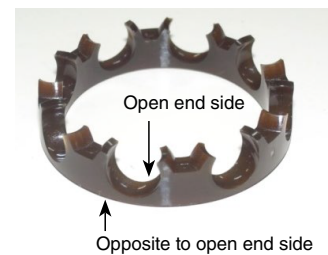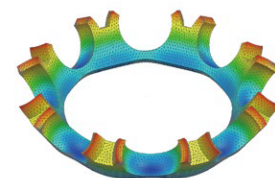

Fig. 11 Resin made snap cage

Fig. 12 Example of deformation analysis of resin made snap cage

Therefore, the thickness of the claw portion was reduced for lightweight and the rigidity of the ring portion on the opposite side of the open end was reduced to allow deformation of the ring to the outer diameter direction, to decrease the impact of the deformation of the claws. **Fig. 13** shows the deformation of the cages of the conventional structure and the developed product in high-speed rotation. In the case of the snap cage, the limitation of the high-speed rotation is not in the cage strength but in the local deformation of the claws. Noticing this fact, the challenge was solved not by providing high rigidity to prevent deformation but conversely, by making the entire piece a flexible structure. For example, the permitted rotational speed of oil lubricated 6206 is 13,000 min^{-1}; however, adoption of this technology achieved a normal operation of 17,000 min^{-1}.

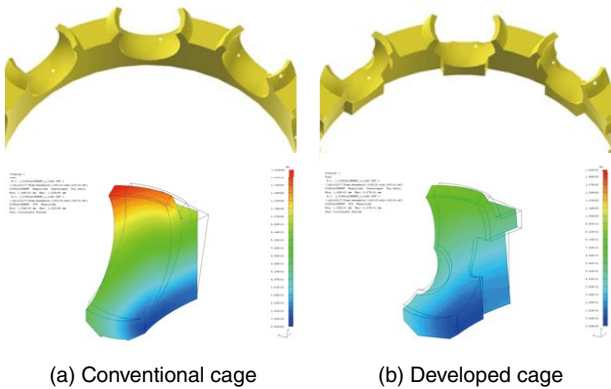(a) Conventional cage   (b) Developed cage

Fig. 13 Example of deformation analysis due to centrifugal force and cage shape

Even higher speed can be achieved by adopting a cage that prevents deformation of the pocket and its surrounding by integrating axially divided components snapped into one[8].

6. Avoidance of Electrical Corrosion

While insulating film made by resin or ceramics may be applied on the outer diameter of the raceway for preventing electrical corrosion of rolling bearings, this article discusses about ceramic balls which are expected to provide highly reliable insulation capability and significant weight reduction.

A type of damages incurred to the bearings used in motors and generators is called electrical corrosion. The electrical corrosion is a phenomenon of damage on the rolling surface by sparks generated at the rolling contact by the electrical current that flows into the bearing. The metallographic structure is deteriorated by the spark generated at the rolling contacts, resulting in vibration, noise and flaking.

Devices equipped with motors, for instance, use carbon brushes for grounding the shaft or shut down the electrical current from the bearings by shaft insulator, etc. However, each of them has issues in durability, such as wear of carbon brushes during operation and thermal degradation of resin, if resin insulator is used for shutting down the electrical current. As a method to solve these issues, a hybrid bearing, where ceramic balls made of silicon nitride are incorporated in the raceway made of steel, is effective.

To verify the insulation capability of the hybrid bearing with the ceramic balls made of silicon nitride, a bearing peel life test was conducted under current carrying condition using direct current, as an example. **Fig. 14** shows an outline of the test equipment. This test equipment supports the rotational shaft by the bearing under the test and a support bearing. The housing is divided into 2 parts by the insulation. The electrical current flows from the terminal A → bearing under test → rotational shaft → support bearing → terminal B when the

terminal A and B are activated. **Table 2** shows the test condition. The test was conducted by applying a constant current (0.5 A) under quick acceleration condition guided by the inner ring (in case of the bearing with ceramic balls made of silicon nitride, the applied voltage was set to 30 V). **Table 3** shows the test results.

As shown in **Table 3**, the ceramic balls made of silicon nitride can contain peeling of rolling element surface due to electrical corrosion, since they are insulating body, compared to the steel balls. Therefore, the ceramic balls made of silicon nitride with insulation capability are expected to be used in the bearings of various types of motors used in the next generation vehicles, which will be widely adopted such as HEVs, PHEVs and EVs.
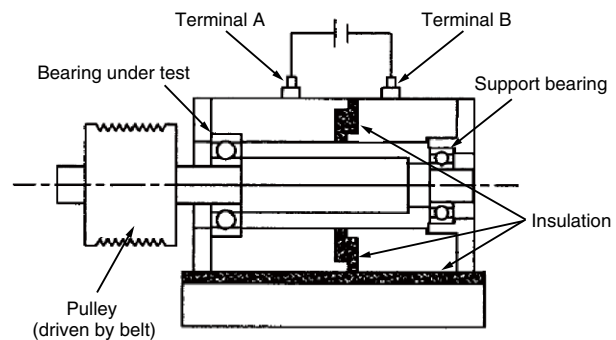

Fig. 14 Peeling life tester under current carrying condition

Table 2 Test condition

Bearing under test	Deep groove ball bearing (6203)	
Rolling element	Steel ball	Ceramic ball
Grease	Nonconductive grease	
Amount of injected grease (g)	0.86	
Rotational speed (min⁻¹)	Quick acceleration/ deceleration from 0 to 20,000	
Atmosphere	Room temperature	
Pulley load (N)	1,617	
Bearing load (N)	2,332	
Current (A)	0.5	–
Stopping condition	When the vibration is 10 times than initial condition	

Table 3 Peeling life test results

	Life (h)	Peeling region
Steel ball	19.6	Ball
Ceramic ball	> 200	None

In addition to the solution for avoidance of electrical corrosion, ceramic balls are also effective for reducing weight. The specific gravity of the ceramic made of silicon nitride is around 40% of the bearing steel; therefore, applying ceramic balls made of silicon nitride for rolling elements makes the bearing lighter than an ordinary bearing with the raceway and rolling elements made of bearing steel (SUJ2). In addition, lighter rolling elements contribute to reduction of centrifugal force applied to the rolling elements during rotation of the bearing, which

helps support the increasing demand of higher speed motors for HEVs, PHEVs and EVs.

In case of deep groove ball bearing 6206, applying ceramic balls made of silicon nitride for rolling elements makes the hybrid bearing lighter than the ordinary bearing with the raceway and rolling elements made of bearing steel (SUJ2) by approx. 10%. As shown in **Fig. 15**, applying ceramic balls made of silicon nitride for hub bearings reduced the weight by approx. 13%, contributing to low fuel consumption of vehicles.

Fig. 15 1st generation hub bearing (using ceramic balls)

In addition, ceramic made of silicon nitride is chemically stable which is expected to help reduce oxidative deterioration of lubricant between the raceway made of bearing steel and the rolling elements and improve anti-galling property by avoiding adhesion if the rolling elements made of bearing steel are replaced with the ceramic made of silicon nitride.

The seizure resistance property was evaluated in the combination of steel ball (SUJ2) and ceramic ball made of silicon nitride (Si3N4) using a four-ball friction tester. The test condition is shown in **Table 4** and the test result is shown in **Fig. 16**. Four-ball friction testing uses three fixed balls on which a rolling ball rotates. Seizure resistance property was evaluated by running the tester for a minute at a constant load and when the friction coefficient did not increase, the load was increased. The test was stopped when the friction coefficient rose more than 5 times the initial condition when the seizure occurred. As shown in **Fig. 16**, a combination of steel balls and a ceramic ball made of silicon nitride indicated the best seizure resistance property.

Since seizure resistance property improves when steel is used for inner/outer rings and ceramic made of silicon nitride is used for rolling elements, low fuel consumption of vehicles can be expected by reduced use of lubricant and therefore, low torque effect.

Table 4 Test condition

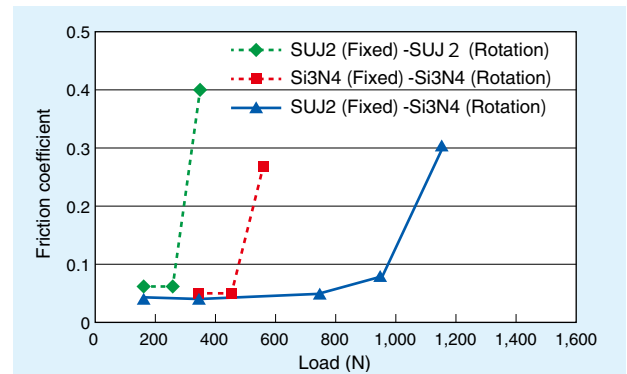| Test equipment	Four-ball friction tester
Material of balls under test	Steel ball (SUJ2), ceramic ball (Si3N4)
Ball size (inch)	3/4
Lubricating oil	Turbine oil grade 68
Lubricating condition	Dipping
Atmosphere	Room temperature
Slide velocity (m/s)	0.86
Stopping condition	When the friction coefficient rose more than 5 times from the initial condition

**Fig. 16** Seizure resistance test result

7. Conclusion

New technologies contributing to low fuel consumption of vehicles, such as design technology by numerical analysis for rolling bearings, weight reduction technologies and low torque technologies were discussed. The hope is these new technologies help support measures against the environmental issues such as global warming and global tendency of fuel cost increase.

References

1) Nakashima: Trends in Materials and Heat Treatments for Rolling Bearings, NTN TECHNICAL REVIEW, No. 76 (2008) 10.
2) Kondo, Kawamura: Impact of grease rheology property on bearing torque, Japanese Society of Tribologists, Proceedings for Tribology Conference 2017 Spring Tokyo, F17.
3) Kawamura: Research on the Lubrication Mechanism of Grease for High Speed Bearings, NTN TECHNICAL REVIEW, No. 76 (2008) 39.
4) Seki: Low Friction Hub Bearing III, NTN TECHNICAL REVIEW, No. 87 (2019) 63-67.
5) Muraki: Illustrated Tribology Science of Friction and Lubrication Technology, Nikkan Kogyo Shimbun, Ltd., 221.
6) Fujiwara, Kawase: Logarithmic Profile of Rollers in Roller Bearing and Optimization of the Profile, Transactions of the JSME C, 72 (2006), 3022.
7) Fujiwara, Yamauchi: Experimental Comparison Between Partially Crowned and Logarithmic Roller Profiles in Cylindrical Roller Bearings, Transactions of the JSME C, 74 (2008), 2308.
8) Katagiri, Naito: Next Generation Deep Groove Ball Bearing for High-Speed Servomotor, NTN TECHNICAL REVIEW, No. 72 (2004) 45.

Photo of authors
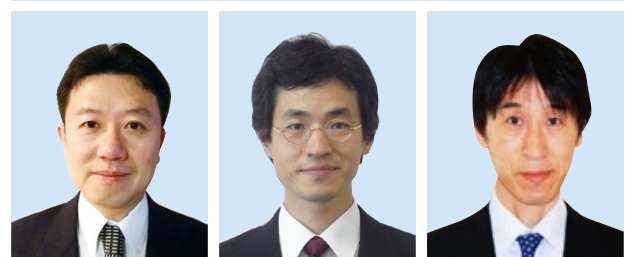
Takayuki KAWAMURA
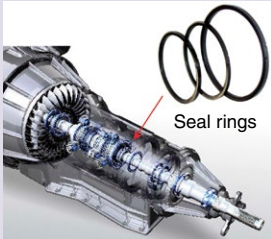Advanced Technology R&D Center

Hiroki FUJIWARA
Advanced Technology R&D Center

Kouya OOHIRA
Advanced Technology R&D Center

Verification of Torque Reduction for Low Torque Seal Ring by Fluid Analysis

Takuya ISHII*
Tomohiko OBATA**

Seal rings

In order to achieve demands of fuel consumption standard, seal rings for automotive transmission are required to further reduce torque and oil leak. **NTN** developed "Low Torque Seal Ring" and started mass production. It has V-shaped lubrication grooves, which reduces torque by 60% in comparison with conventional products. This article introduces fluid analysis results of torque reduction by V-shaped lubrication grooves in "Low Torque Seal Ring".

1. Introduction

Multiple seal rings made of resin with outer diameters ranging from 15-60 mm are used in vehicle transmissions (AT, CVT, etc.). These seal rings are required to have low torque and low oil leakage properties to achieve low fuel consumption of vehicles. In order to respond to this requirement, **NTN** developed "Low Torque Seal Ring"[1), 2)] made of polyether ether ketone (PEEK) resin with a V-shaped lubrication groove and started volume production **(Fig. 1)**.

The number and shape of the V-shaped lubrication grooves was optimized by fluid analysis and experiments to further reduce torque of the low torque seal ring. This article introduces the verification result of the fluid analysis regarding the reduction of torque for the low torque seal ring.
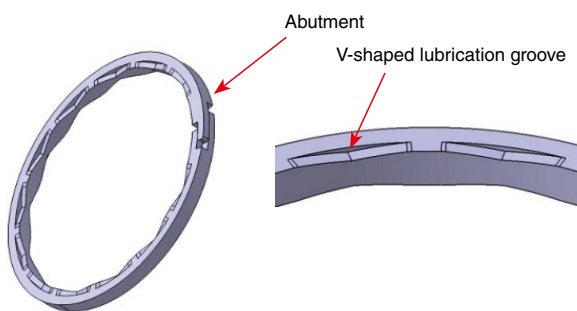
Abutment

V-shaped lubrication groove

Fig. 1 Low torque seal ring

2. Role and Operation of the Seal Ring

Oil is sealed by the seal ring that slides on the moving components. Seal rings are installed between the shaft and housing that moves in relative motion within the oil hydraulic circuits of transmissions. They are pushed to both the inner surface of the housing and the side wall of the shaft groove by oil hydraulics sealing oil and maintaining the pressure inside the oil hydraulic circuit, as they slide.

The required performance of the seal rings is low torque, low oil leakage and high wear resistance. When torque is reduced, transmission efficiency increases achieving higher energy efficiency. Reduced oil leakage leads to a more efficient and smaller oil-hydraulic pump which results in higher energy efficiency. To maintain low torque and low oil leakage operation and realize long operating life, seal rings are required to be wear resistant and at the same time prevent wear of the mating component which the seal rings slide on.

Fig. 2 shows the operation of **NTN**'s conventional product which has a rectangular cross section. Since the contact area of the seal ring and the side wall of the shaft groove is smaller than the contact area of the seal ring and the inner surface of the housing, the seal ring slides on the side wall of the shaft groove. It is this side wall of the shaft groove that has lower sliding resistance when the shaft or the housing rotates. Oil leakage is small as the seal ring has area contact with the side wall of the shaft groove.
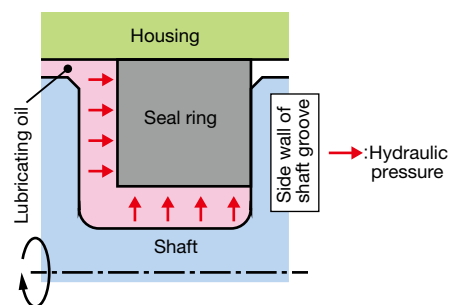
Housing

Lubricating oil

Seal ring

Side wall of shaft groove

→:Hydraulic pressure

Shaft

Fig. 2 Operation of seal ring

* Precision Plastics Engineering Dept., Composite Material Product Division
** Advanced Technology R&D Center

3. Low Torque Seal Ring

3.1 Features

The Low Torque Seal Ring realized low torque and low oil leakage by installing a V-shaped lubrication groove on the surface of the seal ring which slides on the side wall of the shaft groove. It uses BEAREE PK5301, which is a material made of PEEK resin with special additives. It has V-shaped lubrication grooves on the side formed by injection molding and the abutment is made of complex shape. Oil leakage from the abutment is reduced, by making it a complex shape.

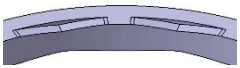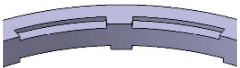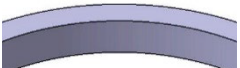The Low Torque Seal Ring has the following features compared with **NTN**'s conventional product.
(Features)
(1) Reduction of torque by up to 60%
(2) 1/10 the wear rate
(3) Equivalent low oil leakage property

3.2 Comparison of the Lubrication Groove Shapes

3.2.1 Torque Measurement Results

Table 1 shows a comparison of torque using 3 types of seal rings with different shapes of lubrication grooves and without grooves. **Fig. 3** shows an outline of the test equipment. Torque was measured by circulating oil between two seal rings installed on the shaft grooves, applying oil pressure and rotating the housing.

Table 1 Seal rings under test

Seal rings under test	Shape of the lubrication grooves on the side
V-shaped lubrication grooves (12 on one side)	
Square-shaped lubrication grooves (12 on one side)	
No lubrication grooves	

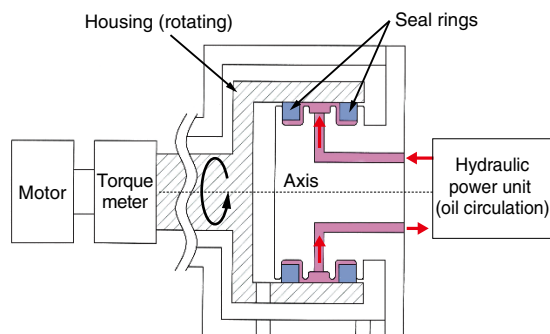Seal ring size: OD: 50 mm, thickness: 1.6 mm, width: 1.5 mm

Fig. 3 Outline of test equipment

Fig. 4 shows the relation between the oil hydraulics and torque. The measured torque for two seal rings was divided by 2 to obtain torque for one seal ring. The seal ring with the V-shaped lubrication grooves showed lower torque than the seal ring without grooves (**NTN**'s conventional product) by 60-70% and the seal ring with square-shaped lubrication grooves by 20%.

[Test condition]
Oil hydraulics: 0.5-2 MPa,
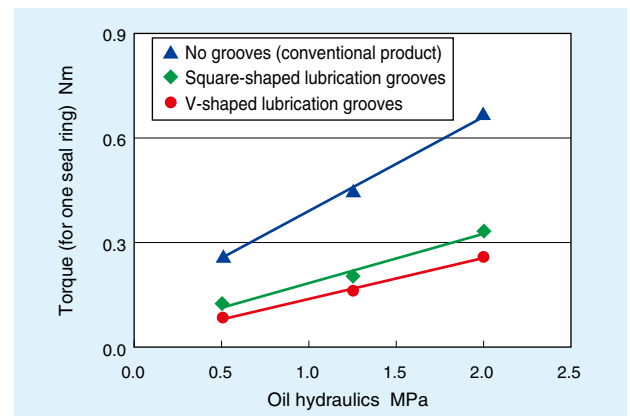rotation speed: 4,000 min^{-1}, ATF: 110°C
S45C Housing/shaft

Fig. 4 Relationship between oil hydraulics and torque

3.2.2 Fluid Analysis Results

As the reason for lower torque, it is assumed that application of the V-shaped lubrication grooves which reduced the contact area between the seal ring and side wall of the shaft groove promoted lubrication of the sliding surface. The difference of torque between two different shapes of the grooves is attributed to the difference of lubricating conditions. This was verified by fluid analysis.

Fig. 5 shows the analysis result of the model extracting fluid region of one lubrication groove. With the V-shaped lubrication groove, oil film pressure at one end of the groove is high due to a hydrodynamic effect. This axial force due to oil film pressure is in the opposite direction from the force that the seal ring is pressed on the side wall of the shaft groove by oil hydraulics; therefore, it reduced the latter force. It is also assumed that oil flowed from the end of the lubrication groove onto the sliding surface between the lubrication grooves due to difference of pressure helped reduce torque. On the other hand, the high pressure observed in the V-shaped lubrication groove is not observed in the square-shaped lubrication groove.

[Analysis condition]
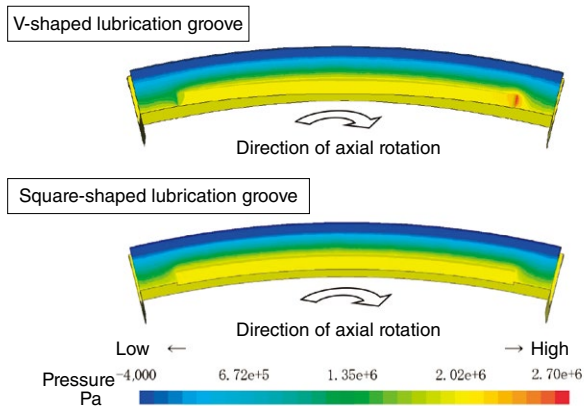Oil film thickness: 5 μm, oil hydraulics: 2 MPa, rotation speed: 4,000 min^{-1}, ATF(20°C)

Fig. 5 Oil film pressure distribution on sliding surface

4. Verification of Torque Reduction by Optimization of V-Shaped Lubrication Grooves

4.1 Fluid Analysis Condition

The torque measurement result and oil film pressure distribution on the sliding surface revealed that the force appearing at the end of the V-shaped lubrication grooves is in the opposite direction from the force due to oil film pressure (oil film reaction force) which contributed to a reduction of torque. When the oil film reaction force is greater, the torque is lower. So, it is assumed that the greater the number of the V-shaped lubrication grooves and the wider the groove widths, the greater the oil film reaction force. Therefore, this was verified by the fluid analysis.

Fig. 6 shows the definition of the length, width, depth, angle of, and the distance between V-shaped lubrication grooves of the seal ring in the analysis. The size was set as: OD: 44 mm, thickness: 2 mm and width: 2.3 mm. The fluid region of one V-shaped lubrication groove of the seal ring was modeled with fluid analysis and the oil film pressure due to hydrodynamic effect was integrated to obtain the oil film reaction force of one groove. The product of this force and the number of grooves was defined as the oil film reaction force for one seal ring and a comparison of different conditions was made. Note that the oil film pressure at the contact area of the side of the seal ring and the side wall of the shaft groove was ignored, as this is very small compared to the V-shaped lubrication groove. In this analysis, the oil film thickness on the sliding surface was assumed to be constant at 5 μm, for ease of calculation, and the operating condition was defined as ATF pressure: 0.6 MPa, temperature: 20°C and rotation speed: 10,000 min^{-1}.
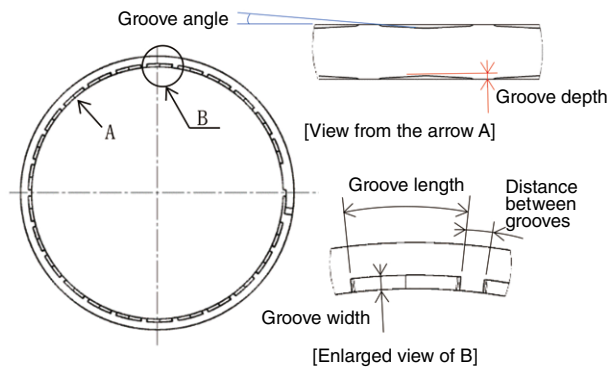

Fig. 6 Analysis of seal ring (24 grooves)

4.2 Fluid Analysis Results
4.2.1 Number of V-Shaped Lubrication Grooves

Oil film reaction force of one seal ring was obtained by fluid analysis for seal rings with 12 and 24 V-shaped lubrication grooves on one side. The distance between V-shaped lubrication grooves was the same and the length was changed between 12 and 24 grooves. The groove angle was also the same but the groove depths are different to allow for 12 or 24 grooves.

Fig. 7 shows the oil film reaction force of seal rings with 12 and 24 V-shaped lubrication grooves. As estimated, it was verified that the oil film reaction force is larger as the number of grooves is greater. Therefore, the greater the number of grooves, the better for reducing torque.
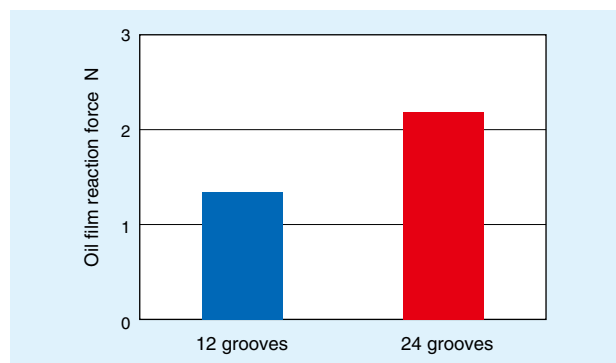

Fig. 7 Number of grooves and oil film reaction force

However, when the number of grooves increases, the number of the spaces between the grooves increases, too, which increases the contact area between the side of the seal ring and the side wall of the shaft groove, which result in higher torque. Therefore, there should be an optimum number of grooves for the minimum torque. To verify this, seal rings with a varying number of grooves were made and the torque measured. The seal ring size was: OD: 51 mm, thickness: 2.4 mm, width: 2.3 mm and the number of grooves: 12-30 on one side. The distance between grooves, groove width and groove angle were the same so the groove lengths and depths were different depending on the number of grooves. The measurement condition was: ATF pressure: 1 MPa, temperature: 80°C, rotation speed: 2,000 min^{-1}.

Fig. 8 shows the relation between the number of grooves and torque. Torque was reduced toward 24 grooves but increased at 30. The measurement results matched with the aforementioned concept, verifying that there is an optimum value for the number of grooves. Since the number of grooves is restricted by design and manufacturing reasons depending on the outer diameter, **NTN**'s Low Torque Seal Rings are lined up with the optimum number of V-shaped lubrication grooves by outer diameter.
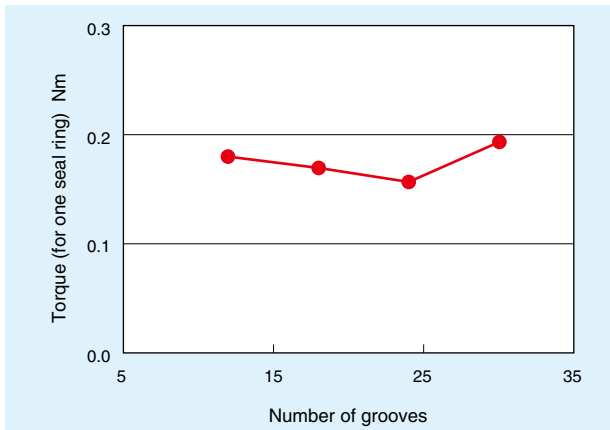

Fig. 8 Relationship between number of grooves and torque

4.2.2 Width of V-Shaped Lubrication Grooves

The oil film reaction force was obtained by fluid analysis for seal rings with V-shaped lubrication grooves with widths ranging from 0.2 to 0.7 mm. The number of grooves was 24 on one side and all the sizes are the same except for the groove width.

Fig. 9 shows the relation between the groove width and oil film reaction force. The verification result obtained matched with the estimate, as the groove width increased, the oil film reaction force increased. However, excessive groove width was found to cause increased oil leakage. Therefore, the groove width must be determined for each case, considering the size of housing and the shaft, eccentricity, wear amount of seal ring and housing, etc.
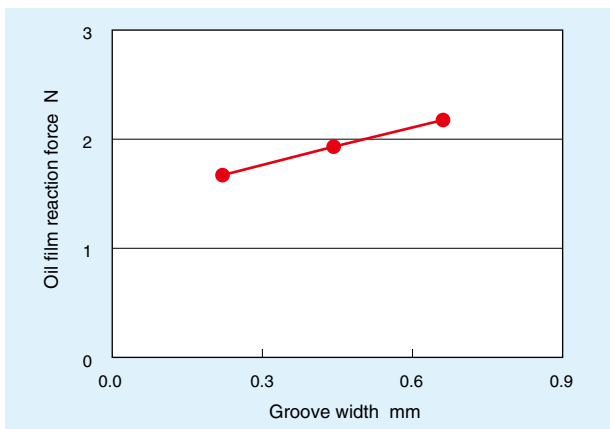

Fig. 9 Relationship between groove width and oil film reaction force

4.2.3 Angle of V-Shaped Lubrication Grooves

The oil film reaction force was obtained using fluid analysis, by increasing or decreasing the angle of the V-shaped lubrication grooves based on the seal ring with 24 grooves on one side described in 4.2.1. Since the distance between the grooves and the groove length and width were the same, only the groove depth is different based on the change of angles.

Fig. 10 shows the relation between the groove angle and oil film reaction force. The horizontal axis is a ratio of angle against the base angle. Within the range of this test, the oil film reaction force is almost the same regardless of the groove angles. Similarly, there is no impact to the groove depth. These results revealed that the number of grooves must be emphasized in the design of the V-shaped lubrication grooves, and the groove angle and depth do not need to be considered, if they are in the appropriate range.
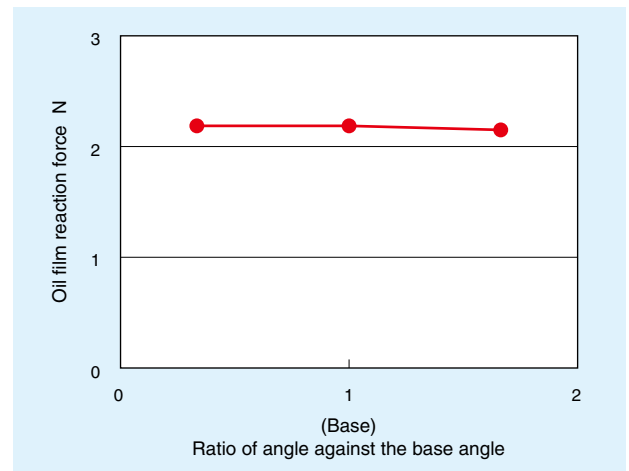

Fig. 10 Relationship between groove angle and oil film reaction force

4.3 Result of Torque Measurement with the Optimum V-Shaped Lubrication Grooves

The number and the shape of the V-shaped lubrication grooves are optimized based on the above fluid analysis. **Fig. 11** shows a comparison of torque from the seal ring with 12 V-shaped lubrication grooves discussed in Section 3.2 and the seal ring with the 24 optimized V-shaped lubrication grooves. The seal ring with 24 optimized grooves showed torque reduction of 10-15% compared to the seal ring with 12 grooves[3), 4)]. A seal ring that was of the following size was used for comparison: OD: 45 mm, thickness: 2 mm, width: 2.4 mm.

[Test condition]
Oil hydraulics: 0.4-1.2 MPa,
rotation speed: 2,000 min^{-1}, ATF: 80°C
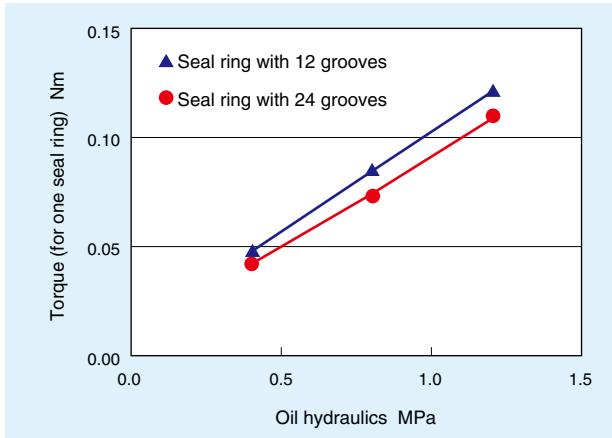Steel base housing/shaft

Fig. 11 Relationship between oil hydraulics and torque

5. Summary

This article introduced the verification result of the fluid analysis regarding reduction of torque of the Low Torque Seal Ring. The number and the shape of V-shaped lubrication grooves are optimized based on the fluid analysis and experiments to successfully reduce torque even further. Adoption of the Low Torque Seal Rings is well in progress as they could respond to the requirement of low fuel consumption of vehicles. We strive for further reduction of torque as we move forward.

Requirements for energy efficiency are increasing in many areas. We are poised to increase the speed of development for enhancing the performance of resin sliding components by adopting analytical approaches such as fluid analysis.

References

1) Kouzou Kakehi, Takumi Kondou, Takuya Ishii, Masato Yoshino: Development of Low Torque Seal Ring for Automotive Transmission, NTN TECHNICAL REVIEW No. 81 (2013) 68.
2) Takuya Ishii: Lower Torque of Seal Ring for Automotive Transmission, Journal of Society of Automotive Engineers of Japan Vol 71, No. 9 (2017) 81.
3) Takuya Ishii: Lower Torque of Seal Ring for Transmission, Automotive Technology Vol. 6, No. 1 (2018) 69.
4) Kayo Sakai, Tomonori Yamashita, Hajime Asada, Takuya Ishii: Proposal of Low Fuel Consumption and High Functionality of Composite Material Products for Automobile, NTN TECHNICAL REVIEW No. 85 (2017) 97.
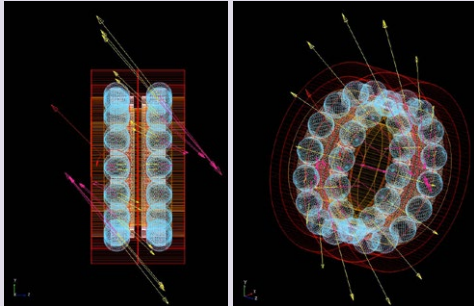
Photo of authors

Takuya ISHII

Precision Plastics Engineering Dept. Composite Material Product Division

Tomohiko OBATA

Advanced Technology R&D Center

Analysis of Dynamics of Hub Bearings under Moment Loads

Tomoya SAKAGUCHI*
Naoto SHIBUTANI*

Stiffness of hub bearings is an important factor for vehicle handling stability. Analysis and measurements for the hub bearing stiffness have been done only under non-rotating inner ring conditions but not done under rotating inner ring conditions. Hence, the authors have examined the rotating hub bearing stiffness by using a bearing dynamic analysis system "IBDAS". This examination shows that rotating hub bearing stiffness coincides with the nonrotating one and hysteresis, that is response delay, exists in displacement curves of inner ring alignment angle against varying moment.

1. Introduction

Even as automated driving technology develops and computers control steering, vehicle handling stability continues to be an important aspect. That is because even with the most advanced computer system if the vehicle response to the steering signal is too slow, then the vehicle will have difficulty driving along the desired path. On the other hand, the stiffness of hub bearings that support the tires of the vehicle is one of the factors that affects vehicle handling stability[1, 2]. Therefore, designing the stiffness of hub bearings appropriately is an important subject.

In general, measuring stiffness of hub bearings is done without rotating the shaft[2]. Although, it is expected that stiffness with a rotating shaft does not differ from the static rigidity, it is not confirmed, yet. To determine if this is valid, dynamic analysis of the relationship between the shaft rotation speed and stiffness of hub bearings was established using an integrated dynamic analysis system "IBDAS"[3], which **NTN** has been developing for the analysis of roller bearings[4]. In this article, the results obtained from these dynamic analyses are reported.

2. Product to Be Analyzed

A hub bearing consists of two rows of balls and a cage, as shown in **Fig. 1**. The inner ring on the inboard side is fixed to the hub ring and a certain axial preload is applied to the balls. Therefore, in this report, the rotation system configured with the double row angular contact ball bearing specified in **Table 1** is calculated.

The operating condition of the bearing is shown in **Table 2** and the load acting point and coordinate system of analysis are shown in **Fig. 2**. This condition assumes a hub bearing of a vehicle, which runs at a constant speed where moment, axial load and radial load periodically change.
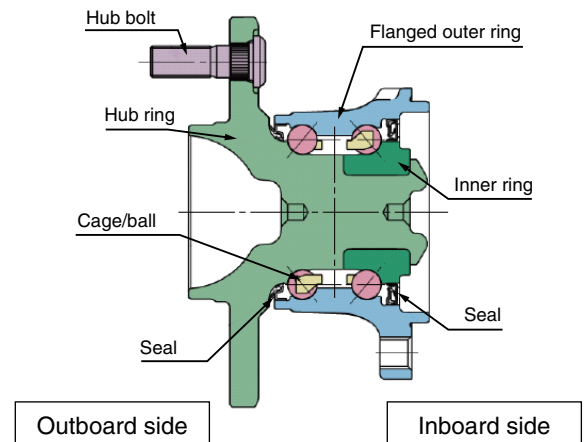
Fig. 1 Example of hub bearings[5]

Table 1: Bearing specification

Ball diameter (mm)	11.1
Number of balls	16
Pitch diameter of ball set (mm)	61
Contact angle (deg)	35
Distance between rows of balls (mm)	18.2
Preload (N)	5,400

* CAE R&D Center

Table 2: Operation condition

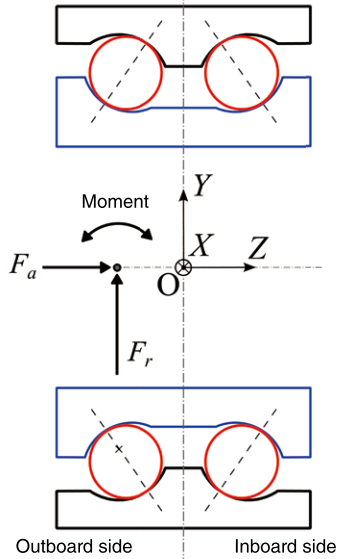| Vehicle speed (km/h)	10, 50, 100
Moment (N mm)	-600×10^3 - 600×10^3
Axial load Fa (N)	$-1,890$ - $1,890$
Radial load Fr (N)	1,820 - 3,750
Load acting point (mm)	10.4
Load variation frequency (Hz)	1, 10, 50

Outboard side　Inboard side

Fig. 2 Load acting position and coordinate system of analysis

3. Method of Analysis

Temporal waveform of the inclining angle of the operating hub bearing under moment load was calculated using an integrated dynamic analysis system "IBDAS"[3], which is **NTN**'s proprietary development for analysis of roller bearings.

The degrees of freedom of motion set for the analytical model and the constraint conditions are as shown in **Table 3**. The outer ring of the bearing is fixed in the space and the inner ring has degrees of freedom of motion excluding rotation. The inner ring was given the weight and the inertial moment of hub ring. The balls and the cage have 3 translational and 3 rotating degrees of freedom. IBDAS can take into account the elastic deformation of the cage using the mode synthesis method. This analysis gives a total of 56 deformation modes to each cage.

Table 3: Degrees of freedom of motion and constraint conditions within the analytical model

Outer ring	Degrees of freedom: None (fixed)
Inner ring	Degrees of freedom: 3 translational, 2 rotating Constraint: rotation at a constant speed
Ball	Degrees of freedom: 3 translational, 3 rotating
Cage	Degrees of freedom: 3 translational, 3 rotating Elastic deformation: 56 modes

In order to dynamically analyze the motion of the ball bearing system with the above degrees of freedom, normal force and tangential force at the contact between the ball/raceway and the ball/cage must be appropriately calculated. The following are the respective methods of calculation. In addition, moments of the balls generated by various forces are also calculated, as required.

3.1 Contact Point Between Balls/Raceway

Normal force is obtained assuming that the contact pressure follows Hertz Theory. In calculating tangential force, the distribution of contact pressure on the major axis of the contact ellipse and sliding velocity are considered as shown in **Fig. 3** for an appropriate expression of 3-dimensional ball motion[6]. The specific calculating method is as follows:

The normal load on one of the nth pieces sliced along the major axis of the contact ellipse under hertzian pressure can be obtained by integrating the contact pressure along the direction of the minor axis, then integrating it along the major axis within the range of the particular sliced piece and can be expressed in the following equation:

$$F_{Nj} = \frac{3F_N}{2n}\left[1 - \frac{12\{j-0.5(n-1)\}^2+1}{3n^2}\right]\quad(1)$$

Where, F_{Nj} is the normal force acted on the jth section, F_N is the normal force of the entire contact area and j is the section number (0 to n-1).
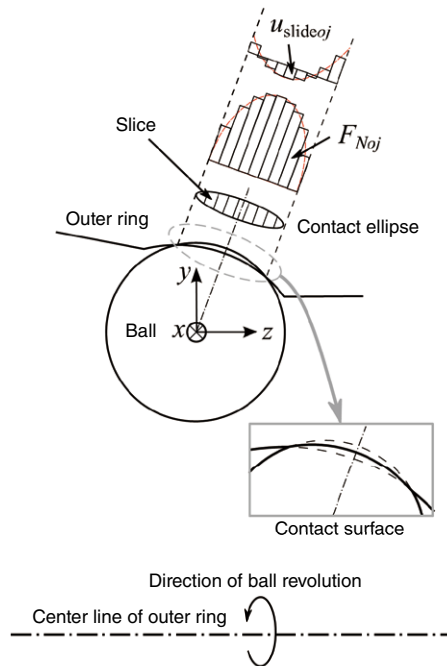
Fig. 3 Calculation model of the contact area between a ball and outer ring (F_{Noj} is the normal force acting on the jth section from the outer ring, $u_{\text{slide}oj}$ is the sliding velocity of the jth section of the ball against outer ring)[6]

For the tangential force, the following 3 types of force elements, which can be assumed in the contact area under oil lubrication, were considered.

    1. Traction[*1]
    2. Rolling viscosity resistance[*2]
    3. Oil film force on the rolling direction[*3]

Since hub bearings are lubricated by grease, this report assumed that the above 3 types of force elements are determined only by the base oil of the grease. The following is an outline of calculation of each force element:

Force acting on each section was calculated using the following equation, assuming that it would act in the opposite direction of the sliding velocity vector of the ball surface against the raceway $\vec{u}_{\mathrm{slide}j}$.

$$\vec{F}_{Tj} = -\phi_j F_{Nj} \frac{\vec{u}_{\mathrm{slide}j}}{\left|\vec{u}_{\mathrm{slide}j}\right|} \qquad (2)$$

Where F_{Tj} is the force acting on the ball, ϕ_j is the friction coefficient and the subscript j represents the jth section. The arrow on top means that it is a vector. ϕ_j under fluid lubrication was obtained using the calculation method that considers the property of lubricating oil[7], ϕ_j under boundary lubrication was obtained by a function with only slide-roll ratio[*4] and ϕ_j under mixed lubrication was obtained by interpolating between those friction coefficients proportionally to the film parameter[8]. The friction coefficient greatly depends on the slide-roll ratio even under fluid lubrication, as shown in the calculation example in **Fig. 4**.
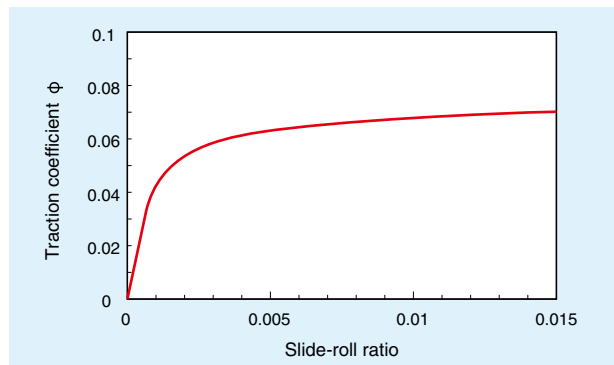
Fig. 4 Example of traction coefficient

The sliding velocity vector of the ball surface against the raceway $\vec{u}_{\mathrm{slide}j}$ was obtained using the following equation:

$$\vec{u}_{\mathrm{slide}j} = \vec{v}_b + \vec{\omega}_b \times \vec{r}_{bcj} - \left(\vec{v}_{\mathrm{race}} + \vec{\omega}_{\mathrm{race}} \times \vec{r}_{\mathrm{race}cj}\right) \qquad (3)$$

*1 On two objects in rolling/sliding contact, this is the tangential force which acts on the opposite direction from the rolling direction at the higher speed side and on the same direction as the rolling direction at the lower speed side.
*2 This is the force caused by shear force of oil film which acts in the direction to prevent rolling of two objects in rolling contact, under oil lubrication.
*3 This is the force that acts on the rolling direction due to the oil film pressure that acts on two objects in rolling contact under oil lubrication. This is generated as the center of oil film pressure shifts to the upstream side.
*4 Sliding velocity of the contact surface divided by the average velocity of the contact surface.

Where, $\vec{v}_b$ is the translational velocity vector of the center of the ball, $\vec{\omega}_b$ is the angular velocity vector of the ball, $\vec{r}_{bcj}$ is the position vector from the center of the ball to the jth section surface, $\vec{v}_{\mathrm{race}}$ is the translational velocity vector of the center of raceway, $\vec{\omega}_{\mathrm{race}}$ is the angular velocity vector of the raceway, and $\vec{r}_{\mathrm{race}cj}$ is the position vector from the center of the raceway to the jth section surface. The method for obtaining the position of the section surface within the contact ellipse is based on the Jones method[9].

The sliding velocity vector of the section on the ball surface, $\vec{u}_{\mathrm{slide}j}$, has a component of the axial direction in addition to the rolling direction, as shown in **Fig. 5**. Therefore, there is a force acting in the direction of major axis of the contact ellipse.

Black: Sliding velocity component in the rolling direction
Blue: Sliding velocity component in the axial direction
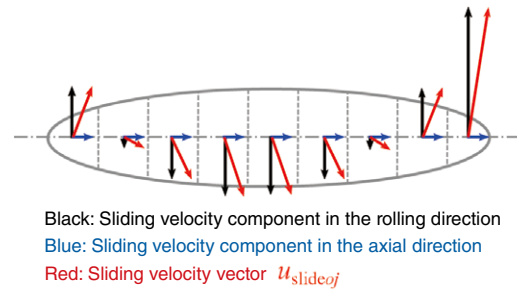Red: Sliding velocity vector $u_{\mathrm{slide}oj}$

Fig. 5 Example of sliding velocity vector on the ball surface

The rolling viscosity resistance acts in the opposite direction of rolling direction against the ball and the raceway. Since it is the force from the lubricating film, it was assumed that this only occurs under fluid lubrication where lubricating film is formed. And the magnitude of the rolling viscosity resistance F_R was obtained, using the equations for[10), 11)] the case of high pressure viscosity elastic body range (PE) and high pressure viscosity rigid body range (PR). The case of isobaric viscosity rigid body range (IR) is also used selectively, depending on the result of the range determination[12].

$$F_{Rj} = \begin{cases} \dfrac{C_t 29.2 R^*_j \left(GU_j\right)^{0.648} W_j^{0.246}}{\alpha_0} \, w & \text{for PE, PR} \\[4mm] 1.70 E^* R^*_j U_j \left(\dfrac{W_{\mathrm{Pmax}}}{U_{\mathrm{Pmax}}}\right)^{0.509} w & \text{for IR} \end{cases} \qquad (4)$$

Where, C_t is the coefficient of thermal correction, R^*_j is the effective radius, G is the material parameter, U_j is the velocity parameter, W_j is the load parameter, w is the section width, E^* is the equivalent elastic modulus and the subscript Pmax refers to the section where the contact pressure is the greatest.

The oil film force on the rolling direction F_P was obtained using the following equation[10] from the rolling viscosity resistance[12].

$$F_{Pj} = \frac{2R_j^* F_{Rj}}{R_{bj}} \qquad (5)$$

Where, R_{bj} is the radius from the rotational axis of the ball to the jth section of the contact area.

As the distribution of forces in the contact ellipse and their 3D effect are put into consideration, the calculation result of rotation and revolution velocity of the balls from IBDAS closely matches[6] the calculation result from Jones Theory[9].

3.2 Contact Point Between Balls/Cage

It was assumed that the normal force, F_{NC}, that corresponds to the interference amount, δ_C, is generated following the Hertz Theory meaning the surface of the cage is divided into finite elements and those nodes geometrically interfere with the balls.

$$F_{NC} = k_{\text{HertzC}} \delta_C^{1.5} \qquad (6)$$

Where, k_{HertzC} is the non-linear spring constant in the Hertz Theory.

In calculating tangential force, only force from sliding friction was considered, as sliding is the only force between the balls and the cage. Sliding friction force was obtained by the following equation.

$$\vec{F}_{TC} = -\mu_S F_{NC} \frac{\vec{u}_C}{|\vec{u}_C|} \qquad (7)$$

Where, μ_S is the friction coefficient and $\vec{u}_C$ is the sliding velocity vector of the ball surface against the cage pocket. For μ_S, 0.06 was used in this calculation.

4. Calculation Result

Fig. 6 shows the calculation result of the inclining angle of the inner ring on the applied moment in each vehicle speed. The load variation frequency is 50 Hz. It revealed that the waveform of the inclining angle of the inner ring on the applied moment has hysteresis. It also revealed that the slopes of the lines for each vehicle speed (compliance) are, although with hysteresis, the same. From these results, it was revealed that the rigidity of hub bearings, which is the inverse number of compliance, is also mutually the same regardless of vehicle speed.
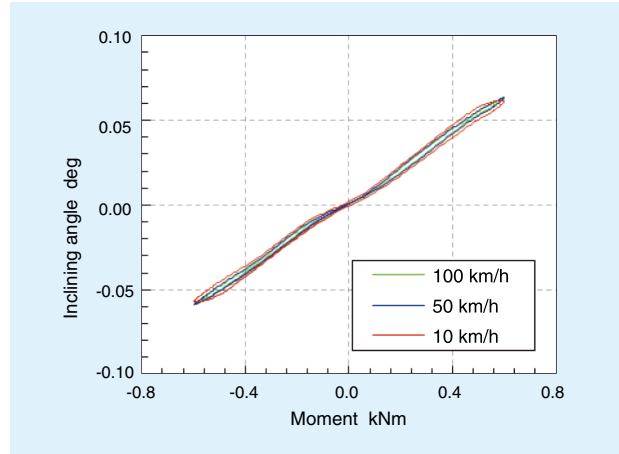

Fig. 6 Calculation result of the inclining angle of the inner ring to the applied moment in each vehicle speed (load variation frequency: 50 Hz)

Fig. 7 shows the calculation result of the inclining angle of the inner ring on the applied moment, when the load variation frequency is changed to 3 different levels with vehicle speed of 10 km/h. The slopes of the lines of the inclining angles of the inner ring on the applied moment remain the same, revealing that the rigidity of hub bearings does not depend on the load variation frequency.
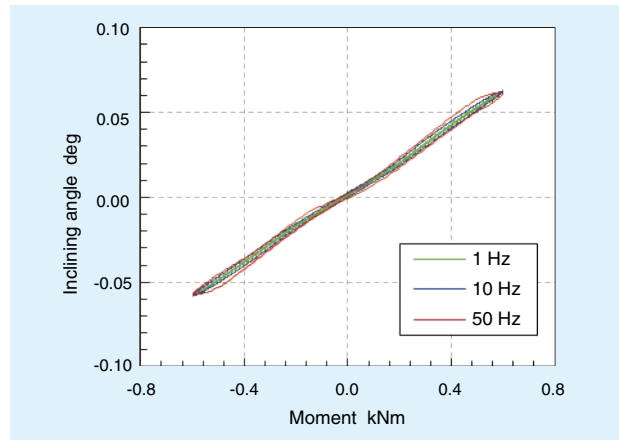

Fig. 7 Calculation result of the inclining angle of the inner ring to each load variation frequency (vehicle speed: 10 km/h)

On the other hand, hysteresis is also observed in the lines of **Fig. 7**. The hysteresis of the inclining angle of the inner ring on the applied moment means that the increase of lateral displacement of the body lags a little behind the tire lateral force input from the ground. If lateral displacement of body against steering is considered, it means the peak of the lateral displacement appears a little late. This reduces vehicle handling stability.

Therefore, the effect of driving conditions on the magnitude of hysteresis is determined by examining the difference of the inclining angle at the moment 0.3 kNm. It is defined as the fluctuation range W_H, as shown in **Fig. 8**.
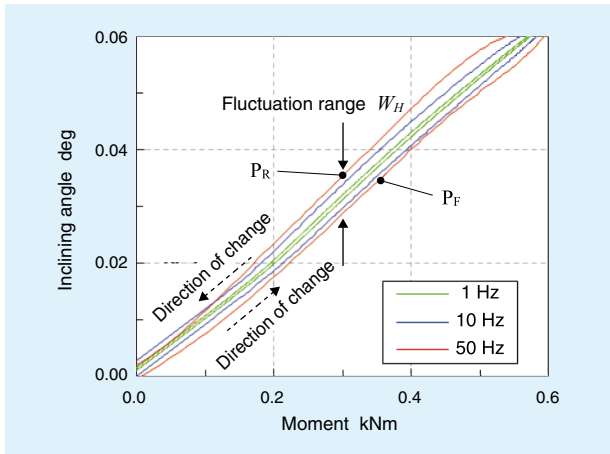
Fig. 8 Definition of fluctuation range W_H, which indicates the magnitude of hysteresis of inclining angle of the inner ring against the moment (Points P_F and P_R are used in Chapter 5)

Fig. 9 shows the fluctuation range of the inclining angle of the inner ring when vehicle speed and load variation frequency are both changed. As shown in **Fig. 9**, the fluctuation range increased as the vehicle speed reduced and the load variation frequency increased.
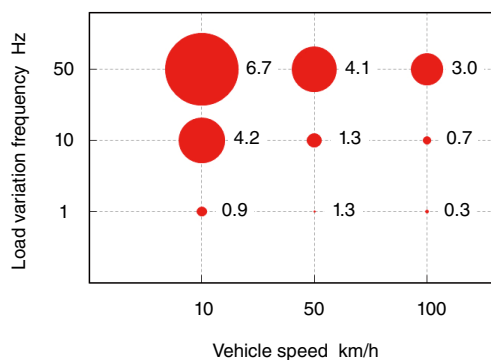

Fig. 9 Calculation result of fluctuation range of inclining angle of the inner ring against the moment W_H when vehicle speed and load variation frequency are changed (bubble diameter is proportional to fluctuation range, numbers next to bubbles are fluctuation range W_H (deg/10^3))

5. Examination

The following discusses the mechanism of how fluctuation range, W_H, affects the waveform of the inclining angle of the inner ring on the applied moment.

The reason for the fluctuation range is shown in **Fig. 10**. The force in the direction of the major axis of the contact ellipse created between the ball and the raceway hinders the movement of the ball in the radial plane. This mechanism is described below, focusing on the forces that act on the upper right ball of **Fig. 10**.
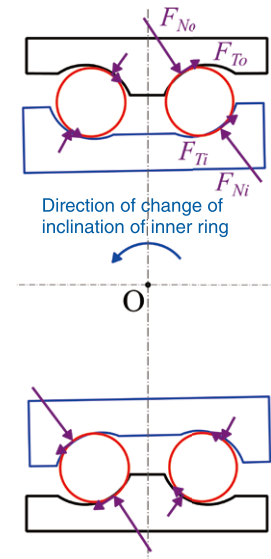

Fig. 10 Overall concept of the normal force and traction that act on the balls from the raceway when the inner ring inclines counterclockwise

The typical state of forces that act on the upper right ball of **Fig. 10** is shown in **Fig. 11**. First, **Fig. 11 a)** shows the state where the inner ring continues to rotate while the inclining angle of the inner ring remains constant. In this case, since the inner ring is rotating with the same inclining angle of the inner ring, the center of the ball is positioned on the line that connects the centers of the grooves of the inner and outer rings. The normal forces, F_{Ni} and F_{No}, which act on the ball from the inner/outer rings are aligned on the same axis and remain balanced (here, the centrifugal force is ignored for ease of explanation). The forces that act on the ball from the inner/outer raceways act only in the direction of the roller, not having the surface component in the figure.

Fig. 11 b) shows the state immediately after the inclining angle of the inner ring increases its magnitude in the counter clockwise direction, where the ball transition is not sufficient. In this case, the normal force, F_{Ni}, from the inner ring changes its direction as shown in the figure (here, force, F_{Ti}, that acts on the ball from the inner ring is ignored for ease of explanation). The resulting force that acts on the ball from the raceway will be toward upper left as shown in the figure.

Immediately after this, the ball moves in the radial plane and the force that acts on the ball and the moment balance out, as shown in **Fig. 11 c)**. As the ball moves, the magnitude and direction of F_{Ni} and F_{No} change and the forces that act on the ball from the inner/outer rings, F_{Ti} and F_{To}, start moving in the upper right direction. Due to these forces, the center of the ball cannot move to the line that connects the centers of the inner/outer raceway grooves, not as **Fig. 11 a)**.

Next, a case where the inclining angle of the inner ring is the same as **Fig. 11 c)**, but the moment is decreasing and

the inclining angle of the inner ring changes in the clockwise direction is considered. Let us consider the case of P_R as the P_F point in **Fig. 8**. The force that acts on the point P_R can be described in **Fig. 12**. Since the forces that act on the ball from the inner/outer rings act in the lower left direction, the ball remains toward to lower left from the line that connects the centers of the inner/outer raceway grooves. The angle of F_{Ni} also becomes smaller. As a result, the magnitude of the moment the ball induces on the inner ring is smaller than **Fig. 11 c**) meaning the moment at the point P_R in **Fig. 8** is smaller than the point P_F.

As seen above, due to the forces acting in the major axis direction of the contact ellipse, the center position of the ball where the inclining angle of the inner ring cannot reach the ball position where the inclining angle of the inner ring is constant. And this force produces the fluctuation range of the inclining angle of the inner ring.
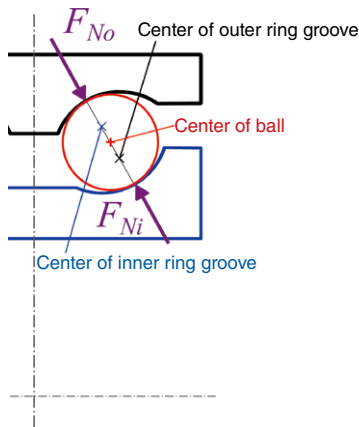
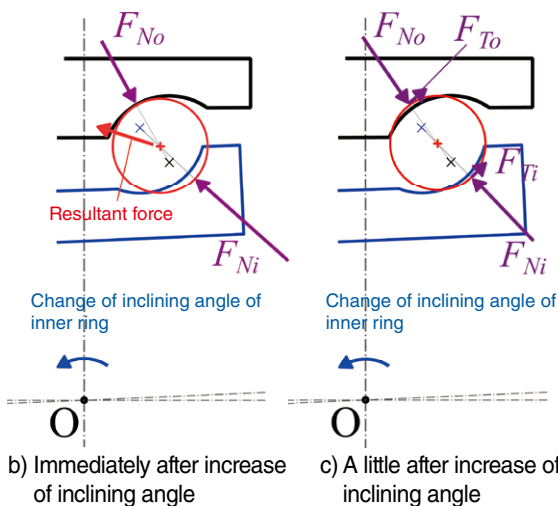a) Inner ring is rotating when inclining angle is constant

b) Immediately after increase of inclining angle

c) A little after increase of inclining angle

Fig. 11 Normal force and traction that act on the balls from the raceway when the inner ring inclines counterclockwise

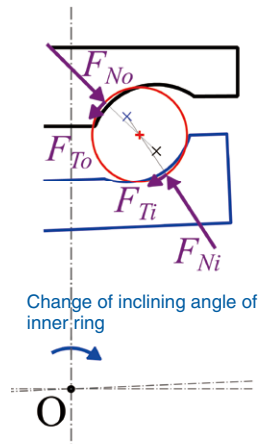Change of inclining angle of inner ring

Fig. 12 Normal force and traction that act on the balls from the raceway when the inner ring inclines clockwise

The fluctuation range, W_H, correlates with the magnitude of the force in the major axis direction of the contact ellipse that acts on the ball, as mentioned above. This magnitude of force greatly depends on the slide-roll ratio as shown in **Fig. 4**. The slide-roll ratio on the ball surface, s_j, is a ratio of the sliding velocity on the ball surface, $\left|\vec{u}_{\text{slide}j}\right|$, over the rolling velocity of the contact area, $\left|\vec{u}_{\text{roll}j}\right|$, and is given in the following equation:

$$s_j = \frac{\left|\vec{u}_{\text{slide}j}\right|}{\left|\vec{u}_{\text{roll}j}\right|} \tag{8}$$

For simplification, slide-roll ratio at the pure rolling position (no sliding in the rolling direction) in the contact area between the ball and raceway is considered. In this case, the sliding velocity and the rolling velocity are proportional to the load variation frequency, f_{load}, and the vehicle speed, u_v, respectively. The slide-roll ratio, s_j, can be expressed as follows:

$$s_j \propto \frac{f_{\text{load}}}{u_v} \tag{9}$$

Therefore, it can be concluded that the increase of f_{load} and decrease of u_v result in the increase of the slide-roll ratio s_j, friction coefficient ϕ_j, force and fluctuation range W_H, which corresponds with the trend in **Fig. 9**.

The above is a discussion of pure rolling position within the rolling contact area. At the position where sliding velocity exists in the rolling direction, the numerator of Equation (8) includes the sliding velocity component in the rolling direction which slightly reduces the impact of f_{load} on s_j. However, since the sliding velocity component in the major axis direction increases, the forces in the major axis still increases.

6. Conclusion

The rigidity of hub bearings with inner ring rotation was analyzed using the dynamic analysis system, IBDAS. As a result, it was verified that the rigidity of hub bearings does not depend on the rotational speed of the inner ring and variation frequency of the moment. It was also verified that the waveform of the inclining angle of the inner ring over the varying moment has hysteresis. The reason for this hysteresis is because of the traction in the direction of major axis of the contact ellipse created between the ball and the raceway. Increasing the load variation frequency and decreasing the vehicle velocity (decreasing the rotational speed of the shaft) increases traction in the major axis direction of the contact ellipse, ultimately increasing the hysteresis range.

The above hysteresis can be interpreted as the delay of response of hub bearing angle to the change of moment. In order to increase vehicle handling stability, it is desirable to reduce this delay. We will continue further analysis using CAE technology to developing hub bearings with reduced hysteresis.

References

1) Eiji Funahashi, History of Hub Bearings and Recent Technology, NTN TECHNICAL REVIEW, No. 70, (2002) 52.

2) Takayasu Takubo, Evaluation Bench Tests for Hub Bearings, NTN TECHNICAL REVIEW, No. 70, (2002) 74.

3) Mariko Sekiya, Integrated Bearing Dynamic Analysis System (IBDAS), NTN TECHNICAL REVIEW, No. 79, (2011) 119.

4) N. Shibutani, D. Imada, T. Sakaguchi, Dynamic Characteristic of Moment Stiffness of Hub Bearing, Proceedings of the 8th Asian Conference on Multibody Dynamics, (2016).

5) NTN Corp. Hub Bearings Catalog, CAT. No. 4601/J.

6) Tomoya Sakaguchi, Mariko Izumi, Tomoya Nakamura, Toshiya Kimura, Masaharu Uchiumi, Dynamic Analysis of Ball Bearings for Turbopumps Considering Force and Moment due to Liquid Hydrogen, The 68th Turbomachinery Society of Japan Conference in Okinawa (2012) 203.

7) Masayoshi Muraki, Yoshitsugu Kimura, Study on Traction Property of Lubricating Oil (2nd Report), Journal of Japan Society of Lubrication Engineers, 28, (1983) 753.

8) T. Sakaguchi, K. Harada, Dynamic Analysis of Cage Behavior in a Tapered Roller Bearing, J. Tribol, 128, (2006) 604.

9) A. B. Jones, A General Theory for Elastically Constrained Ball and Radial Roller Bearings Under Arbitrary Load and Speed Conditions, Trans. ASME, J. Basic Engineering, 82, (1960) 309.

10) R. S. Zhou, M. R. Hoeprich, Torque of Tapered Roller Bearings, J. Tribol., 113, (1991) 590.

11) L. Houpert, Piezoviscous-Rigid Rolling and Sliding Traction Forces, Application: The Rolling Element-Cage Pocket Contact, J. Tribol., 109, (1987) 363.

12) Tomoya Sakaguchi, Calculation Methods of Forces and Cage Stresses in Roller Bearings, Doctoral Dissertation, Nagaoka University of Technology Institutional Repository (2018).

Photo of authors

Tomoya SAKAGUCHI
CAE R&D Center

Naoto SHIBUTANI
CAE R&D Center

Ultra Low Friction Sealed Ball Bearing for Transmission

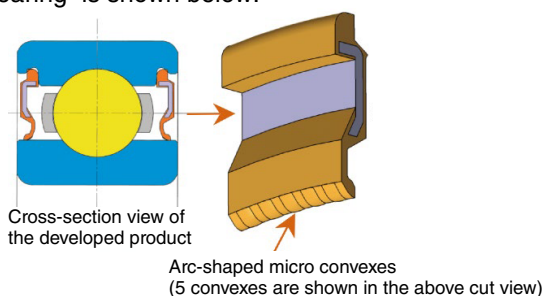**Katsuaki SASAKI**   **Takahiro WAKUDA**   **Tomohiro SUGAI**

1. Introduction

"Ultra low Friction Sealed Ball Bearing for Transmission" was developed. This reduces friction of an application by controlling the fluid lubrication with a new design of a proprietary shaped seal lip.

This product received the Mobility Components Award of the 2018 "CHO" MONODZUKURI Innovative Parts and Components Award sponsored by MONODZUKURI Nippon Conference and Nikkan Kogyo Shimbun, Ltd.

This breakthrough idea achieves both low torque and long operating life simultaneously. The results of this study are based on an unprecedented unique seal philosophy and verified through theory and experiments.

2. Structure

A general structure of the "Ultra Low Friction Sealed Ball Bearing" is shown below:

Cross-section view of the developed product

Arc-shaped micro convexes
(5 convexes are shown in the above cut view)

3. Features

The developed product has the following features:
  (1) Fluid lubrication seal (equivalent to open product)
      Reduction of running torque by 80%
      (compared to contact type seal)
  (2) Longer operational life in comparison to product with special heat treatment 5
      times or longer bearing life
      (compared to open product)
  (3) World's highest seal circumferential speed performance
      Seal circumferential speed of 50 m/s or more
  (4) Sealing properties are equivalent to or better than the conventional contact type seal
      Prevention of penetration from harmful foreign objects

Note: "Open product" is a designation of open type bearing with no seal

The low torque equivalent to non-contact sealed bearings was verified through analysis and experiment. The optimum seal shape was developed to prevent harmful foreign objects from penetrating into bearing.

This long-life bearing has 5 times or more operating life than a product with special heat treatment.
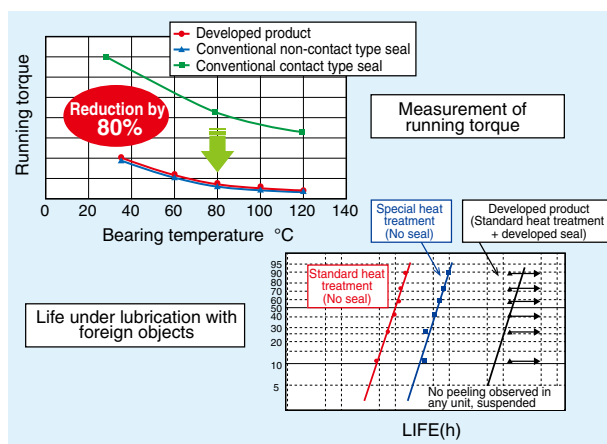

4. Summary

The low torque seal has adopted a new mechanism design to produce a wedge film effect for the seal lip. This creates a low torque equivalent to non-contact type sealed bearings and long operational life that is better than the products with special heat treatment. It exhibits excellent seal durability, even under high rotational speed conditions. This makes this contact type seal suitable for high-speed rotation required by EV/HEV. It is less costly than the bearing with special heat treatment. An active market deployment is planned.

References

1) Tomohiro Sugai, Lubrication Mechanism of Low Friction Seal of Ball Bearing for Transmission, NTN TECHNICAL REVIEW 86, (2018) 78-83.
2) Takumi Fujita, Strategy of Rolling Contact Fatigue Life Testing and Interpretation of Life Data, NTN TECHNICAL REVIEW 84, (2016) 74-79.

Photo of authors
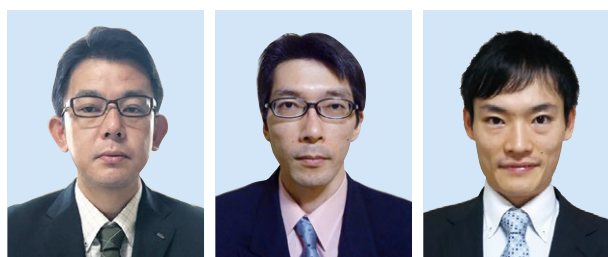
Katsuaki SASAKI

Automotive Bearing
Engineering Dept.
Automotive Business
Headquarters

Takahiro WAKUDA

Automotive Bearing
Engineering Dept.
Automotive Business
Headquarters

Tomohiro SUGAI

Advanced Technology
R&D Center

Micro Hydro Turbine

Masatoshi MIZUTANI*   Fumihiko MATSUURA*   Tomoya KAWAI**   Hiroki MUKAI*   Takashi ITO*

Tomomi GOTO*   Yasunari KANAMURA*   Kanta KIMURA*   Kouji TATEISHI*

1. Introduction

The Micro Hydro Turbine **(Fig. 1)** received the Award for Excellence of 2018 (28th) Nikkei Global Environmental Technology Awards hosted by Nikkei Inc. The Turbine starts generating power by simply placing it in an existing water channel. It is very friendly to the global environment and is contributing to SDGs on a global scale. Features include a highly efficient blade shape that captures water energy and ability to increase generating power. This was evaluated by placing multiple units in series or parallel in the same water channel.

Fig. 1 Micro Hydro Turbine

2. Configuration

Fig. 2 shows the product configuration. It consists of high efficiency blades which connects to a generator and beams for installation on water channels. There are two types of controllers for power generation, one for charging batteries as an independent power source and the other for connecting to the grid so that generated power can be sold. This makes the product versatile to respond to broad market requirements for power generation.
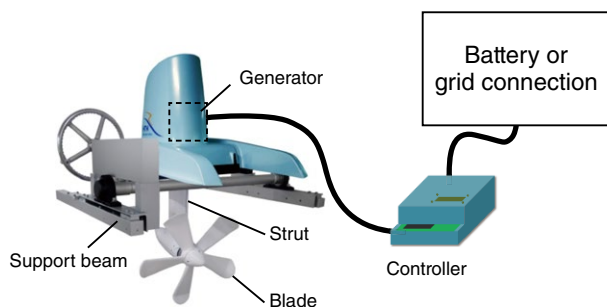

Fig. 2 Configuration of Micro Hydro Turbine

* Engineering Dept., Green Energy Products Division
** Business Promotion Dept., Green Energy Products Division

3. Product Specifications of Typical Models

The model with the blade diameter of 90 cm achieves a rated output of 1 kW when the flow rate is 2 m/sec **(Table 1)**.

Table 1 Product specifications of typical models

Turbine type	Propeller hydro turbine for small water flow
Generator type	Permanent magnet synchronous generator
Blade diameter	60 cm, 90 cm, 130 cm
Rated power output	1 kW (90 cm model at flow rate of 2 m/s)
Recommended water channel	Width 100 cm or more, depth 100 cm or more
Size/weight	H 190 cm × W 230 cm* × D 170 cm, 170 kg

* Varied depending on the width of water channel

4. Summary

Existing hydro turbines in the market by other manufactures require major construction work to create different water levels. The issue with major construction is its cost and damage to the environment. The **NTN** Micro Hydro Turbine can be installed by simply placing the unit on a water channel with the beams to fit the width of the water channel, which can solve the issue construction causes to the environment. This unit can be expected to be used in many fields by utilizing agricultural and industrial water promoting local generation and consumption of renewable energy.

References
1) Tomoya Kawai et al.: Micro Hydro Turbine, NTN TECHNICAL REVIEW No. 84, (2016) 28-33.
2) Takashi Itou et al.: Grid Connectable NTN Micro Hydro Turbine, NTN TECHNICAL REVIEW No. 86, (2018) 102-107.
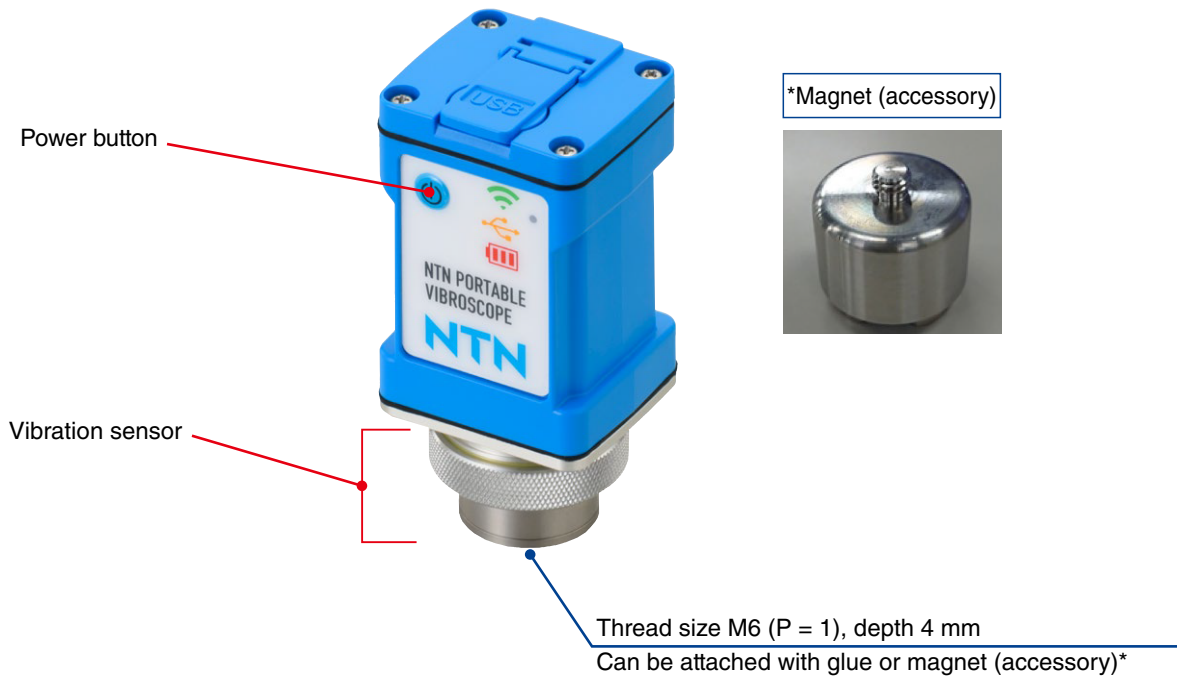
Photo of author (representative)

Kouji TATEISHI*

NTN Portable Vibroscope

This Compact and light sensor unit enables measurement of vibration in various places

Power button

Vibration sensor

*Magnet (accessory)

Thread size M6 (P = 1), depth 4 mm
Can be attached with glue or magnet (accessory)*

Features

(1) Light and compact
The Sensor, power and WiFi wireless units are integrated into a single package
(overall dimensions/weight: W 41 mm × D 36 mm × H 87 mm, 145 g).

(2) Easy measurement
This unit allows for smart devices that support iOS to measure vibration data.

(3) Determines abnormalities
Using OA and FFT methods the user is able to determine abnormalities of bearings via dedicated applications, identifying damaged parts when abnormalities are detected.
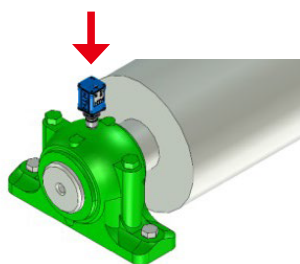Ease of use by graphic display of the measurement history and storage in the smart device allowing for continuous access to the condition of the equipment.
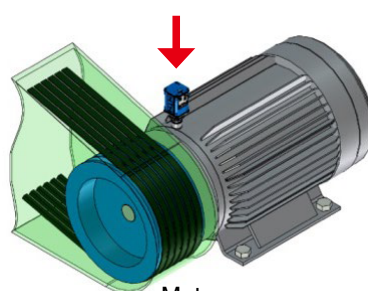
(4) Dust and water resistant
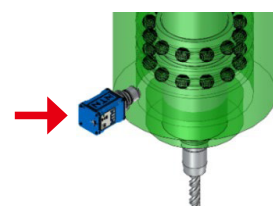IP65 enclosure to assist with portable usage.

Application

· Failure detection, vibration measurement, analysis and trend management of bearings

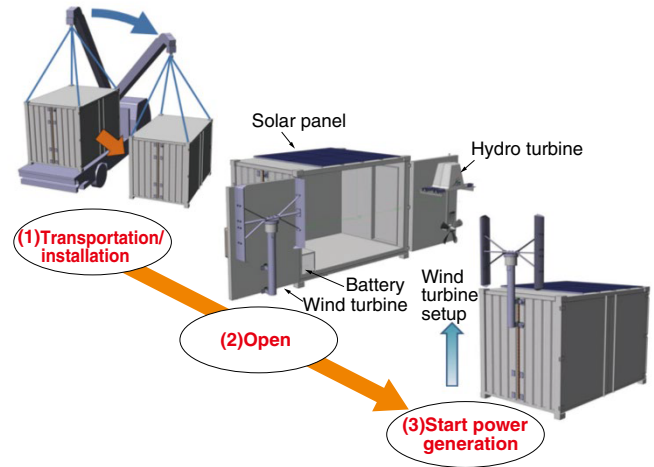Support bearing for conveyor

Motor

Main spindle of machining center

"N^3 N-CUBE," Container Type Transportable Independent Power Supply

Power generation and storage devices by natural energy (wind, water and solar light)
for quick installation

Concept model

Workflow from installation to start of power generation

Features

(1) During an emergency response such as natural disasters, the provided space can be used as storage for supplies or as a living space.
(2) Transportable independent power supply and storage unit with power generation by natural energy (wind, water, and solar light).
(3) Compact package of devices for easy storage
(4) Quick installation and prompt start of power generation/supply

Standard specification

Product type	12-feet container (L 3.7 m × W 2.4 m × H 2.5 m)
Means of transportation	Truck, freight vessel and helicopter
Power devices	Wind turbine: 0.5 kW, hydro turbine: 1.0 kW, solar power generator: 0.9 kW, battery: 8.6 kWh
Installation time	1 hour by 2 persons
Survival wind speed/flow rate	Wind turbine and solar power generator: 30 m/s[*1], hydro turbine: 2 m/s[*2]

*1 Extreme wind speed *2 Maximum water flow

Application

· Power supply to medical devices

· Power supply for cooking/ storage equipment
· Supply of emergency stock
· Supply of drinking water

· Provide space
· Power supply for information devices
· Charging for smartphones
· Power supply to toilets and air conditioners